Organocatalytic access to -amino acids as building blocks for the synthesis of foldamers

Fanelli, Rossana

Awarding institution:
King's College London

Organocatalytic Access to γ-Amino Acids as Building Blocks for the Synthesis of Foldamers

Rossana Fanelli

A dissertation submitted in partial fulfillment

of the requirements for the degree of

Doctor of Philosophy

of

King's College London.

Department of Chemistry

King's College London

December 17, 2019

Abstract

Peptidomimetic foldamers, oligomers that can fold into a well defined conformation in solution, can control functions that would not be possible in nature. Their specific conformation can mimic peptides and therefore control a variety of biological function *via* protein-protein interactions in absence of proteolysis, which is a typical feature of peptidomimetics.

This thesis describes the synthesis of γ-amino acid precursors as building blocks for the synthesis of foldamers. First, an investigation on an envisaged unprece-

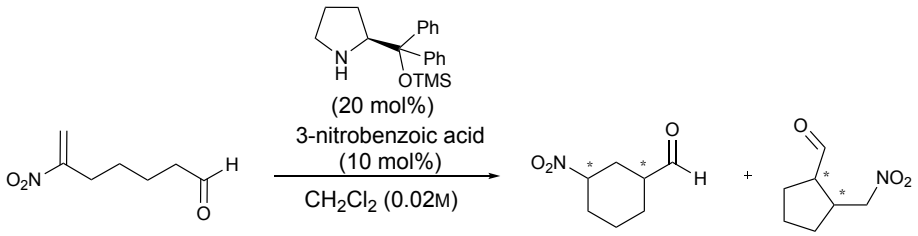

dented mechanistic rearrangement observed during a 6-*endo-trig* cyclisation assisted by organocatalysis was performed. Then, a novel enantio- and diastereoselective synthesis of 5-membered ring *cis*-γ-amino acid precursor was developed. The targeted product was obtained in 72% yield, 9:1 *cis/trans* ratio and 92% *ee*. A mechanistic discussion of the studied 5-*exo-trig* cyclisation is presented. NMR and computational studies suggested that two joint catalytic cycles characterise the synthesis of *cis*- and *trans*-diastereomers. It was found that control of the observed diastere-

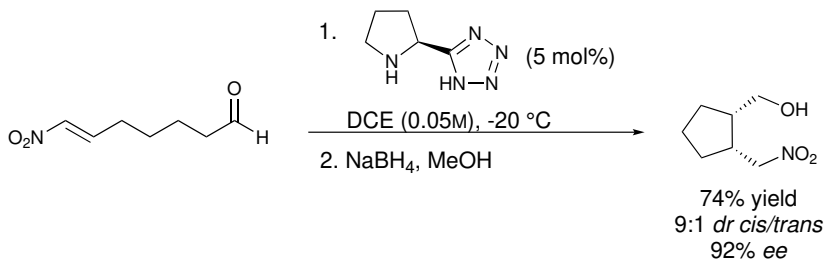

oselectivity degradation may be due to the epimerisation of the *cis*-product to the *trans*-product leading to a change of enantioselectivity with time. Control of this process is crucial to isolate efficiently the *cis*-product.

The synthesised 5-membered ring *cis*-γ-precursor was then incorporated in a γ/α-oligomer. The synthesised peptide proved to populate a 10/12-helical structure in spite of the smallest ζ angle yet observed for a helix of this type, therefore introducing a possible new class of foldamers.

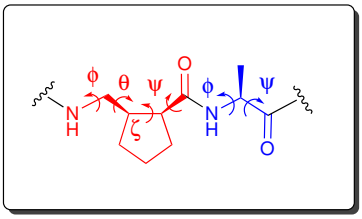

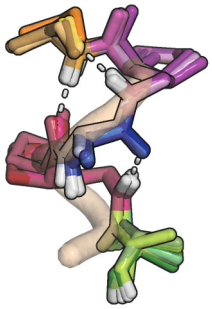

Acknowledgements

Firstly, I would like to thank my supervisor Dr. André Cobb for the guidance and the help that he gave me along these years. A big thank you goes to the whole Cobb group, in Reading and at King's, for the always very useful discussions that we used to have in the lab and for all the help that they gave me all the way to the end of this PhD.

I am grateful to all the collaborators for this project. The Rosta's group and in particular Denés and Tamás for all the help and the very interesting collaboration that we have built together. Dr. Michael Sanders from the Booth's group for the help with the CD. Dr. Andrew Atkinson from Randall Centre of Cell & Molecular Biophysics for working with me on the structural characterisation of foldamers. Dr. Jordi Burés for allowing me to use the NMR facilities at the University of Manchester and for helping me with the kinetic studies.

I would like to express my sincerest thanks to all Reading and BH colleagues. The music of the Osborn's group in Reading made working in the lab even more fun. Thanks to Roberta for the many coffee breaks and for giving me a place to stay whenever I needed it, making my commute to Reading a little easier. Thanks to the many office sharers that we had at King's and in particular Mark for being my desk neighbour and for being very helpful during the writing up of my thesis. Magd and Laura, tea breaks at King's without you would have not been the same. You have been amazing colleagues, but mainly thanks for becoming such good friends.

A huge thanks goes to all my London family. You all were there when I needed it the most. Federica and Tash, thanks for the all fun dinners that definitely helped me going through the writing up of my thesis. Valentina and Natalia, thanks for making your south London flats so welcoming. Kat and Maeve, I would not have survived without you checking on my health and cooking me food. Your presence

has been fantastic.

I cannot thank enough Laura, Danila and Roberta that even if they have never lived in London, it felt like they were there at any time for me. Your calls and your last minute visits made the toughest of times so much easier.

Finally, I would like to thank all the people who encouraged me, my family and most importantly my parents. All this work would have not been possible without you on my side. You gave me all the support I needed along these years, making all my choices much easier than they could have been.

Contents

List of Figures

List of Tables

List of Abbreviations

Ala	Alanine
AMCP	(1*S*,2*R*)-2-(nitromethyl)cyclopentane-1-carboxylic acid
Ar	Aryl
Bn	Benzyl
Boc	*tert*-Butyloxycarbonyl
*n*BuLi	*n*-Butyllithium
CBZ	Carbobenzyloxy
COSY	Correlated Spectroscopy
DBU	1,8-Diazabicyclo[5.4.0]undec-7-ene
DCE	Dichloroethane
DIBAL-H	Diisobutylaluminum hydride
DIPEA	*N,N*-Diisopropylethylamine
DMF	*N,N*-Dimethylformamide
DMSO	Dimethyl sulfoxide
dr	Diastereomeric ratio
E	Electrophile
EDCI	1-Ethyl-3-(3-dimethylaminopropyl)carbodiimide
ee	Enantiomeric excess
eq.	Equivalent

er	Enantiomeric ratio
ESI-MS	Electrospray Ionization Mass Spectrometer
EtOAc	Ethyl Acetate
de	Diastereomeric excess
GABA	γ-aminobutyric acid
Hex	Hexane
HMPA	Hexamethylphosphoramide
HOBt	1-Hydroxybenzotriazole hydrate
HMBC	Heteronuclear Multiple Bond Correlation
HRMS	High Resolution Mass Spectrometry
HSQC	Heteronuclear Single Quantum Coherence Spectroscopy
IR	Infrared spectroscopy
LDA	Lithium diisopropylamide
MHz	Megahertz
MO theory	Molecular orbital theory
mp	Melting point
MS	Mass spectrometry
MW	Molecular weight
NOESY	Nuclear Overhauser Effect Spectroscopy
NMO	*N*-Methylmorpholine *N*-oxide
NMR	Nuclear Magnetic Resonance
Nu	Nucleophile
PCC	Pyridinium chlorochromate
ppm	parts per million
rt	room temperature

R	Alkyl group
T	Temperature
TBAI	Tetra-*n*-butylammonium iodide
TEA	Triethylamine
TEMPO	(2,2,6,6-Tetramethylpiperidin-1-yl)oxyl
TFA	Trifluoroacetic acid
THF	Tetrahydrofuran
TLC	Thin Layer Chromatography
TMS	Tetramethylsilyl
TOCSY	Total Correlation Spectroscopy
TPAP	Tetrapropylammonium perruthenate
TS	Transition state

Chapter 1

Introduction

The control of stereochemistry is one of the main pursuits in organic chemistry because of the different reactivity that the two resulting enantiomers might have in a chiral environment. This was sadly demonstrated in the 1960's in the case of thalidomide; a drug administered to pregnant women to alleviate nausea and morning sickness. Shortly after the drug was released, it was discovered that the two enantiomers of this drug had different effects. The (*R*)-enantiomer produced the desired effect, whereas the (*S*)-enantiomer caused birth defects (Figure 1.1).[1] At

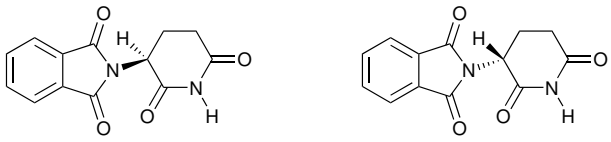

Figure 1.1: The two enantiomeric forms of thalidomide.

first, it was believed that the administration of a single enantiomer would have solved the problem, however they found out that the (*R*)-thalidomide would epimerise to the (*S*)-enantiomer in the body after administration, which meant that even giving the pure enantiomer would have been unsuitable. The negative effect of thalidomide led to more rigorous drug regulations and highlighted the importance of stereoselective synthesis of compounds and in particular of medication.[1]

At first, enantioselective molecules were achieved *via* different routes such as chiral resolution or using chiral auxiliaries. For chiral resolution, a racemic mixture is coupled with a chiral molecule forming diastereomers that can be separated in an achiral environment (*e.g.* chromatography or crystallisation). The two separate compounds can be then converted to the targeted enantiomers but the maximum

achievable yield is 50%. As a result, this is an inefficient method for targeting a single enantiomer. Chiral auxiliaries induce chirality to new forming bonds, however the atom economy is penalised by the presence of the auxiliary. The auxiliary has to be removed after the reaction making this technique undesirable. An alternative method to achieve enantiopure compounds is through use of chiral catalysts. This method is more efficient, enables higher yields and provides a greater atom economy.

1.1 Asymmetric Catalysis

There are three main categories of catalysts that are used for asymmetric synthesis: biocatalysis, metal catalysis and organocatalysis.[2] Biocatalysis uses enzymes that are already used by nature for the synthesis of enantiomerically pure compounds. An example is the dihydroxylation of arenes as described in Scheme 1.1.[3] Enzymes work

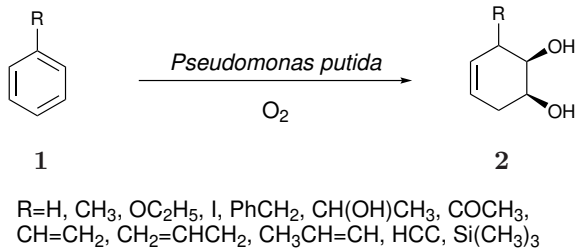

Scheme 1.1: Biocatalysed dihydroxylation of arenes.[3]

extremely well with specific substrates. However, often they require cofactors and specific conditions, making this category incompatible with a variety of substrates and conditions.

Transition metal catalysis originated in the 1950's,[3] and the discovery of tris(triphenylphosphine)rhodium chloride as a catalyst by Wilkinsons and co-workers essentially marks the beginning of the development of asymmetric catalysis. The substitution of phosphines with chiral ligands led to first advances in asymmetric hydrogenation.[4] An example of asymmetric hydrogenation is presented in Scheme 1.2, where compound **4** is obtained in quantitative yield and with 95% *ee*. Following the discovery of Wilkinson's catalyst, transition metal catalysis has been widely used due to low catalyst loading, which has led to high efficiency and good malleability of reactions with a variety of substrates. However, there are growing concerns around metal catalysts due to their costs and sustainability issues. Owing to their toxicity and persistence in the environment, transition metals require a specific disposal

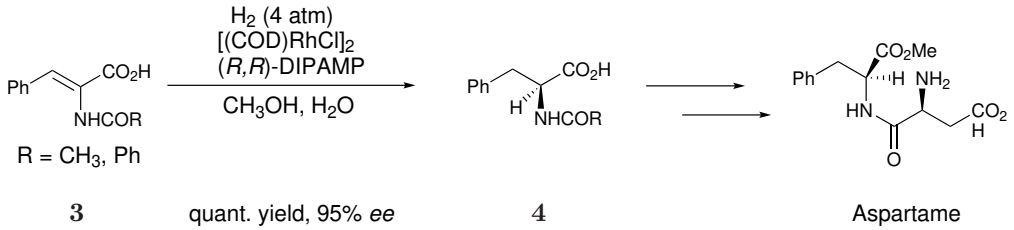

Scheme 1.2: Asymmetric hydrogenation catalysed by the Wilkinson's catalyst.

method. Additionally, the risk of heavy metal residue contamination in medical preparations can make transition metals unsuitable for use by pharmaceutical companies.

Asymmetric organocatalysis is a proficient method to obtain directly only one enantiomer and can be employed to accelerate chemical reactions using organic molecules without the aid of any metal atoms.[5] Compared with metal catalysts, organocatalysis produces less toxic waste and material, are less expensive and more readily available. Organocatalysts tend to be air and water stable, requiring less harsh conditions than metals and they have a wider substrate scope than biocatalysts.[2] There are several classes of organocatalysts and two of the most commonly used involve the use of compounds that act as (i) covalently bonded reagents,[5] and (ii) *via* hydrogen bonding and ion paring.[6]

1.1.1 Covalent organocatalysis

1.1.1.1 Enamine catalysis

Secondary amine catalysis is part of the first class of catalysts. The use of these catalysts in the absence of any metal was first reported in 1971 independently by Hajos and Parrish[7,8] and by Eder, Sauer and Wiechart.[9] Hajos and Parrish cyclised the triketone **5** to compound **7** using (*S*)-proline **6** (3 mol%) as catalyst in anhydrous DMF (Scheme 1.3). Compound **7** was obtained in quantitative yield with a 93% *ee*

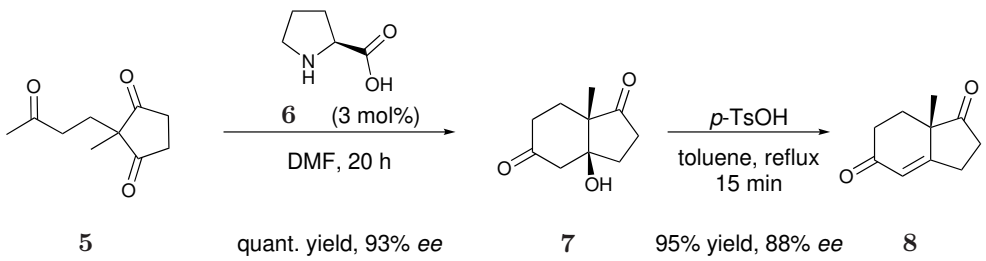

Scheme 1.3: Hajos-Parrish asymmetric aldol reaction catalysed by (*S*)-proline.

and then dehydration was performed to give the optically pure compound **8** in 95% yield and 88% *ee*.

At the same time, Eder, Sauer and Weicher first tested several chiral primary and secondary amines in order to steroselectively cyclise optically active steroids, before finding that natural amino acids achieved better results.[9] They studied the same reaction using a higher catalyst loading and a solution of perchloric acid in acetonitrile at 80 °C, and after 22 hours product **8** was obtained in 87% yield and 84% *ee* (Scheme 1.4).[9]

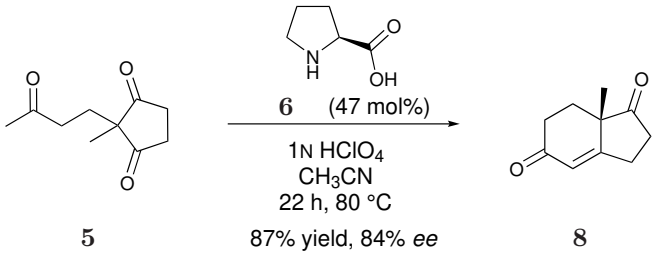

Scheme 1.4: Eder-Sauer-Wiechert aldol reaction catalysed by (S)-proline

After several proposed mechanisms for proline catalysed reactions, in 2004 Houk and co-workers[10] demonstrated, *via* a computational study, that the catalytic reaction involves a proline enamine intermediate. At the same time, List and co-workers reported experimental evidence on the same proposal performing the reaction in ^{18}O enriched water and found that the side chain carbonyl was labelled.[11] This proved the proposed enamine mechanism and it was followed by further ^{1}H NMR studies, which led to the identification of reaction intermediates. These studies led to the currently accepted mechanism of a proline catalysed reaction where the carboxylic acid of proline coordinates to the carbonyl of the electrophile promoting the nucleophilic attack (Figure 1.2).

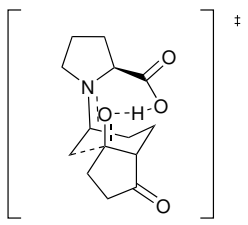

Figure 1.2: Catalytic intermediate proposed by Houk and reported experimentally by List.[10]

In general, secondary amines are Lewis bases and their catalytic mechanism might proceed *via* enamine or iminium mechanism.[11,12] In the first case, the catalyst activates carbonyl compounds (**11**) and generates an enamine intermediate (**12**) that can react with several electrophiles, forming a new bond in α-position (**13**).[13] For an α,β-unsaturated compound, the reactivity will be different and the iminium-form intermediate will react with a nucleophile in the β position (Scheme 1.5).

It was not until the 2000's that, secondary amines became more popular as catalysts.[14] In 2001, List and his research group, studied several proline-catalysed reactions, such as intermolecular aldol, Mannich and Michael reactions (Scheme 1.6).[14] Proline was one of the first catalysts in this category. Proline's efficacy derives from its bifunctionality due to the carboxylic acid group that acts as Brønsted acid together with the secondary amine group which performs as a Lewis Base.[5,15] The bifunctional catalyst can activate both nucleophile and electrophile.[16–19] In particular, the catalyst controls the enantioselectivity of the product through the formation of a H-bond between the electrophile and the carboxylic acid. However, proline presented solubility issues therefore alternative catalysts were designed.

To overcome difficulties encountered with poor H-bonding electrophiles, proline-derivatives were developed. In 2004 several groups reported 5-pyrrolidin-2-yl-1H-

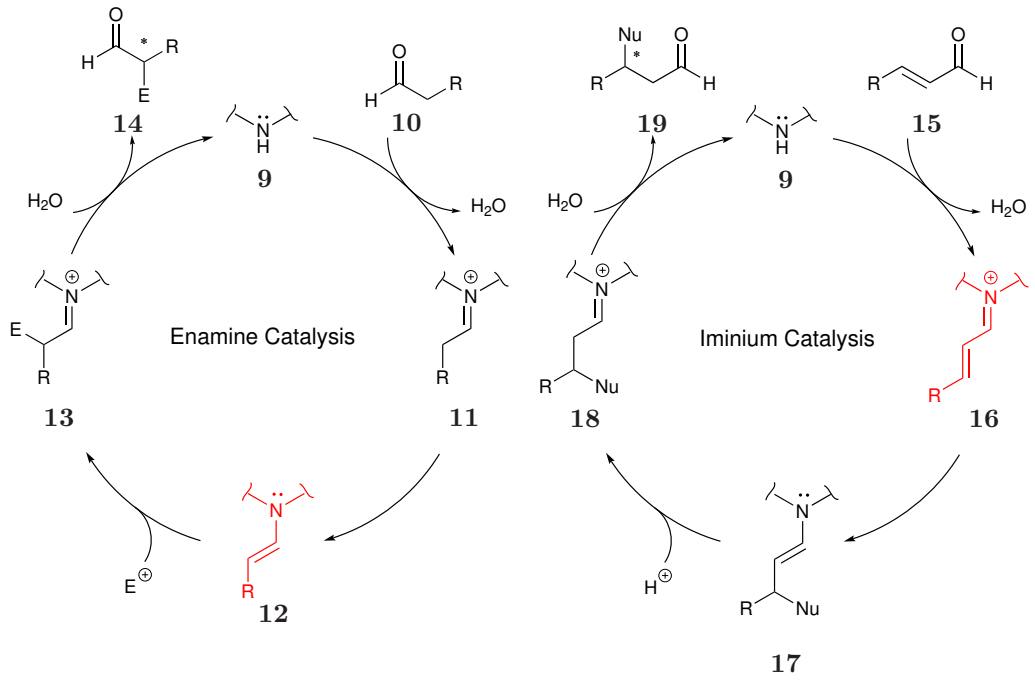

Scheme 1.5: Enamine catalysis and iminium catalysis.

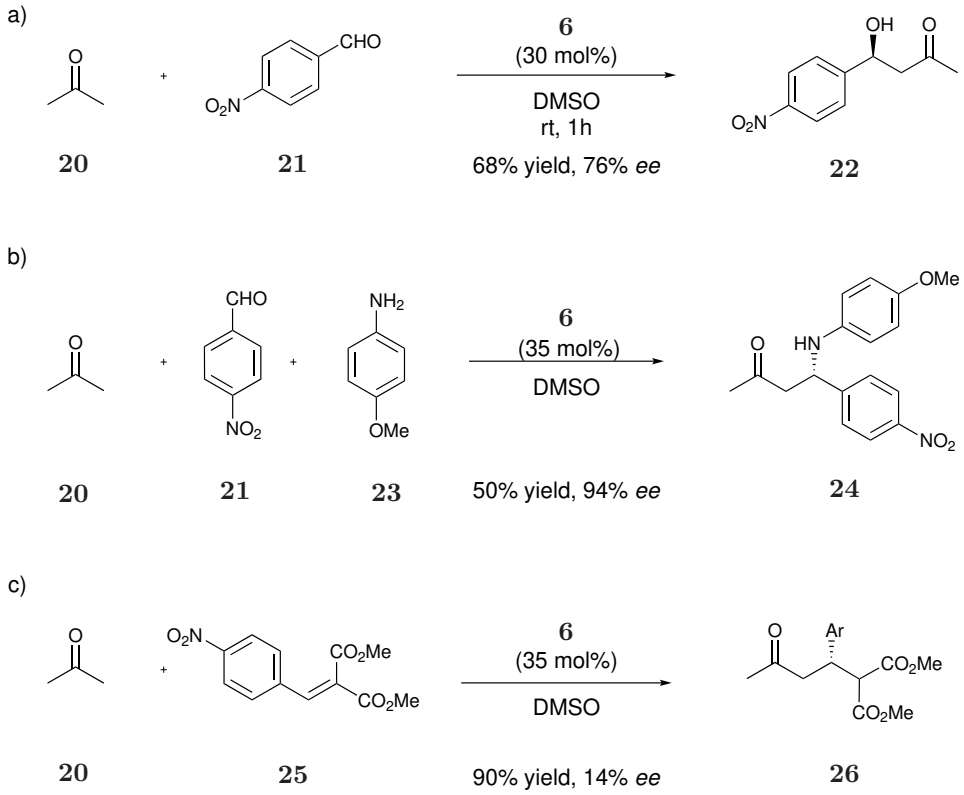

Scheme 1.6: List's proline (**6**) catalysed reactions: (a) intermolecular aldol reaction, (b) first highly enantioselective three-component Mannich reaction and (c) enamine catalysed Michael reaction.

tetrazole **29** as a valid alternative to proline.[20–22] Torii and co-workers reported an asymmetric direct aldol reaction assisted by water (Scheme 1.7).[21] They concluded that the tetrazole catalyst can give highly efficient results if the conditions are adjusted specifically for the reaction. Shortly after, Ley and co-workers reported an asymmetric Mannich-type reaction catalysed by **29**, which gave the targeted product in good yields, excellent *dr* and excellent *ee* (Scheme 1.8).[22] They proposed a hydrogen bonded transition state in a similar manner to the one suggested by Houk

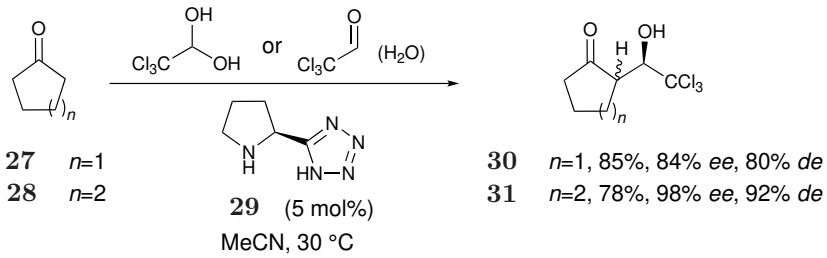

Scheme 1.7: Asymmetric direct aldol reaction assisted by water and catalysed by **29** performed by Torii and co-workers.[21]

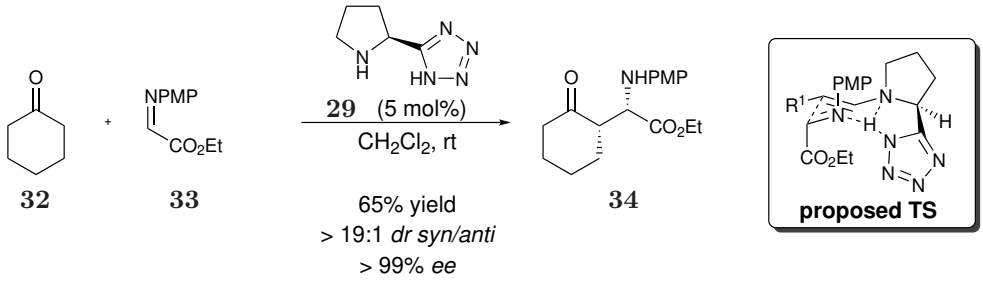

32 33 34

Scheme 1.8: Asymmetric Mannich-type reaction catalysed by **29** performed by Ley and co-workers.[22]

and Bahmanyar (Scheme 1.8).[17,18,23,24] Hartikka and co-workers compared the reactivity of tetrazole catalyst **29** with proline **6** for asymmetric aldol reactions.[25] They observed that the tetrazole catalyst **29** had a higher turnover number than proline **6**. Notably, in the presence of substrates with a lower reactivity, the consumption of starting material occurs at a higher rate with **29**. They suggested that the high efficiency of **29** compared to **6** might derive from the higher lipophilicity of **29**, which provides compatibility with a wider range of solvents due to the presence of the tetrazolic group (Scheme 1.9). The hydrogen bond between the acidic proton of the tetrazole and the carbonylic group of the substrate might be stabilised by charge delocalisation over the tetrazole ring, leading to a stronger hydrogen bond (Scheme 1.9).

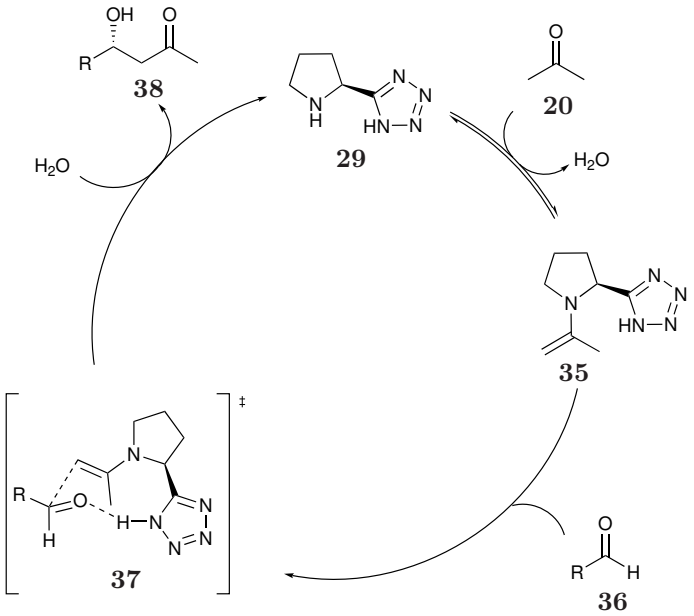

Scheme 1.9: Catalytic cycle proposed by Hartikka and co-workers.[25]

List defined the observed bicyclic oxazolidinone by-product as a parasitic intermediate in reactions carried out in DMSO whereas Blackmond and co-workers thought it was crucial for the reactivity of proline and suggested that it might increase the solubility of the catalyst or allow the catalyst to participate in the reaction (Scheme 1.10).[26–28]

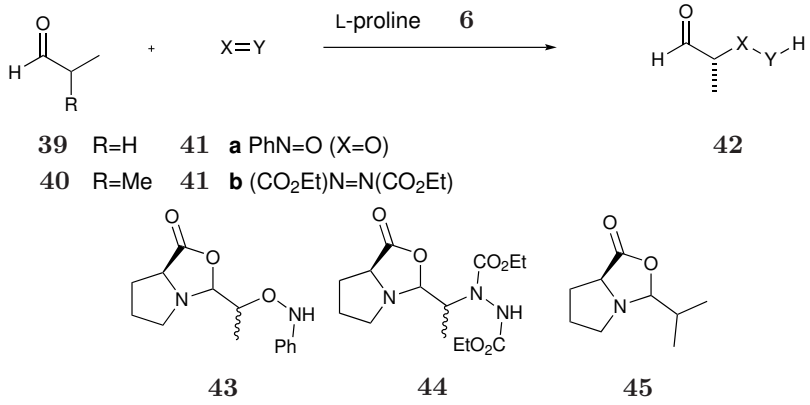

Scheme 1.10: Blackmond and co-workers observation of hemiaminal species as catalytic intermediates in the reaction.[27]

In 2005, Hartikka and co-workers used NMR spectroscopy to rationalise the greater reactivity of the tetrazole catalyst compared to proline.[25] They showed that proline generates parasitic bicyclic oxazolidinone compounds reducing the efficiency of the catalyst, whereas **29** does not.[25] In 2005, Ley and co-workers presented another study where they compared proline derivatives with the proline catalyst for asymmetric Mannich, nitro-Michael and aldol reactions. They found that **29** generated better results than proline in all cases (Scheme 1.11).[29] They suggested that the improvement in enantioselectivity of the tetrazole catalyst **29** over proline **6** might derive from the size difference between the tetrazole and the carboxylic acid which might affect the facial preference of the substrate or possibly different transition states are formed from the two organocatalysts.

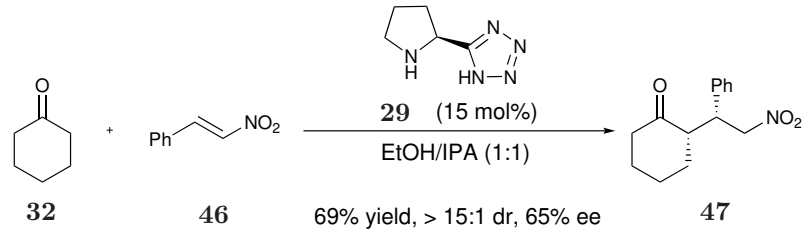

Scheme 1.11: Nitro-Michael addition catalysed by **29** performed by Ley and co-workers.[29]

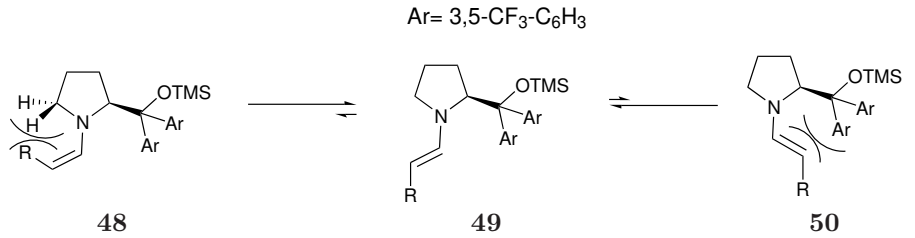

Scheme 1.12: Diarylprolinol silyl ether geometric control.

One of the major exponents of proline-derivative catalysts was Jørgensen, who designed pyrrolidine derivatives with high enantioselectivity due to greater geometry control and efficient face shielding (Scheme 1.12).[30] Several new enamine catalysts were developed (1.3(a)), including the free alcohol **51**, which presented a high stereocontrol, but surprisingly a low turn-over number. They ascribed this problem to the synthesis of an unreactive hemiaminal species (Figure 1.3).[30,31]

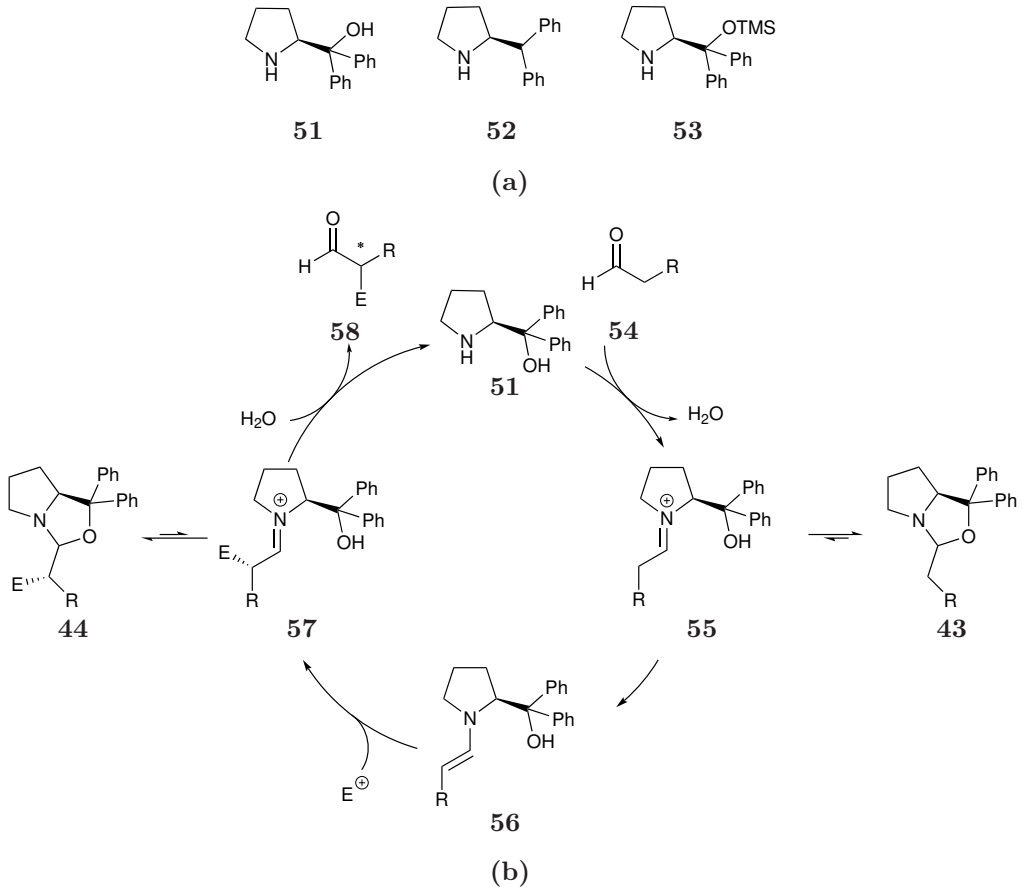

Figure 1.3: (a) Pyrrolidine derivative enamine catalysts; (b) Pyrrolidine derivative catalytic cycle with catalyst **51** showing the hemiaminal side product formation **43** and **44**.

A simple protection of the hydroxyl group (**53**, diphenylprolinol silyl ether) solved the problem, resulting in considerably increased catalytic turnover number. In parallel, Hayashi and co-workers studied the reactivity of the same system **53** in the preparation of nitroalkanes from nitroolefins and aldehydes (Figure 1.3).[32] After a catalyst screen of a test reaction, they showed that catalyst **53** was giving superior results compared to other catalysts. Stirring the reaction at 0 °C for 27 hours gave compound **60** in 80% yield, 99% *ee*, and a ratio of diastereoisomers *syn/anti* of 95:5 (Scheme 1.13).[32] They justify high diastereoselectivities and enantioselectivities

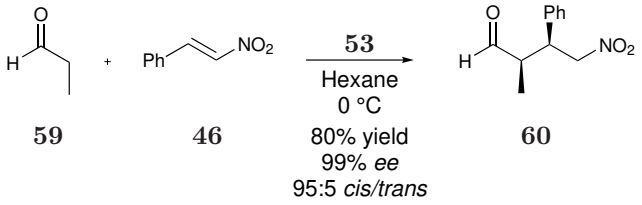

Scheme 1.13: Michael reaction performed by Hayashi and co-workers.

with a transition state model proposed by Seebach and Golinski (Figure 1.4).[33] They showed that the double bond of the enamine is oriented away from the bulky diphenylsiloxymethyl group and the enamine will then react selectively with the nitrostyrene forming an acyclic gauche transition state (Figure 1.4).

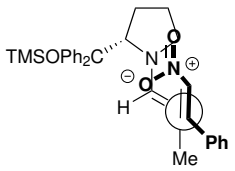

Figure 1.4: Transition state model proposed by Seebach and Golinski.

In the past ten years, several studies have been conducted to investigate the mechanism of action of nitro-Michael additions using organocatalysis. In particular, nitro-Michael reactions mediated by the Hayashi-Jørgensen catalyst have been investigated. Seebach and Hayashi presented a study where they identified a cyclobutane species (CB, **69**) as intermediates of the reaction *via* ^{1}H NMR spectroscopy (Scheme 1.14).[34] Aldehyde **62** condenses into the secondary amine organocatalyst **61**. The enamine formed **63** then reacts with nitroolefin **64** to form the intermediate **65**, which is in equilibrium with a CB species **69**. Hydrolysis leads to the protonation of the nitronate and finally release of the targeted product **67**.[34] They

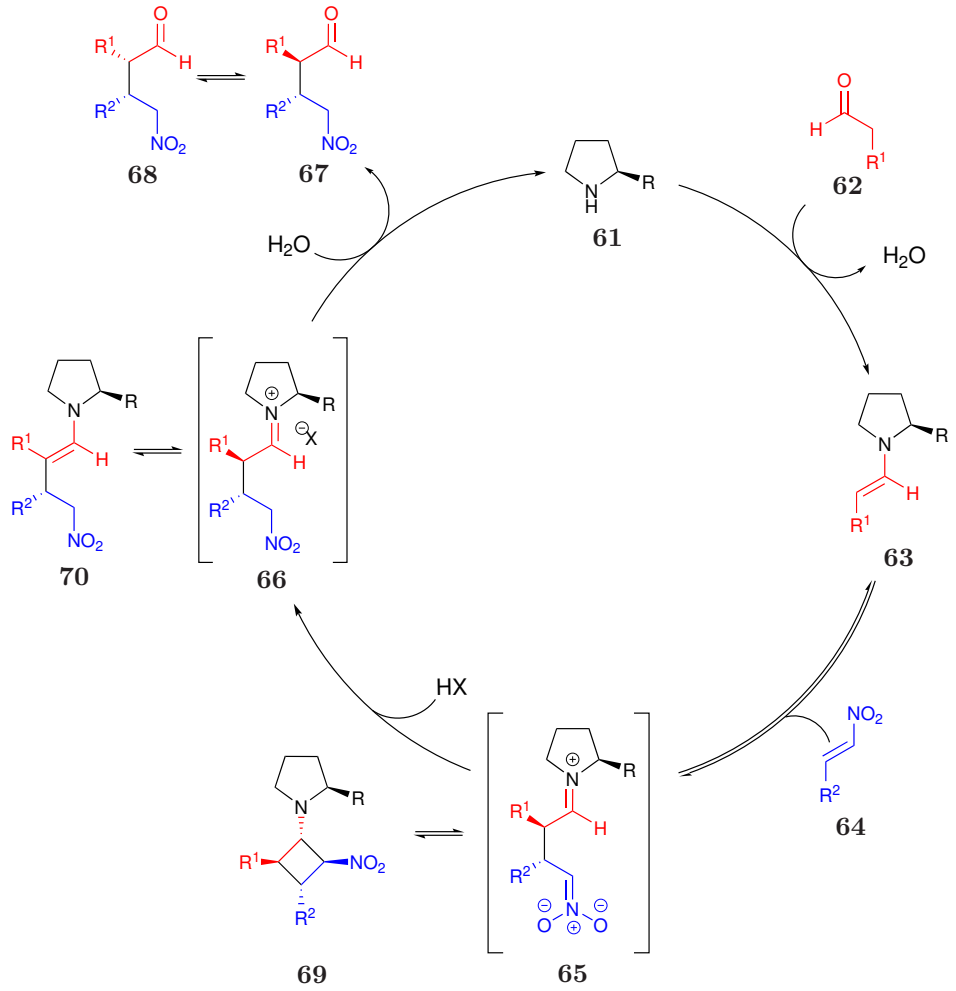

Scheme 1.14: Proposed catalytic cycle by Seebach and Hayashi in 2011.[34]

investigated the addition of different acid co-catalysts to understand why this additive is essential in order to perform more efficient reactions. They confirmed that acid additives (i) accelerate the generation of the enamine, (ii) promote the addition of the enamine to the nitro olefin, (iii) aid the conversion of the CB intermediate **69** with H_2O to Michael addition products, and (iv) affect diastereoselectivity and epimerisation at the α-carbonyl position to the final product. They postulated that the CB intermediate is a "parasitic" species that inhibits the product formation.[34] However, in a parallel work, Blackmond and co-workers found that the formation of these species maintain high stereoselectivity (Scheme 1.15).[27,28] They observed that the formation of the CB intermediate **74** is inversely proportional to the presence of the product enamine which would otherwise lead to a degradation of diastereoselectivity. They monitored reactions *in situ* to observe the effect of water in the reaction

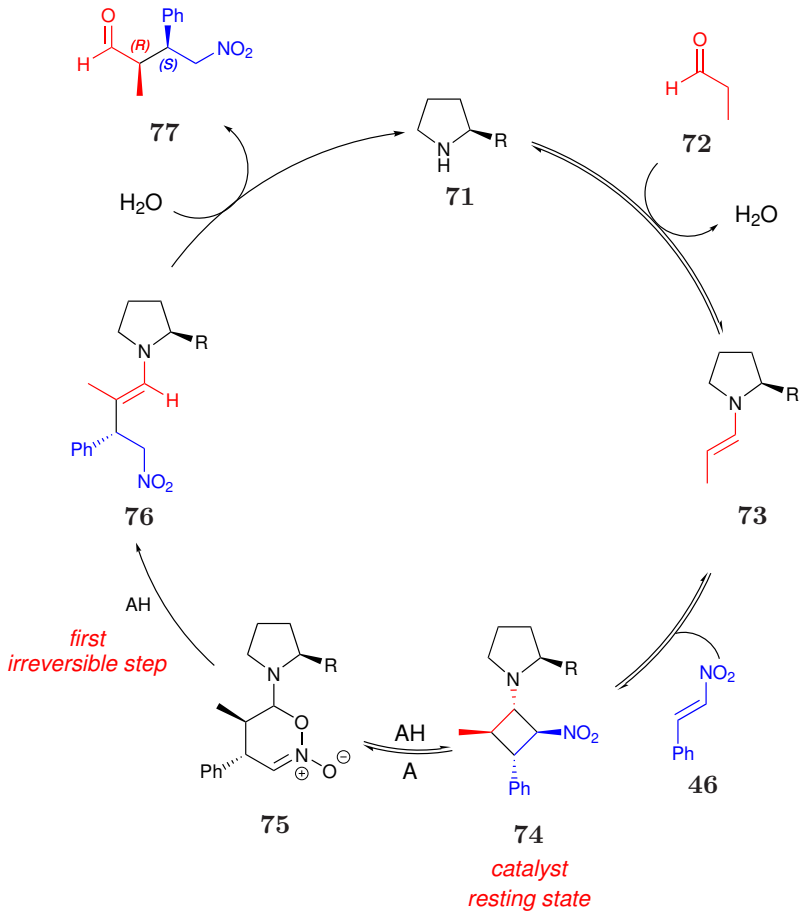

Scheme 1.15: Organocatalytic cycle of a nitro-Michael addition proposed by Blackmond and co-workers in 2012.[35,36]

and have found that there were not substantial changes with or without addition of water and, therefore, conclude is unlikely that the protonation step would be the rate determining step.

In 2012, Pihko and Pápai presented a model where they combined experimental and computational experiments. They suggested that the rate determining step is related to the protonation step of a dihydrooxazine oxide (OO) intermediate **75**, which was fully characterised *via* NMR spectroscopy.[37] They compared the reactivity of α-alkyl substituted and unsubstituted nitro olefins and rationalise the lower reactivity of substituted substrates over unsubstituted. As previous mechanistic studies proved that the rate determining step of this type of reaction was expected after the formation of the intermediate CB, they assumed that the low reactivity of α-alkyl substitued nitro olefins was not an intrinsic problem of the substrate. Instead, they thought it was rather related to the intermediate stability, considering

the slow protonation step in the presence of a substitutent in α-position to the nitro group. The addition of an acid co-catalyst favoured this protonation step allowing the release of the product in high yields, high enantioselectivity and high diastereoselectivity. With this study, Pihko, Papai and co-workers highlight the importance of intermediates stability to predict reactions reactivity.[37]

Pfalz, Wennemers and co-workers *via* an ESI-MS spectroscopic technique analysed the back-reaction of the nitro Michael addition to compare forward and backward reactions and thus identifying the rate determining step. They concluded that in the presence of non-acidic catalysts, such as the Hayashi-Jørgensen catalyst, the rate determining step cannot be the C-C bond formation. This finding would be in line with other mechanistic studies that propose the protonation step that follows the C-C bond formation as the turnover-limiting and stereoselectivity-determining step.[37–39]

However, in 2017 Pápai and co-workers presented a computational study where they observe that nitro-Michael reactions catalysed by Hayashi-Jørgensen catalyst do not meet Curtin-Hammett conditions as previously stated in literature (Figure 1.5).[35,36,39] The Curtin-Hammett principle states that two intermediates or reactants that are rapidly interconverting between each other will generate two irreversible different products. The product ratio is related to the energy of the two conformers and to the energy barrier from each of the isomers to the respective products. They found that the transition state of the protonation occurs at a lower energy compared to C-C bond formation transition states. This outcome would be in contrast with Curtin-Hammett stereoselectivity control since the fast interconversion between the two intermediates would be unfeasible. They explained that even if the rate determining step of this reaction is the protonation step, the stereoselectivity is determined by the C-C bond formation transition states (Figure 1.5(b)). Pápai and co-workers presented a computed free energy profile where the two enantioselective paths are analysed together. The proposed mechanistic discussion concluded that the methodology used by Wennemers and co-workers is valid for most reactions that are characterised by the same turnover-limiting and stereoselectivity-determining step, however in this case the two steps are not coinciding and therefore they suggest that the validity of this method is reduced.[38]

In summary, enamine organocatalysis has been widely studied, however questions related to the behaviour of these catalysts in different reactions are still unanswered.

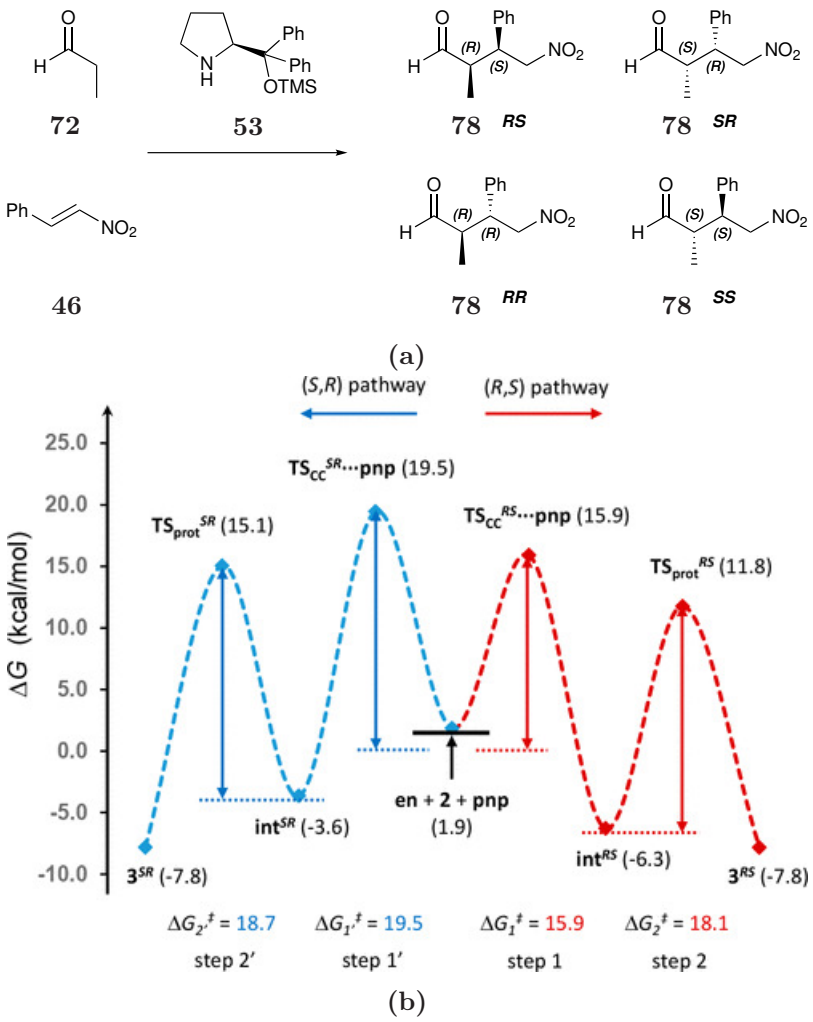

Figure 1.5: (a) Nitro-Michael reaction that was computationally and experimentally studied by Pápai and co-workers. (b) Computed free energy profile of nitro-michael addition catalysed by **53** and performed by Pápai and co-workers.[40]

1.1.1.2 Iminium catalysis

The second type of mechanism in Scheme 1.5 envisages the generation of an iminium ion, formed by the reaction of the catalyst with carbonyl compounds, which then reacts with nucleophiles. For instance, this type of catalysis is utilised to activate α,β-unsaturated compounds generating a new bond in β-position (Scheme 1.16).

In 2000, Macmillan and co-workers presented the first example of highly enan-

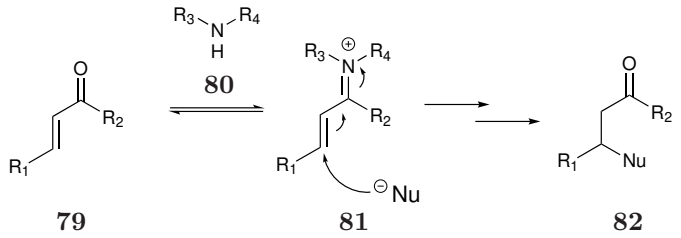

Scheme 1.16: Example of nucleophilic addition to α,β-unsaturated compounds.

tioselective Diels-Alder reaction *via* iminium ion catalysis.[41] The reaction of α,β-unsaturated aldehyde **86** with an enantiopure secondary amine as the catalyst led to the formation of an iminium ion able to react with diene **87** in order to obtain compounds **88** (Scheme 1.17). They tested several secondary amine catalyst but they found that using compound **85** as catalyst product **88** was achieved in 99% yield and only after 8 hours. The ratio between the *exo*- and the *endo*-product was respectively 1.3:1 and the (2*S*)-*exo*-aldehyde was obtained with a 93% *ee*.[41] In 2002, Macmillan and co-workers investigated the enantioselective 1,4-addition of aniline rings **89** to α,β-unsatured aldehydes **90**. They found that in only 20 minutes with 10 mol% of catalyst **91**, product **92** was obtained in 96% yield and with a 95% *ee*

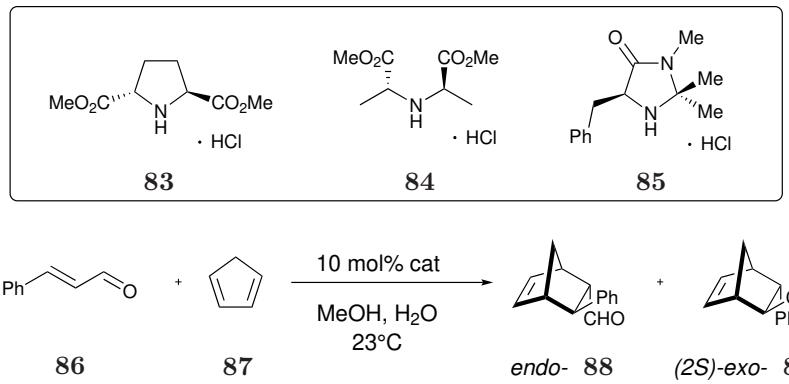

Scheme 1.17: First highly enantioselective amine catalytic Diels-Alder.

(Scheme 1.18).[42]

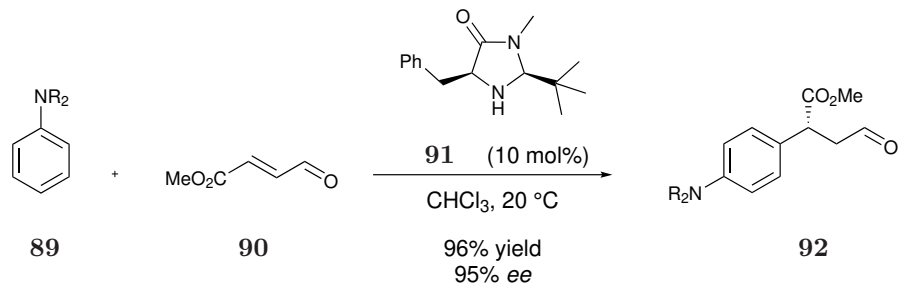

Scheme 1.18: Enantioselective 1,4-addition of aniline rings to α,β-unsaturated aldehydes.

1.1.2 Non-covalent organocatalysis

1.1.2.1 Brønsted base/brønsted acid bifunctional catalysis

In 1923, a Brønsted acid was defined as a proton donor according to the Brønsted-Lowry theory, whereas a Brønsted base was considered a proton acceptor.[43,44] In the same year, Lewis acids were described as substances able to accept a pair of non-bonding electrons and Lewis bases as electron-pair donor.[45] In 1884, Friedel and Crafts used for the first time aluminium chloride as a Lewis acid which was able to catalyse electrophilic aromatic substitutions.[46] Brønsted acids have been known as catalysts since 1942, when Wassermann and co-workers presented a Brønsted acid catalysed Diels-Alder (Scheme 1.19).[47] The ability of a strong acid to catalyse reactions was already known, however they proved difficult to use because of their lack of regioselectivity.[48] Chemists observing natural enzymatic systems began to study systems with weak interactions or H-bonding in order to design new catalysts.[49] The usage of H-bonding to direct molecules' assembly became more prevalent at the end of the 20^{th} century. In 1990, Etter and co-workers set the basis for the following studies on achiral thiourea based H-bond donor catalysts.[50,51] They stud-

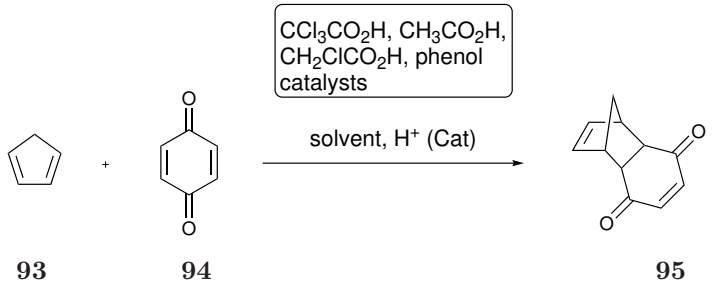

Scheme 1.19: First catalytic Diels-Alder reaction.

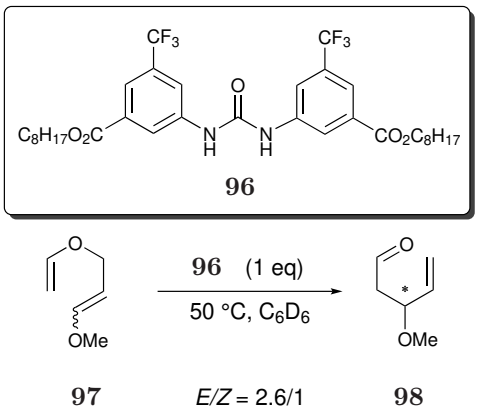

Scheme 1.20: Catalytic Claisen rearrangement.

ied the molecular recognition properties of diarenylureas co-crystallized with Lewis bases.[50,51] In 1994, Curran and Kuo proved that urea derivatives were efficacious organic catalysts.[52] In 1995, they studied a Claisen rearrangement (Scheme 1.20) showing an eminent acceleration of the reaction in the presence of this new catalyst.[53]

In 1998, Sigman and Jacobsen presented their results obtained experimentally using thioureas catalysts in an asymmetric Strecker reaction.[54] Four years later, Jacobsen together with Vachal, presented a structure-based mechanistic analysis which demonstrated the accountability of the thiourea dual H-bond interaction for the catalytic activity in the Strecker reaction (Scheme 1.21).[55]

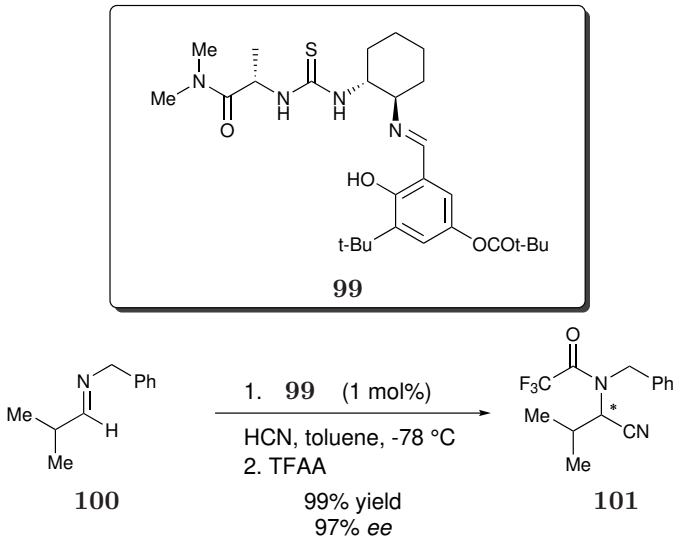

Scheme 1.21: Organocatalysed Strecker reaction.

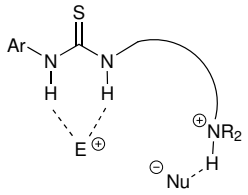

Figure 1.6: Bifunctional thiourea catalyst.

They found *via* isotope shift experiments that the imine substrate exclusively interacts with the urea hydrogens.[55] The thiourea enhances the electrophilicity of the substrate *via* hydrogen bonding activation and the tertiary amino group activates the nucleophile (Figure 1.6).[13,56]

The first enantioselective Aza-Henry reaction catalysed by a bifunctional organocatalyst was conducted by Takemoto and co-workers in 2003 (Scheme 1.22).[57]

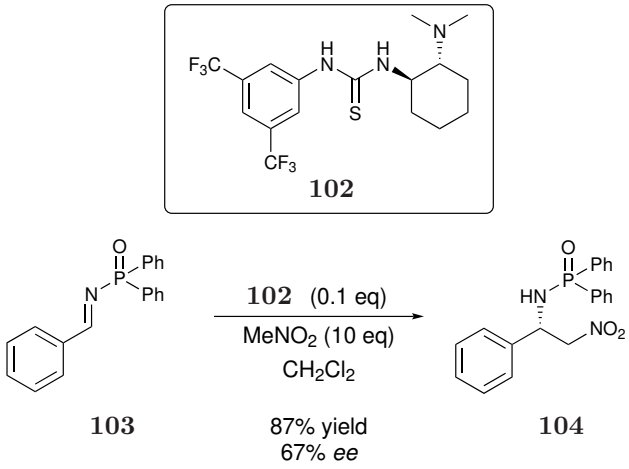

Scheme 1.22: First Aza-Henry reaction catalysed by bifunctional thiourea organocatalyst.

The bifunctionality of this catalyst enables this reaction because it deprotonates the nitro group to give the nitronate enhancing the electrophilicity of the substrate (Scheme 1.23).[57,58]

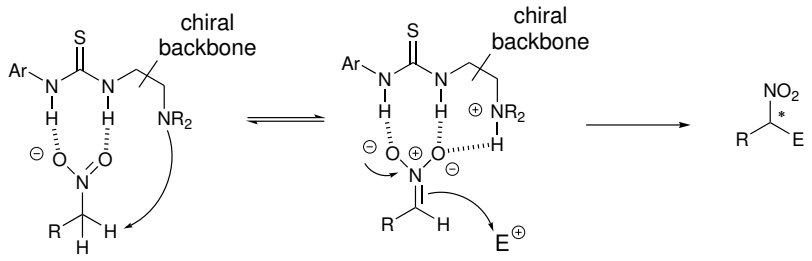

Scheme 1.23: Deprotonation of the nitroalkane to the corresponding nitronate.

1.1.2.2 Phase-transfer catalysts

An example of ion pairing catalysis is phase-transfer catalysis, which involves a system with two different phases, an aqueous and an organic layer, where the anion acts as base or nucleophile. The catalysis is due to the ability of cations to transfer anions in the organic phase in order to react with the substrate.[59,60] An interesting example was reported by Corey *et al.* in 1997. They present the mechanism and the geometrical factors responsible for the enantioselectivity of phase-transfer catalysts based on cinchona alkaloid molecules (Scheme 1.24).[61] They believed that the quaternary bridgehead nitrogen of the cinchona alkaloid **108**, which is the centre of a tetrahedron, should have steric hinderance to three of the faces, leaving the fourth one accessible enough to the counterion of the substrate. They found that the bulkier group R^1 is, the higher the enantioselectivity of these catalysts.[61,62] An example is the reaction described in Scheme 1.24 which reports good yields of **110**

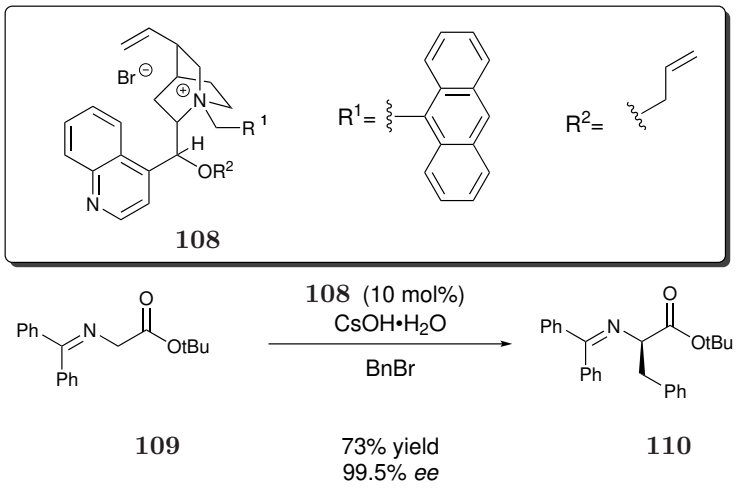

Scheme 1.24: Ion pairing catalysis through cinchona alkaloids.

and excellent *ee* (up to 99% *ee*) in the presence of catalyst **108**.

A multitude of reactions have been made possible with these catalysts (*e.g.* asymmetric aldol, Mannich, Michael and Diels-Alder reactions)[63] including the catalysis of reactions with nitro compounds. An example of asymmetric aza-Henry reaction under phase-transfer catalysis was reported in 2008 by Palomo *et al.* (Scheme 1.25).[64]

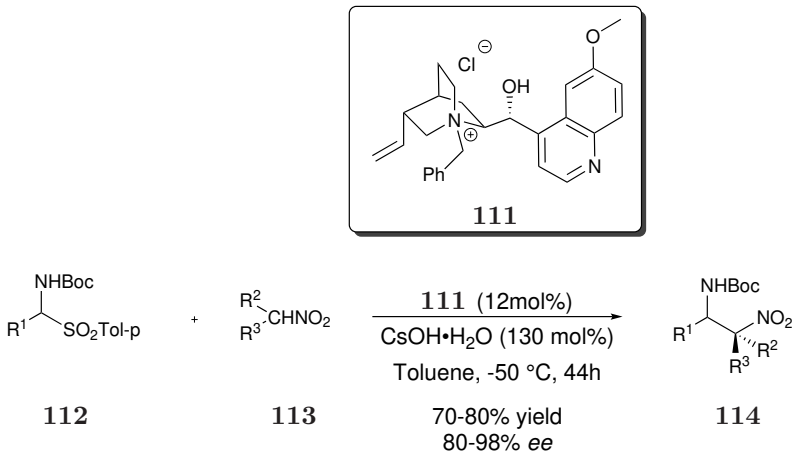

Scheme 1.25: Asymmetric aza-Henry reaction under phase-transfer catalysis.

They demonstrated through experimental and theoretical studies that the catalyst **111** forms hydrogen bonds with the nitro group of the substrate **114**. This interaction leads to a more rigid structure, which is one of the reasons of high enantioselectivity. They obtained **114** in good yield and with excellent enantiomeric excess of *syn* product (up to 99% *ee*).[11]

1.2 Intramolecular Nitro-Michael Additions

The combination of organocatalysis and nitro olefins opened the way to the generation of a multitude of enantioselective compounds containing nitrogen.[58] Several

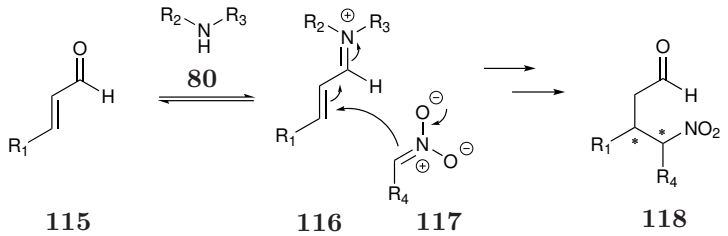

Scheme 1.26: Secondary amine catalysed addition of nitronates to α,β-unsatured aldehydes, achieving γ-amino acid precursors.

examples of nitro-Michael additions have already been described in this chapter because of the high utility of the respective products. The use of organocatalysis for nitro-Michael addition gives way to the synthesis of a variety of γ-amino acid precursors that can be easily achieved by oxidising the carboxylic group and reducing the nitro group to the amine (Scheme 1.26).[58]

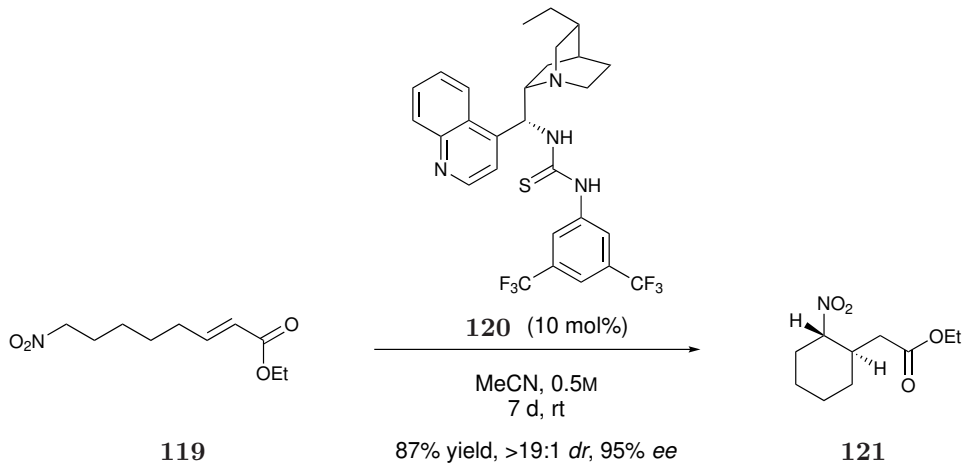

119 87% yield, >19:1 *dr*, 95% *ee* **121**

Scheme 1.27: Enantioselective Michael addition performed by Cobb and co-workers for the synthesis of a γ-amino acid precursor.

Intermolecular Michael additions have been widely studied and reported in literature.[29,32,34] Intramolecular nitro-Michael additions assisted by organocatalysts are reported in the literature but to a lesser extent. An example of enantioselective Michael additions of nitronates onto conjugated esters is described in Scheme 1.27. Cobb and co-workers obtained compound **121** in 87% yield, with excellent *dr* (>19:1) and 95% *ee*.[65] In 2013, an intramolecular Michael addition was reported for the final synthesis of atropurpuran A-ring **124** (Scheme 1.28). After reaction optimisation they obtained moderate *dr* (24:24:11:41) and moderate *ee* of the four diastereomers (28,67, 70, 36 %).

In summary, organocatalysis is a valid method to obtain enantioselective molecules *via* a more environmentally friendly procedure compared to metals. Nitro-Michael addition assisted by organocatalysts can lead to γ-amino acid precursors. However, only a few examples of intramolecular nitro-Michael additions assisted by organocatalysis have been reported in the literature to date. Cyclic γ-amino acids can be used as building blocks for the synthesis of constrained oligomers and this field is still under investigation.

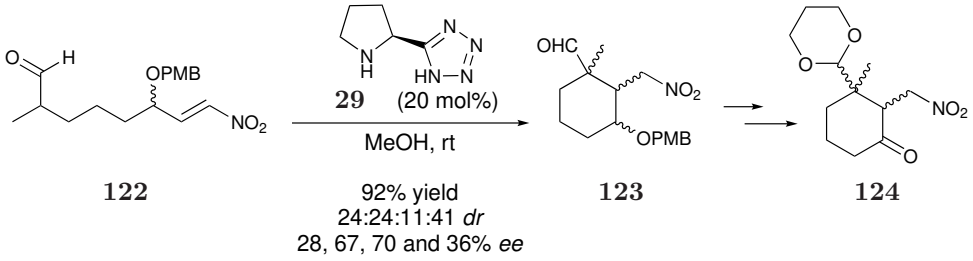

Scheme 1.28: Intramolecular Michael addition performed by Chen and co-workers.[66]

1.3 Peptidomimetic Foldamers

1.3.1 Peptides and peptidomimetics

Peptides are essential to the human body as they control many vital functions. They are responsible for cell-cell communication and they regulate the interaction of ligands with receptors.[67] Peptides and proteins are sequences of amino acids and they are characterised by primary, secondary, tertiary and quaternary structures.[68]

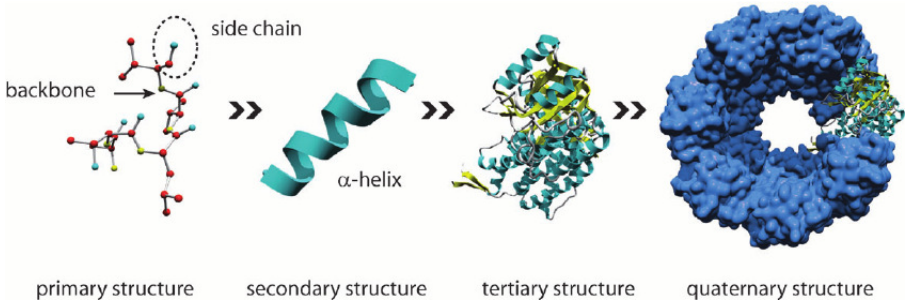

Figure 1.7: The hierarchical structure of proteins.[69]

A primary structure can be defined as a sequence of amino acids linked together through peptide bonds. These types of bonds have a planar structure caused by resonance of the nitrogen lone pair through the carbonyl (n $\rightarrow \pi^*$). The formed double bond prevents rotation of the peptide bond itself, letting free rotation only of fragments connected to the double-ended peptide.

Peptides have two different conformations: a *trans* conformation, which is the most favoured, and a *cis* conformation, which presents a sterically hindered section between the residues (Figure 1.8).

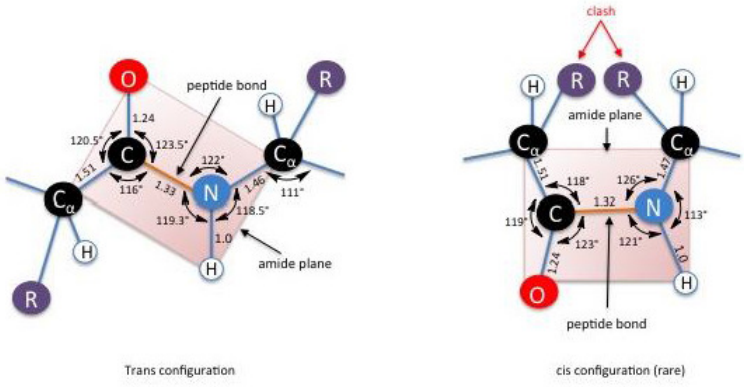

Figure 1.8: *Trans* and *cis* peptide configurations.[70]

The latter conformation is usually seen with proline, forming conformations such as β-turns (Figure 1.9).[68]

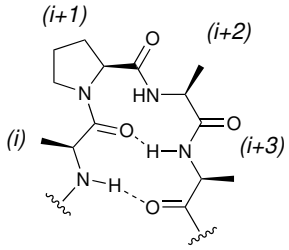

Figure 1.9: Natural Pro-Gly-β-turn as an example of *cis* conformation of a peptide bond.

The folding of the amino acids sequence can be described as secondary structure, which is mainly due to hydrogen bonds between non-adjacent atoms in the main chain. The three major secondary structures are α-helices, β-sheets and β-turns. α-Helices are formed through hydrogen bond interactions between moieties from the same sequence. Side chains are positioned outside the helix in order to reduce steric hinderance. β-Sheet rearrangements are defined as adjacent strands that are joined together through hydrogen bonds, the side chains are arranged at right angles to the sheet to minimise steric issues. The tertiary structure is caused by globular folding of proteins due to polar peptidic interactions with water and apolar side chains' tendency to aggregate minimising contact with polar compounds. Finally, the arrangement of multiple folded proteins is called quaternary structure.[68]

In the last few decades, scientific interest in peptide-based drugs has increased considerably and several therapies have been developed.[71] Peptides exhibit some

problems related to their poor oral bioavailability due to metabolic degradation, their difficulty crossing the blood-brain-barrier and undesired effects caused by the interaction of conformationally flexible peptides with receptors.[67] The introduction of peptidomimetics in drug discovery presented beneficial results in view of the fact that peptidomimetics were able to overcome most of the peptide-based drugs' issues, thus becoming a very interesting tool for drug discovery.[72] A peptidomimetic can be considered as a molecule that can mimic or inhibit a specific biological function of a peptide. They also present some additional advantages compared to peptides: their specific conformational restrictions can minimise undesired interaction with non-targeted receptors, and the presence of extra hydrophobic groups and isosters that substitute the peptide bond enables a better transfer of the peptidomimetic through the cell. All these features lead peptidomimetics to develop resistance to proteases, revealing higher activity than peptides.[67,72]

1.3.2 Peptidomimetic foldamers

In the 1990's, the synthesis of unnatural oligomers that can mimic proteins secondary structure was explored, but it was not until 1998 that a clear definition of foldamers was provided by Gellman. A foldamer was defined as any oligomer that can fold into a well-defined conformation in solution.[73] Foldamers usually have a high molecular weight and, when in solution, they prefer a globular structure due to noncovalent interactions between nonadjacent monomer moieties.[74] They can be categorised in two different classes: bio-inspired foldamers and abiotic foldamers. Bio-inspired foldamers refer to those oligomers that resemble bio-macromolecules such as proteins and nucleic acids, whereas abiotic foldamers describe all the remaining foldamers that do not.[75]

The present study focuses on peptidomimetic foldamers which can mimic peptide substrates of enzymes or peptide ligands of protein receptors which regulate several biological functions. β-peptides were the first foldamers to be extensively studied and it was found that this type of foldamer presented antimicrobial properties.[76] Their amphiphilicity allowed these compounds to penetrate bacterial membranes and disrupt them without leading to bacterial resistance, an effect readily seen with other antibiotics.[76] Following this discovery, the use of foldamers has increased, and they have been adapted for various applications including: (i) molec-

ular recognition opening a new route for receptor design,[77–79] (ii) sensors ("foldamers switching"),[80–84] (iii) enzyme-like catalysts[85,86] and (iv) they could open up the way to the development of new materials, due to their interesting properties.[87,88]

1.3.2.1 Foldamers based on γ-residues

In the last 20 years, the interest towards the study of foldamers based on unnatural amino acids increased as well as the use of γ-amino acids as residues in foldamer synthesis. Hanessian's[89,90] and Seebach's[91,92] groups were the first ones to present γ-peptides with one, two or three substituents that are prone to form specific helical conformations. In 1998, Seebach and co-workers presented a pivotal study, where they synthesised γ-hexamers derived from the homologation of L-Val, L-Ala and L-Leu (Figure 1.10).

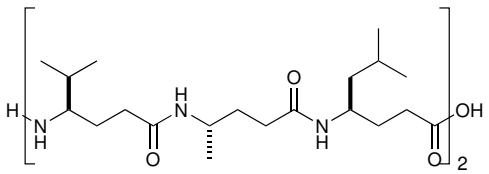

125

Figure 1.10: Oligomer synthesised by Seebach and co-workers which folds into a right handed helix.[92]

They discovered that the stability of the helical conformation increased upon homologation of the residues. Indeed, the synthesised γ-hexapeptide **125**, compared to the α and β peptides, formed 14-membered H-bonding rings between the carbonyl of residue i and the amide proton of residue $i+3$ leading to the formation of a right handed helix (Figure 1.10).[92]

At the same time, Hanessian and co-workers were working on the synthesis of γ-peptides derived by homologation of L-Ala and L-Val and they observed that despite the short length of the peptide, it was already displaying a helical structure. They also reported that α-substitution of γ-residues can stabilise the helical structure even further on the condition that the orientation of the α-group is not disrupting the secondary structure of the main peptide backbone (Figure 1.11).[90]

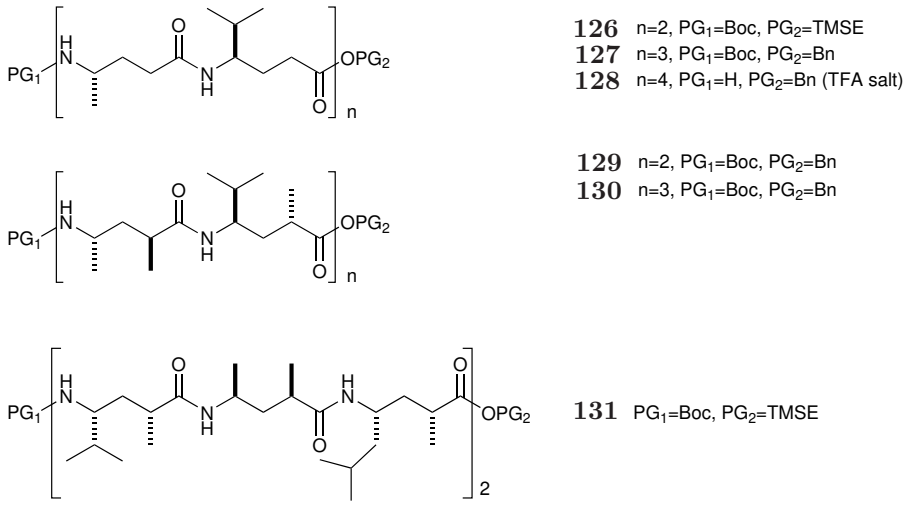

Figure 1.11: Oligomers synthesised by Hanessian and co-workers.[90]

In 2003, *ab initio* MO theory was performed to identify the most stable secondary structures for homogenous oligomers based on γ-amino acids. Hofmann and co-workers found that periodic structures with 14- and 9-membered ring pseudocycles were the most stable and these results were in agreement with the experimental data, which was then available.[89,90,93]

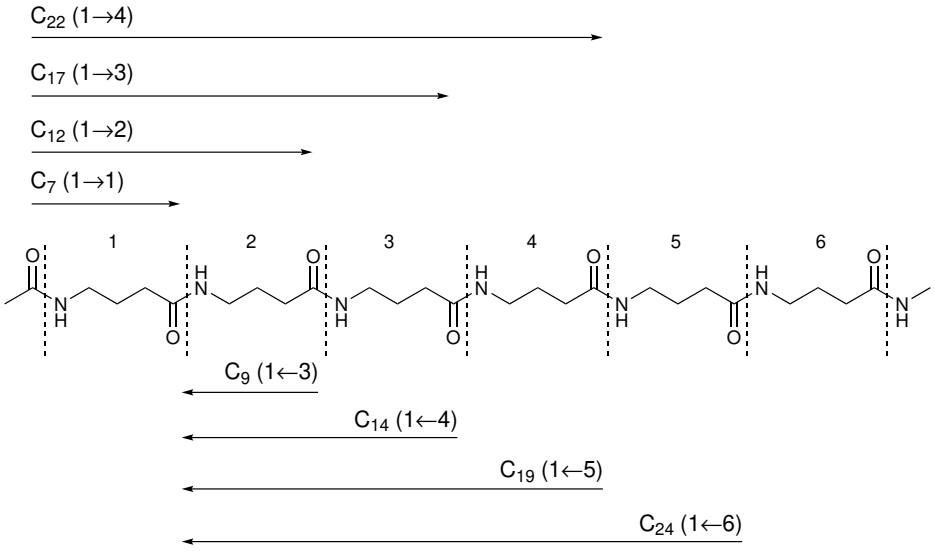

Figure 1.12: Possible hydrogen bonding patterns for helices of γ-peptides studied by Hofmann and co-workers.[93]

1.3.2.2 Foldamers based on vinylogous amino acids

Vinylogous amino acids are rigid systems that could be useful for the synthesis of foldamers. The first synthesis of vinylogous peptides in order to study the secondary

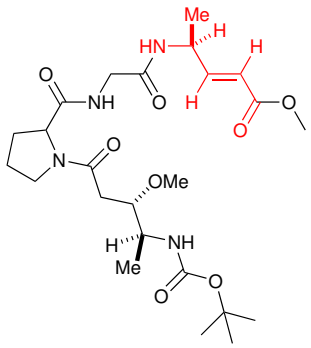

132

Figure 1.13: Oligomer synthesised by Hagihara and co-workers that presents features typical of a secondary structure.[94]

structure was presented by Hagihara and co-workers in 1992.[94] They observed that vinylogous peptide **132** exhibits important characteristics of well defined secondary structures (Figure 1.13). Another example of vinylogous peptides was reported in 1997 by Coutrot and co-workers (Figure 1.14).[95] They found that *trans* CH=CMe groups lead to an open conformer, whereas *cis* CH=CMe groups induced the formation of an intramolecualar 9-membered pseudocycle.[95]

Several further theoretical studies were carried out by Hofmann and co-workers. In 2003 they performed *ab initio* MO theory on vinylogous γ-amino acids comparing them to saturated γ-peptides (Figure 1.15 and Figure 1.16).[93] They found that the introduction of a *E* double bond into the backbone aids the generation of larger

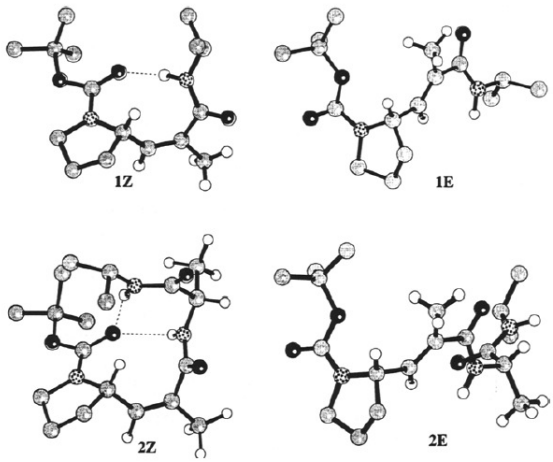

Figure 1.14: Crystal molecular structures of *E* and *Z* oligomers synthesised by Coutrot and co-workers obtaining intramolecular 9-membered ring pseudocycles for *Z*-oligomers.[95]

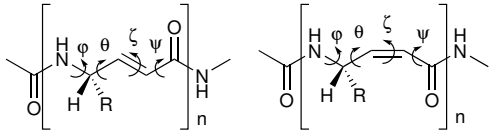

133 **134**

Figure 1.15: *E* and *Z* vinylogous oligomers (n = 1, 6) studied by Hofmann and co-workers.[96]

H-bonded pseudocycles, such as 19- and 22-membered ring pseudocycles compared to *Z* vinylogous γ-peptides which are more stable with 7- and 9-membered ring pseudocycles (Figure 1.15).[96]

Indeed, in 2013 Maillard and co-workers synthesized oligomers based on 5-membered ring constrained γ-amino acids substituted in the γ-position.[97] This new family of ring constrained γ-amino acids exhibited a right-handed 9-helix structure (so named because of the H-bonds occur in 9-atom pseudocycles, Figure 1.17). These γ-peptides proved to be stable in organic and in aqueous media, which is a valuable characteristic for medicinal chemistry applications. Oligomers **136** and **137** were found to form a tight 9-helix secondary structure in organic solvents. Oligomers **139**, **140** and **141** were synthesised in order to obtain soluble structures in aqueous

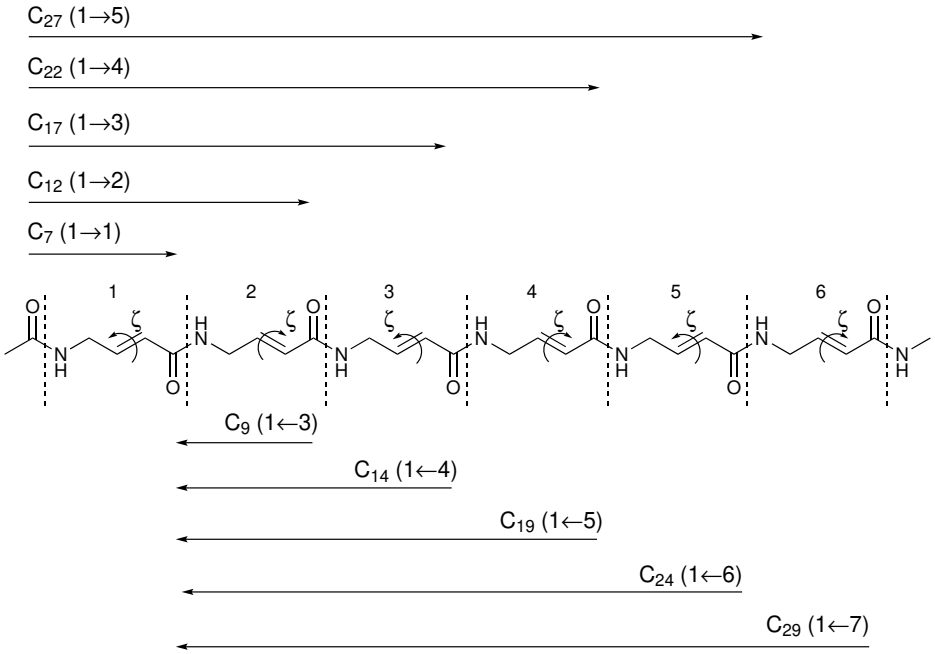

Figure 1.16: Possible hydrogen bonding patterns for helices of *E*-**133** (ζ = 180°) and *Z*-**134** (ζ = 0°) vinylogous γ-peptides with the hydrogen bonds formed in forward and backward direction along the sequence.[96]

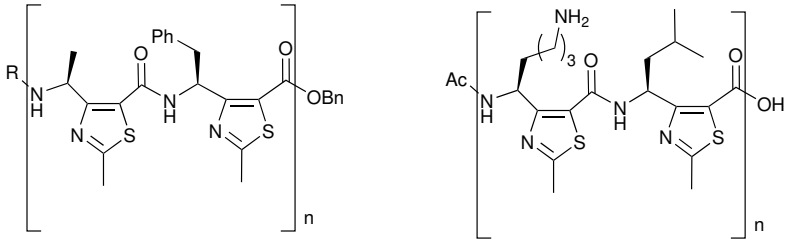

135 *n*=1, R=Fmoc
136 *n*=2, R=Fmoc
137 *n*=3, R=Fmoc
138 *n*=2, R=Boc

139 *n*=1
140 *n*=2
141 *n*=3

Figure 1.17: γ-peptides synthesised by Malliard and co-workers that have been found to form a 9-helix secondary structure.[97]

solvents and they presented similar NOEs signals confirming that the secondary structure is maintained even in aqueous media.[97]

1.3.2.3 α/γ-peptides

Foldamers can control functions that would not be possible in nature.[74] The synthesis of this type of unnatural peptides can be designed according to the type of secondary structure required. γ-Amino acids were chosen as building blocks for the synthesis of foldamers because lengthening the amino acid backbone chain, the number of H-bonds that can form within a few residues increases. Oligomers based on a single monomeric unit have homogeneous backbones and all the examples cited to date belong to this category. Oligomers with heterogeneous backbones are based on different monomeric units which alternate (Figure 1.18).

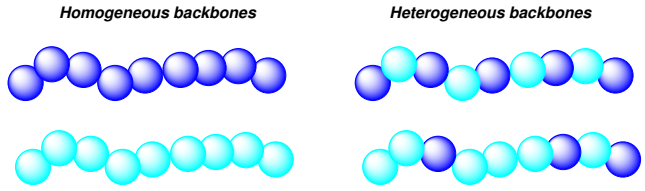

Figure 1.18: Simplistic example of homogeneous and heterogeneous backbones.[98]

This second class of foldamers has proven to be necessary in order to widen the foldamer repertoire and facilitate their design. In 2005, Anada and co-workers, synthesised hybrid peptide sequences containing α-, β- and γ-residues. α/γ-peptides were found to have a 12-helix conformation (Figure 1.19).[99]

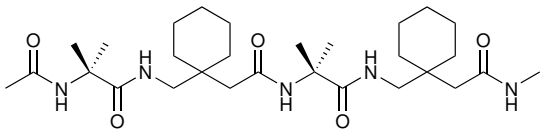

142

Figure 1.19: (a) Oligomer synthesised by Anada and co-workers.[99]

In 2006, Hofmann and co-workers reported that α/γ-peptides present stable secondary structures and if the hydrogen bonding alternates in forward and backward direction along the sequence the conformation is even further stabilised. The most stable helices for α/γ-peptides were found to be H_{12}, $H_{12/10}$ and $H_{18/20}$ (Figure 1.20).[100]

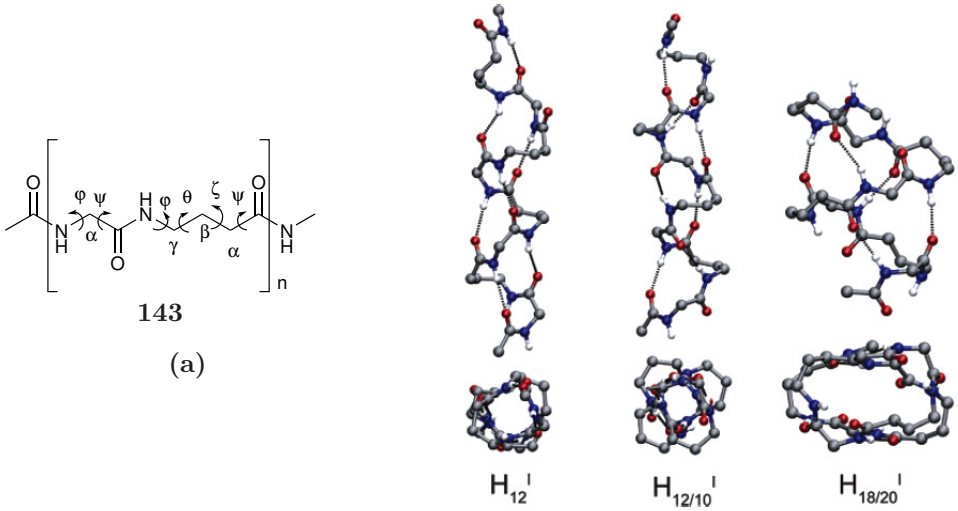

143

(a)

Figure 1.20: (a) α/γ-peptides studied by Baldauf and co-workers. (b) Most stable helices of α/γ-octamers predicted with *ab initio* MO theory by Hofmann *et al.*[100]

Sharma, Kunwar[101] and co-workers presented the first study of α/γ-peptides based on acyclic γ-residues and they reported that these unnatural peptides present a $H_{12/10}$-helix conformation. 12/10-helical structures are characterised by alternation of 12- and 10-membered rings H-bonds with different directionality of the pseudocycles (relative positions of interacting amino acids $\gamma_1 \rightarrow \alpha_2/\gamma_1 \leftarrow \alpha_4$). They report the first example that confirmed the Hofmann group's predictions[100] of the secondary structure in α/γ-peptides was correct (Figure 1.21).

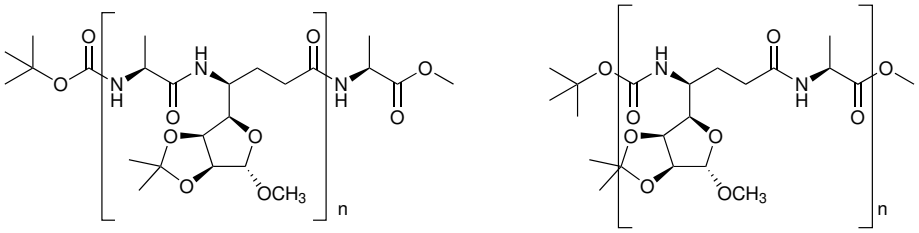

144 n = 1, 3 **145** n = 2, 3

Figure 1.21: Oligomers synthesised by Sharma, Kunwar and co-workers that fold into 12/10-helices.[101]

In 2016, Ganesh Kumar and co-workers reported an example of α/γ-hybrid peptide foldamer containing *cis* C-C double bond in the backbone (Figure 1.22).[102]

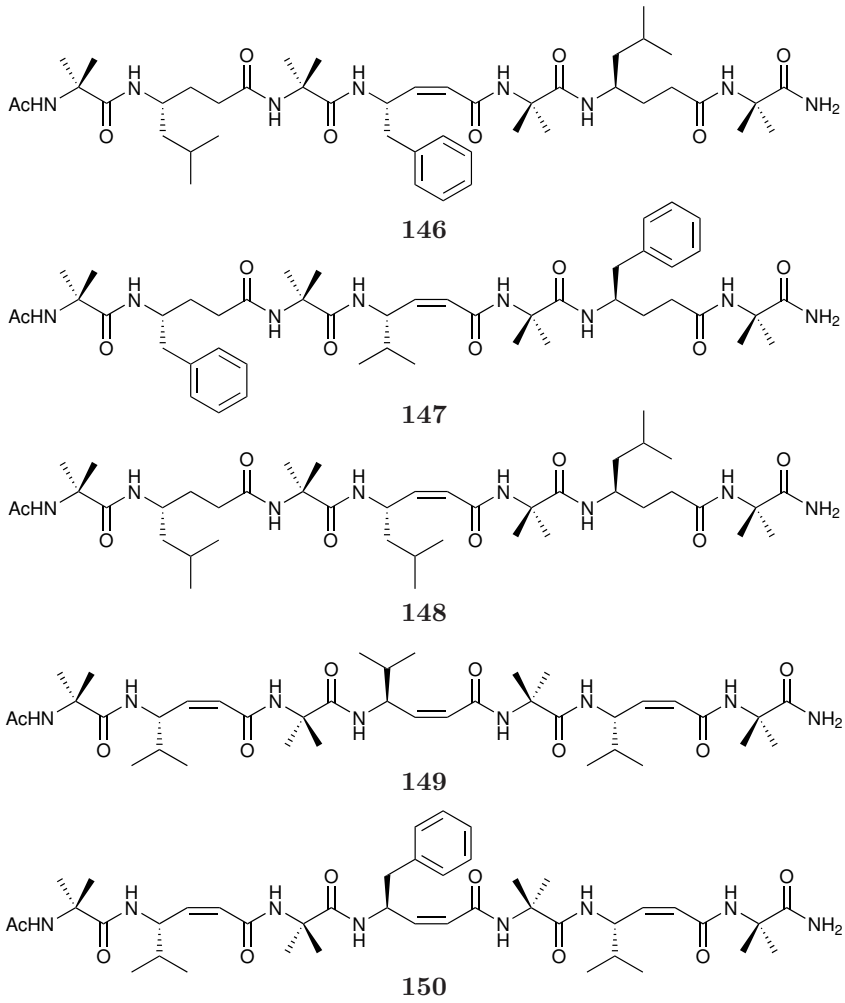

146

147

148

149

150

Figure 1.22: Oligomers synthesised by Ganesh Kumar and co-workers that fold into 12-helices.

Single-crystal and solution conformation showed a 12-helix secondary structure conformation for the designed peptides which contained a *Z*-vinylogous residue (Figure 1.23).

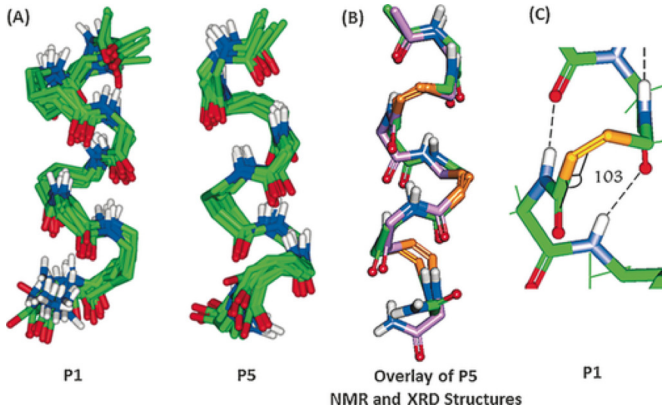

Figure 1.23: A) Solution conformations of the α/γ-hybrid peptides **146** and **150**, from left to right. B) An overlay of the X-ray and NMR structures of **150**. C) The X-ray structure of peptide **146**, illustrating the non-planarity of the C=C and C=O bonds (Cβ-Cα-C-O=103°) in the *Z*-vinylogous residues.[102]

They found that the calculated dihedral angles of the α/γ-peptides containing *Z*-C-C double bond do not match to the theoretical and experimental dihedral angles of saturated α/γ-peptides proposed by Hofmann and co-workers (Table 1.1).[100]

Table 1.1: Comparison of the backbone dihedral angles of the *Z*-vinylogous γ-amino acids synthesised by Ganesh Kumar and co-workers[102] with the theoretical model presented by Hofmann and co-workers for α/γ-hybrid peptides.[100]

α/γ-hybrid 12-Helix	ϕ	θ	ζ	ψ
Theoretical model	$-122 \pm 2°$	$52 \pm 2°$	$62 \pm 2°$	$-125 \pm 4°$
Z-γ-residues	$-119 \pm 4°$	$100 \pm 5°$	$0 \pm 3°$	$-78 \pm 4°$

α/γ-Vinylogous-peptides are therefore considered a new class of peptides and to date the study reported by Ganesh Kumar and co-workers is the only example of heterogeneous peptides containing cyclic vinylogous *cis*-γ-residues that can be found in literature.

1.4 Aims of the Study

Foldamers can fold into specific conformations and they could control several biological functions. The general aim of this work was the identification of new unnatural peptides with specific secondary structures.

The first goal of this thesis was to synthesise novel cyclic γ-amino acid precursors as valuable building blocks for pharmaceutical purposes and for the synthesis of unnatural peptides (Figure 1.24).

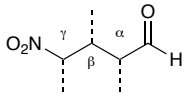

Figure 1.24: Generic γ-amino acid precursor.

The aim was to achieve these pharmaceutical tools enantioselectively *via* organocatalysis. Then, investigation of the mechanism of studied organocatalytic reactions was the consequent goal for further reaction optimisation (Scheme 1.29).

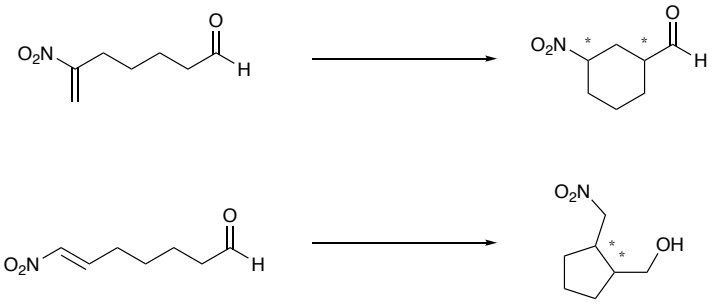

Scheme 1.29: Planned intramolecular nitro-Micheal addition reactions.

The last goal was to synthesise and characterise foldamers based on constrained enantioselective γ-amino acid residues in order to develop new materials (Figure 1.25).

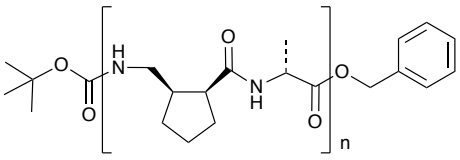

Figure 1.25: Designed foldamer for this thesis.

Chapter 2

Unprecedented Rearrangement during an Intramolecular Michael Organocatalytic Addition for the Synthesis of γ-Amino Acid Precursors

2.1 Background

Cyclic γ-amino acids have many advantages over acyclic γ-amino acids, they both mimic the neurotransmitter γ-aminobutyric acid (GABA), however cyclic γ-amino acids are characterised by a rigid backbone that can be easily functionalised by a variety of groups. For these reasons they are of interest for use in pharmaceuticals and for the synthesis of unnatural peptides as described later. Owing to their intriguing structure, cyclic γ-amino acids have been of interest to our research group for some years. Of particular recent interest has been the synthesis of the γ-amino acid precursor 3-nitrocyclohexane-1-carbaldehyde **151**, which would allow access to the respective γ-amino acid **152** (Scheme 2.1).

Syntheses of 3-aminocyclohexanecarboxylic acids **152** have been reported since 1938, where Greenstein and Wyman described the synthesis of *cis*-**152** (Scheme 2.2)

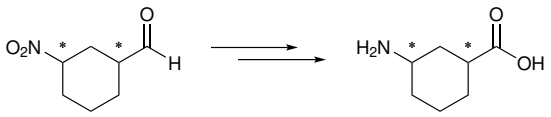

151 **152**

Scheme 2.1: γ-Amino acid precursor **151** and γ-amino acid **152**.

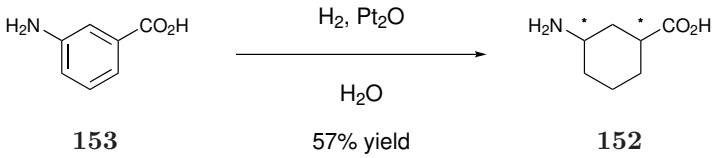

153 57% yield **152**

Scheme 2.2: Catalytic hydrogenation to obtain **152** performed by Greenstein and co-workers.

via hydrogenation of the alkenes **153** using platinum oxide catalyst.[103] However, it was not until 1977 that Johnston and co-workers repeated the synthesis of γ-amino acids with full stereochemical characterisation.[104]

In 1981, Allan and co-workers presented an alternative synthetic pathway to access both *cis*-optical isomers.[105] An allylic bromination of **154** was undertaken to generate **155**. Reaction of this crude product with potassium phtalimide in *N*-methylpyrrolidinone yielded **156** as a mixture of isomers, which was then followed by acid hydrolysis to achieve **157**. L or D-othreinine was used to form crystalline salts, of which **157** gave the resolved phtalimido acids **159** and **161**. The targeted enantiomers of **152** were then obtained *via* a catalytic reduction followed by deprotection of the amine (Scheme 2.3).[105]

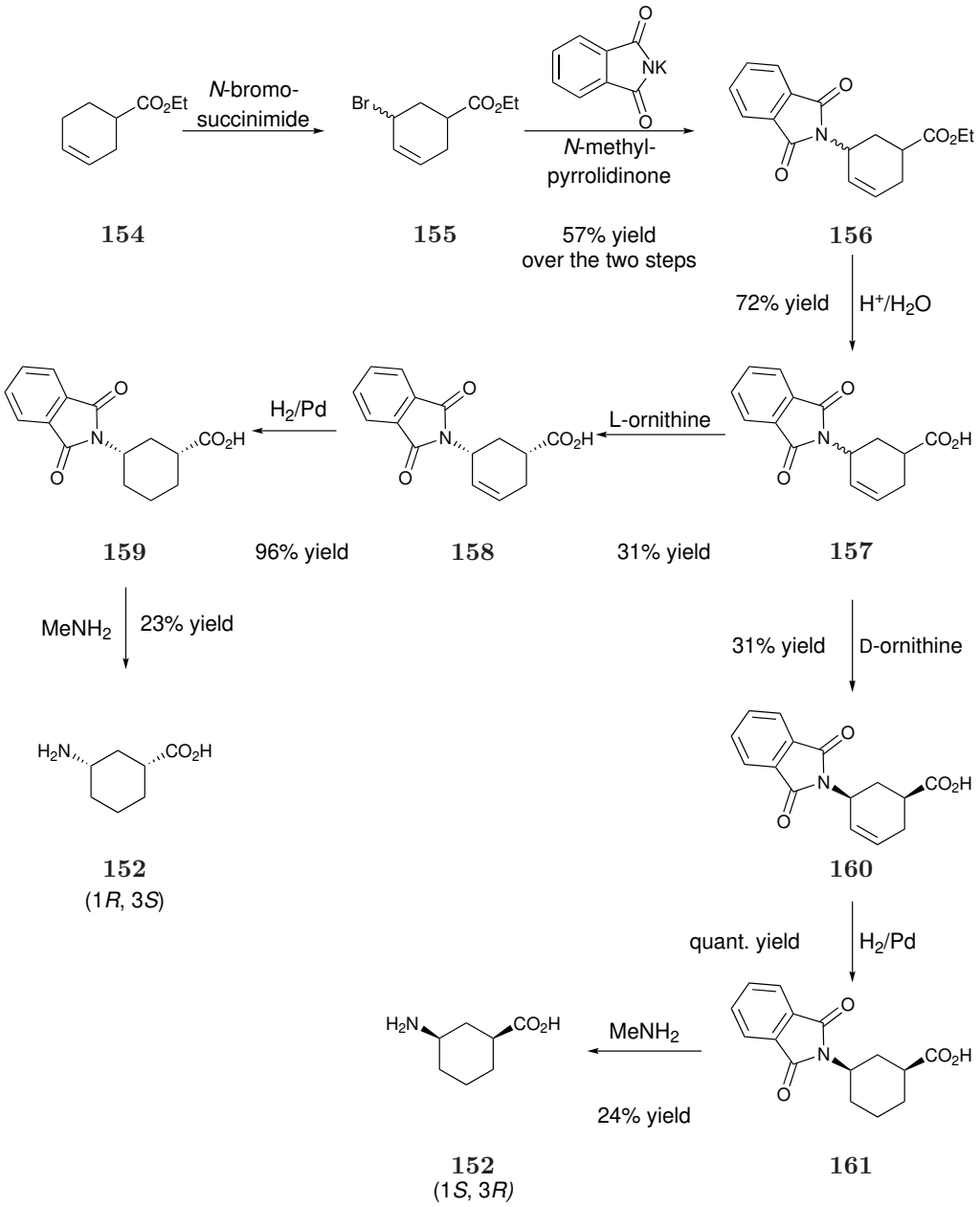

Scheme 2.3: Synthetic procedure of **152** developed by Allan and co-workers.

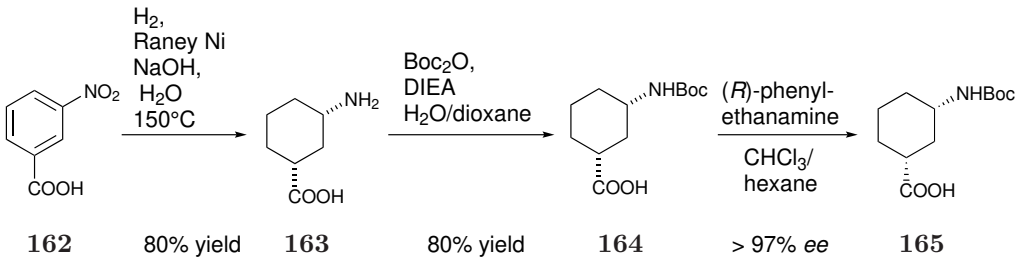

Scheme 2.4: Synthetic procedure presented by Granja and co-workers for the enantioselective synthesis of **165**.

More recently, in 2003, Granja and co-workers presented the synthesis of **165** in three steps.[106,107] First, simultaneous reduction of the aromatic ring and the nitro group was performed under H_2 atmosphere with Raney Nickel under pressure at 150 °C. The reaction yielded a selectively specific diastereomer *cis*, in racemic form. The amine was then protected with di-*tert*-butyl dicarbonate in the presence of *N,N*-diisopropylethylamine and was recrystallised several times with (*R*)-phenylethanamine in order to obtain the protected product **165** in high enantioselectivity (>97% *ee*, Scheme 2.4).[106]

In 2006, Hu and co-workers presented an alternative synthesis of *cis*-**152** and significantly, access to the enantiomerically pure *trans*-**152** (Scheme 2.5).[108] Finally, in the last decade, Newman and co-workers and Karlsson presented an optimised enantioselective synthesis of **152** *via* salt re-crystallisation and enzymatic resolu-

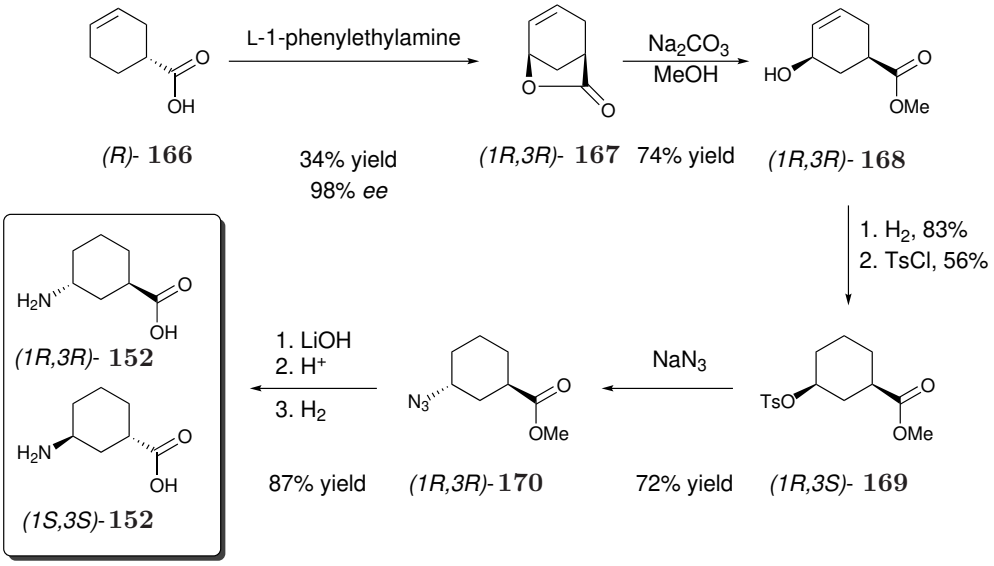

Scheme 2.5: Enantiomeric synthesis of *trans*-**152** developed by Hu and co-workers.

tion using mild and selective conditions which are both important aspects when considering scale-up preparation.[109,110]

To date, the synthesis of the nitroaldehyde γ-amino acid precursor **151** has not been reported in the literature, and thus the development of an organocatalytic route to afford the γ-amino acid was appealing. Therefore, the initial purpose of this study was to define an enantio- and diastereoselective synthesis of **151** using secondary amine catalysts based on work that was started by a previous member of the group.[111] Surprisingly, however, the constitutionally isomeric 5-membered ring was obtained (compound **173**) instead of the expected 6-membered ring **151** (Scheme 2.6).

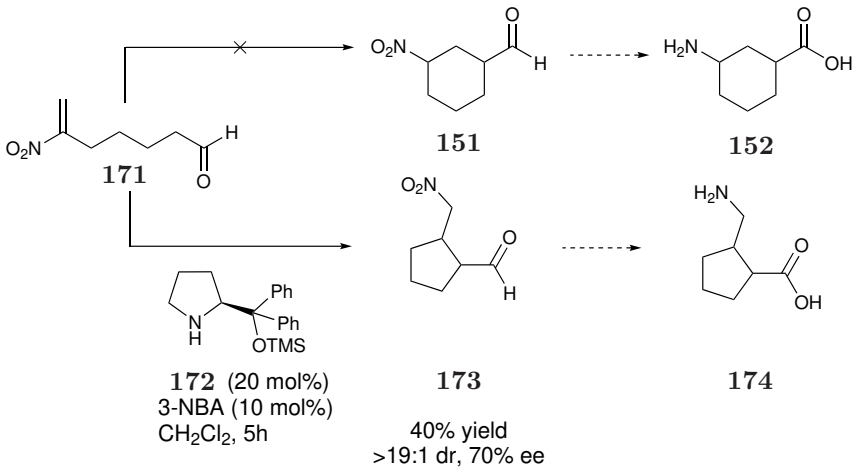

Scheme 2.6: Aim of the study and observation of the unexpected 5-membered ring as side product in previous work by the group

A possible reaction mechanism was initially proposed by the group, and is described in Scheme 2.7.[111] According to this hypothesised mechanism, aldehyde **171** condenses with the catalyst to form enamine **176** *via* the iminium ion. Next, the initially targeted 6-membered ring **177** is generated. A further tautomerisation of the iminium ion to the enamine leads to the synthesis of bicyclic compound **181** through the displacement of the nitro group (Favorskii-like rearrangement). Then, a plausible scenario is that the nitro group nucleophilically attacks the least hindered position of **181**, through the nitrogen lone pair to give intermediate **183** (Path A, Scheme 2.7). A possible alternative route could be that the oxygen atom of the ambident nitrite could react with the iminium ion to form intermediate **182**, which then rearranges with a [2,3]-sigmatropic shift, due to the double bond nature of

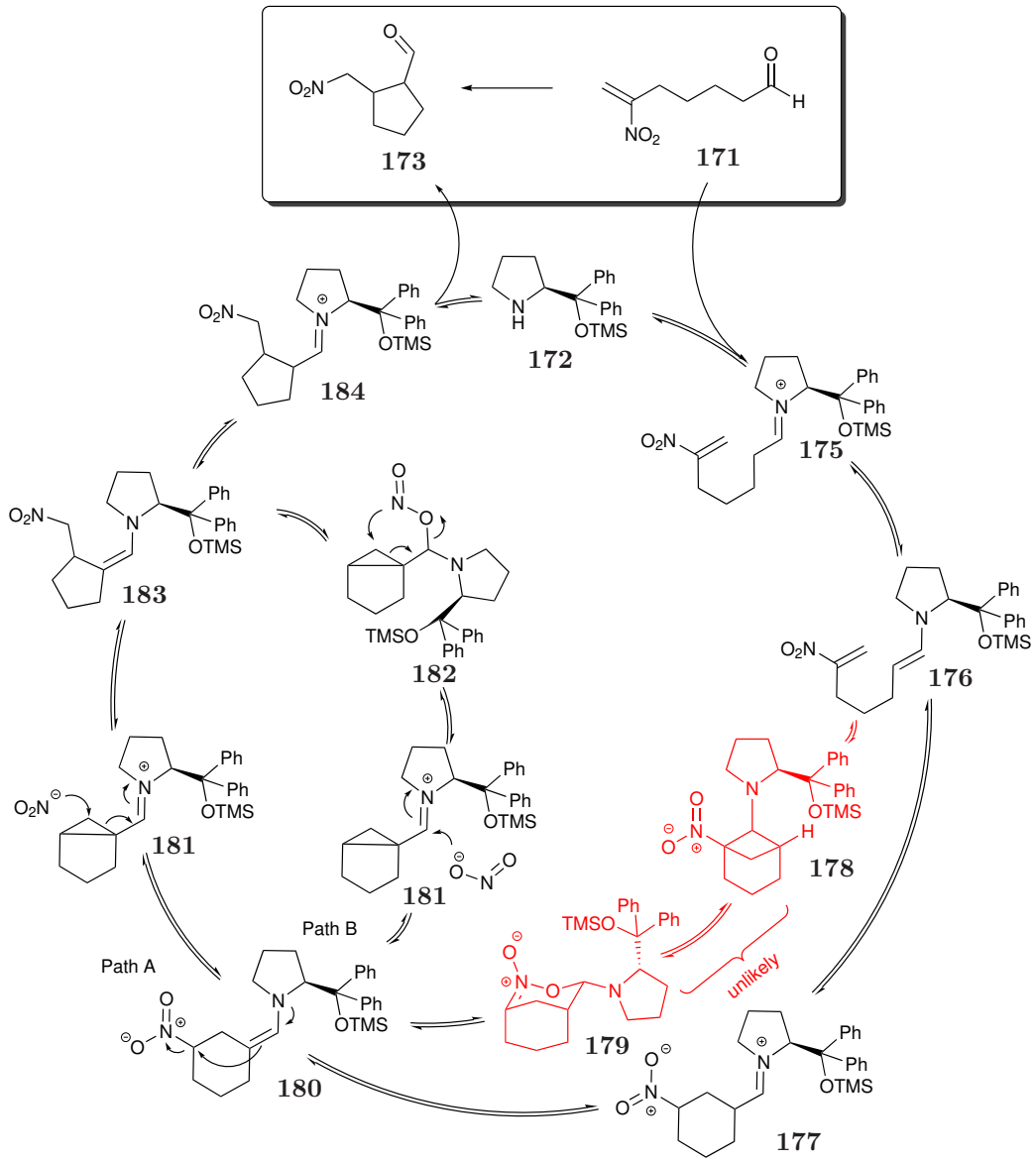

Scheme 2.7: Proposed organocatalytic cycle for the synthesis of **173** from terminal nitro olefin **171**.

cyclopropanes, to produce compound **183** (Path B, Scheme 2.7). Intermediate **183** can then tautomerise to **184**, followed by a final hydrolysis that yields product **173** and releases catalyst **172**. It was believed that the proposed mechanism was more likely to occur compared to the [2+2]-mechanism proposed by Blackmond and co-workers (in red),[35,36] owing to the steric demands of **178** and **179**. However, there was no literature precedent for this reaction pathway.

2.2 Aims and Objectives

The aim of this chapter was to investigate the envisaged unprecedented mechanistic rearrangement observed during a 6-*endo-trig* organocatalytic intramolecular Michael addition. This chapter first describes the attempts to reproduce the organocatalytic synthesis of the 6-membered ring **151**, which previously generated the 5-membered ring **173** as the only observed product (Scheme 2.8). Then, in an attempt to understand the reaction mechanism, synthesis of intermediates, along with *in situ* NMR studies have been undertaken and are discussed herein.

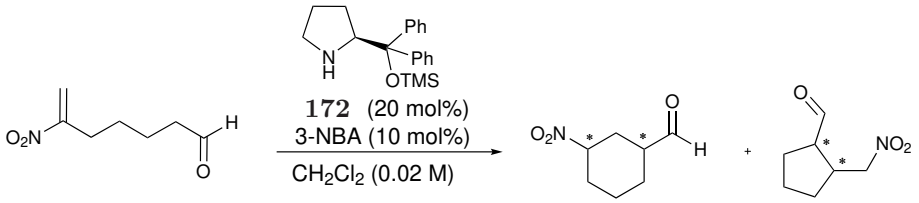

Scheme 2.8: 6-*endo-trig* cyclisation assisted by diarylprolinol silyl ether organocatalyst for the formation of **151** and **173** as a result of a rearrangement.

2.3 Results and Discussion

2.3.1 Synthesis of the terminal nitro olefin substrate

The first synthetic approach to obtain the cyclic 6-membered ring γ-amino acid precursor involved synthesis of the terminal olefin **171** (Scheme 2.9). This procedure began with a nucleophilic substitution of ethyl 6-bromohexanoate **185** with sodium nitrite in 71% yield, followed by reduction of ester **186** to aldehyde **187** in 72% yield. The aldehyde was then protected to form the acetal **188**, which underwent a Henry reaction to give compound **189** in 78% yield. Elimination of the mesylated primary alcohol gave the corresponding nitro olefin **190** in 61% yield. A final deprotection

of the aldehyde generated the target product **171** in 71% yield (17% yield over 6 steps).

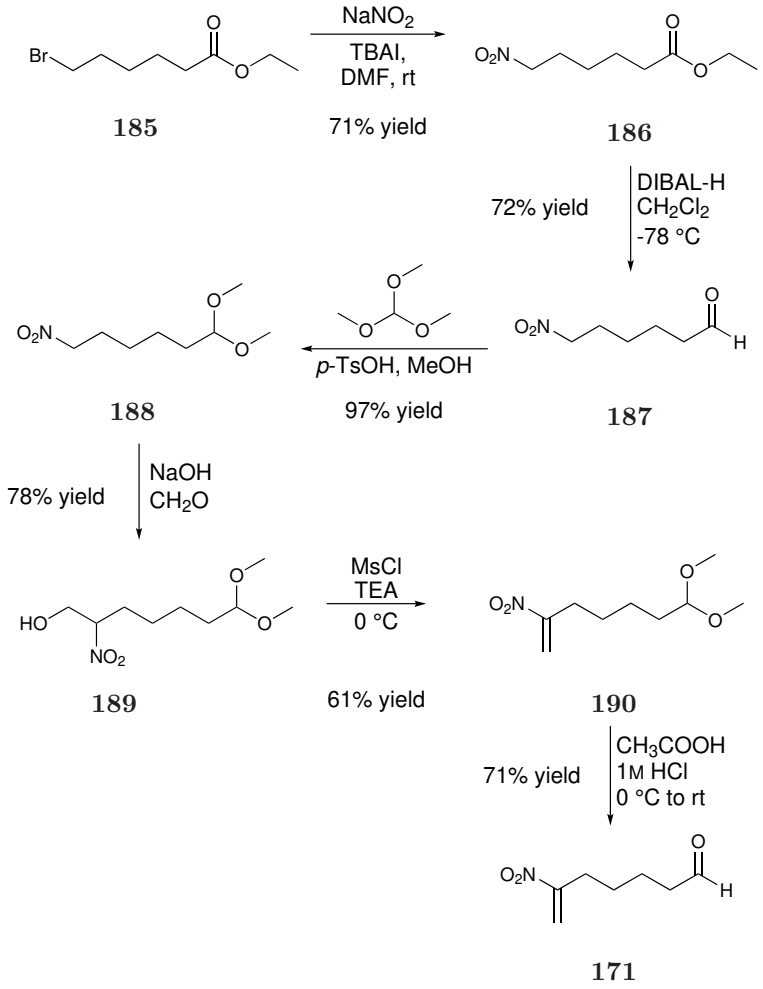

Scheme 2.9: Synthesis of the α-nitro olefin **171**

The multiple synthetic steps, combined with the instability of **171** towards silica made this synthetic route poorly reproducible and, therefore, undesirable, leading to the design of a new synthetic route.[112,113]

The second procedure began with the reduction of ethyl 5-bromovalerate **191** to the aldehyde **192**, which was promptly protected to give the acetal **193**. However, the next steps proved more problematic. It was hoped that selenide **197** could be synthesised from a nucleophilic substitution of bromine with compound **196**, followed by an oxidation with hydrogen peroxide, a concomitant elimination and a final deprotection of the aldehyde to achieve product **171** (Scheme 2.10).[114]

The substitution was attempted with three different reaction conditions: (i) in

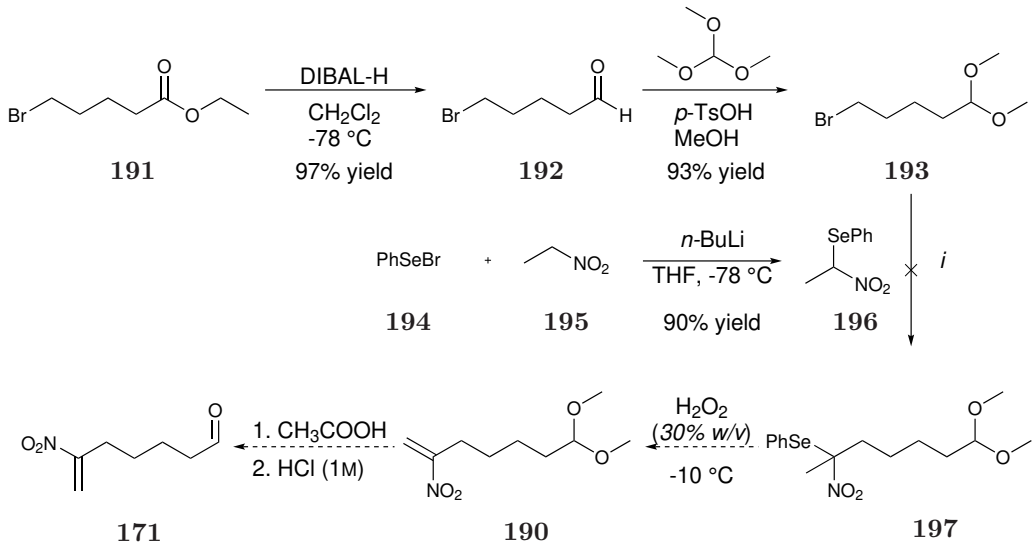

Scheme 2.10: Second synthetic procedure to achieve the α-nitro olefin substrate.(i) a) nBuLi, -78 °C; b) LDA, -78 °C to rt; c) DBU (10 mol%) at rt.

the presence of nBuLi at -78 °C, (ii) with LDA raising the temperature from -78 °C to rt and (iii) with DBU (10 mol%) at rt. In all instances, the reaction failed to form any product and this might be due to the steric hinderance of the nucleophile.

Due to the more significant issues encountered during the second outlined synthetic plan, the first procedure described in Scheme 2.9 was selected for the synthesis of the terminal nitro olefin **171**.

2.3.2 Organocatalytic 6-*endo-trig* cyclisation

As already discussed, a previous group member synthesised the terminal nitro olefin **171** with the intention of performing a 6-*endo-trig* cyclisation, when intriguingly, the 5-membered ring **173** was the observed product instead of the expected 6-membered ring **151** (Scheme 2.6).[111] Therefore, this organocatalytic Michael addition was initially repeated here, however, contradictorily to the previous findings, the 6-membered ring **151** was the main product, and only 1% yield of the 5-membered ring **173** was isolated (Scheme 2.8).

In the presence of the Hayashi-Jørgensen catalyst **53**, compound **171** cyclises to the 6-membered ring with 45% yield and a *dr* calculated after purification *via* flash chromatography of 1:4.5 *cis/trans* ratio. The diastereomer *trans* presented a *ee* of 6%, whereas the enantioselectivity of the *cis* diastereomer was not calculated because of the small amount of isolated material. The low yield compared to

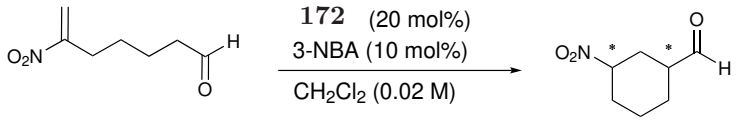

Scheme 2.11: Intramolecular Michael addition of nitro olefin **171** in the presence of the Hayashi-Jørgensencatalyst **172**

Scheme 2.6 could be due to the formation of compounds between the nitro olefin **171** and the catalyst **172** that did not hydrolyse to the final product, inhibiting the regeneration of the catalyst. The obtained side products were isolated *via* flash chromatography, however, characterisation was not possible due to the presence of other impurities. The organocatalytic reaction was not optimised because the focus of the study was the understanding of the observed rearrangement and the isolation of the more appealing 5-membered ring γ-amino acid precursor **173** as will be discussed in chapter 3.

2.3.3 Identification of rearrangement intermediates

Although we managed to synthesise the 6-membered ring **151**, the reaction mechanism was still unclear, and therefore required further investigation. Synthesis of intermediate **151** was undertaken in an attempt to validate the proposed mechanism. The exposure of **151** to the same previous reaction conditions (20 mol% of Hayashi-Jørgensen catalyst **172**, 10 mol% of 3-nitrobenzoic acid and CH_2Cl_2) would have validated the proposed mechanism (Scheme 2.8). If the reaction yielded the 5-membered ring **173** as previously found, that would suggest that compound **151** could plausibly be part of the catalytic cycle.

An alternative synthetic strategy to the organocatalytic 6-*endo-trig* cyclisation was designed in order to achieve **151** on a larger scale. The first synthetic procedure is described in Scheme 2.12. Nucleophilic substitution of the bromine in ethyl 4-bromobutyrate with a nitro group was achieved to afford **199** in 49% yield, followed by reduction of the ester to the aldehyde **200** in 88% yield. The nucleophilic addition of compound **201** to the aldehyde **200** yielded **202** in 61% yield, as a mixture of two different diastereoisomers. Protection of the alcohol of both compounds was then performed, followed by an oxidation with hydrogen peroxide in order to obtain compound **204** in 91% yield. The use of caesium carbonate as a base enabled the

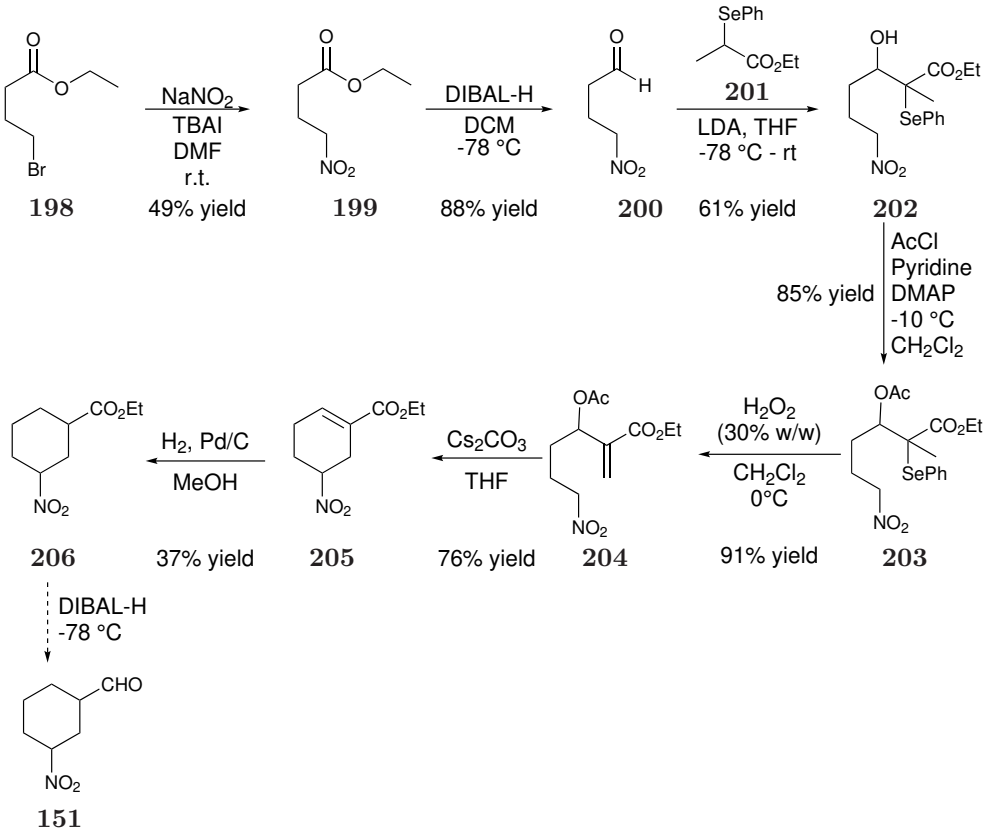

Scheme 2.12: First proposed synthetic pathway for the synthesis of compound **151**.

closure of the ring in 76% yield. The reduction of the alkene gave nitroester **206**. This step was found to be problematic, where several methods were attempted, but only hydrogenation of the alkene **205** catalysed by Pd/C (10 wt%) was found to be successful leading to the desired product **151** in a 37% yield (Table 2.1). The reason for these difficulties can be attributed to (i) the conjugation of the double bond with the electron withdrawing ester, which deactivates the double bond, (ii) the hinderance of the trisubstituted alkene which keeps the structure very rigid, and is thus sterically difficult to reach for the reduction, and (iii) the presence of the nitro group which is also prone to reduction. Due to the difficulties encountered with the reduction of the α,β-unsaturated ester, an alternative route for this specific reduction was established (Scheme 2.13). The reduction of the α,β-unsaturated ester **205** with DIBAL-H directly obtained the allylic alcohol **207**,[115] which was subsequently oxidised to the aldehyde **208**. The organocatalytic reaction was carried out directly with **208** in the presence of a Hantzch Ester, which was chosen as an *in situ* reducing agent of the alkene. Aldehyde **208** was expected to condense with the secondary

Table 2.1: Attempted reaction conditions for the reduction of compound **205** to compound **206**.

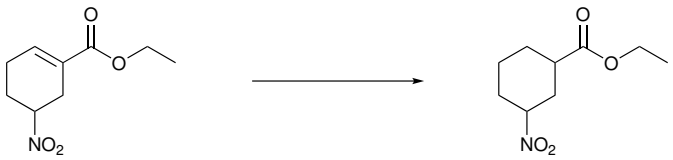

205 **206**

Entry	Reagents	Solvent	T [°C]	Time [h]	Yield[i] [%]
1	H_2, Pd/C[ii]	MeOH	rt	3	37
2	$NaBH(OAc)_3$	CH_3CN[iii]	0	4.5	0
3	$NaBH_4$	MeOH [iii]	0 – rt	2.5	0
4	H_2, $Rh(PPh_3)_3Cl$[iv]	THF [iii]	rt	4 d	0
5	Baker's yeast (S. Caervisiae)	EtOH/ H_2O (1:15)	rt - 35	7 d	0
6	$Rh(PPh_3)_3Cl$)[v], $PhMe_2SiH$	THF[iii]	rt - 50	3 d	0
7	$Rh(PPh_3)_3Cl$[vi], $PhMe_2SiH$	Toluene[iii]	80	5	0

(i) Isolated yield. (ii) 10 wt%. (iii) Anhydrous solvent. (iv) 4 mol%. (v) 10 mol%. (vi) 1 mol%.

amine catalyst **172**, followed by an *in situ* reduction of the alkene performed by the Hantzch ester. The reduced imminium intermediate **177** would then be able to rearrange to **173**. Hantzch esters have been observed to be particularly successful as reducing agents for example in the presence of Macmillan catalysts.[116,117] However, under the ascribed conditions, the targeted rearranged product **173** was not obtained (Scheme 2.13).[118] The unsuccessful outcome of this experiment can be attributed to either: (i) inability of the reaction to occur *via* intermediate **177** or (ii) inefficient reduction of the alkene by the Hantzch ester having prevented the formation of **151**, and therefore prevented the occurrence of the proposed rearrangement. The bulky group of the Hayashi-Jørgensen catalyst **172** might have hindered the alkene, preventing the reduction, therefore, it is not possible to determine between the two possible reasons.

Due to the encountered issue with the Hantzsch ester *in situ* reduction, a new synthetic procedure that bypasses the α/β-unsaturated aldehyde reduction was developed (Scheme 2.14). The new designed strategy involved a lower number of steps to achieve the nitroaldehyde **151**, compared to the one described in Scheme 2.12. A

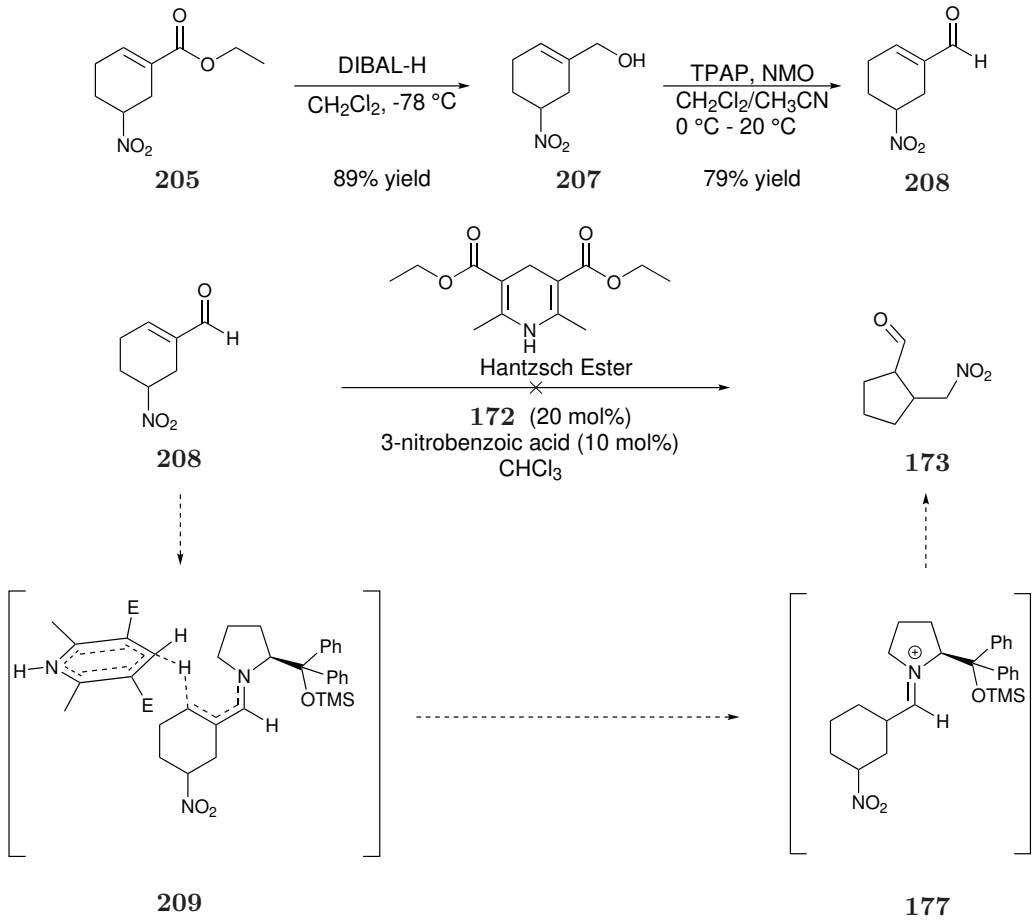

Scheme 2.13: *In situ* reduction of the α,β-unsaturated ester to pursue the targeted organocatalytic reaction.

single nucleophilic substitution of 1,4-dibromo butane with the organoselenide **201** yielded the bromo-organoselenide **211** in 19% yield. The low yield can be accounted for the poor selectivity of the reaction due to the presence of the two bromine atoms of **210**, and thus, formation of side products. The oxidation of the organoselenium compound produced **212** in 55% yield and it was followed by a nucleophilic substitution with sodium nitrite which afforded **213** in 57% yield. Cyclisation was then performed with caesium fluoride to afford **206** in 56% yield and final ester reduction with DIBAL-H led to the synthesis of the targeted 6-membered ring **151** in 96% yield (Scheme 2.14). After the successful synthesis of **151**, it was then reacted under the organocatalytic reaction conditions where previously the 5-membered ring **173** was first observed (20 mol% of Hayashi-Jørgensen catalyst **172**, 10 mol% of 3-nitrobenzoic acid and CH_2Cl_2, entry 1 of Table 2.2). Under reaction conditions

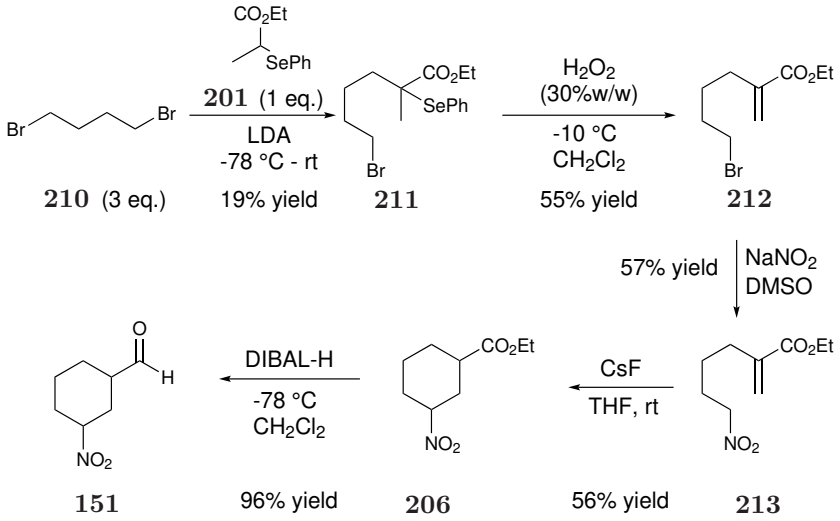

Scheme 2.14: Successful synthetic procedure for the synthesis of compound **151**.

where a mixture of both *cis* and *trans* of **151**, along with 20 or 50 mol% catalyst loading, also varying the co-catalyst loading from 10-25 mol%, no formation of **173** was observed. The reaction was also attempted with a single diastereomer. First the *cis* diastereomer was reacted under the same reaction conditions (20 mol% Hayashi-Jørgensen catalyst **172**, 10 mol% 3-nitrobenzoic acid, CH_2Cl_2), then the *trans* diastereomer was reacted in DMF instead of dichloromethane (Table 2.2). In both cases, the targeted product **173** was not detected and a mixture of *cis* and *trans* of starting material **151** was recovered. As a result, with the intermediate, synthesised and unsuccessfully reacted in equivalent reaction conditions, it is still unclear whether the 6-membered ring **151** is an intermediate of the reaction and further investigation is needed to address this issue.

2.3.4 1,2-nitro shift

As discussed previously, the proposed catalytic cycle could not be confirmed *via* the synthesis of the hypothesised intermediate **151**. The subsequent generation of the 5-membered ring **173** as product of an intended 6-*endo-trig* cyclisation was still ambiguous. Several test reactions were attempted to reproduce the observed rearrangement and to understand the reasons behind the 5-membered ring **173** formation (Table 2.3). The terminal nitro olefin **171** was reacted with 20 mol% of Hayashi-Jørgensen catalyst **172**, 10 mol% 3-nitrobenzoic acid, in CH_2Cl_2 to determine the yield of the 5-membered ring **173**. The formation of **173** was compared

to the percentage of internal nitro olefin **214** present in the starting material and it was found that, even in absence of impurities, the 5-membered ring **173** was formed (Entry 6 and 7 of Table 2.3), suggesting that the initially proposed catalytic cycle was plausible (Scheme 2.7).

Interestingly, a 5-*exo-trig* reaction with the internal nitro olefin **214** under the same adopted conditions (20 mol% of Hayashi-Jørgensen catalyst **172**, 10 mol% 3-nitrobenzoic acid, in CH_2Cl_2) led to prompt formation of the 5-membered ring **173**. This suggested that a 1,2-nitro shift of the substrate from the terminal nitro olefin **171** to the internal nitro olefin **214** might occur. The formation of the internal nitro olefin **214** was hypothesised to derive from the mesylation and elimination step of the nitroalcohol **189** to the nitro olefin **190** (Scheme 2.15). However, a ^{1}H NMR

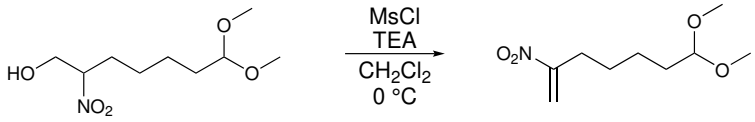

189 **190**

Scheme 2.15: Mesylation of the alcohol **189** to the nitro olefin **190**.

study was performed and the internal nitro olefin was not identified.

This suggests that a 1,2-nitro shift probably occurred during work up and pu-

Table 2.2: Attempted reactions to validate the proposed reaction mechanism.

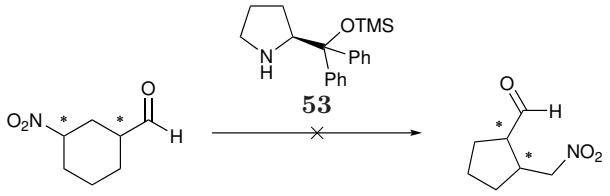

151 **173**

Entry	Diast.	Cat. loading[i] [mol%]	Co-cat. loading[ii] [mol%]	Solvent	Yield[iii] [%]
1	*cis* and *trans*	20	10	CH_2Cl_2	0
2	*cis* and *trans*	50	25	CH_2Cl_2	0
3	*cis*	20	10	CH_2Cl_2	0
4[iv]	*trans*	20	10	DMF	0

(i) Hayashi-Jørgensen catalyst **172**. (ii) 3-nitrobenzoic acid. (iii) Determined by ^{1}H NMR spectroscopy. (iv) In the presence of H_2O (100 mol%).

Table 2.3: Formation of the 5-membered ring **173** as side product of the 6-*endo-trig* cyclisation.

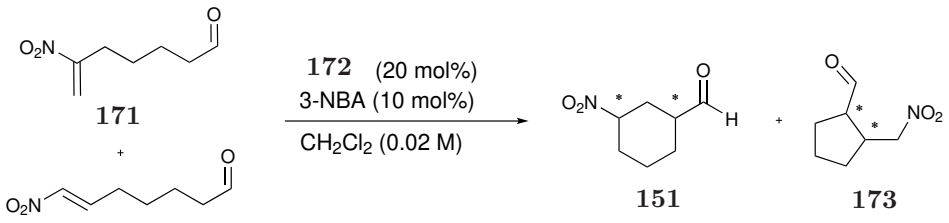

Entry	T [°C]	t	SM impurity[i] (**214**) [%]	Yield[ii] of **173** [%]
1	rt	280 min	18	4
2	rt	10 days	2	<5[iii]
3	rt	70 min	18	10
4	0	5 days	18	10
5	rt	60 min	18	22
6	rt	180 min	0	<5%[iii]
7	rt	90 min	0	<5%[iii]

(i) Percentage of terminal olefin **214** calculated *via* ^{1}H NMR spectroscopy as side product. (ii) Isolated yield. (iii) Yield determined by crude ^{1}H NMR spectra. (iv) Yield determined by ^{1}H NMR spectra of fractions containing a mixture of 6-membered ring **151** and 5-membered ring **173**.

rification over silica gel of the crude nitro olefin **190** leading to a mixture of terminal nitro olefin **171** and internal nitro olefin **214** that were difficult to separate *via* flash chromatography. Table 2.3 presents syntheses of the 5-membered ring **173** under various reaction conditions, with differing quantities of the internal nitro olefin **214** as starting material impurity during the intramolecular cyclisation of the terminal nitro olefin **171**. Despite higher yields of the 5-membered ring **173** being obtained when the starting material contained a higher percentage of the internal nitro olefin **214**, the nitroalkane **173** was also identified when the starting material was pure (Table 2.3).

In an attempt to rationalise the formation of the 5-membered ring **173** from pure starting material **171**, further ^{1}H NMR studies were performed. The 1,2-nitro shift was not observed when the terminal nitro olefin **171** was left in $CDCl_3$ or in CH_2Cl_2 and 3-nitrobenzoic acid (10 mol%) in absence of the Hayashi-Jørgensen catalyst **172**. A ^{1}H NMR study of protected terminal nitro olefin **215** in the presence of the Hayashi-Jørgensen catalyst **172** (20 mol%) and 3-nitrobenzoic acid (10 mol%) in CD_2Cl_2 was then performed (Figure 2.1). Figure 2.1(b) displays the increase

in concentration of the protected internal nitro olefin **216** over time. Figure 2.1(c) shows the overlap of ^{1}H NMR spectra of the monitored reactions. The characteristic peak of the internal alkene proton is shown and increases with time. 3% of nitro olefin **216** is formed in 3 days at room temperature, despite the protection of the aldehyde.

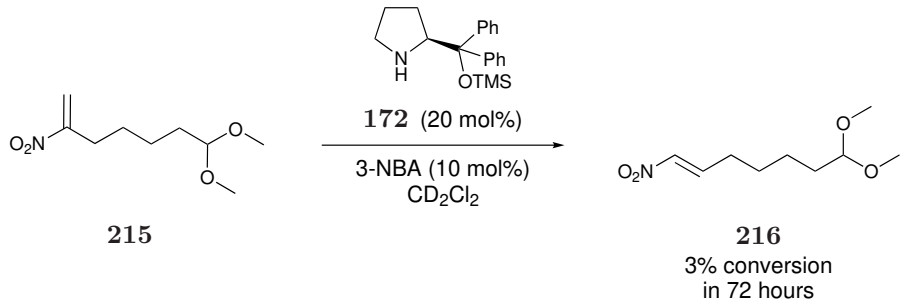

215 **216**
3% conversion
in 72 hours

(a)

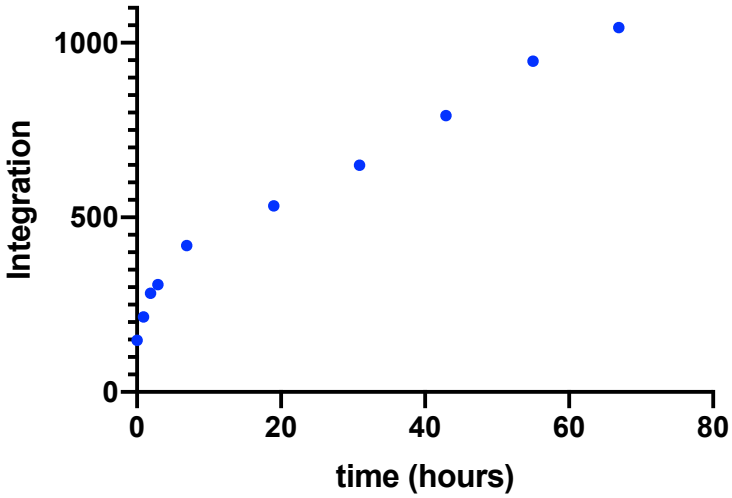

(b)

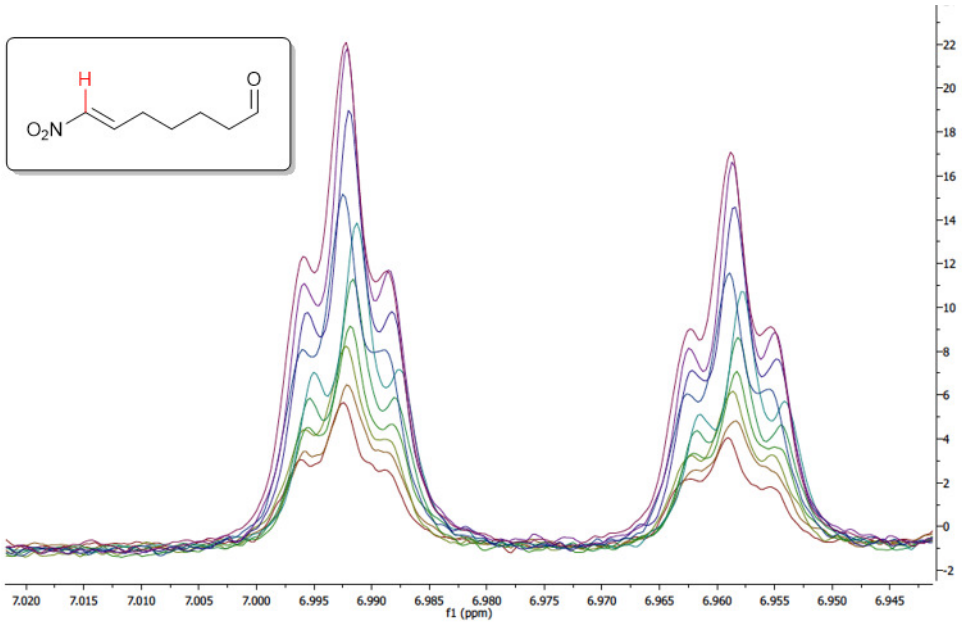

(c)

Figure 2.1: (a) 1,2-nitro shift of **215** to **216** occurring in the presence of catalyst **172**. (b) Plot of the integral, which is proportional to the concentration, of the inserted nitro olefin **214** with time. (c) *In situ* monitored reaction ^{1}H NMR spectra overlap. The spectra are zoomed in on the dt of the characteristic alkene proton which is highlighted in red.

A mechanism has already been proposed for this specific rearrangement.[119–123] Prochazka and co-workers reported in 1971 the mechanism of isomerisation of nitro olefins, where they use triethylamine as base.[119–121] The latter can abstract the β-proton from the nitro olefin, forming the 3-membered ring intermediate, and the conjugated acid. The formation of the internal nitro olefin is then followed and a 1,2-nitro shift can be performed (Scheme 2.16).[119–123]

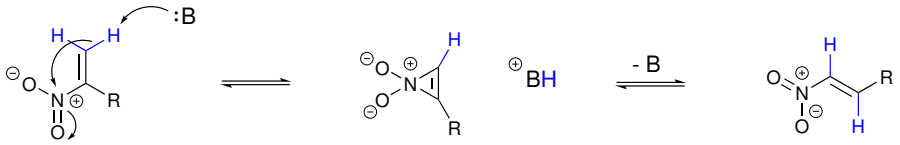

217 **218**

Scheme 2.16: Leseticky and co-workers mechanistic proposal for the isomerisation of nitro olefins.

Of particular note, only 3% of the internal olefin **216** is formed after 3 days when the aldehyde is protected. This suggests that in the presence of the catalyst the aldehyde plays a significant mechanistic role, possibly condensing into the secondary amine, and a concerted mechanism might occur promoting the 1,2-nitro shift. This would explain the previously observed much faster formation of the 5-membered ring **173** when the aldehyde is unprotected.

2.4 Conclusion

In this chapter, the synthesis of the terminal nitro olefin **171** has been optimised with a 17% yield over 6 steps. A preliminary study of a 6-*endo-trig* cyclisation for the final synthesis of γ-amino acid precursor **151** containing a 6-membered ring in 45% yield, has been reported. Interestingly, the 5-membered ring γ-amino acid precursor **173** was observed only as a side product (<5% yield) during a 6-*endo-trig* cyclisation (Scheme 2.17). A preliminary mechanistic study to understand the rearrangement observed during a organocatalytic 6-*endo-trig* cyclisation of nitro olefins was performed (Scheme 2.8). Synthesis of a possible 6-membered ring intermediate **151** was accomplished and was tested under the same reaction conditions where the rearrangement was observed. However, the expected rearrangement to the 5-membered ring **173** was not observed under the catalytic conditions, therefore was unable to confirm the proposed organocatalytic cycle. It was found that the internal

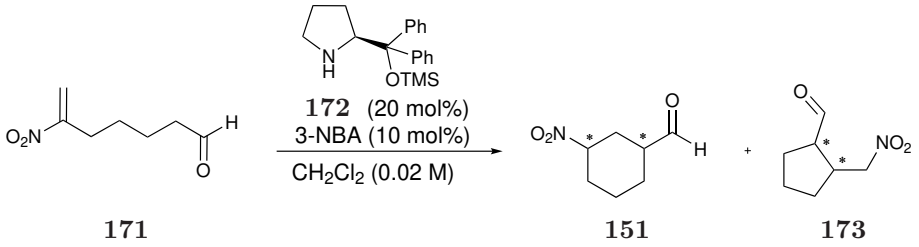

Scheme 2.17: 6-*endo-trig* cyclisation assisted by diarylprolinol silyl ether organocatalyst for the formation of **151** and **173** as a result of a rearrangement.

nitro olefin **214** cyclised promptly to the 5-membered ring **173**, therefore a 1,2-nitro shift of the terminal nitro olefin **171** to the internal nitro olefin **214** was then proposed to explain the formation of **173** (Figure 2.2). However, the 5-membered ring

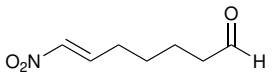

214

Figure 2.2: Internal nitro olefin **214**.

173 was also obtained from pure nitro olefin **171**, therefore a ^{1}H NMR study was performed and it was found that a 1,2-nitro shift of the protected terminal nitro olefin **215** to the protected internal nitro olefin **216** was observed. Only 3% of the protected internal nitro olefin **216** was formed in 3 days suggesting the importance of the free aldehyde in the rearrangement (Figure 2.1). To conclude, a concerted mechanism of the secondary amine catalyst **53** with the nitro olefin substrate **171** could be hypothesised to rationalise the formation of the 5-membered ring **173** during the initally expected 6-*endo-trig* cyclisation.

2.4.1 Future work

Further studies would be necessary to demonstrate if a concerted rearrangement of the terminal nitro olefin **171** to the afforded 5-membered ring **173** is part of the catalytic cycle. Computational and further NMR studies could give a preliminary understanding of a possible concerted mechanism. An optimisation of the envisaged enantio- and diastereoselective 6-*endo-trig* reaction should be performed to develop an organocatytic route to the novel 6-membered ring nitro-aldehyde **151**.

Chapter 3

Organocatalytic access to *cis*-5-membered ring γ-amino acid precursors *via* a 5-*exo-trig* Intramolecular Michael Addition

3.1 Background

During the study of 6-*endo-trig* cyclisation, it was observed the generation of the 5-membered ring **173** that might have resulted from a rearrangement of the terminal nitro olefin **171** to the inserted nitro olefin **214** (Scheme 3.1, chapter 2). We therefore

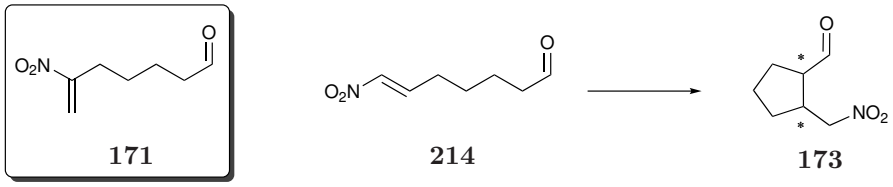

Scheme 3.1: Nitro olefin **171** and 5-*exo-trig* cyclisation of nitro olefin **214** to the γ-amino acid precursor **173**.

felt it was important to investigate the 5-*exo-trig* intramolecular Michael addition of nitro olefin **214** assisted by organocatalysis.

Synthesis of cyclic γ-amino acid precursors is extremely interesting for pharmaceutical purposes and as building blocks for the synthesis of foldamers (chapter 1). Particularly interesting is the synthesis of *cis*-**173** since it has proven difficult in the past. To date, only Ley and co-workers reported in 2002 the synthesis of an enantioselective *cis*-γ-amino acid **174** obtained with enzymatic resolution presenting

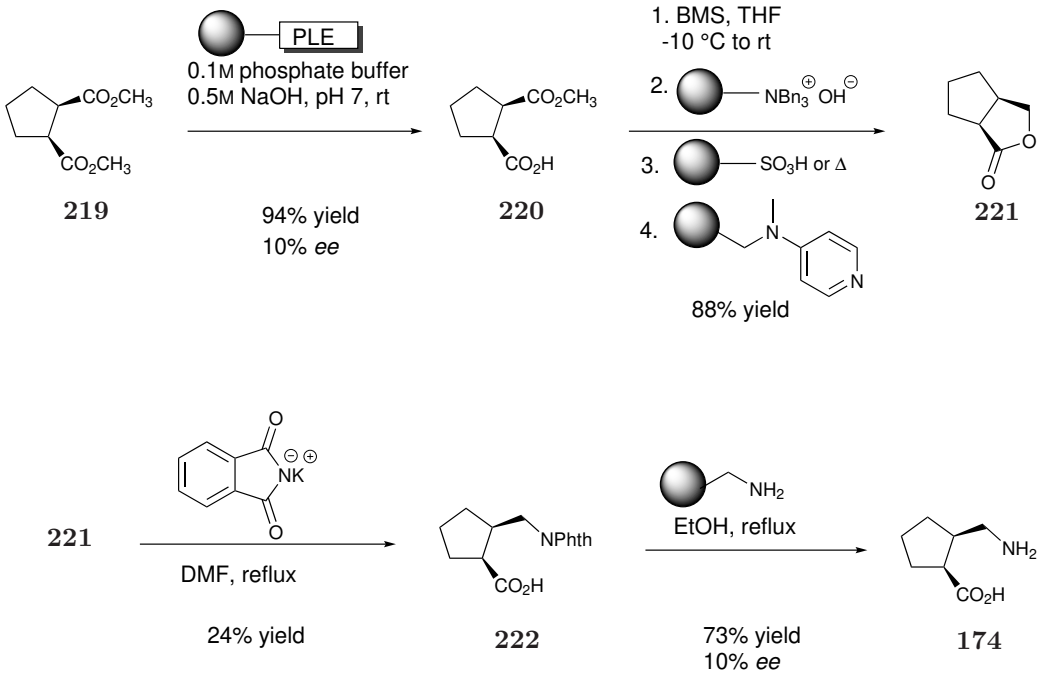

Scheme 3.2: Synthesis of the 5-membered ring *cis*-γ-amino acid **174** developed by Ley and co-workers. PLE = pig liver esterase

only 10% *ee* (Scheme 3.2).[124] In this study, a desymmetrisation of the *meso*-diester **219** with polymer-supported pig liver esterase on Eupergit® was performed.

In 2008, Enders and co-workers presented an organocatalytic asymmetric domino reaction to achieve the 5-membered ring α-substituted γ-amino acid precursors.[125] From the substrate scope, it was apparent that the smaller the R group, the greater the diastereoselectivity towards the *trans* diastereomer and *vice versa* with larger substituents, albeit with lower yields (Table 3.1).

Table 3.1: Substrate scope of an organocatalytic domino reaction of aldehydes **223** and (*E*)-5-iodo-1-nitropent-1-ene developed by Enders and co-workers.[i]

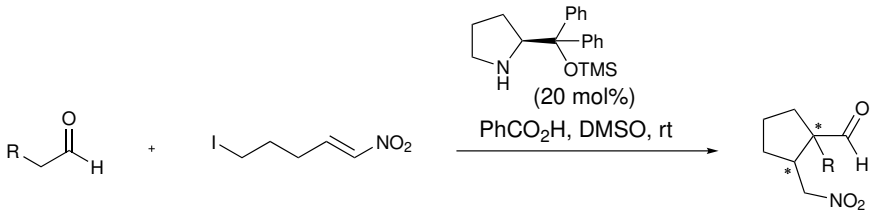

223 (a-e)		**224**			**225 (a-e)**
Prod.	R	t [d]	Yield [%][ii]	*dr*[iii] *trans/cis*	*ee* [%][iv] *trans, cis*
225a	Me	2	62	66:34	94, 96
225b	Et	4	59	13:87	60, 97
225c	*i*Pr	7	40	1:99	-, 93
225d	*n*Pr	4	45	10:90	59,97
225e	*n*Bu	4	41[iii]	11:89	-, 97[vi]

(i) Reaction conditions: 2 mmol **224**, 5 eq. aldehyde **223**, 20 mol% catalyst, and 100 mol% $PhCO_2H$ at rt in 4.0 mL DMSO. (ii) Combined yield of separable diastereomers. (iii) Determined by GC analysis. (iv) Determined by HPLC analysis on a chiral stationary phase on the corresponding aldehyde **225** except **225e**. (v) Yield after reduction of the aldehyde to the alcohol ($NaBH_4$, MeOH, 0 °C). (vi) Determined by HPLC analysis of alcohol **225e** on a chiral stationary phase.

In 2013, Gellman and co-workers reported an asymmetric synthesis of the 5-membered ring **226**.[126] A Michael addition of nitromethane to cyclopentene-1-carboxaldehyde aided by the Hayashi-Jørgensen catalyst **53** was performed to afford the *trans* diastereoisomer in >19:1 *dr*, high yields and high enantioselectivity (Scheme 3.3).

Finally, in 2015 Bernardi and co-workers also reported the synthesis of the 5-

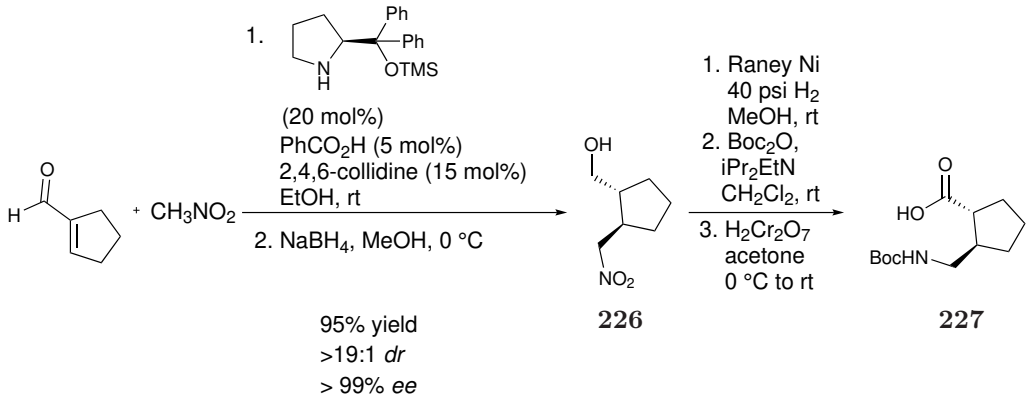

Scheme 3.3: Synthesis of *trans*-5-membered ring γ-amino acid precursors performed by Gellman and co-workers.

membered ring γ-amino acid precursors.[127] A modified procedure inspired by Gellman and co-workers was created with the aim of using it in manufacturing. Catalyst loading as low as 1 mol% was used maintaining high enantioselectivity.

3.2 Aims and Objectives

The aim of the study was to design an enantio- and diastereoselective synthesis of *cis*-γ-amino acid precursor **226** and their analogues assisted by organocatalysis. This chapter first describes the optimisation of the targeted 5-*exo-trig* cyclisation, which is then followed by a mechanistic investigation. *In situ* NMR studies, identification of kinetic profiles, enantioselective and computational studies were performed and discussed further (Scheme 3.4).

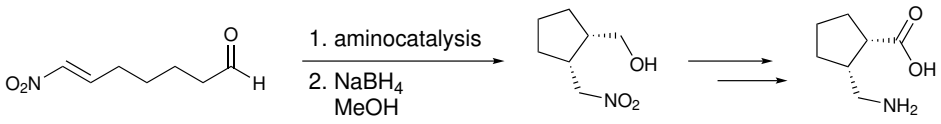

214 **226** **174**

Scheme 3.4: 5-*exo-trig* cyclisation for the final synthesis of **174**.

3.3 Results and Discussion

The present work focused on the optimisation of a 5-*exo-trig* cyclisation assisted by organocatalysis to achieve the desired 5-membered ring γ-amino acid precursor **173**. Synthetic routes to obtain nitro olefin **214** were designed in order to perform the envisaged asymmetric intramolecular Michael addition (Scheme 3.5).

214 **173**

Scheme 3.5: 5-*exo-trig* cyclisation for the synthesis of the aldehyde **173**.

3.3.1 Synthesis of the internal nitro olefin 214.

Two different procedures were explored for the synthesis of nitro olefin **214**. The first procedure began with the nitration of the double bond of ethyl 6-heptenoate **228** *via* a radical process followed by the reduction of the ester to the aldehyde **214** with DIBAL-H.[128] This synthetic procedure lead to the targeted product with a

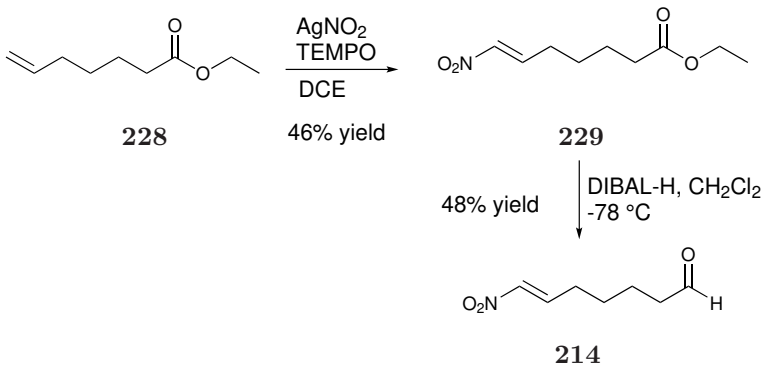

Scheme 3.6: First synthetic procedure for the synthesis of nitro olefin **214**.

22% yield over two steps (Scheme 3.6).

In order to achieve the internal nitro olefin **214** with less impurities a different procedure was designed. First, an oxidation of cyclohexene **230** was performed with ozone at -78 °C, followed by a methylenation. A nitration of the double bond of **232** and deprotection of the acetal **233** achieved the final product **214** in 13% yield over the four steps. The second procedure avoided the synthesis of impurities and racemic cyclised product which were difficult to separate from the nitro olefin **214**. It was speculated that these were obtained as a result of the DIBAL-H reaction and purification on silica. However, the first procedure presented a higher overall yield over fewer steps and therefore chosen as the preferred synthesis of **214** (Scheme 3.7).

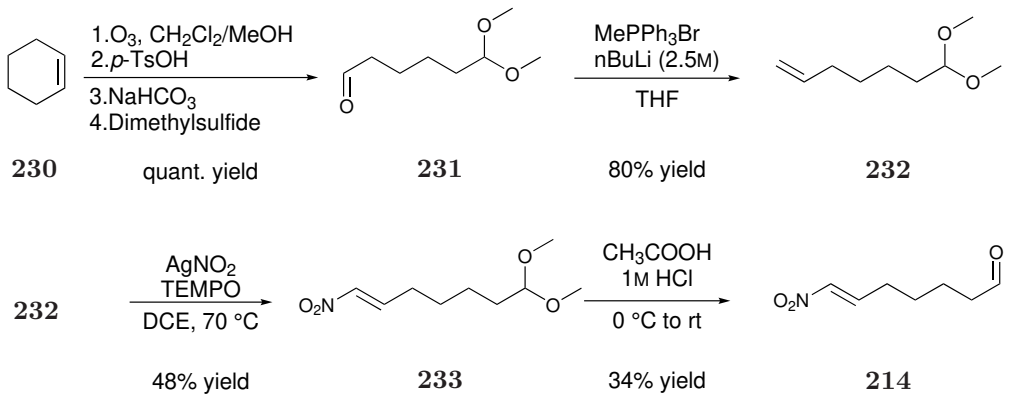

Scheme 3.7: Second synthetic procedure for the synthesis of nitro olefin **214**.

3.3.2 Preliminary optimisation for the synthesis of the γ-amino acid precursor 173.

Once the substrate was synthesised a catalyst screen at room temperature was performed. At first, the investigation was carried out at room temperature without any further reduction as a provisional study. This method led to the synthesis of the *trans* diastereomer **173** as main product of the reaction.

Several amino based catalysts were tested (Figure 3.1).

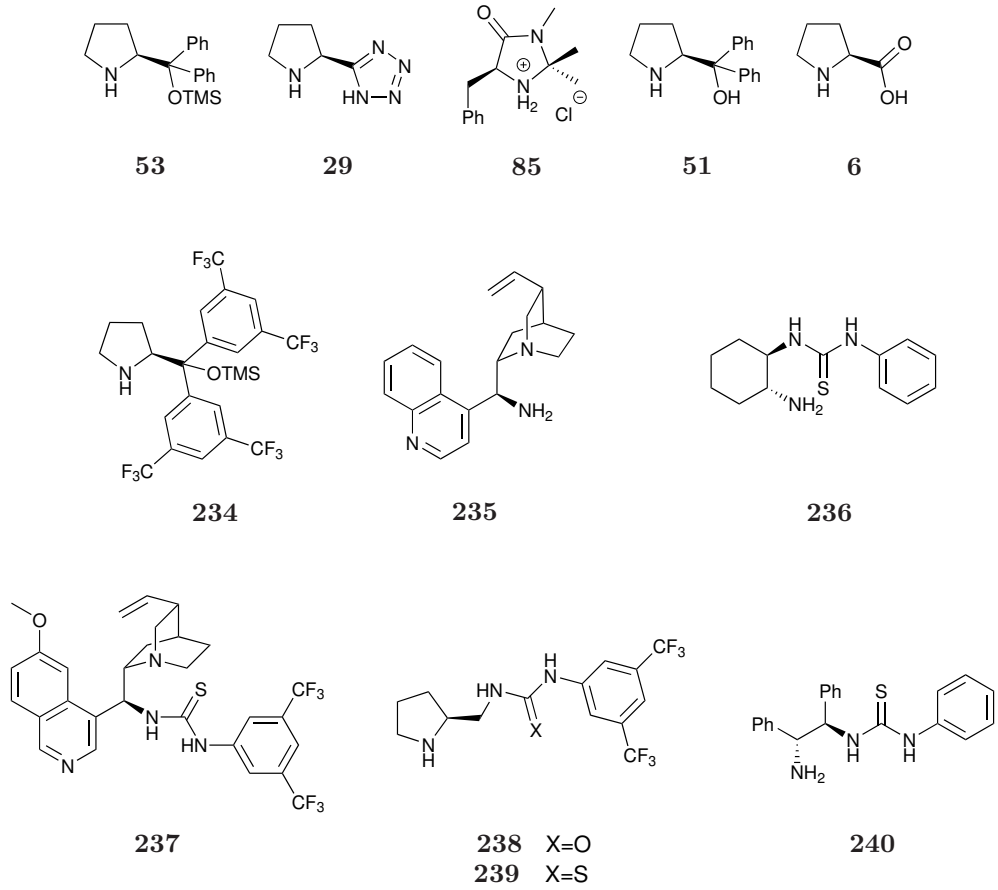

Figure 3.1: Selected catalysts to perform a preliminary screen at rt.

Diastereoselectivity and enantioselectivity were not reported where yields were considerably low and the obtained results were not significant for the optimisation of the reaction. Bifunctional catalysts **238**, **239** and **240** were synthesised according to literature procedures.[129,130] A preliminary catalytic screen was performed with the reaction catalysed by the Hayashi-Jørgensen catalyst **53** reaching completion in 20 minutes, in 62% yield, with a 1:4 *cis/trans* diastereoselectivity and a –59% *ee* of the major diastereomer. The *cis* diastereomer and was confirmed later in the study

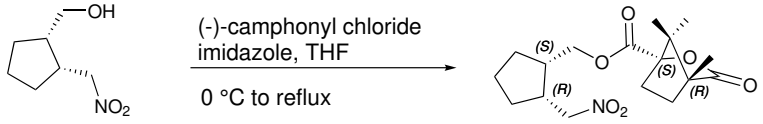

cis- **226** **241**

(a)

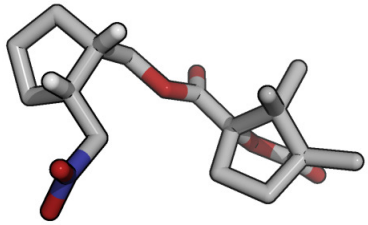

(b)

Figure 3.2: (a) Synthesis of the ester **241** to identify relative stereochemistry. (b) X-ray crystal structure of **241** (CCDC: 1947228).

with a crystal structure (Figure 3.2).

The same reaction was performed in the presence of an acid co-catalyst (3-nitro benzoic acid) at rt and at 0 °C. In both cases, yields, diastereoselectivity and enantioselectivity improved to 94% and 98% yield with a 1:9 and 1:13 *dr* and –62% and –71% *ee* respectively (Entry 2 and 3 of Table 3.2). The yield was improved further with the use of bifunctional catalyst **29** and this is probably due to a lower amount of impurities forming (Table 3.2). As with catalyst **53**, repeating the reaction at 0 °C with tetrazole catalyst **29** the *dr* improved to 1:7, which suggests that at lower temperature the *cis* diastereomer is more likely to be isolated. Several other secondary amine catalysts and bifunctional catalysts were tested (Table 3.2), however all with limited success in terms of *ee* and *dr*.

Interestingly, Hayashi-Jørgensen-CF_3 catalyst **234** produced a 1:2 *dr* in favour of the *trans* product with mismatched enantioselectivity between the *cis* and *trans* diastereomers. This indicates that the formation of the two diastereomeric products may occur *via* different intermediates and a more in depth study of the mechanism is discussed later in this chapter.

Primary amine catalyst **235** was screened alongside benzoic acid as co-catalyst

Table 3.2: Preliminary catalyst screen.

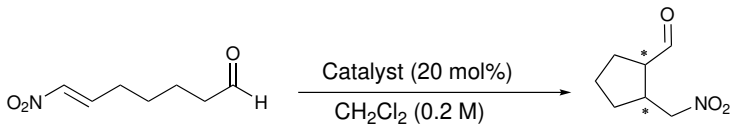

214 **173**

Entry	Cat.	Time [h]	T [°C]	Yield[i] [%]	*dr*[ii] (*cis*/*trans*)	*ee*[iii] [%] (*trans*)
1	**53**	0.3	rt	62	1:4	-59
2	**53**[iv]	0.5	rt	94	1:9	-62
3	**53**[iv]	0.5	0	98	1:13	-71
4	**29**	1.5	rt	91	1:8	72
5	**29**	9.5	0	74	1:7	79
6	**51**	2.5	rt	67	1:2	6
7	**6**	0.7	rt	67	1:9	-7
8	**234**	120	rt	67	1:2	15[v]
9	**85**	2.5	rt	54	1:7	-59
10	**237**	72	rt	26	1:1	ND
11	**235**[vi]	144	rt	11	1:2	-22
12	**236**	18	rt	51	1:5	85
13	**238**	16	rt	50	1:3	63
14	**239**	19	rt	70	1:3	61
15	**240**	96	rt	41[vii]	1:6	88

(i) Combinatorial isolated yield of separable diastereomers. (ii) Determined by crude ^{1}H NMR. (iii) Determined by HPLC analysis on a chiral stationary phase. (iv) In the presence of 3-nitrobenzoic acid (10 mol%) as co-catalyst. (v) -70% *ee* for *cis* diastereomer. (vi) In the presence of benzoic acid (10 mol%) as co-catalyst. (vii) Yield of single *trans* diastereomer because the *cis* diastereomer was not separable from impurities.

to aid the enamine formation and hydrolysis as reported in literature (Table 3.2).[131] However, the reaction presented 1:2 *dr* and –22% *ee* of *trans*-**173** and only 11% yield after 6 days, which is probably due to the slow rate of hydrolysis of the iminium intermediate impeding the catalytic cycle to complete (Entry 11, Table 3.2).

Catalysts **238** and **239** gave moderate to good yields, moderate enantioselectivities (entry 13 and 14 of Table 3.2) and 1:3 *dr*. The inclusion of a primary amine and thiourea moiety within the same catalyst (**236** and **240**) led to high enantioselectivity (entries 12 and 15 of Table 3.2). The reaction catalysed by **240** achieved the best results from the catalyst screen and was used for further optimisation studies.

Mild and strong acids were tested as additives to the reaction, however all led to a reduction in diastereoselectivity and enantioselectivity (Table 3.3).

A different strategy was therefore outlined to optimise the enantioselective syn-

Table 3.3: Co-catalyst screen for the synthesis of the 5-membered ring *trans*-**173**.

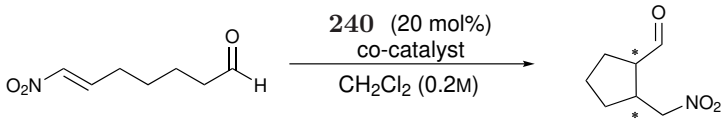

214 **173**

Entry	Co-cat. (20 mol%)	Time [d]	Yield[i] [%]	*dr*[ii] (*cis*/*trans*)	*ee*[iii] (*trans*)[%]
1	-	96	41[iv]	1:6	88
2	Benzoic acid[v]	7	47[vi]	1:4	57
3	4-NBA	7	42	1:3	39
4	*p*-Toluene-sulfonic acid mono-hydrate	7	15	1:1	-
5	*o*-Fluoro benzoic acid	5	43[vi]	1:2	45
6	TFA	7	23[vii]	1:1.5	40
7	3-NBA	6	44	1:1.5	37

(i) Combinatorial isolated yield of separable diastereomers. (ii) Determined by crude ^{1}H NMR. (iii) Determined by HPLC analysis on a chiral stationary phase. (iv)) Yield of single *trans* diastereomer. (v) Co-catalyst loading of 10 mol%. (vi) Yield of single *trans* diastereomer because product *cis* was obtained together with not easily separable impurities. (vii) The reaction did not go to completion.

thesis of the 5-membered ring **173**. This initial study was valuable to deepen our understanding of the targeted reaction and to select the best catalysts for further investigations. The enantioselectivity of *cis*-**173** was not recorded during this first preliminary study apart from entry 9 of Table 3.2 because it was obtained as minor diastereomer (*cis*-**173**) with poor yields. Having focused on the synthesis of the *trans* diastereomer in the first part of the study, the project moved on to target the synthesis of the *cis* diastereomer.

3.3.3 Asymmetric synthesis of *cis*-γ-amino acid precursor 226.

In the past, *cis*-γ-amino acid precursors have proven to be difficult to synthesise enantioselectively and only one example has been reported in literature as previously mentioned (Scheme 3.2).[124] The study of the 5-*exo*-*trig* cyclisation at rt led to the identification of the best catalysts for further optimisation of the *cis*-nitroalcohol **226** synthesis. Five catalysts out of the catalyst screen performed at rt were selected to test at lower temperature followed by an *in situ* reduction in order to isolate *cis*-**226**

Table 3.4: Catalyst screen at 0 °C.

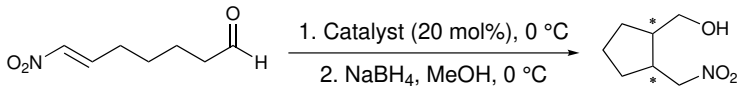

214 **226**

Entry	Catalyst	Time [h]	Yield[i] [%]	*dr*[ii] (*cis/trans*)	*ee*[iii] [%] (*cis,trans*)
1	**53**	1	57	1:1	87[iv], -27
2	**29**	14	62	2:1	-83[iv], 71
3	**51**	96	5[v]	1:1	ND, ND
4	**85**	72	42	1:6	-68, -74
5	**240**[vi]	104	6	1:1.5	-95, ND

(i) Combinatorial isolated yield of separable diastereomers. (ii) Determined by crude ^{1}H NMR. (iii) Determined by HPLC analysis on a chiral stationary phase. (iv) Determined by AD-H HPLC chiral column. (v) The reaction did not go to completion.(vi) The reaction was carried out at rt.

(Table 3.4). The reactions were carried out at 0 °C except from the reaction catalysed by **240**, which was performed at rt due to slow reactivity (Table 3.4). Catalyst **240** gave the highest *ee* for *cis*-**226** albeit with a long reaction time, low yield and *dr*. Catalyst **53** and **29** produced the best results in terms of yields, diastereoselectivity and enantioselectivity and therefore were selected for further investigation.

Interestingly, opposite enantiomers can be selectively obtained using either the Hayashi-Jørgensen catalyst **53** or the 5-pyrrolidin-2-yltetrazole catalyst **29** (entry 1 and 2 of Table 3.4). The reason behind this outcome can be associated to the different mechanism of reaction of the two catalysts. The Hayashi-Jørgensen catalyst **53** controls the enantioselectivity of the reaction *via* the steric hinderance of the bulky TMS group. Although more in depth mechanistic studies conducted independently by Blackmond, Seebach, Hayashi, Pápai and Pihko revealed that intermediates of the reaction might influence the stereoselectivity (chapter 1).[34,35,37,40,132–137] In contrast, the tetrazole catalyst **29** behaves as a bifunctional catalyst and the actractive nature of the tetrazole group, rather than the repulsive hinderance, affects the enanantioselectivity.[25,138,139]

Temperature control of the reaction was unsurprisingly an important aspect of diastereoselecitivity. Temperature plays an important role as *cis*-**226** is the kinetic product and can only be isolated at low temperature after *in situ* reduction to the corresponding alcohol, since the *cis* diastereomer tends to convert to the more sta-

Table 3.5: Temperature screen for the optimisation of the 5-*exo-trig* cyclisation.

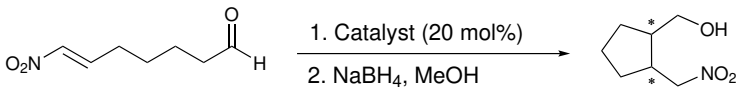

214 **226**

Entry	Catalyst	T [°C]	t [h]	Yield[i] [%]	*dr*[ii] (*cis/trans*)	*ee*[iii] [%] (*cis,trans*)
1	**53**	-20	5	20[iv]	1:1	36, 53
2	**53**	-10	3	64	1:1	-86, -26
3	**29**	-20	22	62	3:1	82, 22
4	**29**	-10	22	68	1:1	83, 67

(i) Combinatorial isolated yield of separable diastereomers. (ii) Determined by crude ^{1}H NMR. (iii) Determined by HPLC analysis on a chiral stationary phase. (iv) The reaction did not go to completion.

ble thermodynamic product *trans* in the presence of the secondary amine catalyst. Each diastereomer may be formed from different mechanisms which may explain the different enantioselectivities of the two diastereomers. A more in depth mechanism discussion is presented later in this chapter. The organocatalytic reaction was tested at 0, -10 and -20°C with catalysts **53** and **29** (Table 3.4 and Table 3.5). The use of tetrazole catalyst **29** at -20°C achieved the highest *dr*; a solvent screen was therefore performed with this catalyst. The intramolecular Michael addition was tested with different solvents, but only chlorinated solvents led to good diastereoselectivity and excellent enantioselectivity (Table 3.6). Protic and polar solvents such as methanol and THF (entry 4 and 6, Table 3.6) were found to have a detrimental effect on yield and enantioselectivity of the reaction and this can be associated to the coordination of the solvent to the tetrazole moiety interfering with the protonation step which might be crucial for the reactivity and the selectivity of the reaction. Interestingly, performing the reaction in dichloroethane gave the best results in terms of *dr* and *ee* (entry 7, Table 3.6). Dichloroethane might reduce the rate of the reaction by stabilising one of the two competing transition states for the *cis* and *trans* diastereomers. This process can lead to the selective synthesis of the *cis* diastereomer, considerably shifting the *dr* towards the synthesis of the intended *cis* diastereomer.[140,141]

The solvent screen was then followed by another co-catalyst screen. In the presence of an acidic co-catalyst, such as entry 1 and entry 2 of Table 3.7, the diastereoselectivity shifted towards the synthesis of *trans*-**226** as the main diastereomer.

Table 3.6: Solvent screen of the 5-*exo-trig* cyclisation.

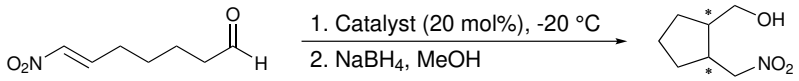

214 **226**

Entry	Solvent (0.2 M)	t [h]	Yield[i] [%]	*dr*[ii] (*cis/trans*)	*ee*[iii] [%] (*cis,trans*)
1	CH_2Cl_2	22	62	3:1	82, 22
2	Toluene	24	57	3:1	70, 32
3	CH_3CN	25	54	1:1	65, 56
4	THF	24	52	1:1	50, 38
5	$CHCl_3$	20	68	3:1	79, 48
6	MeOH	26	11	1.5:1	-10, ND
7	DCE	50	53	7:1	85, 54

(i) Combinatorial isolated yield of separable diastereomers. (ii) Determined by crude ^{1}H NMR. (iii) Determined by HPLC analysis on a chiral stationary phase.

Basic co-catalysts on the other hand favoured the production of *cis*-**226** albeit in low yields (Table 3.7). This type of co-catalyst might promote the formation of side products, reducing the efficiency of the reaction. The next step for the optimisation of the 5-*exo-trig* intramolecular Michael addition was the concentration screen. As

Table 3.7: Co-catalyst screen of 5-*exo-trig* cyclisation for the synthesis of *cis*-**226**.

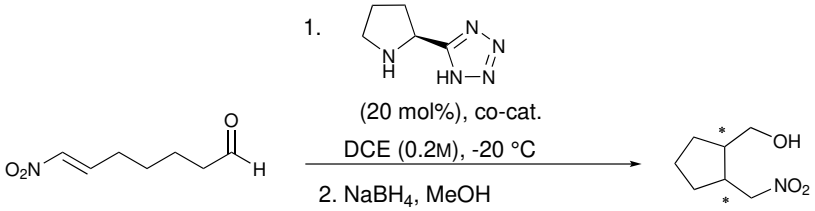

214 **226**

Entry	Co-catalyst (20 mol%)	Time [h]	Yield[i] [%]	*dr*[ii] (*cis/trans*)	*ee*[iii] [%] (*cis,trans*)
1	Benzoic acid	48	53	1:2	78, 80
2	3-NBA	48	68	1:5	70, 82
3	Acetic acid	77	54	2:1	86, 62
4	Catechol	48	47	N.A.[v]	74, 41
5	TEA	20	25	4:1	-26, ND
6	Dimethyl-piperazine	48	18	2.5:1	7, 5

(i) Combinatorial isolated yield of separable diastereomers. (ii) Determined by crude ^{1}H NMR. (iii) Determined by HPLC analysis on a chiral stationary phase. (iv) The reaction did not go to completion.(v) The *dr* cannot be calculated *via* NMR.

Table 3.8: Concentration screen of the 5-*exo-trig* cyclisation.

Entry	Conc. [M]	Time [h]	Yield[i] [%]	*dr*[ii] (*cis/trans*)	*ee*[iii] [%] (*cis,trans*)
1	0.2[iv]	42	58	6:1	83, -
2	**0.05**	**168**	**74**	**8.5:1**	**93, -**
3	0.1	48	66	6:1	89, -
4	0.2	50	60	5.5:1	88, -
5[v]	0.1	72	60	5.5:1	91, -
6[vi]	0.05	168	51	4:1	85, 45

(i) Combinatorial isolated yield of separable diastereomers. (ii) Determined by crude ^{1}H NMR. (iii) Determined by HPLC analysis on a chiral stationary phase. (iv) The reaction was carried out with anhydrous solvents. (v) The reaction was reduced with DIBAL-H. (vi) Cold addition of a solution of substrate (2M in DCE) to the reaction mixture.

expected, yield improved considerably from 58% to 78% when diluting the reaction from 0.2M to 0.05M and this is possibly due to the suppression of side reactions, like nitro olefin polymerisation, which might occur at higher concentrations.[142,143] The diastereoselectivity also increased which can be explained by the fact that at lower concentrations the epimerisation of the product *cis*-**226** to the *trans*-**226** occurs at a lower rate of the reaction. Interestingly, we can also notice an improvement of the enantioselectivity for *cis*-**226** probably due to a reduced self-aggregation phenomena of the catalyst which can lower the efficiency of the catalyst.[144,145]

A catalyst loading screen was performed to complete the reaction optimisation and it was found that the reaction maintains comparable results when using catalyst loading as low as 5 mol% (Table 3.9). Low catalyst loading is an important achievement for organocatalysis and it is likely that the reaction catalysed by 2 mol% catalyst would give higher yield if the reaction was carried out in larger scale due to encountered solubility issues (entry 5, Table 3.9).

Table 3.9: Catalyst loading screen for the optimisation of the 5-*exo-trig* cyclisation.

Entry	Conc. [M]	Catalyst loading [mol%]	Time [h]	Yield[i] [%]	*dr*[ii] (*cis/trans*)	*ee*[iii] [%] (*cis,trans*)
1	0.1	10	70	64	7:1	89, 26
2	0.1	5	168	52	11.5:1	88, 0
3	0.05	10	24	74	9:1	92, 34
4	**0.05**	**5**	**168**	**75**	**10:1**	**89, -56**
5	0.05	2	168	43	10:1	92, -11

(i) Combinatorial isolated yield of separable diastereomers. (ii) Determined by crude ^{1}H NMR. (iii) Determined by HPLC analysis on a chiral stationary phase.

3.3.3.1 Scale up of the reaction

The optimisation of the 5-*exo-trig* cyclisation assisted by the bifunctional tetrazole catalyst **29** produced the desired *cis*-nitroalcohol **226** in high yield, good diastereoselectivity and excellent enantioselectivity. The reaction was then successfully scaled up to 7 mmol and it was stopped after 99 hours instead of 168 hours producing analogous results (Table 3.10). It is believed that the amount of starting material left in solution is not reacting as fast as in the first 4 days and this might be due to the high concentration of the competing product **173** formed that tends to condense again with the catalyst in order to convert to the more stable *trans*-**173**. A more in depth discussion about the diastereoselectivity degradation is presented later in this chapter.

Table 3.10: Scale up of the 5-*exo-trig* cyclisation.

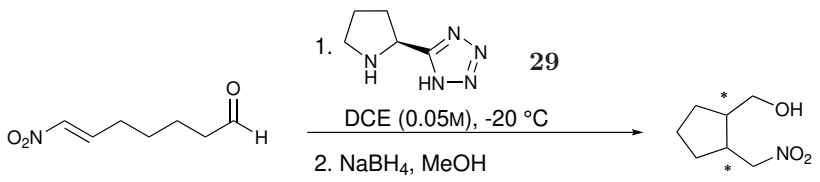

214 **226**

Entry	Reaction scale [mmol]	Catalyst loading [mol%]	Time [h]	Yield[i] [%]	*dr*[ii] (*cis/trans*)	*ee*[iii] (*cis*) [%]
1	0.64	20	168	74	8:1	93
2	0.64	5	168	75	10:1	89
3	**7.0**	**5**	**99**	**74**	**9:1**	**92**

(i) Combinatorial isolated yield of separable diastereomers. (ii) Determined by crude ^{1}H NMR. (iii) Determined by HPLC analysis on a chiral stationary phase.

3.3.3.2 Substrate scope

The optimised conditions were tested with different substrates to prove the generality of the reaction for the synthesis of the desired *cis*-5-membered ring nitroalcohols. First, several α-substituted nitro olefins were synthesised according to Scheme 3.8. The synthesis was performed in 4 steps. An oxidation of cyclohexene was performed with ozone to form the aldehyde **231** in quantitative yield. A Henry reaction was carried out to synthesise the nitro alcohol **242**, which was followed by an elimination to achieve the corresponding nitro olefin **243**. The acetal deprotection was the final step to achieve the aimed nitro olefins. α-Substituted nitro olefins **244a-e** were

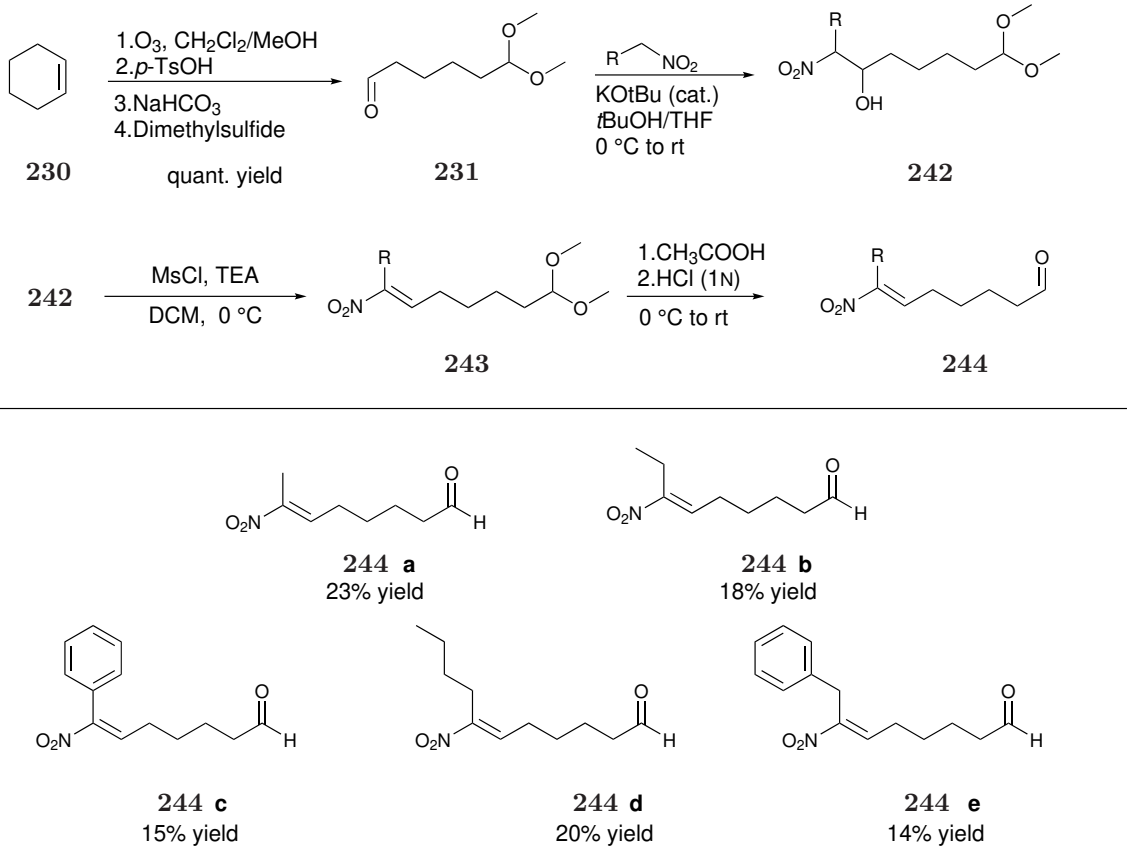

Scheme 3.8: Synthetic procedure to afford α-substituted nitro olefins.

achieved in yields between 15-23% over four steps. Henry reactions are known to produce low yields and instability of acetals in silica gel might have caused even lower yields. The main problem during the synthesis of α-substituted nitro olefins was the uncontrolled deprotection of the aldehyde during the purification on flash chromatography on silica gel and the immediate cyclisation of part of the nitro olefin to the racemic 5-memberered ring **245**.[112,113] The synthesised substrates were tested with the optimised organocatalytic conditions for the synthesis of the *cis*-5-membered ring **245** (Scheme 3.8). The reactions were not as successful as expected

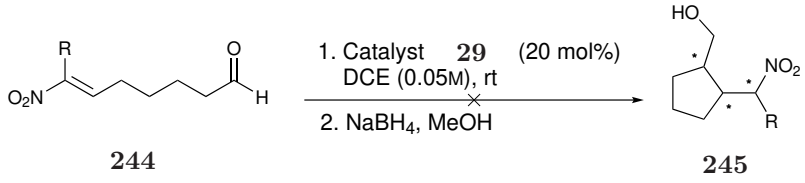

Scheme 3.9: α-substituted nitro olefins synthesised for the substrate scope of the 5-*exo-trig* cyclisation.

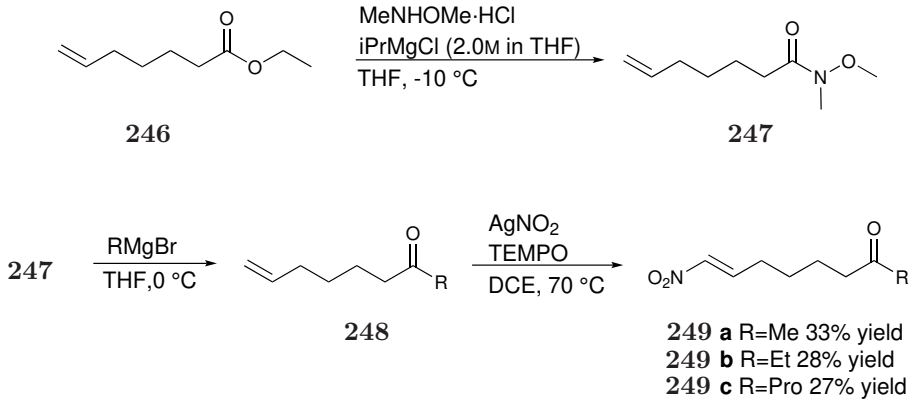

Scheme 3.10: Synthesis of ketones **249a**, **249b** and **249c**.

as no product was isolated. Therefore, the reactions were repeated at 0 °C and at rt, but comparable results were reported. The reason for this outcome might be explained because of the substitution on the α-position to the nitro group.

Ketones have also been tested. Methyl, ethyl and propyl ketones were synthesised in 3 steps following the procedure described in Scheme 3.10. First, ethyl 6-hexenoate **246** was converted to the Weinreb amide **247**, followed by a Grignard reaction to obtain the respective ketones in quantitative yields. Then, the olefin was oxidised to a nitro olefin with a radical nitration reaction obtaining ketones **249a**, **249b** and **249c** in 33%, 28% and 27% yield over the three steps. The intramolecular cyclisation was performed with all three ketones at -20 °C and in the absence of a co-catalyst, however the reactions proved to be very sluggish. Therefore, the

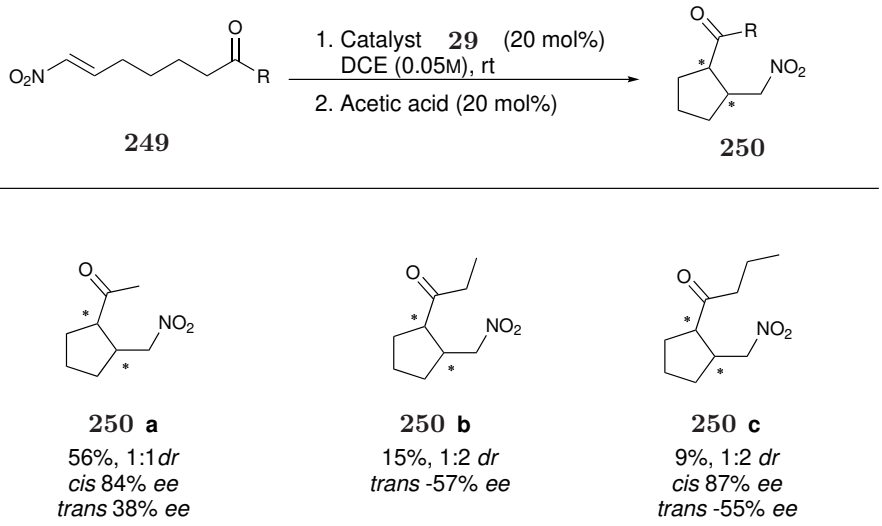

Scheme 3.11: Ketones substrate scope.

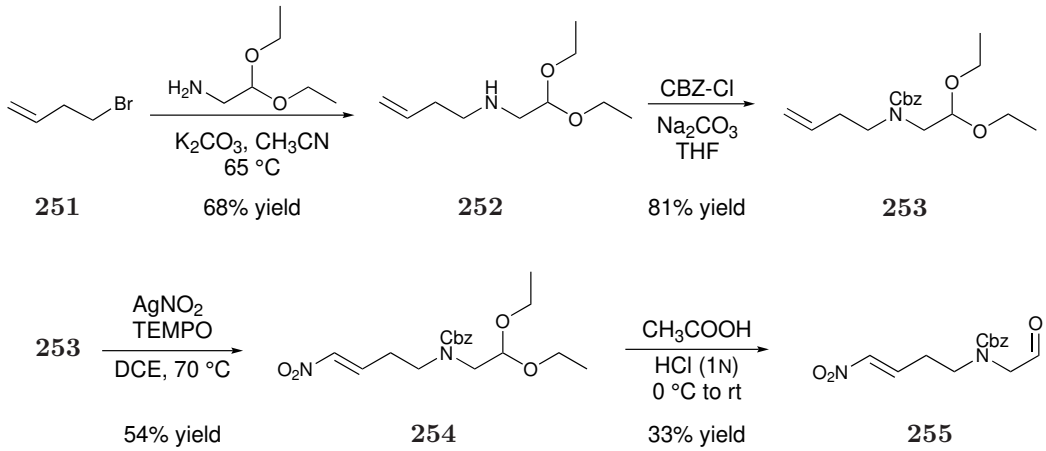

Scheme 3.12: Synthesis of substrate **255**.

reaction was repeated at rt with the addition of an acidic co-catalyst to facilitate the condensation of the catalyst into the substrate. The rate of the reaction was still low and the reaction was stopped after 7 days for the methyl ketone **249a** and 8 days for the ethyl and propyl ketones **249b** and **249c** (Scheme 3.11). Methyl ketone **250a** was the only one that produced a moderate yield of 56% and 1:1 *dr*, whereas substrates **250b** and **250c** presented a much lower yield and 1:2 *dr* with a higher formation of the *trans* diastereomer. The reason for lower yield and diastereoselectivity in favour of *trans* diastereomer for ethyl and propyl ketones **250b** and **250c** can be accounted for the steric hinderance of the substitutents reducing the bifunctionality of the catalyst.

A substrate with a nitrogen embedded in the substrate structure was also synthesised in four steps as shown in Scheme 3.12. A nuclephilic substitution of diethoxyethylamine to 4-bromobut-1-en **251** in the presence of potassium carbonate at 65 °C was carried out in order to achieve the amine **252** in 68% yield. The secondary amine was then protected with a benzyloxy carbamate (CBZ) group ob-

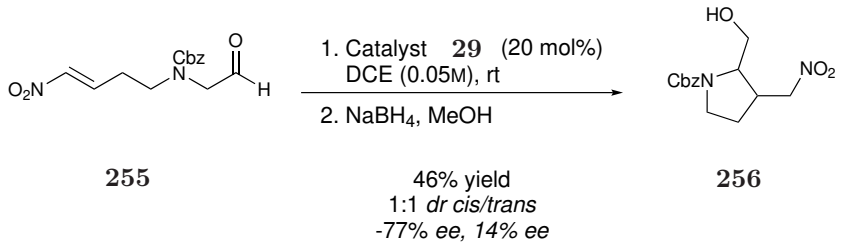

Scheme 3.13: Nitrogen embedded substrate organocatalysis.

taining **253** in 81% yield. Then, a nitration of the olefin was performed achieving **254** in 54% yield, which was then followed by an aldehyde deprotection with acetic acid and 1M HCl at 0 °C to achieve the targeted substrate **255** in 40% yield. The reason of the low yield of the deprotection might be due to a high reactivity of this substrate and to the instability of this compound on silica as the acetal can deprotect and induce a racemic intramolecular cyclisation which could be aided by the mild acidic conditions of the silica. The reaction was carried out under the same optimised reaction conditions for nitro olefin **214**. The reaction presented 1:1 *dr* and 48% yield. The *ee* of the 5-membered ring *cis*-**256** is -77% whereas the *ee* of *trans*-**256** is 14% (Scheme 3.13). This can be explained by the fact that the reaction should undergo the same mechanism described for substrate **214**, leading to a high enantioselective *cis*-product and a less enantioselective *trans*-product. A full discussion of the mechanism is presented later in this chapter.

A substrate containing an aromatic ring was synthesised to finally achieve an enantioselective indane derivative. The dihydrobenzyofuran **259** was first enantio- and diastereoselectively synthesised by Tang and co-workers targeting the *trans* diastereomer (Scheme 3.14).[146]

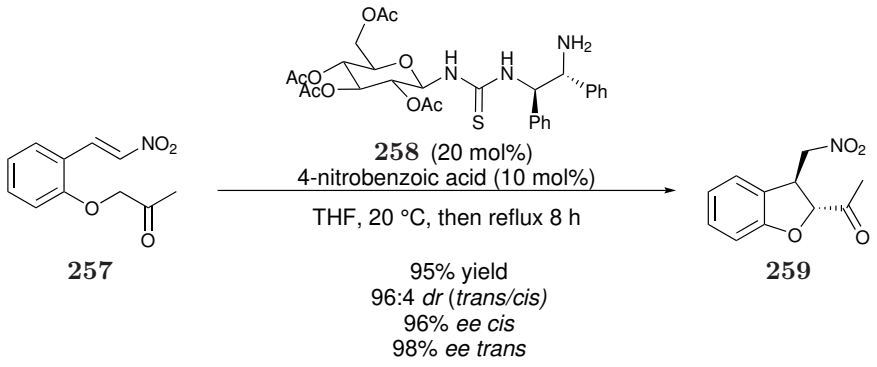

Scheme 3.14: Enantio- and diastereoselective synthesis of the dihydrobenzofuran **259** performed by Tang and co-workers.

In contrast to the literature precedent, the current work presents the synthesis of a bicyclic compound in absence of any heteroatom adopting the optimised methodology for the selective synthesis of *cis* diastereomers.

Substrate **265** was synthesised *via* a 5-step route (Scheme 3.15). The first step was an oxidation of 1,2-dihydronaphthalene (**260**) with ozone, followed by an *in situ* reduction to compound **261**. The benzylic alcohol was than selectively oxidised

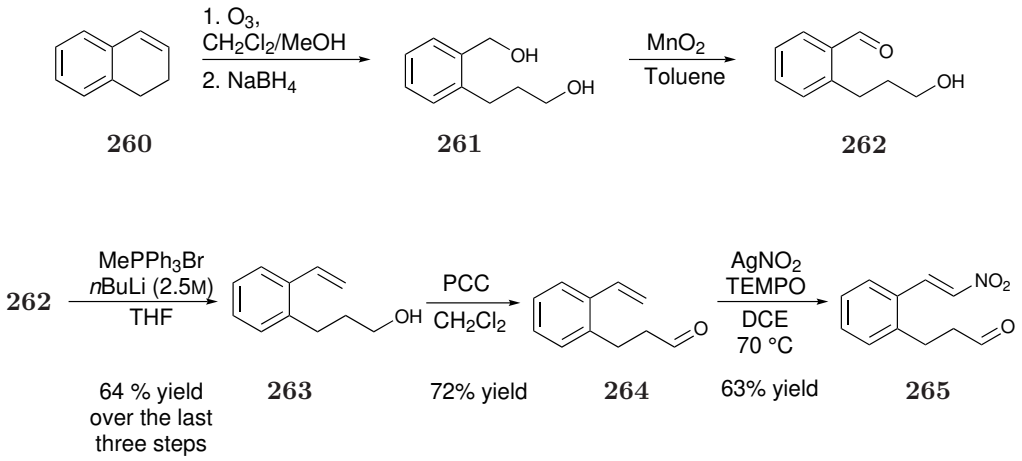

Scheme 3.15: Synthesis of the indane derivative precursor.

to the aldehyde **262** in order to perform a Wittig reaction to achieve the olefin **263**. The alcohol moiety is then oxidised to the aldehyde **264**, followed by the final nitration of the olefin with silver nitrite and TEMPO. The designed synthesis of the nitro olefin **265** was achieved with an overall yield of 29% over the 5 steps (Scheme 3.15). The organocatalytic intramolecular Michael addition was performed using optimised conditions. The indane derivative **266** was achieved in 72% yield, with 1:1 *dr*, 90% *ee* for *cis*-**266** and 52% *ee* for *trans*-**266** (Scheme 3.16).

Assignment of diastereomers of the synthesised substrates was performed by comparison of ^{1}H NMR splitting patterns of protons on the methyl next to the nitro group (ABX systems). It is possible to observe a regular pattern between *cis*-products and *trans*-products. *Cis* diastereomers will show a higher difference

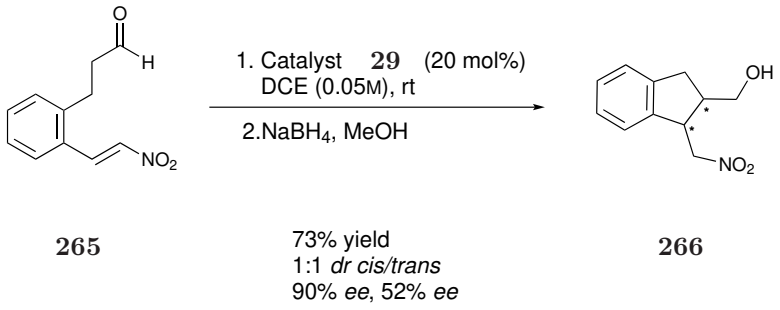

Scheme 3.16: Organocatalytic reaction for the synthesis of the indane derivative **266**.

in resonance frequencies then the *trans* $\delta\nu_{ABcis} \gg \delta\nu_{ABtrans}$ as shown in Figure 3.3. The difference of $\delta\nu_{AB}$ is related to the magnetic field generated by the electrons moving in their orbitals caused in the first place by the external field. The different orientation of the groups generates a magnetic field that shields the external field in different ways therefore it is possible to discriminate between the two isomers without further degenerative derivatization.[147–149]

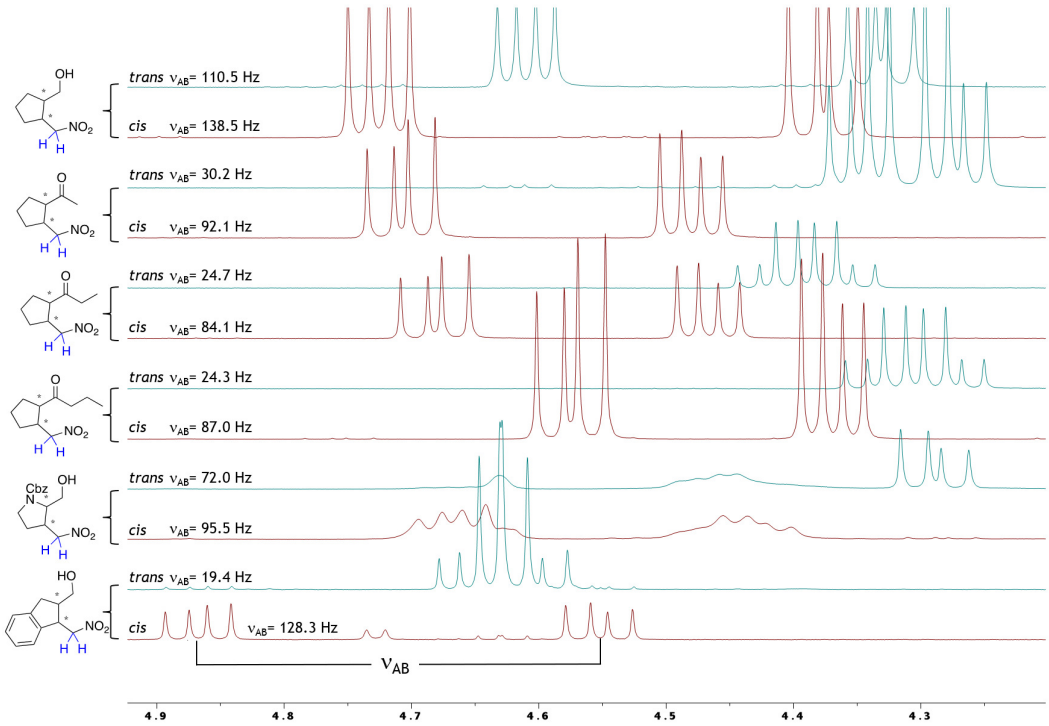

Figure 3.3: Stacked ^{1}H NMR spectra showing the peaks of the protons highlighted in blue of the respective substrates and the different $\delta\nu$ for *cis*- and *trans*-products.

3.3.4 Mechanistic study of the 5-*exo-trig* cyclisation

The optimisation of the 5-*exo-trig* cyclisation assisted by the secondary amine tetrazole catalyst **29** was previously described. Owing to the observed diastereoselectivity degradation, a mechanistic study was performed to understand and optimise further the target 5-*exo-trig* reaction.

3.3.4.1 Kinetic study

A kinetic study was carried out in order to investigate the progress of the reaction and to have a better understanding of the mechanism of the reaction (Scheme 3.17). The optimised 5-*exo-trig* organocatalytic reaction was carried out in a NMR tube in a 0.1M solution of the substrate in CD_2Cl_2 and in the presence of 5 mol% of 5-(pyrrolidin-2-yl)-1H-tetrazole catalyst (**29**). The reaction was first monitored *in situ*

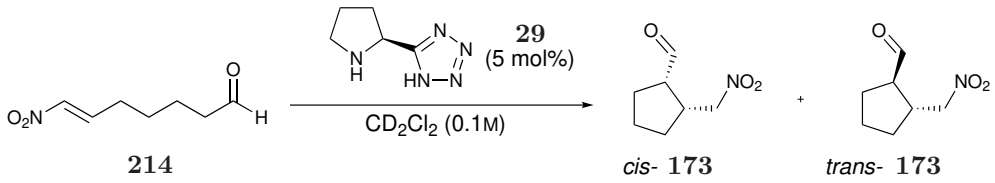

214 *cis*- **173** *trans*- **173**

Scheme 3.17: 5-*exo-trig* organocatalytic cyclisation studied *via in situ* NMR spectroscopy.

at -20 °C and then at 0 °C, but in both cases the reaction rate was still very low and the catalyst was not soluble enough in solution without stirring. Therefore, temperature was raised to 25 °C in order to study the kinetic profile of the reaction. As already discussed, increase in temperature influenced the *cis*:*trans* ratio conversion, however *in situ* monitoring of the reaction provided a general understanding of the kinetic profile of the reaction for further optimisation. Figure 3.4 shows the kinetic profile of the studied 5-*exo-trig* cyclisation until full consumption of the starting material **214**. The concentration of starting material (in blue) decreases whereas the concentration of *cis*-**173** and *trans*-**173** increases (respectively in red and green) with different reaction rates. The reaction was analysed in the first 2 hours of the reaction to interpolate the functions of the different lines in order to determine the initial rate of the reaction for the two diastereomers (1.4 x 10^{-2} mol L^{-1} s^{-1} for the *cis* and 3.0 x 10^{-3} mol L^{-1} s^{-1} for the *trans*, Figure 3.5). The rate of the reaction for the synthesis of the *cis* diastereomer was significantly faster than the reaction rate for the *trans* diastereomer.

After 7 h with complete conversion of the starting material, the formation of *cis*

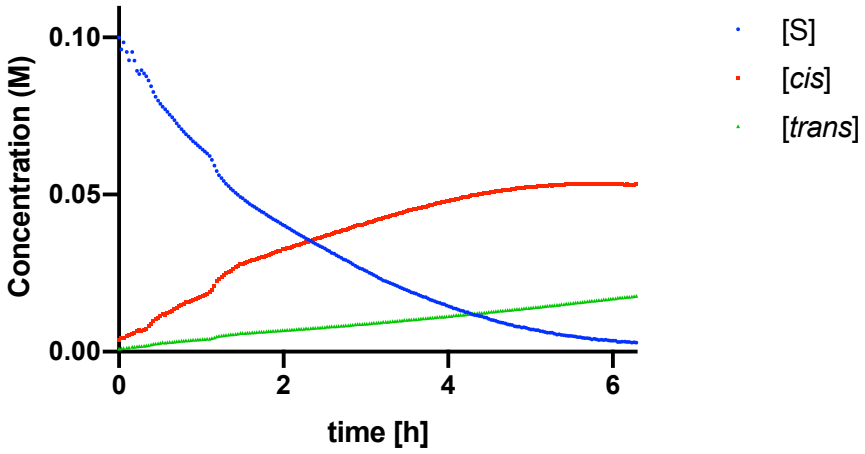

Figure 3.4: Progress of reaction until consumption of starting material.

diastereomer decreases, whereas an increase of the *trans* concentration is observed (Figure 3.6(a)). The reason for this outcome can be accounted for the stability of *cis* and *trans* diastereomers in presence of the catalyst once the starting material has been all consumed. The *cis* is the kinetic product and therefore less stable than the *trans*, which is the thermodynamic product. With time, diastereoselectivity degradation occurs and figure 3.6(a) displays the reduction of the *cis* concentration and a rise of the *trans* concentration. In particular, in figure 3.6(b) it is possible to observe that once the concentration of the starting material is low, the concentration of the *cis* formed decreases and the concentration of the *trans* increases. The loss

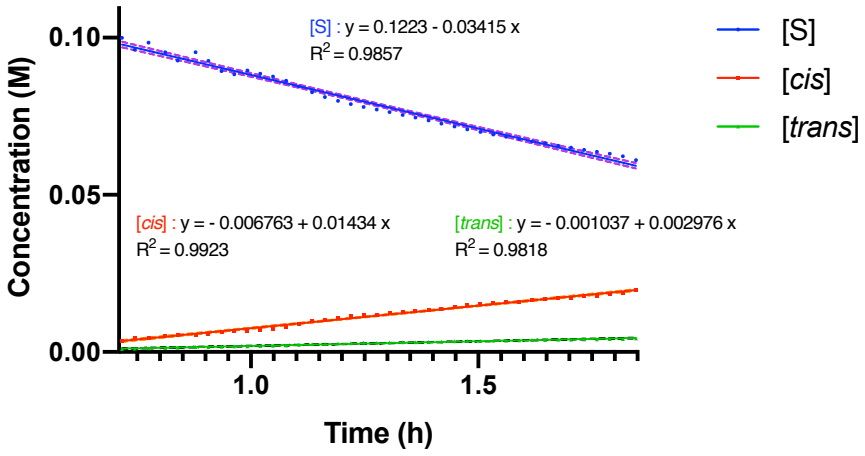

Figure 3.5: Progress of the reaction up to 1.84 hours in order to define the rate of the reaction.

of material observed in Figure 3.6(b) can be accounted for intermediate species and impurities probably due to the polymerisation of the nitro olefin **214** that were not identified.

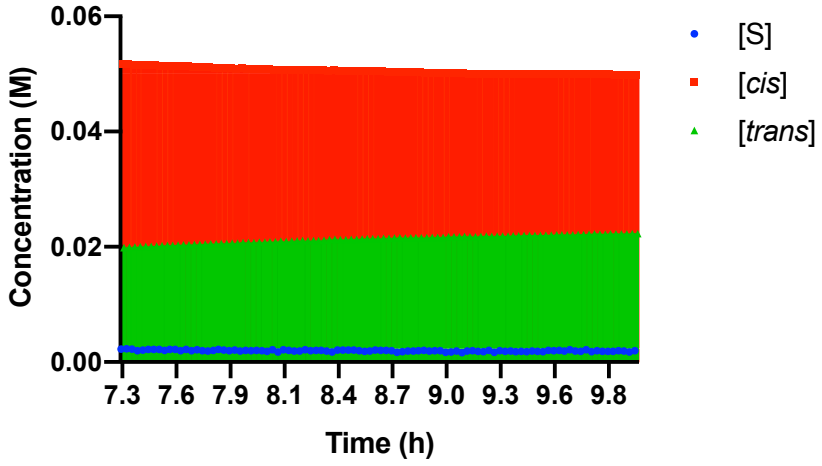

(a)

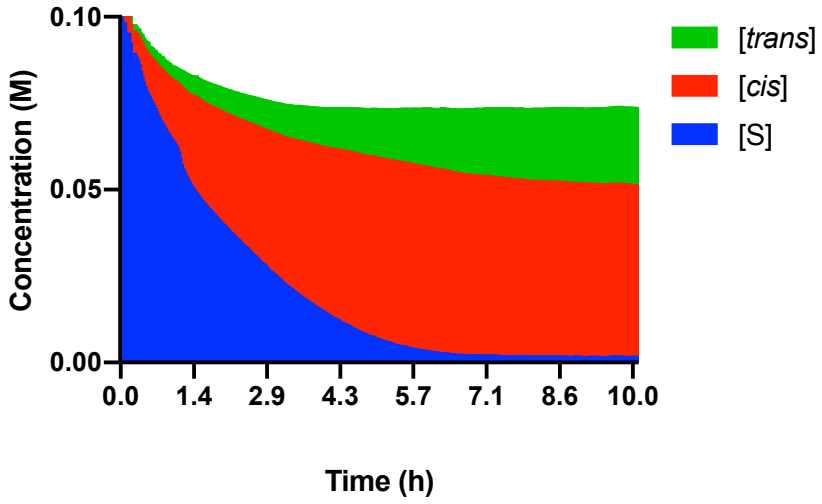

(b)

Figure 3.6: (a) Plot of concentration of *cis*- and *trans*-**173** with time once the starting material was completely consumed.(b) Plot of concentration of starting material, *cis*- and *trans*-**173** normalised to 0.1.

The ratio *cis*/*trans* was analysed together with the concentration of the starting material normalised to 100 so that the ratio of the two diastereomers is easily comparable to the progress of the reaction and at the concentration of the starting material in the reaction mixture (Figure 3.7).

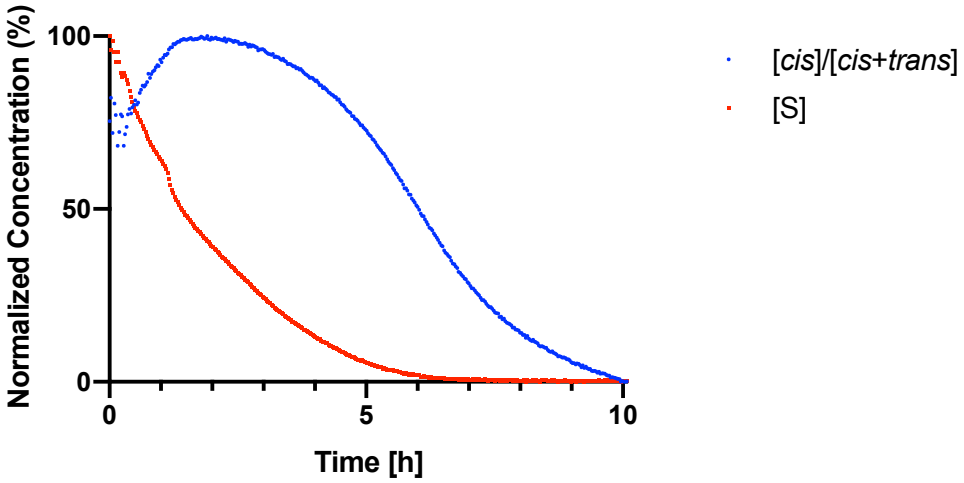

Figure 3.7: Plot of *[cis]/([cis]+[trans])vs* time to study the ratio of formation of *cis*-**173** and *trans*-**173** in comparison with the progress of the reaction. The concentration of the starting material was normalised to 100 in order to compare the different species during the progress of the reaction.

At first, both diastereomers are formed even if the concentration of the *cis* is still higher then the *trans*. Then, there is an increase on the production of *cis*-**173** up to a maximum at 2.62 h. The decline in the rate of formation of *cis*-product is likely to be linked to the decrease in the concentration of substrate present. In contrast to the beginning of the reaction, the catalyst at this point could condense into both product **173** or substrate **214** thus slowing down the formation of the *cis*-product.

In conclusion, the preliminary kinetic profile of the 5-*exo*-*trig* cyclisation catalysed by **29** highlights the fact that to isolate the product with the hightest ratio of *cis* diastereomer, the reaction must be stopped before full consumption of starting material and a decrease of temperature might reduce diastereoselectivity degradation that accelerates as soon as the concentration of product is higher than the concentration of starting material.

3.3.4.2 Kinetic profiles of reactions catalysed by MacMillan and Hayashi-Jørgensen catalysts

The determination of the kinetic profile of the 5-e*xo-trig* cyclisation catalysed by the bifunctional tetrazole catalyst **29** led to a general understanding of the reaction. The comparison of the obtained results with kinetic profiles of the same intramolecular reaction catalysed by other catalysts could provide significant information about the efficacy of the chosen tetrazole catalyst **29** for the synthesis of the *cis*-5-membered ring **226**. A preliminary kinetic study of the 5-*exo-trig* cyclisation was performed with Macmillan and Hayashi-Jørgensen catalysts. A 0.1M solution of substrate **214** in CD_2Cl_2 was reacted respectively with 5 mol% of catalyst **85** and **53** and the reaction was monitored *in situ* at 25 °C to achieve *cis*- and *trans*-**173** (Scheme 3.18). The reaction was also performed in larger scale at rt and at 0 °C and the results were presented in Table 3.2 and Table 3.5 at the beginning of this chapter. The reaction

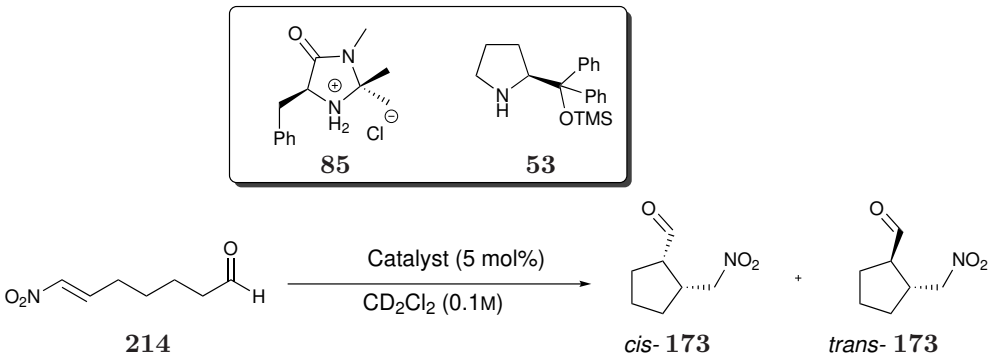

Scheme 3.18: Kinetic study performed at 25 °C and monitored *in situ* by ^{1}H NMR spectroscopy.

performed in the presence of Macmillan catalyst **85** did not go to completion in 12 hours. The highest concentration of the *cis* diastereomer was formed during the first hour of the reaction and then it slightly decreased over time. The *trans* was the main product of this reaction and the initial reaction rates are 3.4 x 10^{-3} mol L^{-1} s^{-1} for the *cis* formation and 4.4 x 10^{-3} mol L^{-1} s^{-1} for the *trans* formation (Figure 3.8).

The reaction catalysed by Hayashi-Jørgensen catalyst **53** went to completion in 4 hours (Figure 3.9). The concentration of the starting material decreases in a linear way, which could be associated to a 0^{th} order of the reaction. However, at 60.3 minutes the concentration of substrate is shifted from the expected linear trend and this could be related to the autocatalytic effect of the product formed.

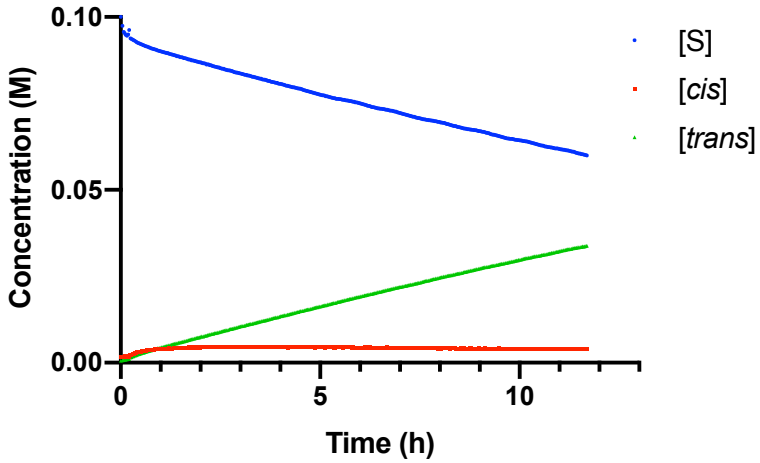

(a)

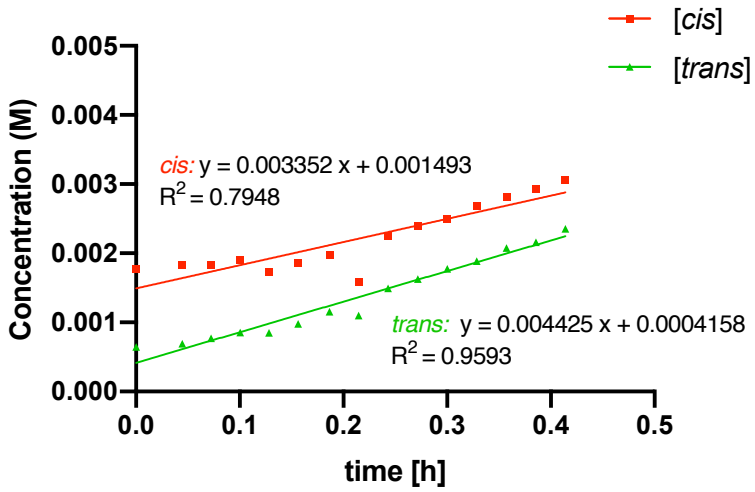

(b)

Figure 3.8: Kinetic profile of the 5-*exo-trig* cyclisation catalysed by Macmillan catalyst **85**.

The concentration of the nitro alkane formed is at this point of the reaction high enough that the acidic protons in α-position to the nitro group could behave as acidic co-catalyst, accelerating the reaction as reported by Burés and co-workers for a similar nitro-Michael addition.[132] Diastereoselectivity degradation is also observed in the presence of the Hayashi-Jørgensen catalyst **53** at a much higher rate than for catalysts **29** and **85**, especially once the concentration of the substrate is lower than the concentration of the products (Figure 3.9). The rate of the reaction for *cis*- and *trans*-**173** formation are respectively 3.4 x 10^{-4} mol L^{-1} s^{-1} and 2.5 x 10^{-4} mol L^{-1} s^{-1}.

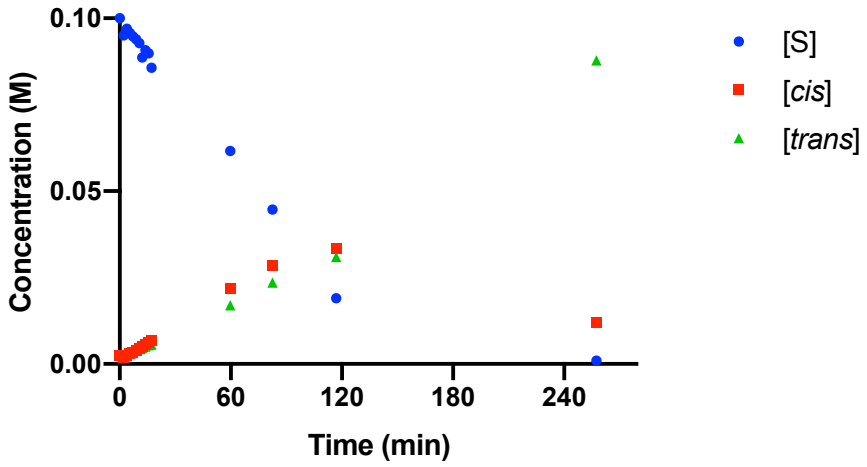

(a)

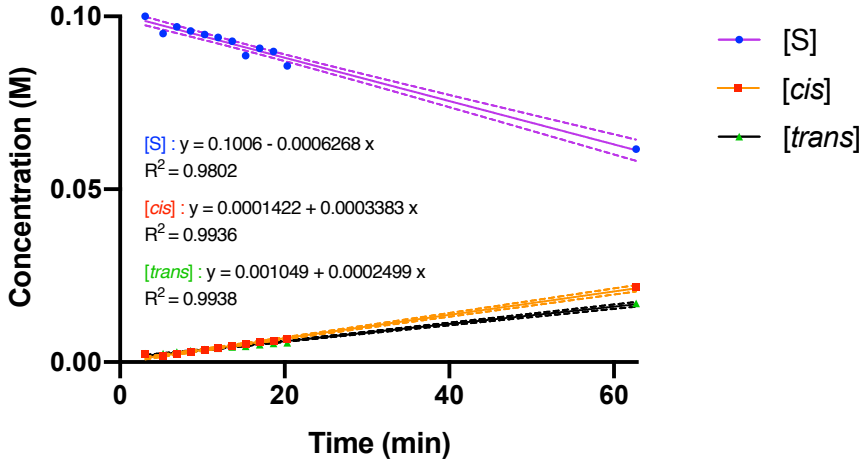

(b)

Figure 3.9: Kinetic profile of the 5-*exo-trig* cyclisation catalysed by Hayashi-Jørgensen catalyst **53**.

In summary, the kinetic profiles of the same reaction catalysed by different secondary amine catalysts (**29**, **85** and **53**) exhibit different reactivity between the three cases. All studied reactions presented a higher concentration of *cis* diastereomer at the beginning of the reaction but only the reaction catalysed by 5-(pyrrolidin-2-yl)-1H-tetrazole (**29**) maintains a high concentration nearly to the end of the reaction. The reaction catalysed by the Hayashi-Jørgensen catalyst **53** shows a similar rate of *cis* and *trans* production, however a drastic diastereoselectivity degradation is observed as soon as the starting material concentration is lower than the concentration of the *cis* and *trans* product, whereas the reaction catalysed by the Macmillan catalyst **85** presents a fast conversion of the *cis* diastereomer to the most stable

trans.

3.3.4.3 Enantioselective study

An investigation on diastereoselectivity degradation was performed. One of the reasons that could lead to the conversion of *cis*- to *trans*-product could be assigned to an epimerisation on C2.

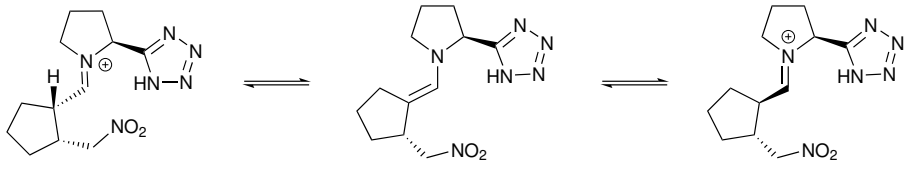

267 **268** **269**

Scheme 3.19: epimerisationmechanism from *cis* to *trans* diastereomer.

In this case the proton α to the carbonyl has a pk_a of $\sim$ 15 and it is likely that once the product is formed and the concentration of the substrate is lower than the concentration of the product, the catalyst can condense again into the formed cyclic aldehyde and promote the epimerisationto the more stable *trans*-product. A retro-Michael reaction could also hypothetically occur because of the acidity of the protons in the α-position to the nitro group, promoting the opening of the cycle again. The following cyclisation could lead to the more stable thermodynamic *trans*-product **273**, however the opening of the cycle to **272** would make accessible all four enantiomers (Scheme 3.20).

In order to gain a better understanding of the mechanism of the reaction, an enantioselective study was performed (Table 3.11). The reaction was carried out under the same reaction conditions used for the NMR kinetic study at rt in CH_2Cl_2 (0.1M) and in the presence of 5 mol% of the catalyst (Table 3.11). After 2 hours, 14

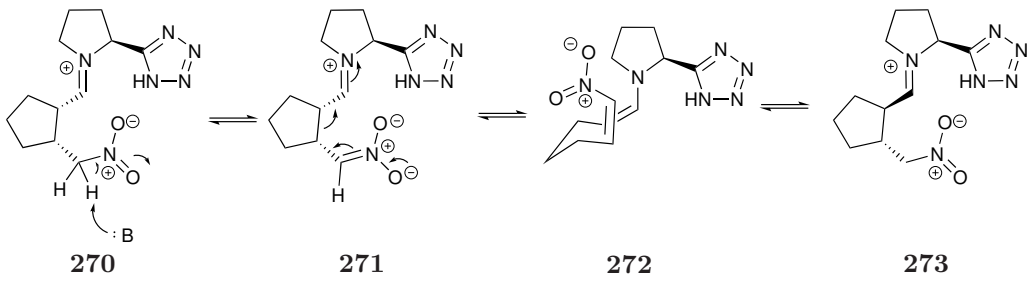

270 **271** **272** **273**

Scheme 3.20: Retro-Michael reaction mechanism leading to the conversion of the *cis* diastereomer to the *trans* one.

Table 3.11: Enantioselective study of 5-*exo-trig* cyclisation.

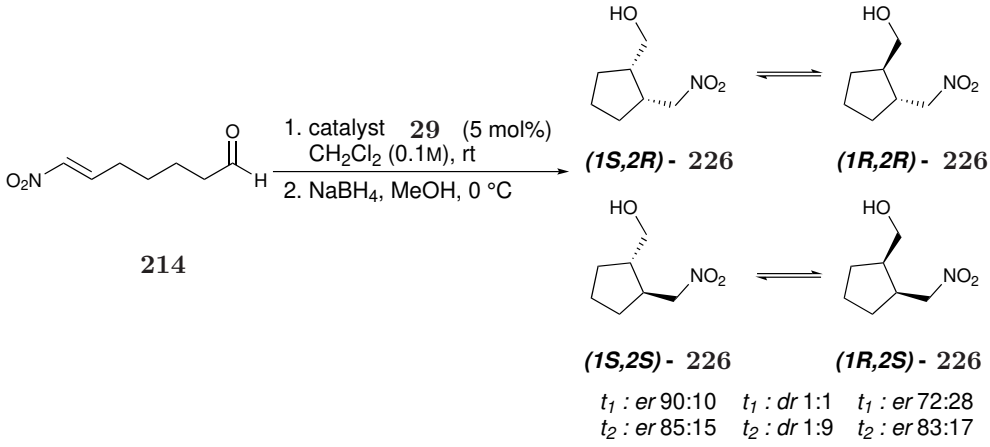

Entry	Time [h]	Yield [%]	*dr* (*cis*/*trans*)	*ee* − *cis*[%]	*ee* − *trans*[%]
1	2	62[i]	55:45	80	43
2	23	64	11:89	70	66

mL out of 28.7 mL of the reaction mixture was transferred in to a separate flask and the reaction was reduced *in situ* with $NaBH_4$ at 0 °C to afford **226** in 62% yield, 1:1 *dr*, 80% *ee* for the *cis* diastereomer and 44% *ee* for the *trans* diastereomer. The rest of the reaction mixture was left stirring at rt for 23 hours and then reduced *in situ* to achieve **226** in 64% yield. Diastereoselectivity degradation to 1:9 *dr* in favour of the *trans* was then observed. Enantioselectivity diminished to 70% *ee* for the *cis*-**226** and raised to 66% *ee* for the *trans*-**226**. Examining the ratio of the four enantiomers during and after the reaction, one can notice a redistribution driven by thermodynamics converting both *cis*-products to their respective C1-epimeric *trans*-products (Figure 3.10). The normalised concentration to 100 of each enantiomer was calculated at two different times (2 h and 23 h from beginning of the reaction) and it was possible to observe that the major *(1S,2R)-cis*-enantiomer concentration decreased as much as the major *(1R,2R)-trans*-enantiomer increased. In a similar manner the minor *(1R,2S)-cis*-enantiomer decreased in concentration as much as the minor *(1S,2S)-trans*-enantiomer increased (Figure 3.10). Change of stereochemistry of only one chiral centre led to an increase of enantioselectivity of the *trans*-product and a decrease of enantioselectivity of the *cis*-product. As a consequence, the overall impression given is that the *trans*-adduct becomes increasingly enantioenriched as more of the corresponding *cis*-adduct epimerises to it. On the other hand, the

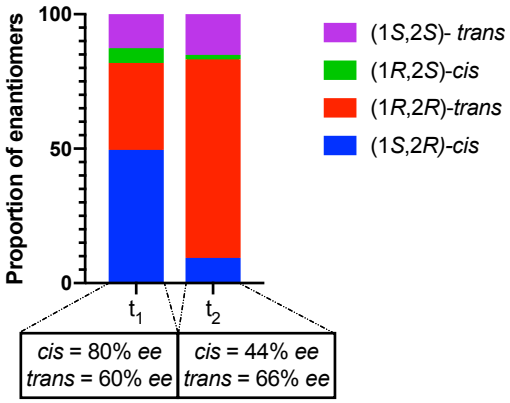

Figure 3.10: Concentration of the four enantiomers normalised to 100 at 2 and 23 h in order to exhibit the corresponding change of concentration of enantiomer *(1R,2S)-cis*-**173** to *(1S,2S)-trans*-**173** and of enantiomer *(1S,2R)-cis*-**173** to *(1R,2R)-trans*-**173**.

decrease of enantioselectivity of the *cis*-enantiomer can be explained by the fact that the high difference of concentration of the two enantiomers leads to the epimerisation in greater quantities of the major *(1S,2R)-cis* enantiomer, likely *via* 1^{st} order kinetics, and ultimately adversely effecting the *er* of that system. Theoretically, a retro-Michael reaction could also lead to the conversion of *cis*-enantiomers to the more thermodynamically favoured *trans*-enantiomers (Scheme 3.20). Interestingly, however, this study shows that the enantiomeric ratio of the *trans*-product is not maintained as one would expect if this were the case, but instead undergoes an enantioenrichment (Figure 3.10).

To conclude, epimerisation at C2 could be considered the major cause for the diastereoselectivity degradation, however we cannot exclude a scenario where epimerisation and, at a less significant level, retro-Michael reaction are both occurring.

3.3.4.4 Mechanistic Proposal Assisted by a Computational Study

The 5-*exo*-*trig* cyclisation under investigation was also analysed from a mechanistic point of view. Different enantioselectivity and reaction rates for the synthesis of *cis* and *trans* diastereomers suggest that the two diastereomers might be formed from two different intermediates following two different organocatalytic cycles. A mechanistic proposal is outlined in Scheme 3.21. First, the secondary amine catalyst **29** could condense into the aldehyde **214** forming the iminium ion **214a**. Then, following path A, the tautomerisation of the iminium ion to the enamine would form transition state **214b**, followed by the CC bond formation step to form the

CB intermediate **214d**. The protonation step would be the next following step that allows the opening of the oxazine oxide ring (OO) leading to the 5-membered ring iminium intermediate **214f** and the release of the *cis*-**173** product regenerating the free catalyst **29**. Path B would go *via* a similar mechanism, however the iminium ion **214a** would tautomerise to the different CC bond transition state **214b**. The following formation of an oxazine oxide intermediate OO **214e** instead of the CB would be expected because of *trans* conformers would lead to a twisted and unstable four membered ring. The protonation step would then allow the opening of the intermediate to lead to the final product *trans*-**173**.

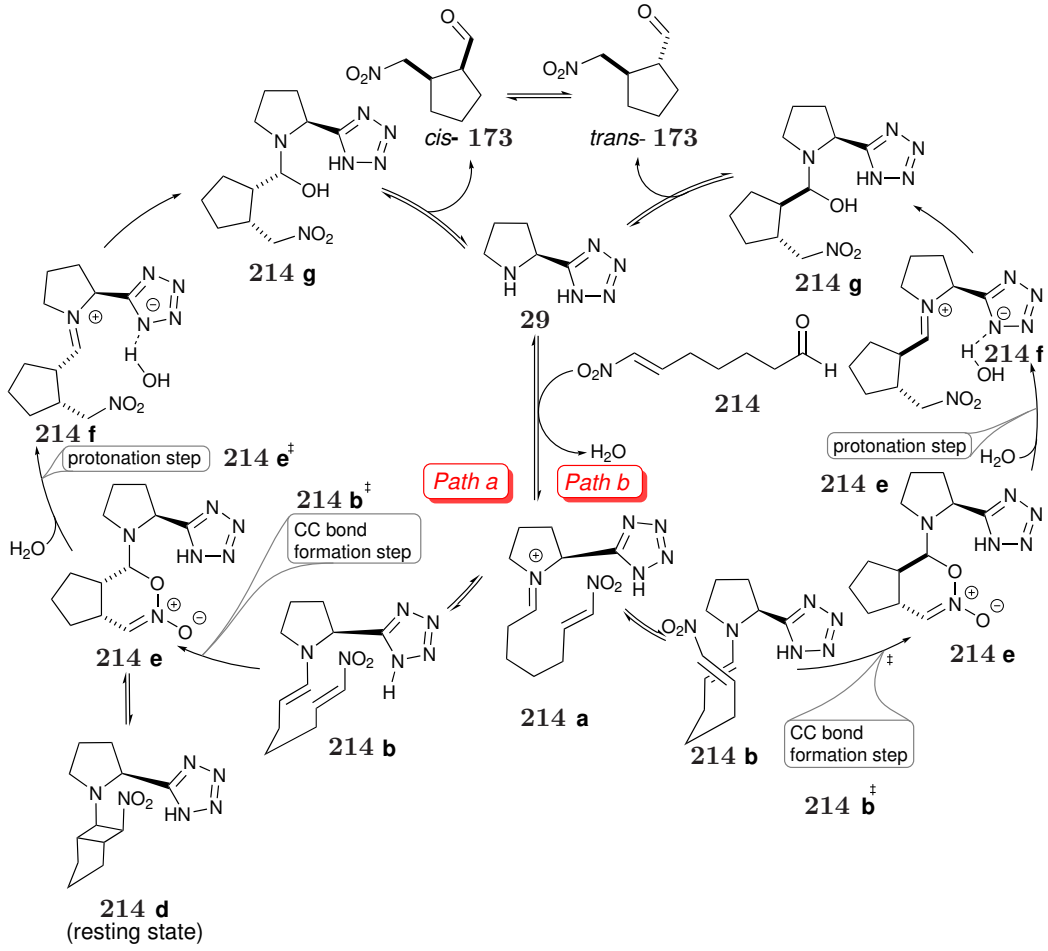

Scheme 3.21: Proposed organocatalytic cycle for the synthesis of *cis*- and *trans*-**173**.

The double cycle could explain the different enantioselectivity of the two diastereomers, therefore, in collaboration with Rosta and co-workers, a computational study was performed to investigate further the proposed mechanism of the 5-*exo*-*trig* cyclisation.[150–152] Calculated energies and Gibbs free energies were obtained at the

ω-B97X-D/6-311G(d,p) level of theory.

The study focused on the CC bond formation and on the protonation step in view of the fact that condensation of the catalyst into the aldehyde and final hydrolysis of the catalytic intermediate have already been extensively studied and reported in literature. In a similar manner to the intermediates observed by See-

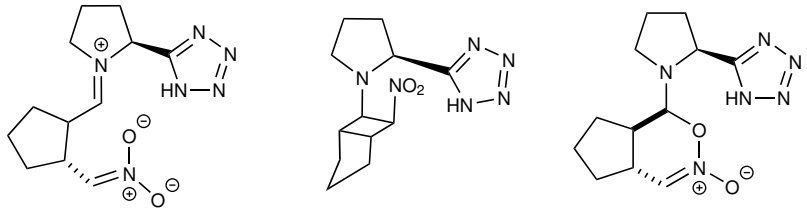

Figure 3.11: Possible intermediates after the CC bond formation.

bach, Hayashi,[34] Blackmond,[27,28,35,36] Wennemers,[38] Pihko and Papái[37,40] in studies performed with the Hayashi-Jørgensen catalyst (chapter 1), there are three intermediates the addition step can result in (Figure 3.11). In a moderately polar solvent such as DCE, the zwitterionic structure **214c** is thermodynamically unfavoured. The formation of a four-membered ring (**214d**) in a *trans*-configuration is rendered impossible due to extreme ring strain, while it is found to be rather stable in the *cis*-path, (although the applied level of theory might overestimate its stability). Thus the oxazine oxide (OO) **214e** intermediate is left the sole option in the *trans*-path, as shown in Scheme 3.21. A free energy profile at -20 °C was obtained (Figure 3.12). The CC bond forming step favoured the major *(1S,2R)-cis*-enantiomer with high enantioselectivity, whereas the protonation step favoured the major *(1S,2S)-trans*-enantiomer with low enantioselectivity. The free energy profile at -20 °C shows that the transition states for the CC bond forming step and the protonation step have similar energies, suggesting that the stereochemistry of the reaction is determined by both states. Experimental observations suggest that the computational model overestimates the barrier of the protonation step, which is likely to be due to the thermochemical correction and different molecularity. Thus, we assume that the initial selectivity is determined in the CC bond forming step and altered by the epimerisationdiscussed before. The obtained results suggest that the relative value of the two TS is heavily influenced by the entropy correction, thus uncertain, there-

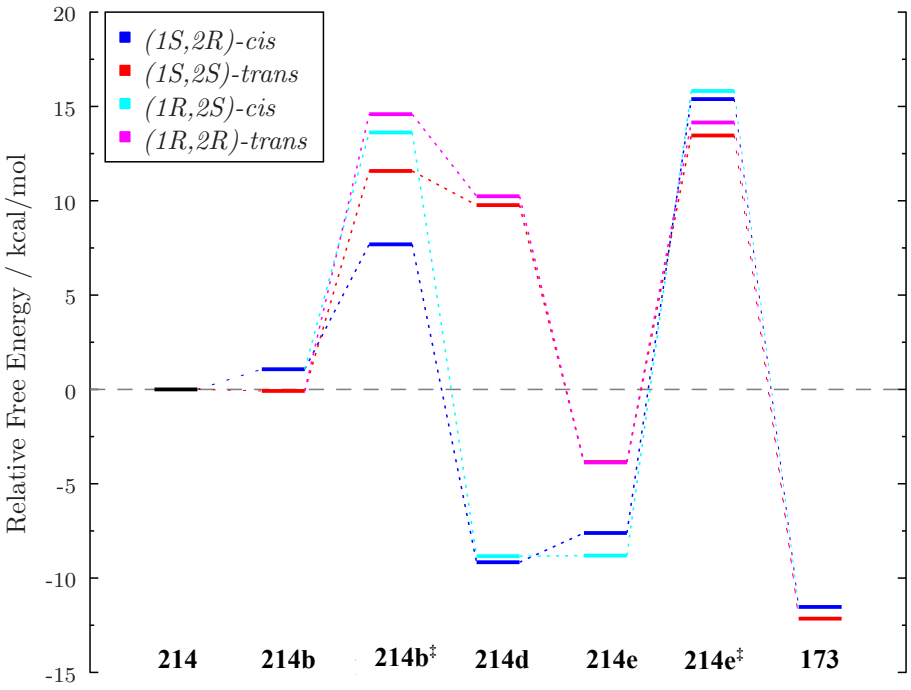

Figure 3.12: Free energy profile at -20 °C.

fore computation might overestimate the energy barrier height of the protonation step. In contrast with the free energy profile, electronic energy and solvent corrected electronic energy profiles at -20 °C were performed and it was found that the free energy of the transition states of the protonation step were much lower than those found in the free energy profile, exhibiting results that are in line with the experimental data as the major *(1S,2R)-cis*-**173** is the favoured enantiomer at -20 °C. The significant difference in free energy for the TS of the protonation step confirms that the computational experiments might overestimate the free energy of the TS of the protonation step (Figure 3.13(a)).

TS for the CC bond forming step were then determined showing that the tetrazole moiety is always involved in the reaction thus confirming the bifunctionality of the catalyst (Figure 3.14). The energy of CB **214d** and OO **214e** intermediates for each enantiomer were then calculated. The CB *trans* configuration results in a high energy twisted 4-membered ring rendering this unavailable in the *trans* paths, whereas the OO intermediate is possible for all diastereomers, although less stable than the CB in the *cis* structures. The formation of CB and OO intermediates is then followed by the protonation step. TSs for this final step were also identified.

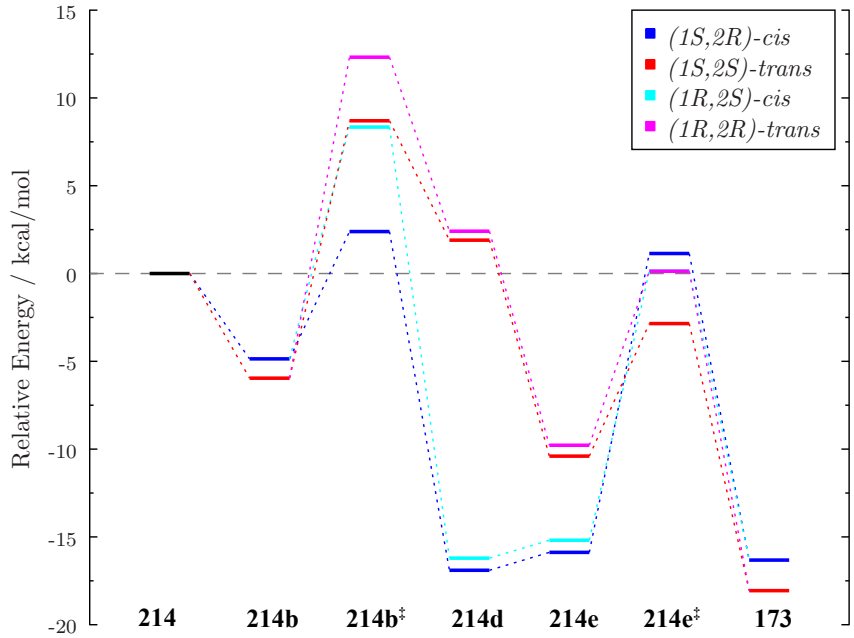

(a)

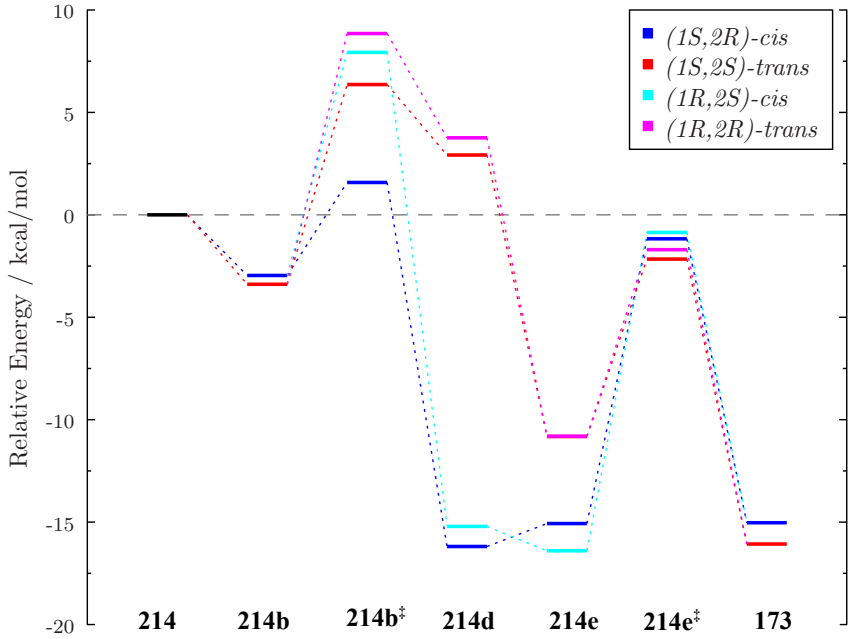

(b)

Figure 3.13: (a) Electronic energy profile at -20 °C; (b) Solvent corrected electronic energy profile at -20 °C.

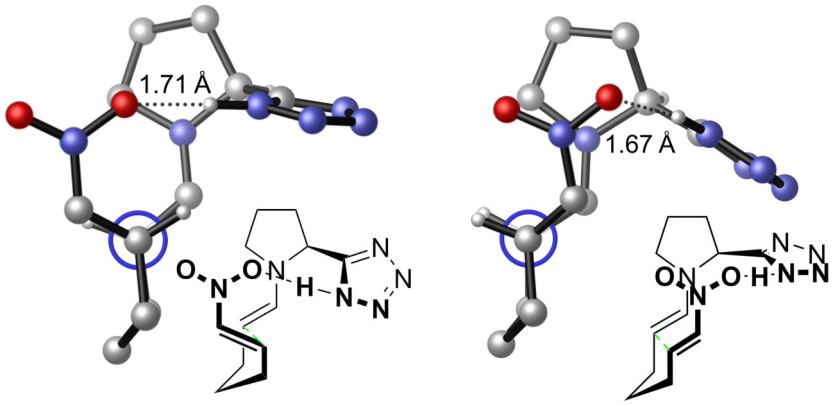

Figure 3.14: Transition states for the CC bond forming step.

The protonation step to form the hemiaminal product **214g** can occur in two ways. Either the oxygen of the water molecule undergoes a nucleophilic attack on the iminium carbon, which is unlikely since in abundant intermediates the centre does not bear a positive charge, or the water protonates the nitronate moiety ultimately breaking the oxazine oxide ring **214e** formed as intermediate. The latter scenario is favoured by the assistance of the tetrazole ring acting as a Brønsted acid to stabilise the transiently forming hydroxide anion. Interestingly, the protonation step favours the *trans* products, because the ring configuration enables a more concerted set of bonds forming and breaking as depicted in Figure 3.15. The relative free energies of the transition states of the aforementioned steps are close to each other. Due to the involvement of the water in the second step, the thermodynamic corrections,

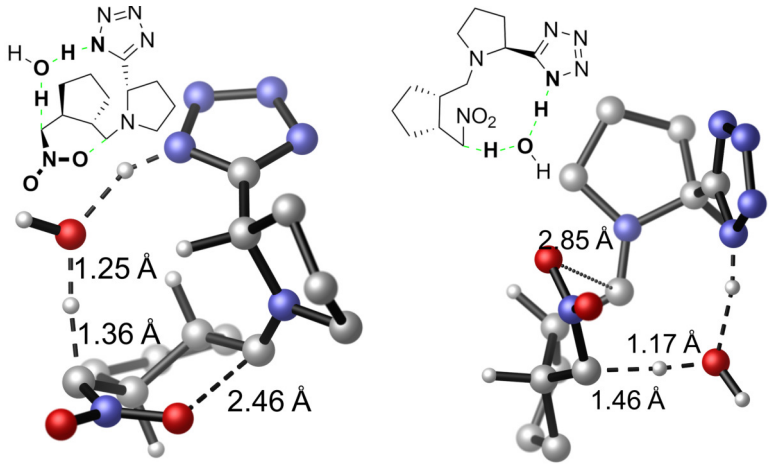

Figure 3.15: Transition states for the protonation step.

introduced as Grimme's qRRHO,[153] increase the uncertainty of the comparison of these steps, possible overestimating the barrier of the protonation step (chapter 6). The free energy profile was also obtained at rt and it was observed that changing the temperature, results in a change to the energy barrier of the protonation step (Figure 3.16). Nevertheless, the temperature dependence of the qRRHO term of the protonation transition state is considerably higher than the that of the first step (Figure 3.16), which may also account for the temperature dependent selectivity.

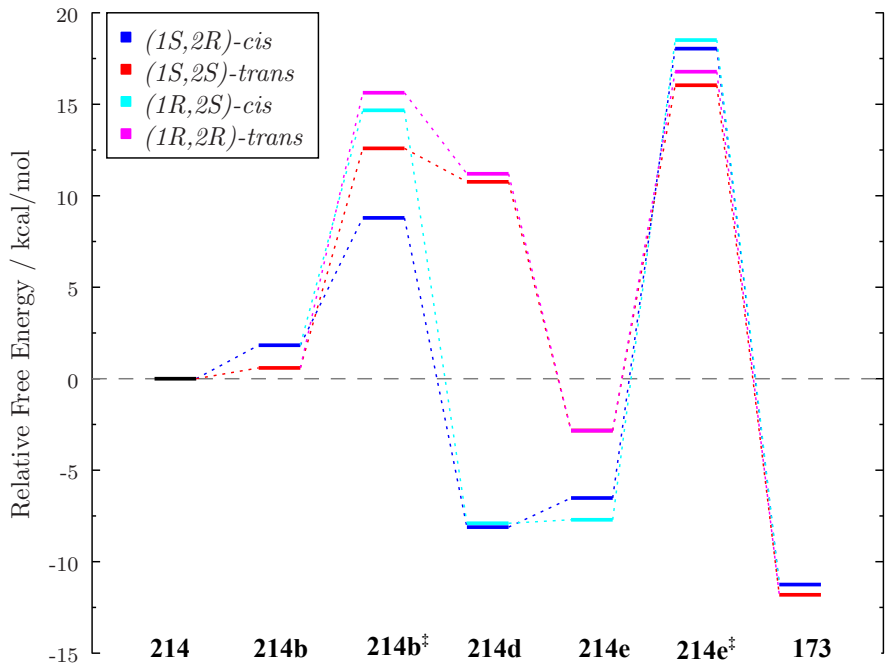

Figure 3.16: Free energy profile at 25 °C.

3.4 Conclusion

An initial catalyst screen at rt led to the understanding that the diastereoselectivity could be temperature controlled and a more detailed optimisation at lower temperature followed by an *in situ* reduction, guided the study to the isolation of the more unstable and more difficult to achieve *cis*-γ-amino acid precursor **226**. The reaction was then scaled up to 7 mmol and using only 5 mol% of the catalyst the targeted asymmetric product **226** was achieved in 74% yield with 9:1 *cis/trans* ratio and 92% *ee*. A substrate scope was carried out to prove the generality of the reaction. However, α-substituted nitro olefin substrates were unable to perform the intended

5-*exo-trig* cyclisation under the optimised conditions probably because of their substitution in α-position to the nitro group (Scheme 3.9). Different types of ketones were tested as alternative substrates, but only the methyl ketone **250a** presented significant results which confirmed that the bifunctional function of the catalyst is essential for the efficiency of the reaction (Scheme 3.11). Synthesis and cyclisation of nitrogen containing substrate **255** afforded **256** in 46% yield (Scheme 3.13). Finally, an indane derivative was also obtained in good yield (73%), 1:1 *dr* and good *ee* (-70% *ee*) for the *cis* diastereomer (Scheme 3.16). The project then focused on the understanding of the mechanism of the 5-*exo-trig* reaction. A kinetic study was performed and it was possible to see that the highest concentration of *cis*-**173** can be isolated before the complete consumption of starting material as the diastereoselective degradation is accelerated when the concentration of starting material is low. The kinetic profile of the reaction catalysed by tetrazole catalyst **29** was compared with the kinetic profile of reactions catalysed by the Macmillan catalyst **85** and the Hayashi-Jørgensen catalyst **53**. All studied reactions exhibited higher concentration of *cis* than *trans* diastereomer at the beginning of the reaction which then decreased with associated increased concentration of the *trans* diastereomer. This observation suggested that the control of diastereoselectivity degradation is crucial to efficiently isolate the *cis* product. An enantioselective study was also performed to gain a deeper understanding of the observed diastereoselectivity degradation and the agreement between the different changes in concentration of the four enantiomers proves that retro-Michael reaction is less likely compared to the epimerisation process. A computational study then confirmed a proposed double catalytic cycle and it was found that the rate determining step of the reaction might be able to change with temperature, which is extremely interesting in order to control the selectivity in the synthesis of different enantiomers.

3.5 Future work

This chapter describes a new methodology developed for the synthesis of *cis*-enantioselective γ-amino acid precursors. In the future the reaction could be performed in flow to develop an even more efficient isolation of the *cis* product. Proline and indane derivatives were synthesised using the developed methodology. The next steps would be the final synthesis of their respective γ-amino acids, **274** and **275**

respectively (Figure 3.17) leading to very interesting building blocks for pharmaceutical purposes.

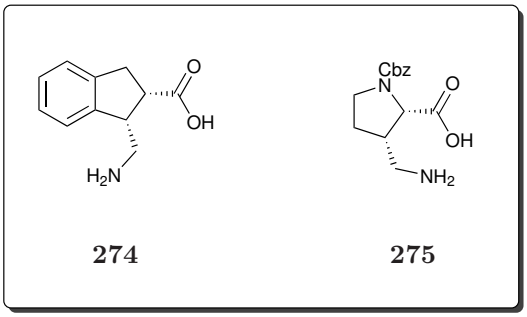

Figure 3.17: Respective γ-amino acid derived from substrates **266** and **256**.

Chapter 4

Foldamers

4.1 Introduction

The selection of constrained residues can lead to specific secondary structures, which might affect the biological function. More recently, research has focused on the synthesis of foldamers based on constrained cyclic-γ-residues to achieve a higher control of the secondary structure. Gellman and co-workers presented several studies where α/γ-peptides based on cyclic γ-residues were synthesised.[126,154–157] In 2009, they presented a synthesis of γ-amino acid residues containing a cyclohexyl constraint on the C_β-C_γ and a variable side chain at C_α. The enantio- and diastereoselective γ-residue was coupled with D-α-amino acid residues to achieve the heterogeneous tetramer **276** and hexamer **277** (Figure 4.1). The X-ray crystal structure of the synthesised foldamers showed a 12-helical secondary structure, which was also confirmed in solution with NOESY analysis (Figure 4.2).

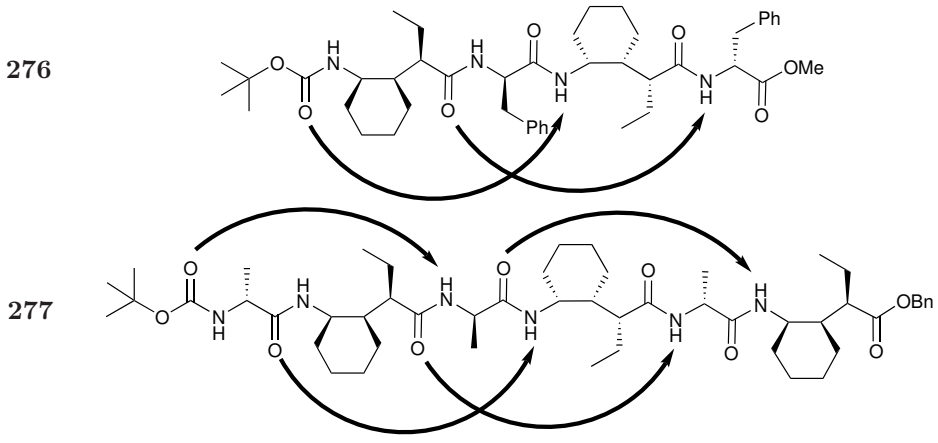

Figure 4.1: α/γ-Peptides **276** and **277** synthesised by Gellman and co-workers.

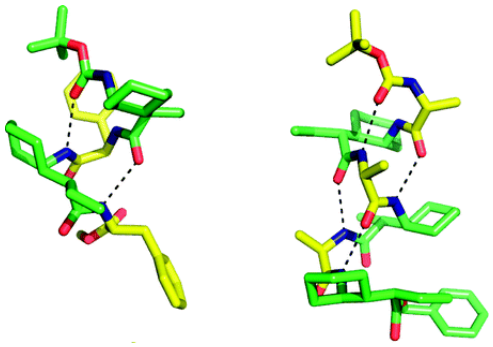

Figure 4.2: From left to right, X-ray crystal structure of tetramer **276** and hexamer **277**.[154]

In 2012, Gellman and co-workers built foldamers based on 6-membered ring γ-residues constraint on the C_α-C_β. Heterogeneous foldamers were generated by the combination of γ-residues with D-Ala or L-Ala respectively for the oligomers based on *trans* or *cis* residues (Figure 4.3).[157] They compared α/γ-peptides based on *cis*- and *trans*-γ-residues, interestingly the peptide based on *cis*-residues revealed a strong helix-propensity forming 12-helices (**278** and **279**), whereas peptides based on *trans*-residues (**280** and **281**) did not display any secondary structure (Figure 4.3).

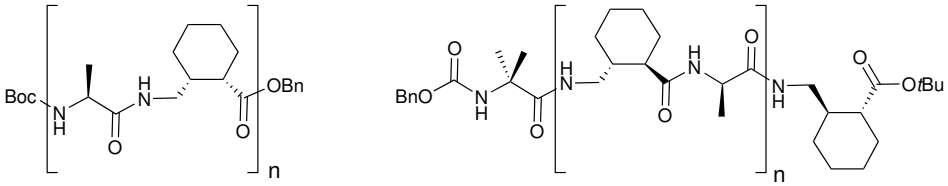

278 $n = 2$ **280** $n = 2$

279 $n = 3$ **281** $n = 3$

Figure 4.3: α/γ-peptides based on the *cis*- and *trans*-6-membered ring moieties synthesised by Gellman and co-workers.[157]

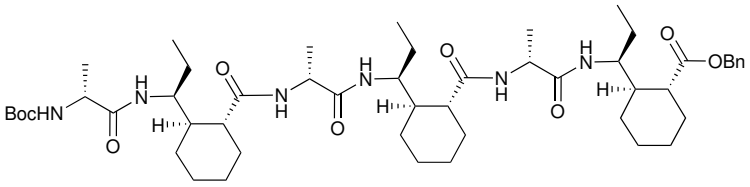

282

Figure 4.4: α/γ-peptide based on *trans*-6-membered ring residues and D-Ala synthesised by Giuliano and co-workers.[156]

In 2014, Gellman and co-workers proved that the introduction of a substituent in the γ-position can give higher control of the secondary structure leading to helical conformations even in peptides based on *trans*-6-membered ring γ-residues (Figure 4.4).[156] α/γ-Peptide **282** was found to fold into 12/10-helices.[156]

They then synthesised heterogeneous foldamers based on *trans*-γ-residues (1*R*,2*R*)-2-aminomethyl-1-cyclopentane carboxylic acid (AMCP, **227**) and D-Ala.[126] Enantio- and diastereoselective synthesis of *trans*-5-membered ring residues was undertaken *via* an organocatalysed Michael addition which produced *trans*-**227** in high yields, in 1:19 *cis/trans* ratio and high enantioselectivity (Scheme 4.1).

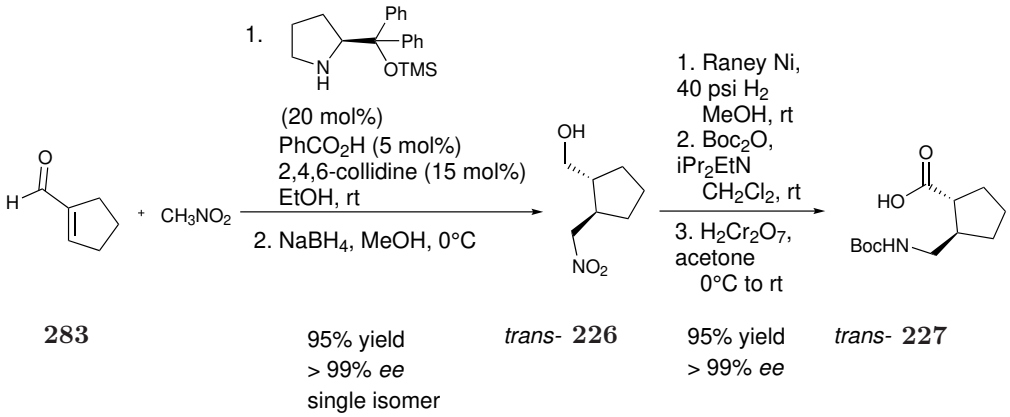

Scheme 4.1: Synthesis of the *trans*-**227** performed by Gellman and co-workers.[126]

With this study, they concluded that α/γ-peptides **285** and **286** moderately populate 12/10-helical conformations as well as other conformations, suggesting that this type of peptide do not display a tendency to adopt a specific secondary structure (Scheme 4.2).[126] In spite of the previous studies demonstrating that different residue isomers can lead to different conformational structures,[156,157] they only focused on the synthesis of peptides based on *trans*-AMCP residues.

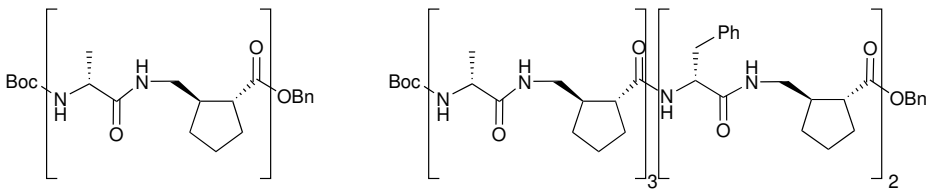

284 n = 3
285 n = 4

286

Scheme 4.2: α/γ-peptides based on *trans*-5-membered ring residues and D-Ala achieved by Gellman and co-workers.[126]

4.2 Aims and Objectives

Owing to difficulties found in the isolation of the enantioselective (1*S*,2*R*)-2-(nitromethyl)cyclopentane-1-carboxylic acid (*cis*-AMCP **287**),[125,126] syntheses of foldamers based on *cis*-5-membered ring γ-amino acid building blocks have not been previously explored (Figure 4.5). After the development of the enantio- and diastereoselective synthesis of the 5-membered ring *cis*-γ-amino acid precursor **226** described in chapter 3, the aim of this chapter was the synthesis of foldamers based on *cis*-AMCP **287** residues. Herein a discussion of synthesis and structural characterisation of the desired γ/α-peptides is presented.

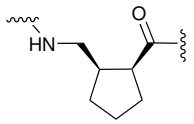

287

Figure 4.5: *Cis*-AMCP-γ-residue subject of this study.

4.3 Results and Discussion

4.3.1 Synthetic procedure

Nitroalcohol *cis*-**226** synthesised using the organocatalytic procedure described in chapter 3 was oxidized to carboxylic acid **288** in 92% yield. Alanine was chosen as α-residue to couple with γ-units to synthesise heterogeneous γ/α-peptides in a similar manner to those presented by Gellman and co-workers for the synthesis of oligomers based on *trans*-AMCP-residues.[126]

Both nitro-dimers with D-Ala (**289**) and with L-Ala (**290**) were synthesised (Scheme 4.3 and Scheme 4.4).

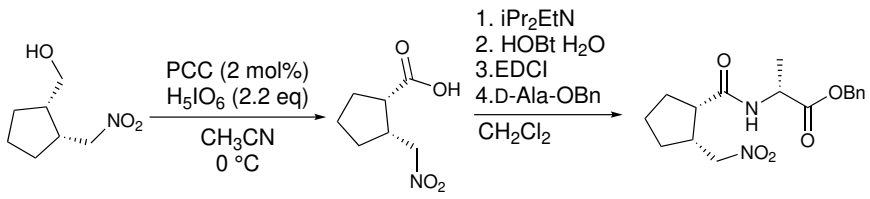

226 92% yield **288** 34% yield **289**

Scheme 4.3: Synthesis of the nitro-dimer **289**.

The carboxylic acid **288** was coupled with D-Alanine benzyl ester to afford the nitro-dimer **289** in 34% yield (Scheme 4.3), and with L-Alanine benzyl ester *p*-toluenesulfonate salt to achieve the nitro-dimer **290** in 43% yield (Scheme 4.4).

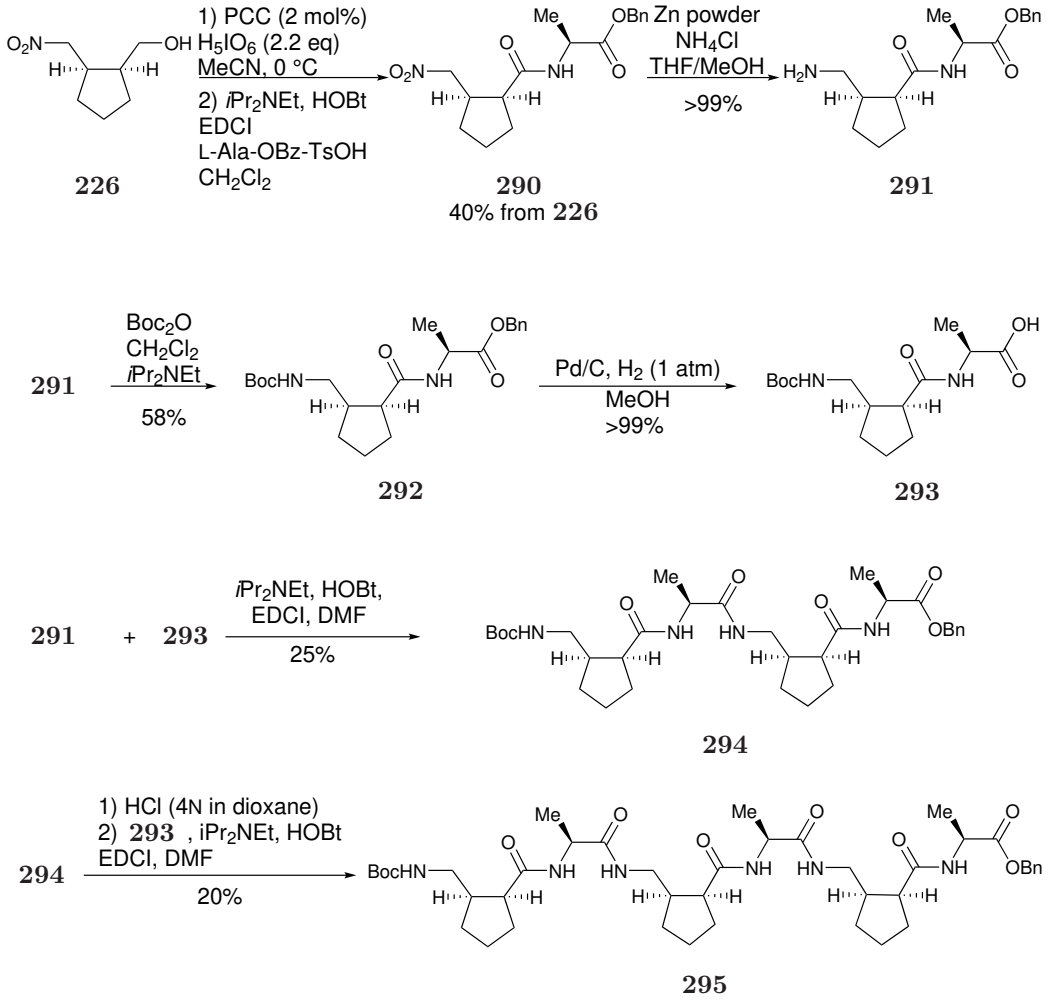

Scheme 4.4: Synthetic procedure for the synthesis of α/γ-peptides **292**, **294** and **295**.

However, comparing the oligomer based on the 5-membered ring with oligomers based on a *cis*-6-membered ring unit[157] and performing preliminary structural predictions using ChemDraw 3D software, L-Ala was considered more suitable for the synthesis of oligomers with a well defined secondary structure, therefore only the synthesis of these types of foldamers were pursued.[156] The nitro group of the nitro-dimer **290** was reduced to the amine and then protected to afford the dimer **292** in 58% yield.

Instead of generating α/γ-peptides, γ/α-peptides were synthesised.[126] This synthetic choice was carried out taking into account that *cis*-AMCP moieties are prone

to epimerisation at the C-terminus as previously shown in chapter 3. It is reported that α-amino acids tend to epimerise at the C-terminus under peptide coupling conditions and for this reason Gellman and co-workers deprotected the acid moiety on the γ-residue. The hypothesised intermediate that leads to the epimerisation is an oxazolone formed after the activation of the carboxylic acid. Activations of the carboxylic acids for the synthesis of the α/γ-peptide **298** and the γ/α-peptide **302** were compared (Scheme 4.5).

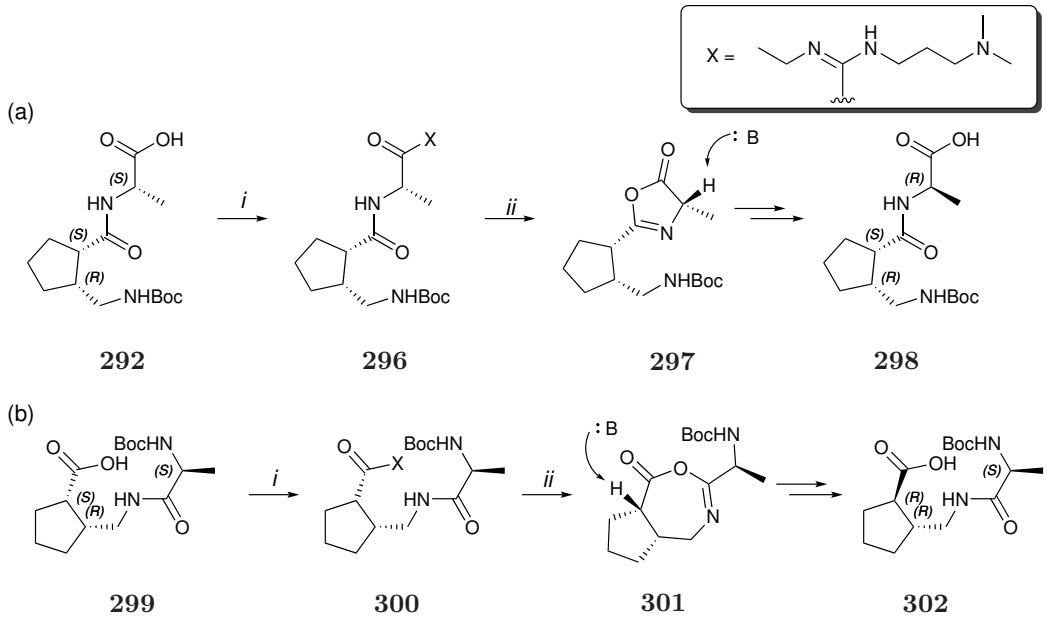

Scheme 4.5: (*i*) activation, (*ii*) cyclisation. (a) Possible epimerisation mechanism for the activation of the α-residue. (b) Possible epimerisation mechanism for the activation of the γ-residue.

The activation of the carboxylic acid on the γ-residue might lead to the formation of a 7-membered ring which is enabled by Baldwin rules in a similar manner to the formation of the 5-membered ring and therefore it might lead to the epimerisation of AMCP residues (Scheme 4.5).[158,159] As a result the coupling was performed by deprotecting the acid moiety of the α-residue. This was believed to create less epimerisation in comparison to the deprotection of the γ-unit. The minimal amount of opposite diastereomer formed by the epimerisation of L-Ala residue was easily separated by flash chromatography. Furthermore, HOBt and EDCI were chosen as coupling reagents in order to minimise the epimerisation process.

Following the coupling with L-Ala, a reduction of the nitro group of **290** produced amine **291** in quantitative yield which was then protected to achieve dimer

292 in a 58% yield (Scheme 4.4). γ/α-Peptide **292** was then deprotected on the acid moiety to give **293** and then coupled with the free amine **291** to obtain tetramer **294** in 25% yield over the last three steps. Finally, the amine of tetramer **294** was also deprotected and coupled with the free acid **293** to achieve hexamer **295** in 20% yield (Scheme 4.4). The decreased yield of coupling with increased chain length can be accounted for the epimerisation on the C-terminus of L-Ala yielding to different diastereomers of the oligomer.

4.3.2 Structural characterisation of the synthesised γ/α-peptides

4.3.2.1 X-ray Crystallography

The stereochemistry of the dimer precursor **290** was confirmed by X-ray crystallography (Figure 4.6). The single crystal was obtained after slow evaporation at 4 °C in a mixture of $CHCl_3$ and heptane (v/v 1:3).

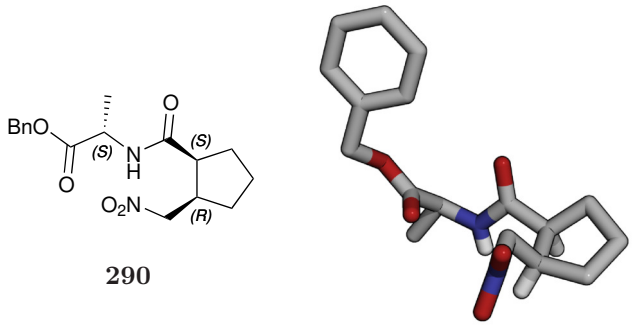

290

Figure 4.6: X-ray crystal structure of compound **290**.

Dimer **292** was also crystallised with slow evaporation at 4 °C in a mixture of $CHCl_3$ and heptane (v/v 1:3). The length of the crystallised γ/α-oligomer **292** was still too short to observe any H-bonds, therefore the crystal structure's dihedral angles were compared to those obtained from the computational study, which will be discussed later in the chapter.

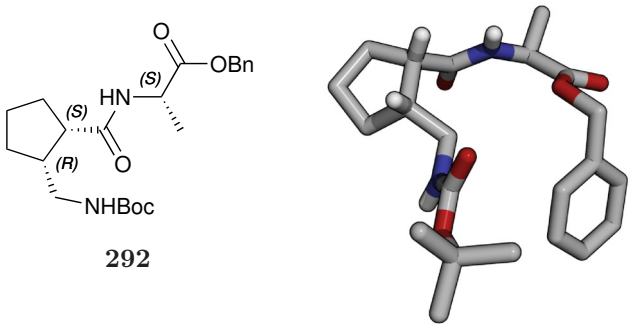

292

Figure 4.7: X-ray crystal structure of α/γ-peptide **292** (CCDC: 1947227).

4.3.2.2 γ/α-Peptides NMR characterisation

Structural characterisation of γ/α-oligomers **294** and **295** was performed using 1D and 2D NMR spectroscopy (COSY, TOCSY, ROESY, HSQC and HMBC), however chemical shift overlap prevented the assignment of ring protons of **295**.

NOEs cross peaks of γ/α-peptide **294** were poor. This may be related to the short length of the peptide which prevents it from folding. However, **294** based on *cis*-γ-residues exhibits a higher number of H-bond interactions than the correspond-

Table 4.1: ^{1}H NMR spectra and δ (ppm) for the characterisation of α/γ peptide **294** recorded at rt in 0.2 mM in $CDCl_3$ (600 MHz).

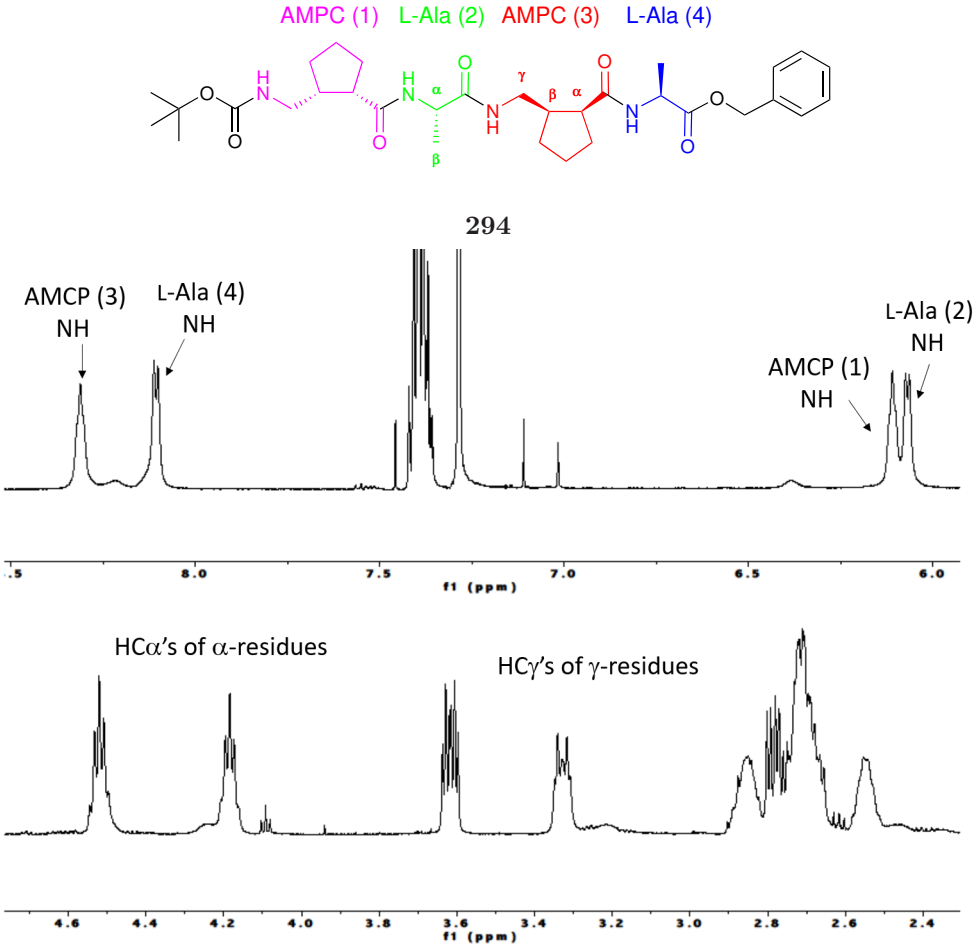

Residue	Hα [ppm]	Hβ [ppm]	Hγ1 [ppm]	Hγ2 [ppm]	NH [ppm]	CH_2 [ppm]
AMCP(1)	2.73	2.54	3.33	2.69	6.10	-
L-Ala(2)	4.19	1.41	-	-	6.08	-
AMCP(3)	2.71	2.87	3.62	2.79	8.31	-
L-Ala(4)	4.52	1.45	-	-	8.11	-
Benzyl	-	-	-	-	-	5.23

ing oligomer based on *trans*-γ-residues (Table 4.1 and Figure 4.8).[160] γ/α-Peptide **294** showed two downfield amide peaks ($\delta > 7$ ppm) in contrast with same length oligomer based on *trans*-γ-residues reported by Gellman and co-workers, which presented only one amide peak just above 7 ppm (Scheme 4.2).[126] The different outcome for the two different oligomers may be accounted for the different stereochemistry of the γ-residues influencing the oligomers conformation.

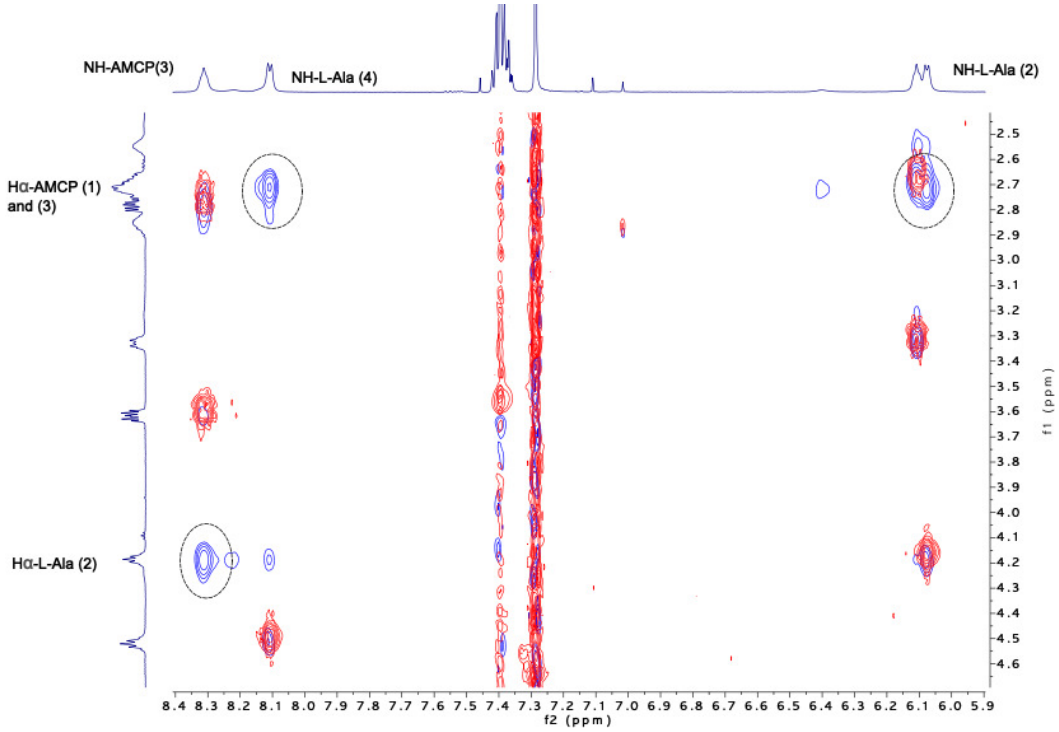

Figure 4.8: Overlap of TOCSY (red) and ROESY (blue) 2D NMR spectra for the assignment of the sequential residues of γ/α-peptide **294**. The spectra were recorded at rt, in a 0.2 mM solution in $CDCl_3$ (600 MHz).

The residues of γ/α-oligomer **295** were also identified *via* 2D NMR spectroscopy. First, L-Ala (6) was identified *via* HMBC NMR: the benzylic carbonyl was assigned *via* a cross peak with the benzylic methylene; the carbonyl then would also display another cross peak with the HC[α] (6) confirming the assignment of L-Ala (6) residue. The rest of the consecutive assignments were done *via* ROESY cross peaks of the HC[α](i) with the NH (i+1) of the following residue (Table 4.2 and Figure 4.9).

Table 4.2: ^{1}H NMR spectra and δ (ppm) for the characterisation of α/γ peptide **295** recorded at rt in 0.2 mM in $CDCl_3$ (600 MHz).

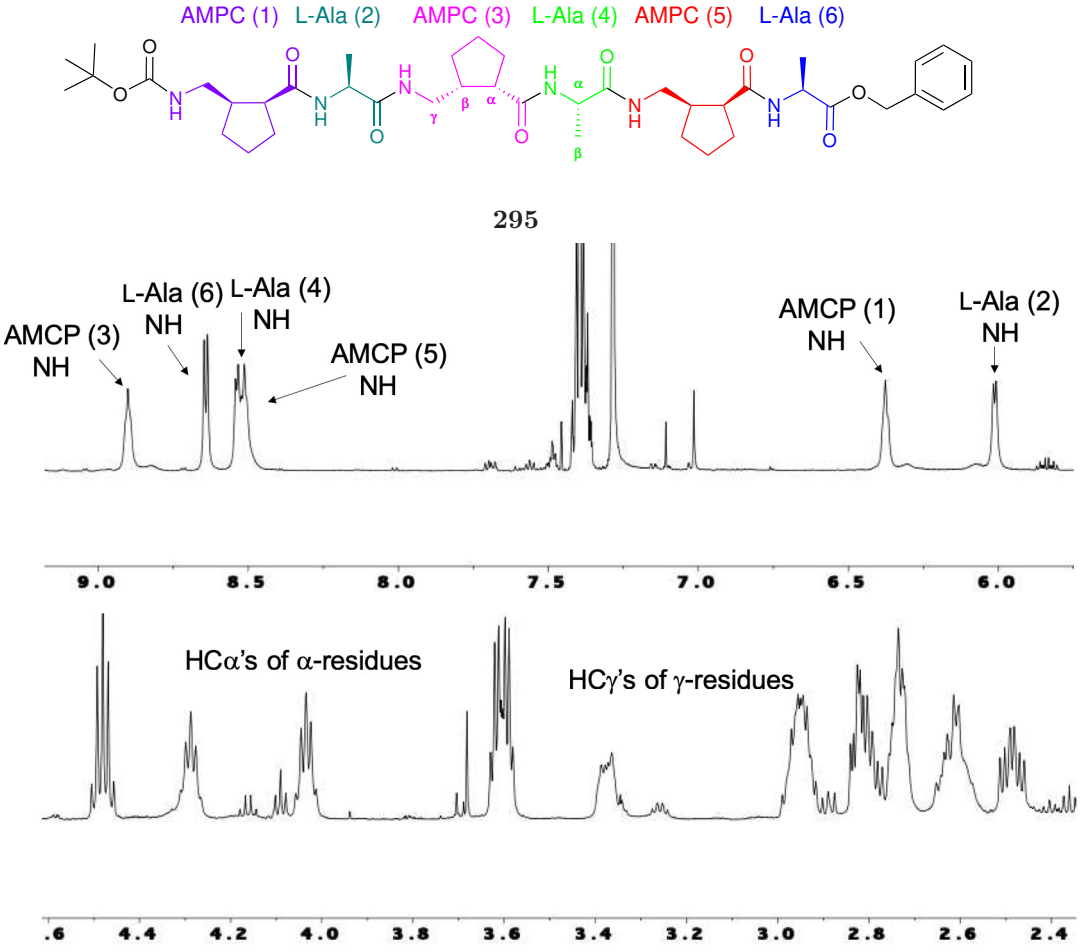

Residue	Hα [ppm]	Hβ [ppm]	Hγ1 [ppm]	Hγ2 [ppm]	NH [ppm]	CH_2 [ppm]
AMCP(1)	2.73	2.6	3.38	2.61	6.38	-
L-Ala(2)	4.29	1.44	-	-	6.01	-
AMCP(3)	2.74	2.95	3.60	2.48	8.90	-
L-Ala(4)	4.03	1.39	-	-	8.54	-
AMCP(5)	2.82	2.95	3.61	2.80	8.51	-
L-Ala(6)	4.48	1.41	-	-	8.64	-
Benzyl	-	-	-	-	-	5.24

It is possible to observe that four out of the six amide peaks are displayed at chemical shifts > 7.0 ppm, characteristic sign of H-bonded protons (Figure 4.9).[160]

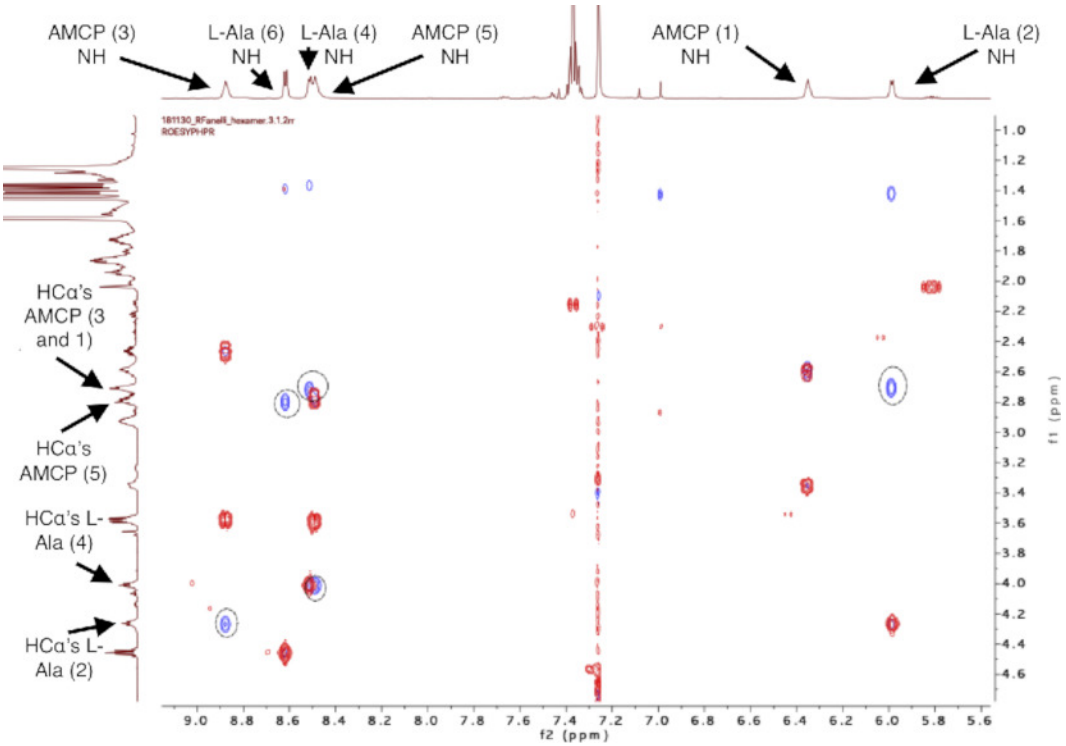

Figure 4.9: Overlap of TOCSY (red) and ROESY (blue) 2D NMR spectra for the assignment of sequential residues of the γ/α-peptide **295**. The spectra were recorded at rt, in a 0.2 mM solution in $CDCl_3$ (600 MHz).

4.3.2.3 Aggregation control experiment

An aggregation control experiment was conducted on hexamer **295** to prove there was no self-association and confirm that the downfield detected amide peaks are due to intramolecular interactions rather than intermolecular interactions. ^{1}H NMR of γ/α-peptide **295** was measured in $CDCl_3$ at different concentrations (0.04mM – 4 mM). This experiment displays the amide peaks at the same chemical shifts for all different concentrations, which confirms the fact that the downfield NH peaks are due to intramolecular H-bonds, rather than intermolecular H-bonds (Figure 4.10).[126,160] The experiment was conducted on the longest oligomer that was synthesised (**295**), which is also the one that presents a more defined secondary structure.

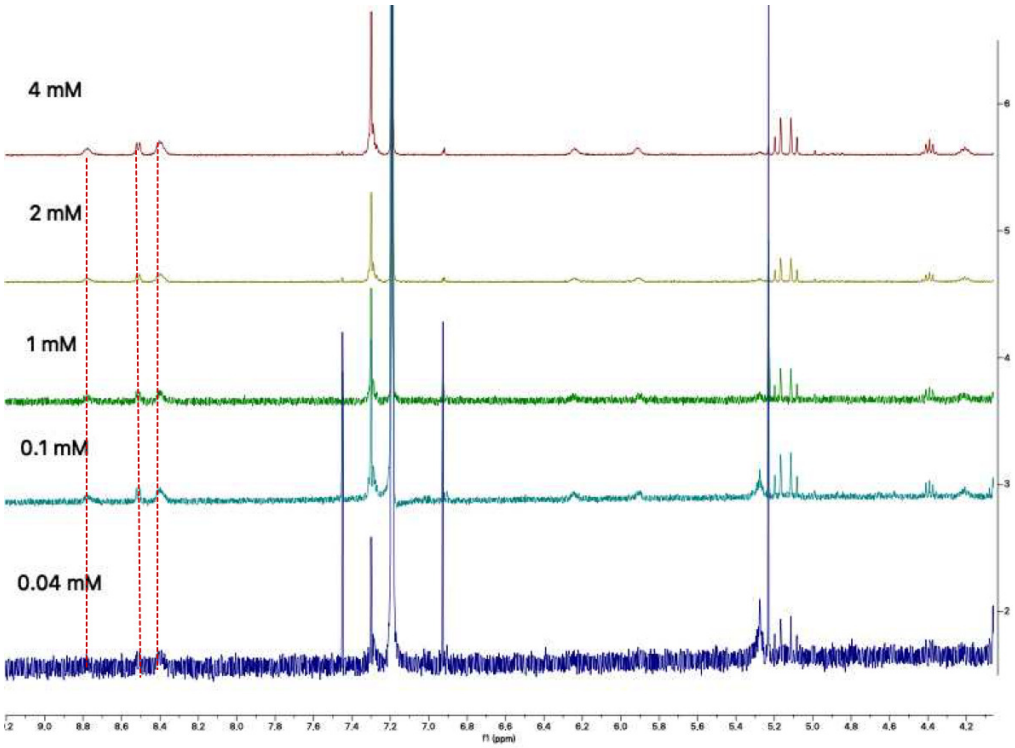

Figure 4.10: ^{1}H NMR spectra (400 MHz) in $CDCl_3$ of the γ/α-peptide **295** at 0.4, 0.1, 1, 2 and 4mM concentration for an aggregation control experiment.

4.3.2.4 NOEs cross peaks for secondary structure designation

Structural NMR characterisation was performed using ROESY NMR analysis. Rotating frame nuclear Overhauser Effect Spectroscopy (ROESY) is a spectroscopic technique employed to study the stereochemistry of molecules in solution. ROESY technique was utilised instead of NOESY because of the nature of the synthesised peptides. ROESY is preferred to NOESY for medium size molecules (MW range 700-1200 Da) whose rotational correlation time falls in a range where the nuclear overhauser effect is too weak to be detectable. NOE signals are positive for small molecules (MW $<$ 600 Da), negative for large molecules (MW $>$ 1200 Da) and zero for medium sized molecules.[161,162] This technique has been used to identify the distance between atoms that couples to each other in the same molecule. The average distance between Hγ_1 and Hγ_2 of the AMCP residues was known from literature and used as reference. Then, the distance of all the other identified cross peaks were defined (Table 4.3) and then compared with cross peaks of 12/10-helices reported in the literature by Sharma, Kunwar, Gellman and co-workers, which are listed below together with the strength of the observed cross peaks:[101,126,156]

I HC[α] of [α]-residue (i) to NH of [α]-residue (i + 2) **strong and medium**

II NH of [γ]-residue (i) to NH of [α]-residue (i+ 1) **medium and weak**

III HC[γ] of [γ]-residue (i) to NH of [α]-residue (i +1)

IV HC[α] of [α] residue (i) to HC[α] of [γ]-residue (i +1) **weak**

V NH of [γ]-residue (i) to HC[α] of [α]-residue (i +1)

The observed cross peaks for γ/α-peptide **295** are shown in Table 4.3. Characteristic peaks of 12/10-helical structures for α/γ-peptides[101,126,156] (relative positions of interacting amino acids $\gamma_1 \rightarrow \alpha_2/\gamma_1 \leftarrow \alpha_4$)[100] I, II and IV were identified and highlighted in bold (Table 4.3) suggesting that the proposed 10/12-helical structure for γ/α-peptides($\alpha_1 \rightarrow \gamma_2/\alpha_1 \leftarrow \gamma_4$)[100] is the most populated conformation for the γ/α-oligomer.[101,126,156] Like Gellman, interaction III was not observed,[126] however the observation of interaction IV might be one reason why we do see a more ordered structure. In addition, the different sequencing might have led to different NOE

Table 4.3: Unambiguous observed NOE cross peaks for hexamer **295**.

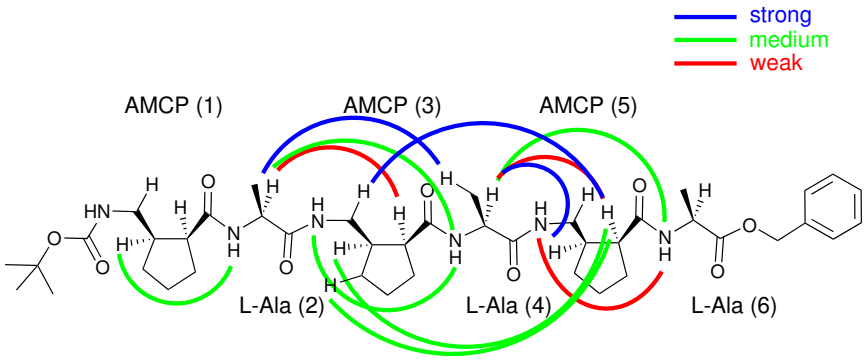

295

NOE cross peak	NMR distance Å	Designation
NH (1) - HCα (2)	4.95	weak
α (1) - NH (2)	2.38	strong
HCα (1) - HCα (2)	4.28	weak
HCβ (1) - NH (2)	3.42	medium
HCβ (1) - HCα (2)	4.68	weak
NH (1) - Hβ (3)	3.90	weak
NH (1) - Hγ''(3)	4.20	weak
HC_1'(1) - HCγ''(3)	3.91	weak
HCα (2) - HCα (3)	**4.28**	**weak** (IV)
HCα (2) - HCβ (3)	4.27	weak
HCα (2) - HCγ''(3)	5.33	weak
HCα (2) - NH (4)	**3.47**	**medium** (I)
HCα (2) - HCβ (4)	2.99	strong
HCβ (3) - NH (3)	4.09	weak
NH (3) - NH (4)	**3.46**	**medium** (II)
HCα (3) - NH (4)	2.68	strong
HCα (3) - HCα (4)	4.30	weak
HCγ'(3) - HCα (4)	5.1	weak
HC_1'(3) - HCα (4)	5.03	weak
HCβ (3) - HCα (5)	3.27	medium
HCγ''(3) - HCα (5)	2.62	strong
HC_3''(3) - HCα (5)	3.25	medium
HCα (4) - NH (5)	2.48	strong
HCα (4) - HCβ (5)	2.96	strong
HCβ (4) - HCγ'(5)	4.27	weak
HCα (4) - NH (6)	**3.47**	**medium** (I)
HCα (4) - HCα (5)	**3.96**	**weak** (IV)
NH (5) - NH (6)	**3.79**	**weak** (II)
HCα (5) - NH (6)	2.58	strong
HCβ (5) - NH (6)	4.40	weak
HCα (5) - HCα (6)	4.73	weak
HC_1'(5) - HCα (6)	4.73	weak

patterns such as strong interactions between HCα of α residues with HCβ of *i +1* α-residues and HCγ of γ-residues with HCα of the i+2 γ-residues (Table 4.3).

4.3.2.5 Computational study

Unambiguous NOEs cross peaks were used as molecular constraints for the original Monte-Carlo conformational search. Fifty five conformers were identified and optimised with DFT optimisation without any molecular constraint to define more accurate energies and confirm the validity of the obtained conformers. The five most populated conformers with the lowest energy have residues (2) to (6) of **295** that overlap in a similar conformation, which can be identified as a 10/12-helical structure (Figure 4.11).

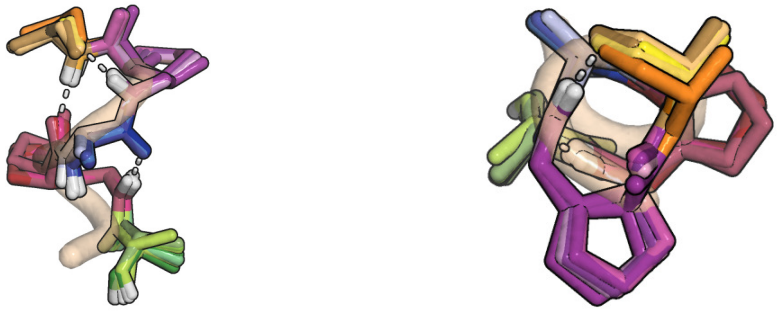

(a) **(b)**

Figure 4.11: Overlap of the 9 lowest energy structures of **295** obtained with a computational study. Residue AMCP (1) and the protecting groups have been omitted for clarity. (a) Side view. (b) Top view.

The conformation of the 9 lowest energy structures is a right handed helix and is in agreement with the conformation prediction given by the previously described analyses. The dihedral angles of **295** have been calculated from the 9 lowest energy structures (Table 4.4). They display the same sign between ψ of residue *i* and ϕ of the following residue *i+1* and this was found to be an essential characteristic for helices to form.[163,164] Subsequent pairs of $\psi(i)/\phi(i+1)$ alternate in sign which implies that amide/amide H-bonds alternate in their directionality, which is a typical feature of 12/10-helices of α/γ-oligomers and therefore 10/12-helices for γ/α-oligomers.[156,163]

By comparing the dihedral angles of the α- and γ-residues of the nine lowest energy structures with the theoretical model for a 12/10-helix, it is possible to observe that the dihedral angles of residues (2) to (6) have similar values with an opposite sign to the theoretical dihedral angles.[100] Different sequencing of the

Table 4.4: Dihedral angles of **295** compared with theoretical values and X-ray crystal structure **292** values.

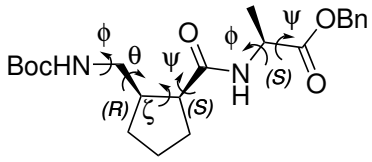

	Residue	ϕ	θ	ζ	ψ
Hexamer **295**	AMCP (1)	26.0±75	9.7±50	35.3±23	-103.0±8
	L-Ala (2)	-72.8±8	-	-	128.7±34
	AMCP (3)	61.0±3	43.5±3	41.9±1	-119.0±4
	L-Ala (4)	-72.8±4	-	-	141.7±2
	AMCP (5)	59.0±1	46.2±2	28.4±1	-119.7±3
	L-Ala (6)	-63.9±1	-	-	139.9±10
X-ray Dipeptide crystal **292**	*cis*-AMCP (1)	-96.3	176.7	29.4	-100.1
	L-Ala(2)	-125.7	-	-	1.1
Hofmann prediction H12/10	γ-residue	-64±1	-32±1	-48±1	132±5
	α-residue	68±2	-	-	-148±1

residues caused the opposite sign of the dihedral angles, however the values similarity is a further confirmation that **295** populates a 10/12-helical conformation. The characteristic small ζ dihedral angle of the γ-residue of the γ/α-oligomer **295** (ζ = 25 - 45°) highlights a similar feature to α/γ-vinylogous peptides. However, the hexamer **295** did not display the main NOEs interactions reported by Ganesh Kumar and co-workers for their α/γ-*Z*-vinylogous peptides (HC$\gamma(i)$ - NH$(i + 2)$ and HC$\gamma(i)$ - NH$(i + 1)$) as they observed a 12-helical conformation.[102]

To date, only Balaram and co-workers presented a stable α/γ helix with a constrained ζ-torsion angle (ϕ = -135°, θ =38°, ζ = 45°, ψ =-108°) using gabapentin as γ-residue.[165] These small values corresponds to the requirements of a helix formation for a *cis*-cyclopentane ring configuration confirming that the γ/α-peptide **295** populates a 10/12-helix. The situation is completely different in the case of the corresponding *trans*-configuration presented by Gellman and co-workers.[126] A much larger range of possible ζ-angles values can be covered and therefore a greater number of helical structures can populate a single ordered structure.

4.3.2.6 DMSO titration experiment

A DMSO titration experiment was performed to identify protons that are not engaged in intramolecular H-bonds, discriminating free NH from H-bonded NH and giving support to the proposed H-bonded 10/12-helical structure. ^{1}H NMR spectra of a 2mM solution of hexamer **295** in $CDCl_3$ were measured, followed by the addition of aliquots of DMSO. Amides that are already engaged in intramolecular hydrogen bonding, should not form any hydrogen bonds with DMSO as DMSO cannot displace pre-existing secondary interactions. Therefore consistent deshielding of amide peaks can be observed only for free amides. This experiment showed that only L-Ala (2) amide peak, which is circled in red, is strongly shifted downfield after the addition of DMSO. Amides that are solvent inaccessible do not shift considerably either and this can be the case for the NH of AMCP(1) since the chemical shift of the NH is below 7 ppm. Therefore, it is believed that the only two residues that are not intramolecularly H-bonded, whereas all the other amide protons are involved in intramolecular secondary interactions (Figure 4.12). Figure 4.12(c) shows shift in chemical shift ($\Delta\ \delta$) of each residue after the addition of DMSO (5, 10, 15, 25, 50, 100 µL). The obtained results confirm H-bonding within the γ/α-hexamer **295**.

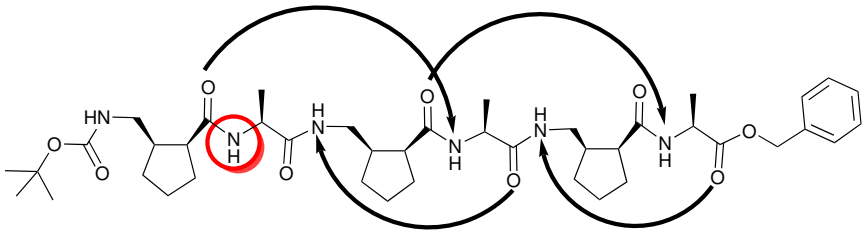

(a)

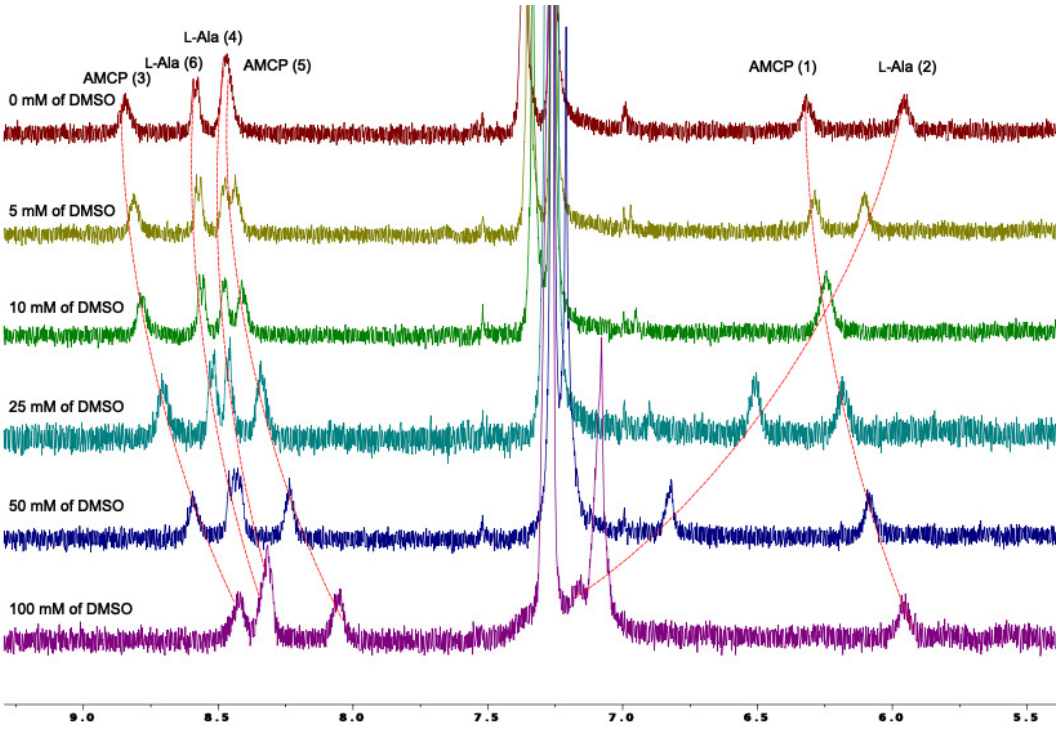

(b)

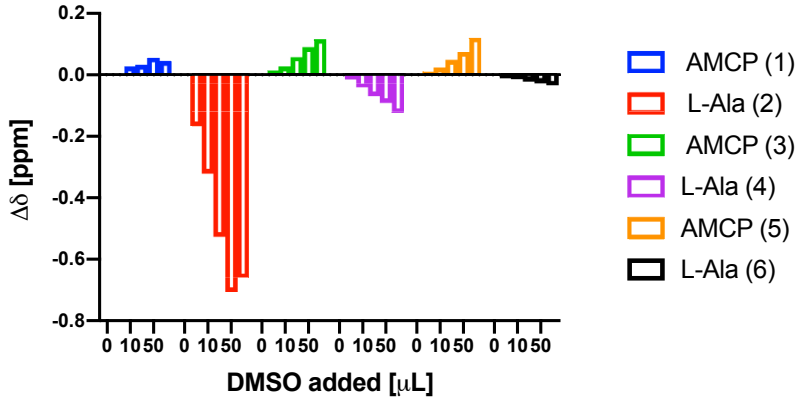

(c)

Figure 4.12: DMSO titration experiment: (a) H-bonding and solvent exposed amide protons in the proposed γ/α-peptide 10/12-helical structure. The amide proton circled in red is expected to exhibit the largest chemical shift change upon DMSO addition. (b) Amide peak region of ^{1}H NMR spectra collected with addition of 0, 10, 25, 50 and 100 µL of DMSO added to a 2 mM solution of **295** in $CDCl_3$. (c) Change of chemical shift of NH peaks with progressive DMSO addition.

4.4 Conclusions

In summary, successful synthesis and in depth structural characterisation of γ/α-peptides **292**, **294** and **295** were performed. A self-aggregation control was carried out confirming that the observed H-bonding are due to intramolecular rather than intermolecular interactions. Crystal structures of nitro-dimer **290** and of γ/α-oligomer **292** were obtained to confirm the stereochemistry and as additional information required for the computational study. NOEs analyses were performed and compared to previously reported characteristic NOE cross peaks of 12/10-helical conformations, of which a large proportion was identified. NOEs cross peaks were used as constraints to calculate the 9 lowest energy structures. Their overlap presented a right handed helical structure confirming the conformational hypothesis of a 10/12-helical structure. A DMSO titration in $CDCl_3$ was accomplished which confirmed that γ/α-hexamer **295** populates a helical conformation.

As a result, *cis*-γ-residues have properties that other peptides synthesised to date do not have. Their specific small ζ dihedral angles of *cis*-CC bond led the γ/α-oligomer **295** to populate a 10/12-helical structure. Owing to their unique properties they can pave the way to a new foldamer family.

4.5 Future Work

In chapter 3, the synthesis of asymmetric proline and indane derivatives (**317** and **266**) was described. γ-Amino acids can be derived from these substrates and coupled with α-amino acids in a similar manner to the method used to synthesise the γ/α-oligomers **292**, **294** and **295** (Figure 4.13).

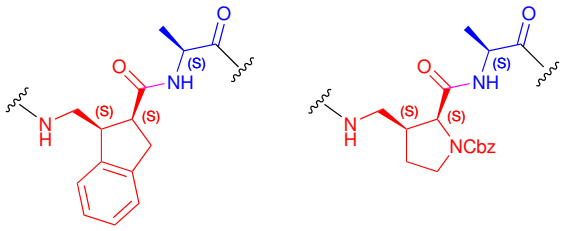

303 **304**

Figure 4.13: α/γ-Oligomers based on substrates synthesised with the optimised reaction conditions described in chapter 2.

Synthesis of foldamers based on these substrates could prove to be very interesting as it is still unexplored. In particular, the study of foldamers based on indane derivatives could investigate how side chains might influence the secondary structure of the main backbone. π-Interactions might play an important role for this type of peptide as Bornhof and Maity have recently reported.[166,167] The presence of aromatic groups as side chains of the γ-amino acid might lead to more stable and more complex secondary structures such as double helical conformations due to the formation of additional non-covalent bonds with the aromatic groups. Therefore, additional studies of constrained aromatic γ-amino acid based foldamers are valuable for further understanding and use of these novel biomaterials.[167,168]

Chapter 5

General Conclusions

In the past 20 years, the progress made on synthesis and characterisation of foldamers has been remarkable. The current study shows that the field of foldamers holds great potential to be explored and a more in depth understanding of this field could lead to the development of new materials.

In summary, a 1,2-nitro shift was identified during an intramolecular Michael addition assisted by organocatalysts for the synthesis of a 6-membered-ring γ-amino acid precursor. The envisioned rearrangment produced a 5-membered ring γ-amino acid precursor that proved to be an interesting molecular target. An enantio- and diastereoselective organocatalytic synthesis of *cis*-5-membered-ring-γ-amino acid precursor was presented. The corresponding γ-amino acid was then used as monomeric unit for the synthesis of γ/α-peptides. Synthesis and characterisation of heterogeneous oligomers established that the synthesised hexamer presented a 10/12-helical conformation. The novel peptide, with its distinctive backbone dihedral angles, could therefore open the way to a new class of foldamers.

Chapter 6

Experimental Session

6.1 General

All reactions were carried out at room temperature and magnetically stirred unless otherwise stated. Anhydrous CH_2Cl_2, THF, MeOH, DMF and toluene solvents were obtained from a dry solvent system all other solvents were supplied as Sureseal® bottles by Sigma Aldrich. All reagents were supplied by Sigma Aldrich, Alfa-Aesar, Fisher and VWR unless otherwise stated.

NMR data: Nuclear Magnetic Resonance (NMR) spectra were recorded using a Bruker Ascend 400 (400 MHz) or a Bruker NEO 600 (600 MHz) spectrometer using TMS as an internal standard. Chemical shifts (δ) are quoted in parts per million (ppm) using the abbreviations: s, singlet; d, doublet; dd, double of doublets; t, triplet; dt, doublet of triplets; ddt, doublet of doublet of triplets; td, triplet of doublets; q, quartet. Resonances that could not be easily interpreted were designated multiplets (m) or broad (br). Coupling constants J are quoted in Hz. ^{13}C NMR spectra were recorded at 100 MHz on a Bruker Ascend 400 (400 MHz) or a Bruker NEO 600 (600 MHz) spectrometer. Two-dimensional spectroscopy (COSY, HSQC, HMBC, TOCSY, ROESY) was used to confirm the assignments where necessary. NMRs taken on the Bruker NEO 600 (600 MHz) were carried out at the NMR facility of the Centre for Biomolecular Spectroscopy at King's College London. Crosspeaks were integrated manually within Topspin 3.5. The average of the intensities of AMCP Hγ_1-Hγ_2 cross peaks was used as a reference, I_0, set to correspond to a distance, r_0, of 1.763 Å. All other upper limits for distance constraints were calculated using: $r_1 = [(I_0/I_1)(r_0^6)]^{1/6}$. Lower limits for all distance constraints were set to 1.8 Å.

IR data: IR spectra were recorded on a Shimadzu IRAffinity-1S FTIR Spectrophotometer as a thin film. The selected absorptions are quoted in wavenumbers (cm^{-1}).

MS data: High-resolution mass spectra were recorded on either Waters LCT Premier (ES-Tof), Thermo Scientific Q-Exactive (APCI) and Micromass Autospec Premier (EI) using the Imperial College London, Department of Chemistry Mass Spectrometry Service.

Optical Rotation: Optical rotation readings were recorded using an Anton Parr MCP100 Polarimeter. Specific rotations ($[\alpha]^{20}{}_D$) were recorded at the sodium D line (589 nm) in methanol or CH_2Cl_2 and are quoted in: deg cm^2 g^{-1}. Solution concentrations (c) are given in units of 10^{-2} g mL^{-1}. Temperatures are in degrees Celsius (°C). The prefixes (+) and (-) indicate the sign of the optical rotation. Correct units: deg cm^2 g^{-1}

Melting point: Melting points were determined on a Stuart SMP30 melting point apparatus and are uncorrected.

HPLC Profiles: HPLC analysis was determined on Agilent Technologies 1200 Series HPLC, using a ratio of HPLC grade hexanes and propan-1-ol as the eluent, using a Chiralpak AD-H, OD or AS column (0.46 cm x 25 cm) and detection by UV at 210 nm. Peaks were assigned by spiking the enantioselective sample with the racemate.

Chromatography: Reactions were monitored by thin layer chromatography on silica gel precoated aluminium sheets (TLC Silica Gel 60 F254, Merck). Visualisation was accomplished by irradiation by UV light at 254 nm and/or ninhydrin stain, potassium permanganate stain, *p*-anisaldehyde, dinitrophenylhydrazine or vanilline. Column chromatography was performed on Merck silica gel (60 Å, 230 - 400 mesh, 40 - 63 μm) or on a CombiflashRF+ system.

Single Crystal X-ray: X-ray data was collected on an Oxford Gemini S-ultra diffractometer using Kalpha ($\lambda = 1.54180$ Å) radiation at the University of Reading.

Circular Dichroism: All CD spectra were measured in an Aviv Circular Dichroism Spectrophotometer, Model 410 (Biomedical Inc., Lakewood, NJ, USA), with specially adapted sample detection to eliminate scattering artefacts, or at the Karlsruhe synchrotron. A final oligomer concentration 1.6 mgmL^{-1} for **292**, 1.2

mgmL^{-1} for **294** and 1.6 mgmL^{-1} for **295** was used in quartz rectangular Suprasil demountable cells of pathlength 0.2 mm (Hellma or 0.5 mm Analytics). Each sample was scanned two to four times from 270 to 185 nm, at 1-nm intervals with an averaging time of 0.5 s. The same cell containing buffer only was also measured for background subtraction during data analysis. All CD spectra were processed using CDTool.[169] First, the multiple scans were averaged and the buffer background was subtracted. These subtracted spectra were zeroed and smoothed, which set the baseline at zero between 255 and 270 nm. **Computational methods:** Conformational sampling was carried out using mixed low-mode Monte-Carlo search[150–152] as implemented in Schrodinger 2017-1[170] based on the OPLS 2005 all atom force field,[171–173] followed by conformational clustering.

Kohn-Sham DFT calculations were done for the mechanistic studies using Gaussian09 Rev.E.[174] The presented result were obtained employing the ω-B97X-D range separated hybrid functional,[175] with the basis 6-311G(d,p) for optimization, frequency and solvent calculations and the 6-311++G(3df,3pd) basis for electronic energies.[176–178] Thermochemical corrections were calculated according to Grimme's quasi-RRHO[153] approximation as implemented in goodvibes.[179] Solvent corrections are determined for DCE using PCM solvent model with Truhlar's SMD parametrization.[180,181]

6.2 Synthesis of the terminal nitro olefin 171

6.2.1 Method A for the synthesis of the nitro olefin 171

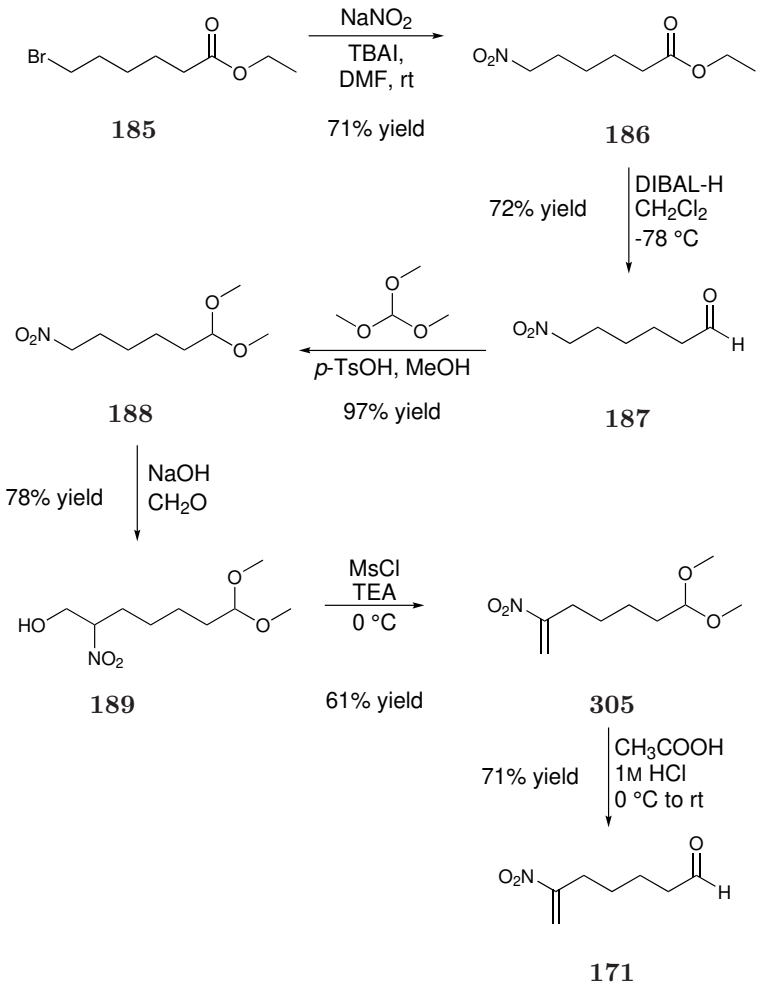

Ethyl 6-nitrohexanoate **186**

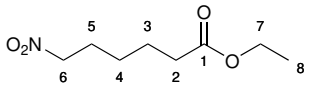

186

To a solution of ethyl 6-bromohexanoate (19.9 mL, 112.1 mmol) in DMF (1 L) was added $NaNO_2$ (11.6 g, 69.0 mmol) and *tert*-butyl ammonium iodide (8.28 g, 22.4 mmol). After 4.5 hours the reaction was quenched with the addition of H_2O (600 mL) and the mixture was extracted with diethyl ether (400 mLx 3). The organic layers were washed twice with brine, and then dried over $MgSO_4$ and concentrated *in vacuo*. The crude of the reaction was purified *via* an automated

flash chromatography (gradient mobile phase 6%– 40% diethyl ether in hexane) giving compound **186** as a pale yellow liquid (53% yield, 11.350 g). IR (neat, cm^{-1}) 2938, 1728, 1549, 1435, 1374, 1351, 1182, 1156, 1096, 1030; ^{1}H NMR ($CDCl_3$, 400 MHz) δ 4.39 (2H, t, J = 7.0 Hz, H-6), 4.13 (2H, q, J = 7.1 Hz, H-7), 2.32 (2H, t, J = 7.4 Hz, H-2), 2.18 - 2.00 (2H, m, H-5), 1.73 - 1.65 (2H, m, H-3), 1.47 - 1.39 (2H, m, H-4), 1.26 (3H, t, J = 7.1 Hz, H-8); ^{13}C NMR ($CDCl_3$, 400 MHz) δ 173.2 (C-1), 75.4 (C-6), 60.4 (C-7), 33.8 (C-2), 27.0 (C-5), 25.7 (C-3), 24.1 (C-4), 14.2 (C-8); HRMS required for $C_8H_{15}NO_4$ $[M+H]^+$ 190.1079, found 190.1077.

6-Nitrobutanal **187**[182]

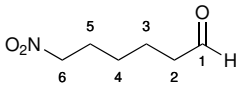

187

To a solution of ethyl-6-nitronate **186** (15.0 g, 79.3 mmol) in anhydrous CH_2Cl_2 (450 mL) at -78 °C was added a solution of DIBAL-H 1M in hexane (111 mL, 111 mmol) dropwise over 45 minutes. After 6 hours the reaction was quenched with 1M aqueous hydrochloric acid (260 mL) and it was left stirring overnight at 3 °C. The aqueous phase was then extracted with CH_2Cl_2 (3 x 150 mL) dried over $MgSO_4$, filtered and concentrated *in vacuo*. The product **187** was obtained as an oil and it did not require further purification (72% yield, 8.259 g). IR (neat, cm^{-1}) 3393, 2933, 1547, 1463, 1434, 1382, 1125; ^{1}H NMR ($CDCl_3$, 400 MHz) δ 9.78 (1H, s, H-1), 4.40 (2H, t, J = 6.9 Hz, H-6), 2.48 (2H, t, J = 7.2 Hz, H-2), 2.16 - 1.86 (2H, m, H-5), 1.80 - 1.56 (2H, m, H-3), 1.43 (2H, tt, J = 10.0, 6.7 Hz, H-4); ^{13}C NMR ($CDCl_3$, 400 MHz) δ 201.8 (C-1), 75.3 (C-6), 43.4 (C-2), 27.1 (C-5), 25.8 (C-4), 21.2 (C-3).

1,1-Dimethoxy-6-nitrohexane **188**

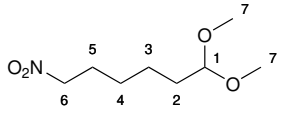

188

To a solution of **187** (8.30 g, 56.9 mmol) in anhydrous methanol (70 mL) was added trimethyl orthoformate (7.5 mL, 68.3 mmol) followed by *p*-toluene sulfonic acid monohydride (2.71 g, 14.2 mmol) dissolved in 15 mLof methanol. The reaction

was left stirring for 14 hours and then, the reaction was quenched adding triethylamine (3.3 mL). The methanol was evaporated under high pressure and then H_2O (30 mL) was and extracted with CH_2Cl_2 (3 x 30 mL), dried over $MgSO_4$, filtered and concentrated *in vacuo*. Compound **188** was obtained pure enough to carry out the next step (93% yield, 10.107 g). IR (neat, cm^{-1}) 3418, 2936, 2862, 1548, 1434, 1383, 1190; ^1H NMR ($CDCl_3$, 400 MHz) δ 4.52 - 4.26 (3H, m, H-1 and H-6), 3.32 (6H, s, H-7), 2.13 - 1.88 (2H, m, H-5), 1.69 - 1.52 (2H, m, H-2), 1.49 - 1.32 (4H, m, H-3 and H-4); ^{13}C NMR ($CDCl_3$, 400 MHz) δ 104.3 (C-1), 75.6 (C-6), 52.8 (C-7), 32.2 (C-2), 27.3 (C-5), 26.1 (C-4), 23.9 (C-3); HRMS required for $C_8H_{17}NO_4$ $[M+NH_4]^+$ 209.1496, found 209.1496.

7,7-Dimethoxy-2-nitroheptan-1-ol **189**[111]

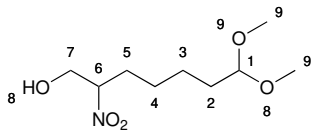

189

An aqueous 3N solution of NaOH (6 mL, 1.2 mL/mmol) was added to compound **188** (0.96 g, 5.0 mmol) at 0 °C. After 2 hours, a 37% w/v solution of formaldehyde (0.21 mL, 7.5 mmol) was added and the mixture was stirred for 5 hours at ice-cold condition. Then, acetic acid (0.57 mL, 10 mmol) was added and stirred at rt for 68 hours. H_2O (15 mL) was added and the reaction mixture was then extracted with ethyl acetate (3x 15 mL). The combined organic layers were dried over $MgSO_4$ and concentrated under reduced pressure. The product achieved (**189**) did not require further purification and it was obtained as a colourless oil (46% yield, 0.505 g). IR (neat, cm^{-1}) 3405, 2943, 1540, 1463, 1353, 1192, 1126, 1050; ^1H NMR ($CDCl_3$, 400 MHz) δ 4.60 (1H, tdd, J = 8.5, 5.5, 3.2 Hz, H-6), 4.34 (1H, t, J = 5.6 Hz, H-1), 3.90 – 4.02 (2H, m, H-7), 3.31 (6H, s, H-9), 2.29 (1H, bs, H-8), 1.98 (1H, dtd, J = 17.1, 8.6, 4.2 Hz, H-5), 1.89 – 1.69 (1H, m, H-5), 1.69 – 1.51 (2H, m, H-2), 1.51 – 1.30 (4H, m, H-3 and H-4); ^{13}C NMR ($CDCl_3$, 400 MHz) δ 104.2 (C-1), 89.2 (C-6), 63.2 (C-7), 52.8 (C-9), 32.1 (C-2), 29.7 (C-5), 25.5 (C-4), 24.0 (C-3).

7,7-Dimethoxy-2-nitrohept-1-ene **306**[111]

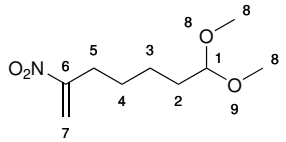

306

To a solution of **189** (5.91 g, 26.7 mmol) in anhydrous CH_2Cl_2 (110 mL) at ice-cold condition was added mesyl chloride (2.7 mL, 34.6 mmol) and TEA (14.8 mL, 106 mmol). After 2 hours stirring at 0 °C, the reaction was quenched with aqueous hydrochloric acid (0.1N, 14.3 mL). H_2O (50 mL) was added, and the mixture was extracted with CH_2Cl_2 (3 x 70 mL). The organic layers were dried over Na_2SO_4 and concentrated under reduced pressure. The crude of the product was purified *via* flash chromatography (20% of ethyl acetate in hexane) achieving the nitro olefin **306** as a colourless oil (66% yield, 3.58 g). IR (neat, cm^{-1}) 2939, 1718, 1553, 1462, 1349, 1173; ^{1}H NMR ($CDCl_3$, 400 MHz) δ 6.43 (1H, d, J = 1.8 Hz, H-7'), 5.55 (1H, d, J = 2.0, H-7''), 4.37 (1H, t, J = 5.6, H-1), 3.32 (6H, s, H-8), 2.61 (2H, t, J = 7.5 Hz, H-5), 1.71 – 1.51 (4H, m, H-2 and H-4), 1.51 – 1.35 (2H, m, H-3); ^{13}C NMR ($CDCl_3$, 400 MHz) δ 158.0 (C-6), 117.1 (C-7), 104.2 (C-1), 52.8 (C-8), 32.2 (C-2), 30.1 (C-5), 27.0 (C-4), 23.8 (C-3).

6-Nitrohept-6-enal **171**[111]

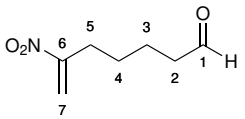

171

To compound **306** (0.019g, 0.089 mmol) at ice-cold condition was added acetic acid (89 μl). After the solution started to freeze HCl (1N, 29 μl) was added and the mixture was left stirring at rt for 24 hours. CH_2Cl_2 (15 mL) was added and washed with H_2O (2 x 1 mL) and saturated aqueous $NaHCO_3$ (1 mL). The organic phase was then dried over $MgSO_4$, filtered, concentrated under reduced pressure to afford the nitro olefin **171** as a colourless oil (64% yield, 0.009 g). ^{1}H NMR ($CDCl_3$, 400 MHz) δ 9.79 (1 H, t, J = 1.5, H-1), 6.45 (1 H, d, J = 1.9, H-7'), 5.58 (1 H, s, H-7''), 2.63 (2 H, t, J 7.5, H-5), 2.51 (2 H, td, J 7.0, 1.4, H-2), 1.77 – 1.65 (2 H, m, H-3), 1.65 – 1.53 (2H, m, H-4). ^{13}C NMR ($CDCl_3$, 400 MHz) δ 201.7 (C-1), 157.6

(C-6), 117.4 (C-7), 43.4 (C-2), 30.0 (C-5), 26.6 (C-4), 21.2 (C-3). HRMS required for $C_7H_{10}NO_3$ $[M\text{-}H]^-$ 156.0661, found 156.0657.

6.2.2 Method B for the synthesis of the terminal nitro olefin 171

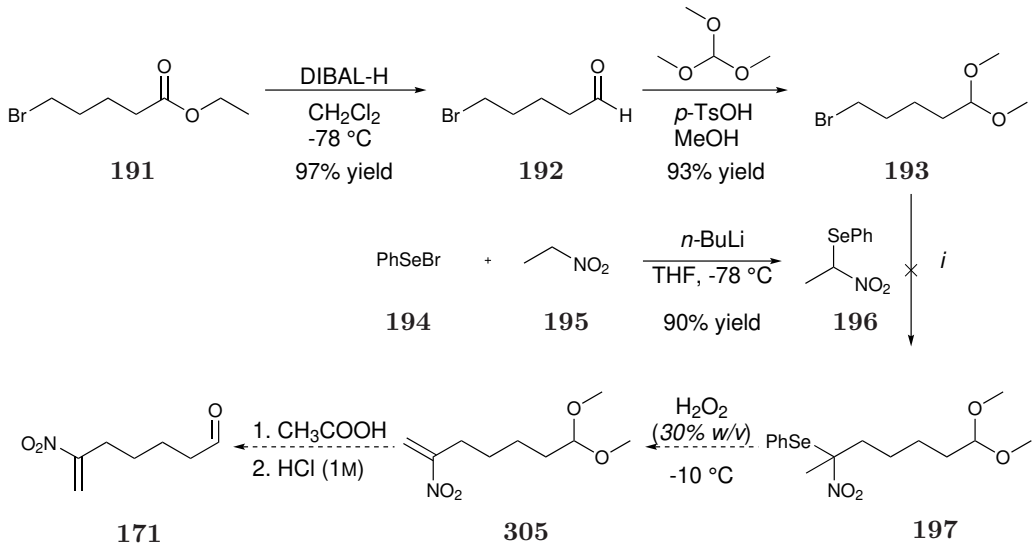

Scheme 6.1: Synthetic procedure for the synthesis of the nitroolefin **171**.

5-Bromopentanal **192**

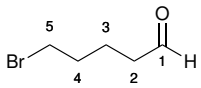

192

To a solution of **191** (5.3 mL, 33.5 mmol) in anhydrous CH_2Cl_2 (184 mL) was added DIBAL-H (1M in hexane, 46.9 mL, 46.9 mmol) dropwise over 25 minutes. After 2 hours and 40 minutes the reaction was quenched with aqueous hydrochloric acid (1M, 108 mL) and it was left stirring at rt for 2 hours. H_2O (100 mL) was added to the mixture and the aqueous phase was extracted in CH_2Cl_2 (3 x 90 mL).The combined organic layers were dried over Na_2SO_4, filtered and concentrated *in vacuo*. The product **192** was then obtained as a colourless oil (97% yield, 5.317 g) and it did not require further purification. IR (neat, cm^{-1}) 3425, 2940, 2866, 2725, 1721, 1433, 1409, 1391, 1252, 1202, 1113,1050; ^{1}H NMR ($CDCl_3$, 400 MHz) δ 9.79 (1H, t, J = 1.5 Hz H-1), 3.43(2H, td, J = 6.7, 2.1 Hz, H-5), 2.50 (2H, td, J = 7.1, 1.4 Hz, H-2), 1.95 - 1.85 (2H, m, H-3), 1.85 - 1.74 (2H, m, H-4); ^{13}C NMR ($CDCl_3$, 400 MHz) δ 201.8 (C-1), 42.9 (C-2), 33.0 (C-5), 31.8 (C-3), 20.6 (C-4). HRMS required for C_6H_12OBr $[M\text{-}CH_2O+H]^+$ 179.0066, found 179.0064.

5-Bromo-1,1-dimethoxypentane **193**

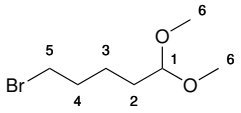

193

To a solution of **192** (5.300 g, 31.9 mmol) in anhydrous methanol (40 mL) was added trimethyl orthoformate (4.2 mL, 38.3 mmol) followed by *p*-toluene sulfonic acid monohydride (1.518 g, 8.0 mmol) dissolved in 10 mL of methanol. The reaction was left stirring for 18 hours and then, the reaction was quenched adding TEA (1.9 mL). The methanol was evaporated under high pressure and then H_2O (50 mL) was added and extracted with CH_2Cl_2 (3 x 40 mL), dried over Na_2SO_4, filtered and concentrated *in vacuo*. Compound **193** was obtained as an oil and did not require further purification (93% yield, 6.26 g). IR (neat, cm^{-1}) 2944, 2829, 1455, 1385, 1287, 1243, 1191, 1101, 1051; ^{1}H NMR ($CDCl_3$, 400 MHz) δ 4.37 (1H, t, 5.6 Hz, H-1), 3.41 (2H, t, J = 6.8 Hz, H-5), 3.32 (6H, s, H-6), 1.95 - 1.82 (2H, m, H-4), 1.68

- 1.56 (2H, m, H-2), 1.56 - 1.43 (2H, m, H-3); ^{13}C NMR ($CDCl_3$, 400 MHz) δ 104.3 (C-1), 52.8 (C-6), 32.1 (c-5), 31.6 (C-4), 23.3 (C-3); HRMS required for $C_5H_{10}Br$ [M-$C_2H_6O_2$+H]$^+$ 150.9940, found m/z 150.9936.

(1-Nitroethyl)(phenyl)selane **194**[114]

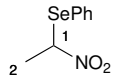

194

A 1.6 M solution of *n*-BuLi (10.0 mL, 16.0 mmol) in hexane was added dropwise to a solution of nitroethane (1.2 mL, 16.4 mmol) in anhydrous THF (145 mL) under inert atmosphere at -78 °C. After 1 hour stirring at -78 °C, a solution of phenylselenyl bromide (1.80 g, 7.6 mmol) in THF (24 mL) was added rapidly in one portion. The mixture was left stirring at -78 °C for 3.5 hours and a saturated aqueous solution of ammonium chloride (24 mL) was added and left stirring at rt for 15 min. H_2O (100 mL) was then added and extracted with ethyl acetate (3x 50 mL). Brine was also used to eliminate the emulsions experienced during the last extraction. The organic phase was dried over Na_2SO_4, filtered and concentrated *in vacuo*. The nitroselenide **194** was achieved as a yellow solid (90% yield, 1.58 g) and there was no need of any further purification. IR (neat, cm^{-1}) 2931, 1550, 1476, 1438, 1381, 1352; ^{1}H NMR ($CDCl_3$, 400 MHz) δ 7.75 - 7.53 (2H, m, Ar-H), 7.49 - 7.40 (1H, m, Ar-H), 7.40 - 7.33 (2H, m, Ar-H), 5.68 (1H, q, J = 6.9 Hz, H-1), 1.83 (3H, d, J = 6.9 Hz, H-2); ^{13}C NMR ($CDCl_3$, 400 MHz) δ 136.3 (C-Ar), 129.9 (C-Ar), 129.5 (C-Ar), 78.7 (C-1), 19.7 (C-2).

6.3 Synthesis of 6-membered ring 151

6.3.1 Method C for the synthesis of the 6-membered ring 151

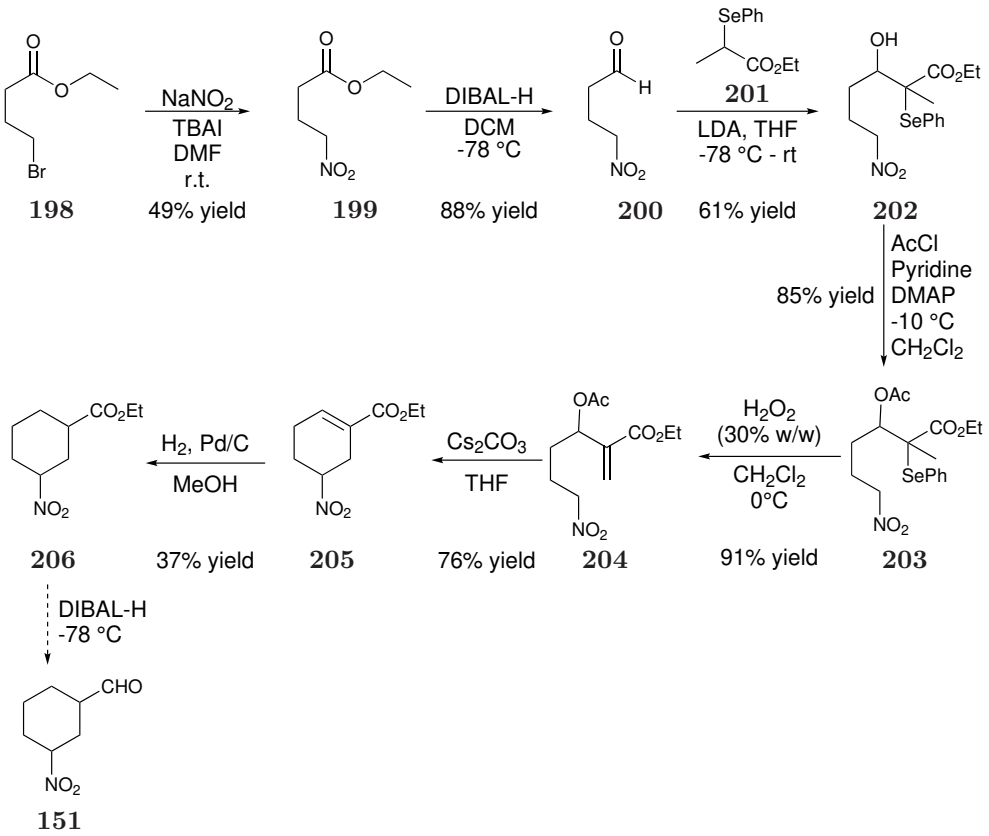

Scheme 6.2: First synthetic plan for the synthesis of the intermediate of reaction.

Ethyl 4-nitrobutanoate **199**

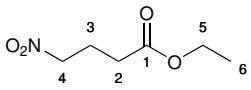

199

To a solution of ethyl 4-bromo butyrate (18.34 mL, 128 mmol) in DMF (1 L) was added sodium nitrite (13.248 g, 192 mmol) and *tert*-butyl ammonium iodide (9.456, 25.6 mmol). The reaction was left stirring at rt for 4 hours and then it was quenched with the addition of water (500 mL). The mixture was extracted in diethyl ether (3 x 1L), it was washed twice with a solution of saturated LiCl and twice with brine, dried over $MgSO_4$ and concentrated *in vacuo*. Flash chromatography (30% ethyl acetate in hexane) was required to obtain the purified product **199** (49% yield, 10.001 g) as an oil. IR (neat, cm^{-1}) 2984, 1728, 1550, 1435, 1375, 1176; ^1H NMR

($CDCl_3$, 400 MHz) δ 4.49 (2H, t, J = 6.7 Hz, H-4), 4.16 (2H, q, J = 7.1 Hz, H-5), 2.54 - 2.39 (2H, m, H-2), 2.42 - 2.22 (2H, m, H-3), 1.27 (3H, t, J = 7.1 Hz, H-6); ^{13}C NMR ($CDCl_3$, 400 MHz) δ 171.9 (C-1), 74.4 (C-4), 50.9 (C-5), 30.5 (C-2), 22.4 (C-3), 14.2 (C-6); HRMS required for $C_6H_{11}NO_4$ $[M+NH_4]^+$ 179.1026, found 179.1024.

4-Nitrobutanal **200**

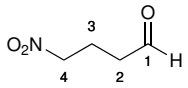

200

To a solution of **199** (0.400 g, 2.48 mmol) in anhydrous CH_2Cl_2 (14 mL) was added DIBAL-H (1M in hexane, 3.47 mL, 3.47 mmol) dropwise over 2 minutes. After 4 hours the reaction was quenched with aqueous hydrochloric acid (1M, 8 mL) and it was left stirring at rt for an hour. Water (15 mL) was added and it was extracted in CH_2Cl_2 (3 x 15 mL) and through the help of brine to reduce emulsions. The combined organic layers were dried over $MgSO_4$, filtered and concentrated *in vacuo*. Product **200** was achieved (93% yield, 0.270 g) as a colourless oil and it did not require further purification. ^{1}H NMR ($CDCl_3$, 400 MHz) δ 9.81 (1H, s, H-1), 4.46 (2H, t, J = 6.3 Hz, H-4), 2.68 (2H, t, J = 6.8 Hz, H-2), 2.32 (2H, p, J = 6.8 Hz, H-3); ^{13}C NMR ($CDCl_3$, 400 MHz) δ 199.7 (C-1), 74.3 (C-4), 40.0 (C-2), 19.7 (C-3).

Ethyl 2-(phenylselanyl)propanoate **201**[183]

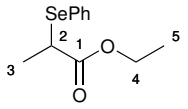

201

Sodium borohydride (3.1 g, 81.6 mmol) was added to a solution of diphenyl diselenide (25 g, 80.1 mmol) in EtOH (250 mL) dried over activated molecular sieves (4Å) in ice-cold condition. Ethyl 2-chloropropionate (9.7 mL, 75.6 mmol) dissolved in EtOH (126 mL) was then added to the reaction mixture. After 3 hours stirring at 0 °C, H_2O (500 mL) was added and the aqueous phase was extracted with diethyl ether (1.2 L). The organic phase was then washed with H_2O again (2 x 500 mL), dried over Na_2SO_4, filtered and concentrated under reduced pressure. A purification *via* flash chromatography (6% ethyl acetate in hexane) was required to

achieve product **201** as a yellow solid (13.99 g, 54.4 mmol, 72% yield). IR (neat, cm^{-1}) 2980, 1726, 1578, 1477, 1438, 1368, 1326, 1256, 1207, 1146, 1057, 1021; ^{1}H NMR ($CDCl_3$, 400 MHz) δ 7.75 -7.49 (2H, m, Ar-H), 7.44 - 7.12 (3H, m, Ar-H), 4.09 (2H, q, J = 7.1 Hz, H-4), 3.77 (1H, q, J = 7.1 Hz, H-2), 1.54 (3H, d, J = 7.1 Hz, H-3), 1.17 (3H, t, J = 7.1 Hz, H-5); ^{13}C NMR ($CDCl_3$, 400 MHz) δ 173.5 (C-1), 135.7 (Ar-C), 129.0 (Ar-C), 128.5 (Ar-C), 127.9 (Ar-C), 61.0 (C-4), 37.4 (C-2), 17.7 (C-3), 14.0 (C-5); HRMS required for $C_{11}H_{15}O_2Se$ $[M+H]^+$ 258.0159, found 258.0168.

Ethyl 3-hydroxy-2-methyl-6-nitro-2-(phenylselanyl)hexanoate **202**[114]

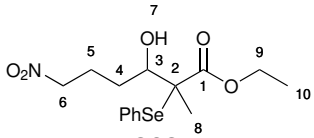

202

n-BuLi (1.6 M in hexane, 1.83 mL, 2.93 mmol) was added dropwise to a cooled (-78 °C) solution of isopropyl amine (0.41 mL, 2.93 mmol) in anhydrous THF (14 mL). The mixture was left stirring at -78 °C for 1 hour and then a solution of **201** (0.753 g, 2.93 mmol) in 1.8 mL of THF was added dropwise. After 90 minutes a solution of **200** (0.264 g, 2.25 mmol) in 2 mL of THF was added dropwise to the cooled mixture (-78 °C). After 40 minutes, the mixture was then quenched with saturated aqueous solution of NH_4Cl (17.5 mL). The cold bath was then removed and stirring at rt was continued for 15 minutes. The mixture was then diluted with water (50 mL) and the aqueous phase was extracted with ethyl acetate (3 x 35 mL). The combined organic layers were washed with brine, dried ($MgSO_4$) and concentrated *in vacuo*. Flash chromatography (10% ethyl acetate in hexane) over silica gel was then required to separate the two diastereoisomers. The less polar diastereoisomer **202a** was achieved as an colourless oil (19% yield, 0.158 g) and the more polar **202b** was obtained along with the other diasteroisomer as an colourless oil (32% yield, 0.268 g). Diastereomer **202a** had: ^{1}H NMR ($CDCl_3$, 400 MHz) δ 7.62 – 7.52 (2H, m, Ar-H), 7.49 – 7.39 (1H, m, Ar-H), 7.39 – 7.29 (2H, m, Ar-H), 4.54 – 4.34 (1H, m, H-6), 4.20 – 3.93 (1H, m, H-9), 3.87 (1H, dt, J = 10.1, 2.0 Hz, H-3), 3.20 (1H, t, J = 2.3 Hz, H-7), 2.36 – 2.21 (1H, m, H-5'), 2.19 – 2.06 (1H, m, H-5''), 1.72 – 1.58 (1H, m, H-4'), 1.54 – 1.43 (1H, m, H-4''), 1.37 (3H, s, H-8), 1.16 (3H, t, J = 7.1 Hz, H-10); ^{13}C NMR ($CDCl_3$, 400 MHz) δ 173.2 (C-1), 138.1

(Ar-C), 129.7 (Ar-C), 129.0 (Ar-C), 126.0 (Ar-C), 75.3 (C-6), 72.2 (C-3), 61.3 (C-9), 56.9 (C-2), 28.1 (C-4), 24.8 (C-5), 17.1 (C-8), 13.8 (C-10). Diastereomer **202b** had: IR (neat, cm^{-1}) 3501, 2934, 1704, 1548, 1476, 1437; ^{1}H NMR ($CDCl_3$, 400 MHz) δ 7.65 – 7.50 (1H, m, Ar-H), 7.49 – 7.38 (2H, m, Ar-H), 7.38 – 7.28 (2H, m, Ar-H), 4.58 – 4.34 (2H, m, H-6), 4.13 (2H, qd, J = 7.2, 1.3 Hz, H-9), 3.86 (1H, ddd, J = 10.8, 6.4, 1.6 Hz, H-3), 2.94 (1H, d, J = 6.5 Hz, H-7), 2.38 – 2.20 (1H, m, H-5'), 2.20 – 1.97 (1H, m, H-5''), 1.50 (2H, ddd, J = 10.7, 8.2, 5.0 Hz, H-4), 1.41 (3H, s, H-8), 1.22 (3H, t, J = 7.1 Hz, H-10); ^{13}C NMR ($CDCl_3$, 400 MHz) δ 174.0 (C-1), 138.0 (Ar-C), 129.6 (Ar-C), 129.0 (Ar-C), 126.2 (Ar-C), 75.4 (C-6), 74.6 (C-3), 61.5 (C-9), 54.0 (C-2), 27.9 (C-4), 24.9 (C-5),17.9 (C-8), 14.0 (C-10); HRMS required for $C_{15}H_{21}NO_5Se$ $[M+NH_4]^+$ 393.0924, found 393.0920.

Ethyl 3-acetoxy-2-methyl-6-nitro-2-(phenylselanyl)hexanoate **203**[114]

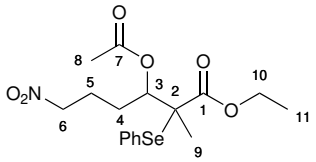

203

To a stirred and cooled (-10 °C , ice-acetone bath) solution of **202b** (0.260 g, 0.69 mmol) and DMAP (0.0084 g, 0.069 mmol), pyridine (0.334 mL, 4.14 mmol) and acetyl chloride (0.150 mL, 2.1 mmol) were added sequentially dropwise. The cold bath was left in place but not recharged and stirring was continued for 18 hours by which the time the temperature has risen to rt. The mixture was then diluted with water (8.6 mL), acidified with aqueous hydrochloric acid (1M, 3.5 mL) and extracted with CH_2Cl_2 (3 x 5 mL). The combined organic extracts were washed with brine, dried over $MgSO_4$, filtered and concentrated *in vacuo*. Flash chromatography of the crude over silica gel (19:50, Ethyl Acetate – Hexane) gave the product **203** (67% yield, 0.192 g) as an colourless oil. IR (neat, cm^{-1}) 2982, 1741, 1723, 1476, 1438, 1371, 1224; ^{1}H NMR ($CDCl_3$, 400 MHz) δ 7.66 - 7.52 (2H, m, Ar-H), 7.52 -7.39 (1H, m, Ar-H), 7.37 - 7.29 (3H, m, Ar-H), 5.41 (1H, dd, J = 10.5, 1.3 Hz, H-3), 4.44 (2H, t, J = 6.6 Hz, H-6), 4.12 - 3.77 (2H, m , H-10), 2.38 - 2.19 (1H, m, H-4'), 2.17 - 1.99 (2H, m, H-5), 1.97 (3H, s, H-8), 1.69 (1H, dddd, J = 14.1, 10.6, 9.2, 4.9 Hz, H-4''), 1.50 (3H, s, H-9), 1.10 (3H, t, J = 7.1 Hz, H-11); ^{13}C NMR ($CDCl_3$, 400 MHz) δ 171.9 (C-1), 170.0 (C-7), 137.9 (Ar-C), 129.8 (Ar-C), 129.0 (Ar-C), 126.0

(Ar-C), 74.9 (C-6), 74.6 (C-3), 61.3 (C-10), 52.4 (C-2), 27.3 (C-4), 24.1 (C-5), 20.8 (C-8), 17.6 (C-9), 13.8 (C-11); HRMS required for $C_{17}H_{23}NO_6Se{\cdot}NH_4$ $[M+NH_4]^+$ 435.1030, found 435.1025.

Ethyl 3-acetoxy-2-methylene-6-nitrohexanoate **204**[114]

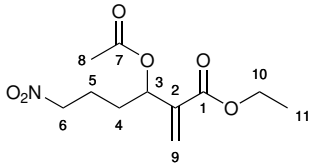

204

A solution of 30%w/v hydrogen peroxide (0.6 mL, 5.28 mmol) was added dropwise to a stirred and cooled (0 °C) solution of **203** (0.188 g, 0.45 mmol) in CH_2Cl_2 (4.5 mL). After 1 hour and 15 minutes the reaction was quenched with saturated aqueous $Na_2S_2O_3$ (3 mL). The mixture was stirred at 0 °C for 5 minutes and then the ice-bath was removed, stirring was continued for 30 minutes and water (15 mL) was added. The aqueous phase was extracted with CH_2Cl_2 (3x 15 mL) and the combined organic layers were washed with brine, dried ($MgSO_4$) and concentrated *in vacuo*. The crude of the reaction was purified *via* flash chromatography (7 : 20, ethyl acetate-hexane) to give product **204** (81% yield, 0.095 g) as a viscous oil. IR (neat, cm^{-1}) 2984, 2363, 1741, 1713, 1633, 1551, 1435, 1370, 1267, 1228; ^{1}H NMR ($CDCl_3$, 400 MHz) δ 6.33 (1H, s, H-9'), 5.78 (1H, s, H-9''), 5.66 (1H, dd, J = 7.6, 4.1 Hz, H-3), 4.41 (2H, t, J = 6.9 Hz, H-6), 4.29 – 4.19 (2H, m, H-10), 2.11 (3H, s, H-8), 2.10 - 1.98 (2H, m, H-5), 1.98 - 1.73 (2H, m, H-4), 1.31 (3H, t, J = 7.1 Hz, H-11); ^{13}C NMR ($CDCl_3$, 400 MHz) δ 169.8 (C-7), 165.0 (C-1), 139.4 (C-2), 125.4 (C-9), 74.9 (C-6), 70.6 (C-3), 61.1 (C-10), 30.8 (C-4), 23.2 (C-5), 21.0 (C-8), 14.1 (C-11); HRMS required for $C_{11}H_{17}NO_6NH_4$ $[M+H]^+$ 277.1394, found 277.1396.

Ethyl 5-nitrocyclohex-1-ene-1-carboxylate **205**[114]

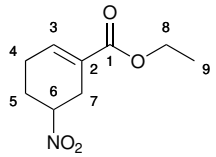

205

Caesium carbonate (0.229 g, 0.702 mmol) was added to a stirred solution of **204** (91 mg, 0.351 mmol) in THF (3.5 mL). The mixture was left stirring at rt for 6 hours, the solvent was evaporated and flash chromatography of the residue over silica gel (1:2, ethyl acetate-hexane) was then followed to give the product **205** (57% yield, 0.041 g) as a colourless oil. IR (neat, cm^{-1}) 2980, 1707, 1652, 1544, 1429, 1372, 1243; ^{1}H NMR ($CDCl_3$, 400 MHz) δ 7.00 (1H, dd, J = 4.6, 2.9 Hz, H-3), 4.63 -4.73 (1H, m, H-6), 4.17 – 4.27 (2H, q, J = 6.8 Hz, H-8), 2.83 – 3.01 (2H, m, H-7), 2.30 – 2.53 (2H, m, H-4), 2.13 – 2.30 (2H, m , H-5), 1.30 (3H, t, J = 7.2 Hz, H-9); ^{13}C NMR ($CDCl_3$, 400 MHz) δ 165.9 (C-1), 137.8 (c-3), 126.9 (C-2), 80.5 (C-6), 60.8 (C-8), 28.2 (C-7), 25.8 (C-5), 23.6 (C-4), 14.2 (C-9); HRMS required for $C_9H_{14}NO_4$ $[M+H]^+$ 200.0917, found 200.0916.

Ethyl 3-nitrocyclohexane-1-carboxylate **206**

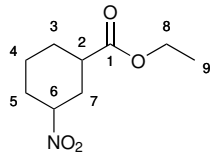

206

Pd/C (10 wt%, 0.010 g) was added to a stirred solution of compound **205** (0.100 g, 0.50 mmol) in MeOH (2 mL) under inert atmosphere (N_2). H_2 (1 atm) was then added and the mixture was left stirring at rt for 3 hours. The mixture was filtered through a pad of celite and it was washed again with MeOH. The crude product was purified *via* flash chromatography (1:2 ethyl acetate-hexane) giving two different inseparable diastereoisomers of the ester **206** as a colourless oil (37% yield, 0.037 g). Mixture of the two diastereomers a and b in a 1:1.5 ratio: ^{1}H NMR ($CDCl_3$, 400 MHz) δ 4.73 (0.4H, tt, J 7.4, 4.6, H-6a), 4.40 (0.6H, tt, J 12.1, 4.0, H-6b), 4.16 (2H, qd, J 7.1, 3.6, H-8), 2.82 (0.4H, p, J = 5.9, H-2a), 2.57 (0.6 H, ddq, J = 12.2,

3.7, 1.9, H-7b), 2.46 – 2.22 (2 H, m, H-2b, H-5b and H-7a), 2.20-2.05 (0.4 H, m, H-5a), 2.07 – 1.89 (2 H, m, H-3b, H-4b, H-7b, H-5a), 1.86 – 1.72 (1 H, m, H-5b and H-3a), 1.72 – 1.51 (1 H, m, H-4a), 1.49 – 1.34 (1 H, m, H-3b and H-4b), 1.27 (3 H, td, *J* 7.1, 3.4, H-9); ^{13}C NMR ($CDCl_3$, 400 MHz) δ 174.2 (C-1a), 173.5 (C-1b), 83.7 (C-6b), 81.1 (C-6a), 60.9 (C-8a), 60.8 (C-8b), 41.5 (C-2b), 38.4 (C-2a), 32.6 (C-7b), 30.5 (C-7a), 30.4 (C-5b), 29.6 (C-5a), 27.6 (C-3b), 27.2 (C-3a), 23.4 (C-4b), 20.7 (C-4a), 14.2 (C-9b), 14.2 (C-9a); HRMS required for $C_9H_{16}NO_4$ $[M+H]^+$ 202.1079, found 202.1085.

6.3.2 Method D for the synthesis of the 6-membered ring 151

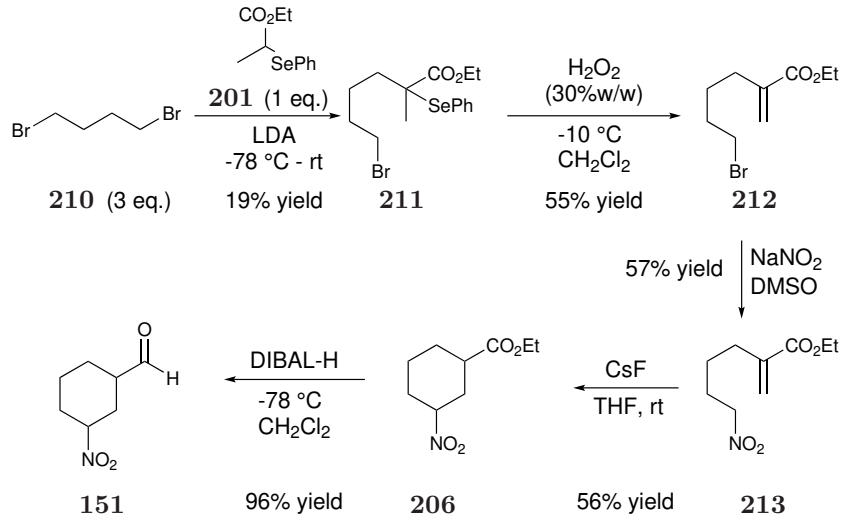

Scheme 6.3: Second synthetic procedure for the synthesis of the intermediate of reaction.

Ethyl 6-bromo-2-methyl-2-(phenylselanyl)hexanoate **211**

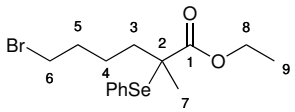

211

A 1.6M solution of *n*-BuLi (2.75 mL, 4.4 mmol) in hexane was added dropwise over 2 minutes to a solution of isopropyl amine (0.68 mL, 4.8 mmol) in anhydrous THF (8 mL) at -78 °C. The reaction mixture was left stirring at this temperature for 45 minutes when a solution of compound **201** (1.03 g, 4.0 mmol) in THF (3 mL + 1 mL to rinse the vial) was added dropwise over 5 min. After 1.5 hours stirring at -78 °C, 1,4-dibromobutane (0.96 mL, 8 mmol) in THF (3 mL) and HMPA (1

mL) was added dropwise over 5 min. The reaction mixture was stirred at -78 °C for additional 2 hours and then the cooling bath was removed and stirring at rt was continued for 2 h. At 0 °C, H_2O (1 mL) and saturated aqueous NH_4Cl (5 mL) were used to quech the reaction, stirring was continued at rt for 10 minutes and then the mixture was diluted with water (50 mL) and extracted with ethyl acetate (3 x 20 mL). The organic layers were dried (Na_2SO_4), filtered and concentrated *in vacuo*. Flash chromatography of the crude was required to achieve compound **211** (19% yield, 0.297g) as a viscous oil. IR (neat, cm^{-1}) 2931, 1717, 1578, 1475, 1437, 1377, 1301, 1260, 1238, 1152, 1099, 1066, 1022, 1000; ^{1}H NMR ($CDCl_3$, 400 MHz) δ 7.74 – 7.48 (2 H, m, Ar-H), 7.44 – 7.35 (1 H, m, Ar-H), 7.35 – 7.20 (2 H, m, Ar-H), 4.18 – 3.99 (2 H, m, H-8), 3.39 (2 H, t, J = 6.7, H-6), 1.95 (1 H, ddd, J = 13.5, 11.9, 4.5, H-3'), 1.89 – 1.79 (2 H, m, H-5), 1.75 (1 H, ddd, J = 13.5, 12.0, 4.4, H-3''), 1.69 – 1.58 (1 H, m, H-4'),1.51 (3 H, s, H-7), 1.38 (1 H, dddd, J 17.2, 8.5, 7.2, 4.4, H-4''), 1.19 (3 H, t, J 7.1, H-9); ^{13}C NMR ($CDCl_3$, 400 MHz) δ 173.8 138.1 (Ar-C), 129.2 (Ar-C), 128.7 (Ar-C), 61.0 (C-8), 37.5 (C-3), 33.4 (C-6), 32.7 (C-5), 24.1 (C-4), 22.7 (C-7), 14.0 (C-9); HRMS required for $C_{15}H_{21}BrO_2Se$ $[M]^+$ 391.9888, found 391.9893.

Ethyl 6-bromo-2-methylenehexanoate **212**

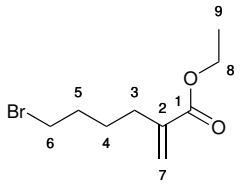

212

Hydrogen peroxide (30% w/v, 36.3 mL, 0.32 mol) was added dropwise to a solution of compound **211** (12.2 g, 0.31 mol) in CH_2Cl_2 (650 mL) at -10 °C (ice-acetone cooling bath 1:1). After 1.5 hours the reaction was quenched dropwise with saturated aqueous $NaHCO_3$ (1.9 L) and then with saturated aqueous solution of $Na_2S_2O_3$ (430 mL). Stirring was continued for 10 minutes at -10 °C, then the cooling bath was removed. The reaction mixture was left stirring for additional 10 minutes at rt, it was diluted with water (850 mL), extracted with CH_2Cl_2 (3 x 450 mL) , dried (Na_2SO_4), filtered and concentrated *in vacuo*. The crude product was purified *via* flash chromatography to afford the title product **212** as an oil (57%

yield, 4.04 g). IR (neat, cm^{-1}) 2937, 1701, 1631, 1444, 1409, 1368, 1300, 1282, 1254, 1179, 1028; ^{1}H NMR ($CDCl_3$, 400 MHz) δ 6.17 (1H, d, J = 1.4 Hz, H-7'), 5.55 (1H, d, J = 1.4 Hz, H-7''), 4.21 (2H, q, J = 7.1 Hz, H-8), 3.43 (2H, t, J = 6.8 Hz, H-6), 2.38 - 2.29 (2H, t, J = 7.6 Hz, H-3), 1.96 - 1.83 (2H, m, H-5), 1.73 - 1.53 (2H, m, H-4), 1.31 (3H, t, J = 7.1 Hz, H-9); ^{13}C NMR ($CDCl_3$, 400 MHz) δ 167.1 (C-1), 140.3 (C-5), 124.8 (C-7), 60.7 (C-8), 33.5 (C-6), 32.2 (C-5), 31.0 (C-3), 27.0 (C-4), 14.2 (C-9); HMRS required for $C_9H_{15}BrO_2$ $[M+H]^+$ 235.0334, found 235.0331.

Ethyl 2-methylene-6-nitrohexanoate **213**

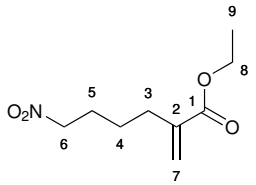

213

Sodium nitrite (1.77 g, 25.7 mmol) and TBAI (1.26 g, 3.4 mmol) were added to a solution of compound **212** (4.0 g, 17.1 mmol) and DMF (170 mL). Stirring at rt was continued for 6 hours. H_2O (170 mL) was then added and the organic phase was extracted with diethyl ether (3 x 300 mL). The organic layers were washed with a saturated aqueous solution of LiCl (150 mL x2) and then brine (150 mL x 2). The combined organic layers were then dried (Na_2SO_4), filtered and concentrated *in vacuo*. Purification *via* flash chromatography was required (15% ethyl acetate in hexane) . The title product was obtained as a yellow oil (57% yield, 1.953 g). IR (neat, cm^{-1}) 2932, 1713, 1632, 1552, 1436, 1382, 1302, 1259, 1185, 1146, 1026; ^{1}H NMR ($CDCl_3$, 400 MHz) δ 6.19 (1H, d, J = 1.3 Hz, H-7'), 5.55 (1H, d, J = 1.4 Hz, H-7''), 4.41 (2H, t, J = 7.0 Hz, H-6), 4.21 (2H, q, J =7.1 Hz, H-8), 2.37 (2H, td, J = 7.5, 1.3 Hz, H-3), 2.15 - 1.92 (2H, m, H-5), 1.66 - 1.49 (2H, m, H-4), 1.31 (3H, t, J = 7.1 Hz, H-9); ^{13}C NMR ($CDCl_3$, 400 MHz) δ 166.9 (C-1), 139.7 (C-2), 125.3 (C-7), 75.4 (C-6), 60.8 (C-8), 31.1 (C-3), 26.8 (C-5), 25.2 (C-4), 14.2 (C-9);

Ethyl 3-nitrocyclohexane-1-carboxylate **206**

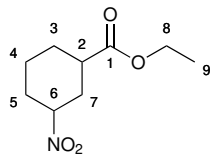

206

To a solution of **213** (1.50 g, 7.4 mmol) in THF (75 mL) was added CsF (2.26 g, 14.9 mmol) and the reaction mixture was then left stirring at rt for 24 h. The reaction mixture was then concentrated under reduced pressure and the residue was purified *via* flash chromatography on silica gel (25% ethyl acetate in hexane) to afford the title compound as a colourless oil (0.831 g, 56% yield). Characterisation of the ester **206** is shown in Method A.

3-nitrocyclohexane-1-carbaldehyde **151**

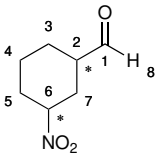

151

To a solution of **206** (1.00 g, 5.0 mmol) in anhydrous CH_2Cl_2 (28 mL) at -78°C was added dropwise DIBAL-H (1M in hexane, 7 mL). The reaction was left stirring at -78°C for 2 hours and then it was quenched with 1M aq. solution of HCl (16 mL). The reaction mixture was left stirring at rt overnight, then H_2O (16 mL) was added and the organic phase was extracted with CH_2Cl_2 (3 x 30 mL). The product was obtained as a colourless oil as a mixture of diastereoisomers and it was used without further purification for the following step (0.753 g, 96% yield). *cis* **151**: IR (neat, cm^{-1}) 2944, 1725, 1539, 1378, 1019, 749; ^{1}H NMR ($CDCl_3$, 400 MHz) δ 9.68 (1H, s, H-8), 4.62 (1H, t, J = 7.6, 4.8 Hz, H-6), 2.80 (1H, p, J = 5.7 Hz, H-2), 2.39 – 2.23 (2H, m, H-7), 2.09 (2H, ttt, J = 17.3, 9.2, 3.9 Hz, H-3), 1.94 – 1.65 (3H, m, H-4 and H-5), 1.57 – 1.41 (1H, m, H-4). ^{13}C NMR ($CDCl_3$, 101 MHz) δ 202.6 (C-1), 80.7 (C-6), 45.6 (C-2), 29.7 (C-3), 27.9 (C-7), 24.0 (C-5), 20.8 (C-4). HRMS required for $C_7H_{11}NO_3$ $[M+H]^+$ 158.0817, found m/z 158.0814. *trans* **151**: ^{1}H NMR ($CDCl_3$, 400 MHz) δ 9.66 (1H, d, J = 1.1 Hz, H-8), 4.43 (1H, tt, J = 12.0, 4.0 Hz, H-6), 2.64

– 2.53 (1H, m, H-7), 2.48 – 2.31 (2H, m, H-2 and H-5), 2.16 – 1.98 (2H, m, H-4 and H-3), 1.95 – 1.68 (2H, m, H-7 and H-5), 1.52 – 1.37 (1H, m, H-4), 1.33 – 1.16 (1H, m, H-3). ^{13}C NMR ($CDCl_3$, 101 MHz) δ 201.1 (C-1), 83.6 (C-6), 48.2 (C-2), 30.7 (C-5), 30.0 (C-7), 24.8 (C-3), 23.3 (C-4).

6.4 Synthesis of the α/β-unsaturated aldehyde 208

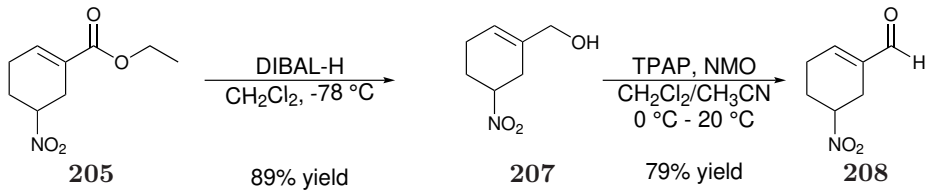

Scheme 6.4

(5-Nitrocyclohex-1-en-1-yl)methanol **207**

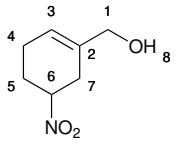

207

To a solution of **205** (0.300 g, 1.51 mmol) in anhydrous CH_2Cl_2 (8.5 mL) at -78 °C was added DIBAL-H (1M in Hex, 2.1 mL, 2.11 mmol) dropwise over 2 minutes. After 5.5 hours the reaction mixture still displayed starting material *via* TLC, so supplementary DIBAL-H was added (1M in Hex, 1 mL, 1 mmol). After 1 more hour the reaction was quenched with aqueous hydrochloric acid (1M, 7.5 mL) and it was left stirring at rt overnight. Water (15 mL) was added and it was extracted in CH_2Cl_2 (3 x 15 mL). The combined organic layers were dried(Na_2SO_4), filtered and concentrated *in vacuo*. The product **207** was obtained as a colourless oil (89% yield, 0.211 g) and it did not require further purification. IR (neat, cm^{-1}) 3347, 2923, 2360, 1359, 1438, 1378, 1286, 1221, 1142, 1063, 1008; ^{1}H NMR ($CDCl_3$, 400 MHz) δ 5.85 – 5.62 (1H, m, H-3), 4.83 – 4.51 (1H, m, H-6), 4.06 (2H, s, H-1), 2.84 – 2.50 (2H, m, H-7), 2.46 – 2.08 (4H, m, H-4 and H-5); ^{13}C NMR ($CDCl_3$, 400 MHz) δ 133.8 (C-2), 122.2 (C-3), 81.3 (C-6), 66.5 (C-1), 29.7 (C-7), 26.7 (C-5), 23.0 (C-4).

5-Nitrocyclohex-1-ene-1-carbaldehyde **208**

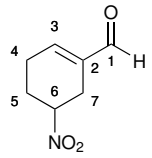

208

In a dry flask containing activated 4Å molecular sieves (0.085 g), compound **207** (0.200 g, 1.27 mmol) was dissolved in an anhydrous mixture of CH_2Cl_2 (17 mL) and acetonitrile (3.4 mL) in a ratio of 40:8. *N*-Methylmorpholine N-oxide (0.373 g, 3.2 mmol) was added to the solution at 0 °C. Once dissolved, TPAP (0.067 g, 0.19 mmol) was then added and it was left stirring at rt for 1.5 h. The reaction mixture was then filtered through a short pad of celite and silica and washed with 10% ethyl acetate-hexane (1.5 L). Compound **208** was obtained as an oil (79% yield, 0.156 g) and it did not require any further purification. IR (neat, cm^{-1}) 2922, 2850, 2361, 1765, 1695, 1647, 1545, 1430, 1385, 1301, 1279, 1172, 1117, 1070, 1001; ^{1}H NMR ($CDCl_3$, 400 MHz) δ 9.49 (s, 1H), 6.85 (1H, tt, J = 3.7, 1.7 Hz, H-3), 4.85 - 4.62 (1H, m, H-6), 3.01 - 2.76 (2H, m, H-7), 2.74 - 2.41 (2H, m, H-4), 2.41 - 2.16 (2H, m, H-5); ^{13}C NMR ($CDCl_3$, 400 MHz) δ 192.3 (C-1), 148.2 (C-3), 137.5 (C-2), 79.7 (C-6), 26.2 (C-5), 25.5 (C-7), 24.0 (C-4).

6.5 Synthesis of the internal nitro olefin 214

6.5.1 Method E for the synthesis of the nitro olefin 214

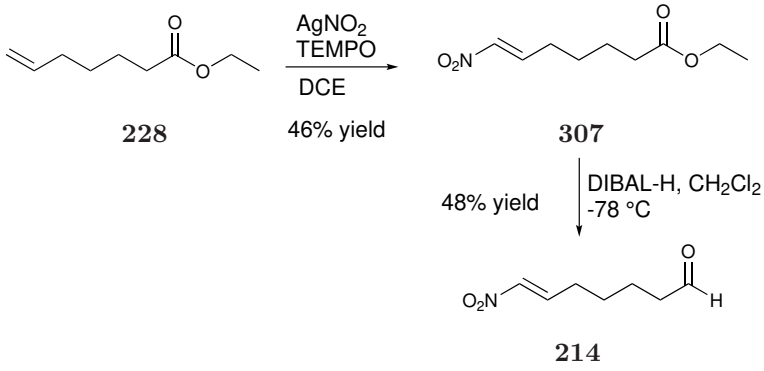

228 46% yield **307** 48% yield **214**

Figure 6.1: Synthesis of substrate **214** according to the synthetic procedure described in method E.

Ethyl (*E*)-7-nitrohept-6-enoate **307**

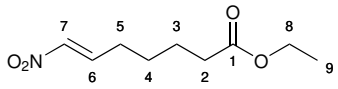

307

To an oven-dried quick-fit cap test tube charged with magnetic stir-bar was added activated 4Å molecular sieves (1.5 g), $AgNO_2$ (21.7 g, 128 mmol) and TEMPO (2.0 g, 12.8 mmol). Ethyl-6-heptenoate (5.6 mL, 32.0 mmol) and anhydrous DCE (100 mL) were added. The tube was then placed in a preheated oil bath at 70 °C and the reaction mixture was left stirring vigorously for 18 hours. The progress of the reaction was monitored by TLC and then the reaction mixture was left to cool down to rt. The reaction mixture was then filtered through a short pad of celite washed with ethyl acetate (500 mL) and concentrated *in vacuum*. The crude product was then purified *via* combiflash using silica gel columns and a gradient solution of ethyl acetate and hexane up to 20% ethyl acetate in hexane to afford the title compound **307** as a colourless oil (2.96 g, 14.7 mmol, 46%). IR (neat, cm^{-1}) 2936, 1728, 1650, 1522, 1462, 1349, 1179, 1152, 1097, 1030; ^{1}H NMR (400 MHz, $CDCl_3$) δ 7.37 – 7.21 (1H, m, H-7), 7.01 (1H, dt, J = 13.4, 1.6 Hz, H-6), 4.15 (2H, q, J = 7.1 Hz, H-8), 2.43 – 2.23 (4H, m, H-2 and H-5), 1.74 – 1.56 (2H, m, H-4), 1.64 – 1.50 (2H, m, H-3), 1.28 (3H, t, J = 7.1 Hz, H-9). ^{13}C NMR ($CDCl_3$, 101 MHz) δ 173.1 (C-1), 141.9 (C-6), 139.8 (C-7), 60.4 (C-8), 33.8 (C-2), 28.1 (C-5), 27.2 (C-3), 24.3 (C-4), 14.2 (C-9); HRMS required for $C_9H_{14}NO_4$ $[M\text{-}H]^+$ is 200.0923, found 200.0931.

(*E*)-7-nitrohept-6-enal **214**

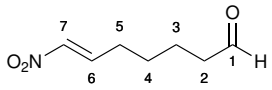

214

To a solution of ethyl **307** (2.95 g, 14.7 mmol) and anhydrous CH_2Cl_2 (80 mL) at -78 °C was added DIBAL-H (1M in hexane, 16.9 mL, 16.9 mmol) dropwise in 15 minutes. The progress of the reaction was monitored by TLC and the reaction went to completion in 4 hours. An aqueous solution of HCl (1M, 50 mL) was added and the reaction mixture was left to stir overnight at rt. Then, H_2O (80 mL) was added and the organic phase was extracted with CH_2Cl_2 (3 x 80 mL). The combined

organic phase was dried (Na_2SO_4), filtered and concentrated *in vacuo*. Purification by combiflash (silica gel, gradient up to 40% diethyl ether in hexane) afforded the title compound **214** as a colourless oil (0.864 g, 5.5 mmol, 37% yield). IR (neat, cm^{-1}) 2937 , 1719, 1648, 1517, 1347; ^{1}H NMR (400 MHz, $CDCl_3$) δ 9.78 (1H, t, J = 1.4 Hz, H-1), 7.33 - 7.13 (1H, m, H-6), 6.99 (1H, dt, J = 13.4, 1.6 Hz, H-7), 2.50 (2H, td, J = 7.1, 1.4 Hz, H-2), 2.30 (2H, td, J = 7.4, 1.6 Hz, H-5), 1.92 - 1.60 (2H, m, H-3), 1.62 - 1.37 (2H, m, H-4). ^{13}C NMR (101 MHz, $CDCl_3$) δ 201.6 (C-1), 141.78 (C-6), 139.90 (C-7), 43.41 (C-2), 28.26 (C-5), 27.19 (C-4), 21.42(C-3). HRMS required for $C_7H_{12}NO_3$ $[M+H]^+$ is 158.0817, found 158.0821.

6.5.2 Method F for the synthesis of 214

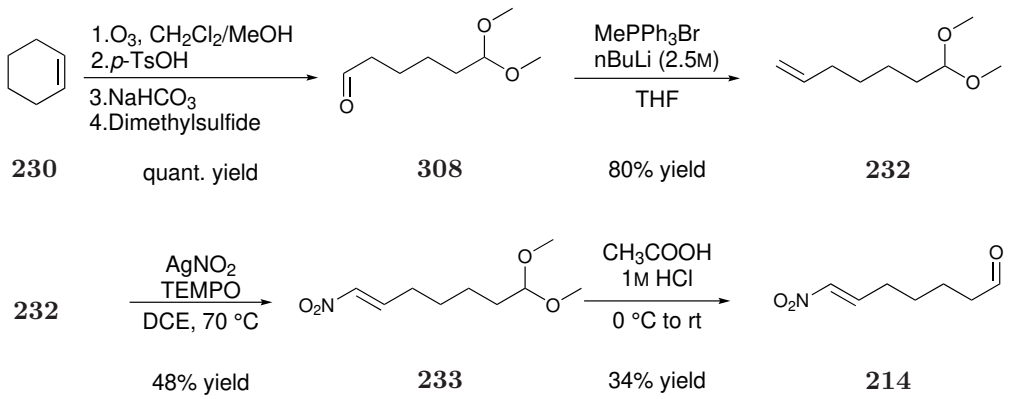

Figure 6.2: Synthesis of the nitro olefin **214** according to the synthetic procedure described in method F.

6,6-dimethoxyhexanal **308**[184]

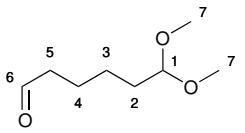

308

A three neck round bottom flask was heat dried and each neck was respectively occupied by a drying tube loaded with CaCl as outlet, a glass stopper and the ozoniser inlet. Cyclohexene (7.6 mL, 75 mmol) was dissolved in a solution of CH_2Cl_2 (250 mL) and MeOH (50 mL) and it was then cooled to -78 °C. O_3 was then bubbled through the solution until a light blue colour developed. Excess of O_3 was removed by bubbling through the reaction mixture N_2 until the blue colour was discharged.

The reaction mixture was then left to warm up to rt and the drying tube and the ozone inlet were replaced with rubber septums. *p*-Tosylic acid monohydride (10% *w/w*, 1.22 g) was added to the solution and then it was left stirring at rt under N_2 for 90 min. $NaHCO_3$ (4mol-eq, 2.15 g) was added followed by dimethyl sulphide (12 mL, 163.4 mmol) after 15 minutes. The reaction mixture was left stirring overnight and then concentrated up to 50 mL of solution. Then, it was diluted with CH_2Cl_2 (100 mL) and washed with H_2O (75 mL). The aqueous phase was extracted with CH_2Cl_2 (2 x 100 mL). The combined organic layers were washed with H_2O (100 mL) and the aqueous phase was extracted with a final portion of CH_2Cl_2 (100 mL). The organic layers were dried over Na_2SO_4, filtered and concentrated *in vacuo*. The product **308** was obtained as a colourless oil (12.6 g, 12 mmol, quantitative yield) and it was used for the following reaction without further purification. IR (neat, cm^{-1}) 2946, 2830, 1724, 1460, 1387, 1191, 1126, 1071, 1050; ^{1}H NMR (400 MHz, $CDCl_3$) δ 9.75 (1 H, s, H-6), 4.34 (1 H, t, *J* 5.7, H-1), 3.30 (6 H, s, H-7), 2.43 (2 H, td, *J* 7.3, 1.7, H-5), 1.82 – 1.51 (4 H, m, H-4, H-2), 1.45 – 1.31 (2 H, m, H-3). ^{13}C NMR (101 MHz, $CDCl_3$) δ 202.5 (C-6), 104.3 (C-1), 52.8 (C-7), 43.8 (C-5), 32.3 (C-2), 24.2 (C-3), 21.9 (C-4); HRMS required for $C_8H_{17}O_3$ $[M+H]^+$ is 161.1178, found 161.1180.

7,7-dimethoxyhept-1-ene **232**[185]

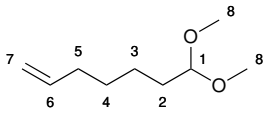

232

To a suspension solution of $MePPh_3Br$ (53.6 g, 150 mmol) in THF (180 mL) at 0 °C was added *n*BuLi (2.5M in hexane, 60 mL, 150 mmol) dropwise and the reaction mixture was left stirring at 0 °C for 30 minutes. A solution of **308** in THF (48 mL) was then added dropwise in 15 minutes. The reaction mixture was then left stirring at rt for 46 hours. A saturated aqueous solution of NH_4Cl (420 mL) was added. The organic phase was extracted with diethyl ether (3 x 300 mL) and then washed with brine (250 mL). The combined organic phases were dried over Na_2SO_4, filtered and then concentrated *in vacuo* keeping the water bath at a max temperature of 30 °C and a pressure of 100 mbar to avoid any evaporation of the

targeted product. The concentrated organic phase was then filtered through a short pad of silica and washed with a mixture of diethyl ether and pentane (1:1, 1.2 L). The organic solvent was concentrated again *in vacuo* to afford a colourless oil as pure product **232** (9.5 g, 60.0 mmol, 80% yield). ^{1}H NMR (400 MHz, $CDCl_3$) δ 5.80 (1 H, ddt, J = 16.9, 10.2, 6.7, H-6), 5.05 – 4.87 (1 H, m, H-7), 4.36 (1 H, t, J = 5.8, H-1), 3.31 (6 H, s, H-8), 2.19 – 1.94 (2 H, m, H-5), 1.73 – 1.47 (2 H, m, H-2), 1.49 – 1.25 (4 H, m, H-4, H-3). ^{13}C NMR (101 MHz, $CDCl_3$) δ 138.8 (C-6), 114.4 (C-7), 104.5 (C-1), 52.6 (C-8), 33.7 (C-5), 32.3 (C-2), 28.8 (C-4), 24.1 (C-3).

(*E*)-7,7-dimethoxy-1-nitrohept-1-ene **233**

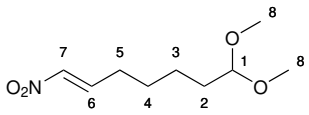

233

To a heat dried two-neck round bottomed flask charged with magnetic stir-bar was added activated 4Å molecular sieves (2 g), $AgNO_2$ (40.4 g, 238 mmol) and TEMPO (3.7 g, 23.8 mmol). Olefin **232** (9.4 g, 59.6 mmol) and anhydrous DCE (186 mL) were added. The round bottomed flask was then placed in a preheated oil bath at 70 °C and the reaction mixture was left stirring vigorously. The progress of the reaction was monitored by TLC and after 17 hours the reaction mixture was left to cool down to rt. The reaction mixture was then filtered through a short pad of celite washed with ethyl acetate (1 L) and concentrated *in vacuum*. The crude product was then purified *via* combiflash using silica gel columns and a gradient solution of ethyl acetate and hexane up to 30% diethyl ether in hexane to afford the title compound **233** as a colourless oil (5.8, 28.5 mmol, 48%). ^{1}H NMR (400 MHz, $CDCl_3$) δ 7.23 – 7.12 (1 H, m, H-6), 6.89 (1 H, dt, J = 13.4, 1.5, H-7), 4.47 – 4.03 (1 H, m, H-1), 3.22 (6 H, d, J = 3.8, H-8), 2.19 (2 H, qd, J = 7.4, 1.6, H-5), 1.72 – 1.39 (4 H, m, H-2, H-4), 1.39 – 1.22 (2 H, m, H-3). ^{13}C NMR (101 MHz, $CDCl_3$) δ 142.3 (C-6), 139.7 (C-7), 104.3 (C-1), 52.9 (C-8), 32.2(C-2), 28.4(C-5), 27.6 (C-4), 24.1 (C-3).

(*E*)-7-nitrohept-6-enal **214**

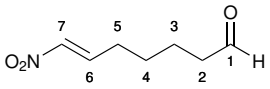

214

To neat acetal **233** (2.940 g, 14.5 mmol), glacial acetic acid (14.5 mL) was added at 0 °C and, as soon as frozen, HCl (1N, 4.8 mL) was added. The reaction mixture was left stirring at rt. The progress of the reaction was monitored by TLC and ^{1}H NMR and after 20 hours CH_2Cl_2 (30 mL) was added to the reaction mixture and washed with H_2O (2 x 50 mL) and a saturated aqueous solution of $NaHCO_3$ (50mL). The organic phase was back extracted with CH_2Cl_2 (3 x 50 mL) and then the organic phases were combined, dried (Na_2SO_4), filtered and concentrated *in vacuo* with a 30 °C water bath temperature at a max pressure of 100 mbar. Purification by combiflash (silica gel, gradient up to 55% diethyl ether in pentane) afforded the title compound as a colourless oil (0.760 g, 4.8 mmol, 34% yield). The characterisation of compound **214** was described in method E.

6.6 General procedure G for the synthesis of catalysts 238 and 239[130]

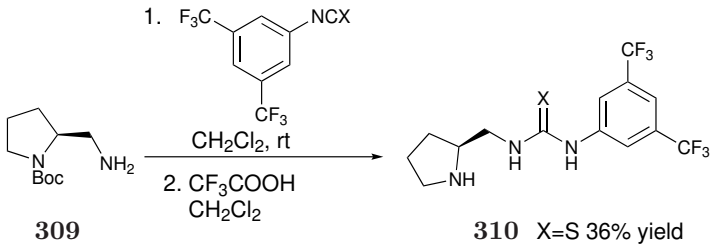

Scheme 6.5: Synthetic procedure for the synthesis of bifunctional catalysts **238** and **239**.

To a stirred solution of **309** in anhydrous CH_2Cl_2 was added the isocyanate at rt. The reaction mixture was stirred at rt for 18 hours and then concentrated *in vacuo* to afford the crude protected product as a white solid and it was used without further purification for the following step. The N-Boc derivative was dissolved in a mixture of trifluoroacetic acid and CH_2Cl_2 (40 mL, v/v = 1:1) and the solution was stirred at rt for 3 h. The pH was then adjusted to 8 with saturated aqueous solution

of $NaHCO_3$ and then the organic phase was extracted with CH_2Cl_2 (3 x 150 mL). Organic layers were combined and dried over $MgSO_4$, filtered and concentrated *in vacuo*. The crude product was then purified *via* flash chromatography on alumina (gradient from 7:1 to 1:2 ethyl acetate/MeOH).

(*S*)-1-(3,5-bis(trifluoromethyl)phenyl)-3-(pyrrolidin-2-ylmethyl) urea **238**[130]

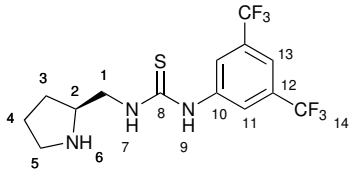

238

Following general procedure G, the urea catalyst **238** was obtained from the nucleophilic addition of the amine **309** (4.35 mmol, 0.871 g) in anhydrous CH_2Cl_2 (30 mL) to isothiocyanate (4.35 mmol, 0.8 mL). The obtained crude protected amine was deprotected with trifluoroacetic acid and CH_2Cl_2 (40 mL, *v/v* = 1:1) to afford the thiourea **239** as a white powder (0.565g, 36% yield). $[\alpha]^{20}{}_D$ + 30.0 (c = 0.1, CH_2Cl_2); ^{1}H NMR (400 MHz, CD_3OD) δ 7.97 (2H, s, H-11), 7.43 (1H, s, H-13), 3.71 – 3.55 (1H, m, H-2), 3.42 (1H, d, J = 6.6 Hz, H-1), 3.32 - 3.07 (1H, m, H-5), 2.21 – 2.01 (1H, m, H-3), 2.01 – 1.84 (2H, m, H-4), 1.79 - 1.59 (1H, m, H-3).^{13}C NMR (101 MHz, CD_3OD) δ 156.9 (C-8), 141.8 (C-10), 131.7 (q, J = 33.0 Hz, C-14), 123.4 (q, J = 271.7 Hz, C-12), 117.8 (d, J = 4.0 Hz, C-11), 114.6 – 114.1 (m, C-13), 61.3 (C-2), 45.2, 40.7 (C-1), 27.0 (C-3), 23.1 (C-4).

(*S*)-1-(3,5-bis(trifluoromethyl)phenyl)-3-(pyrrolidin-2-ylmethyl) thiourea **239**[130]

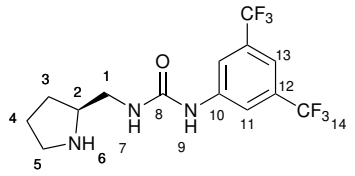

239

Following general procedure G, the thiourea catalyst **239** was obtained from the nucleophilic addition of the amine **309** (4.35 mmol, 0.871 g) in anhydrous CH_2Cl_2 (30 mL) to isothiocyanate (4.35 mmol, 0.75 mL). The obtained crude protected amine was deprotected with trifluoroacetic acid and CH_2Cl_2 (40 mL, *v/v* = 1:1) to

afford the thiourea **239** as a white powder (0.86 g, 56% yield). $[\alpha]^{20}{}_D$ - 29.0 (c = 0.1, CH_2Cl_2) ^{1}H NMR (400 MHz, CD_3OD) δ 8.18 (2H, s, H-11), 7.57 (1H, s, H-13), 3.98 – 3.79 (3H, m, H-1 and H-2), 3.40 – 3.11 (2H, m, H-5), 2.18 – 2.05 (1H, m, H-3'), 2.04 – 1.87 (2H, m, H-4), 1.76 (1H, qd, J = 8.2, 3.8 Hz, H-3''). ^{13}C NMR (101 MHz, CD_3OD) δ 184.2 (C-8), 142.9 (C-10), 133.8 – 131.6 (m, C-12), 126.1 (C-14), 124.8 – 123.5 (m, C-11), 118.8 – 117.4 (m, C-13), 61.8 (C-2), 46.6 (C-5), 45.6 (C-1), 28.7 (C-3), 24.4 (C-4).

6.7 Synthesis of catalyst 240[129]

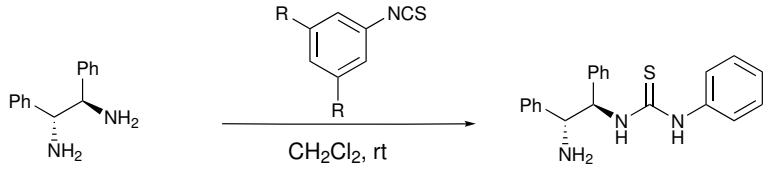

311 **240** R=H 59% yield

Scheme 6.6: Synthetic procedure for the synthesis of bifunctional catalysts **240**.

1-((1*R*,2*R*)-2-amino-1,2-diphenylethyl)-3-phenylthiourea **240**[129]

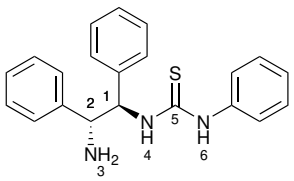

240

A solution of isothiocyanate (2 mmol) in CH_2Cl_2 (10 mL) was added dropwise over 2 hours *via* a syringe pump to a stirred solution of (1*R*,2*R*)-1,2-diphenylethane-1,2-diamine (4 mmol) in anhydrous CH_2Cl_2 (10 mL) at 0 °C. The reaction mixture was stirred at rt for 14 hours. Then, the reaction mixture was concentrated *in vacuo* and the residue was purified by flash chromatography on silica gel (eluent phase: 10% MeOH in CH_2Cl_2) to afford the corresponding thiourea. White solid, 59% yield; $[\alpha]^{20}{}_D$ + 109.0 (c = 0.1, CH_2Cl_2); ^{1}H NMR ($CDCl_3$, 400 MHz) δ 7.56 (1H, br s, H-4), 7.55 – 7.37 (2H, m, H-1 and Ar-H), 7.37 - 7.05 (14H, m, Ar-H), 5.47 (1H, s, H-6), 4.35 (1H, d, J = 3.1 Hz, H-2), 1.40 (2H, br s, H-3). ^{13}C NMR ($CDCl_3$, 101 MHz) δ 180.7 (C-5), 141.5 (Ar-C), 140.0 (Ar-C), 136.1 (Ar-C), 130.0 (Ar-C), 128.8 (Ar-C), 128.5 (Ar-C), 128.5 (Ar-C), 127.8 (Ar-C), 127.5 (Ar-C), 126.4 (Ar-C),

126.3 (Ar-C), 125.7 (Ar-C), 64.3 (C-1), 59.3 (C-2).

6.8 Optimised synthesis of the nitroalcohol *cis*-226

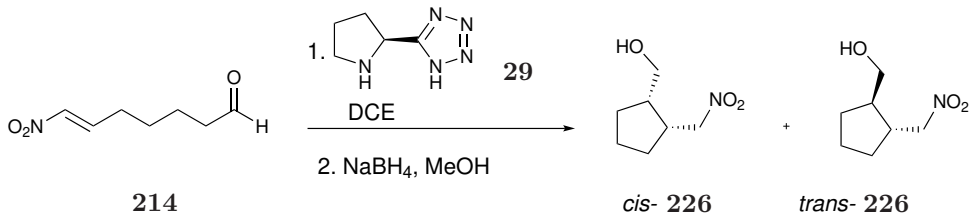

214 *cis*- **226** *trans*- **226**

Figure 6.3: Synthetic procedure for the synthesis of *cis*-**226**.

((1*S*,2*R*)-2-(nitromethyl)cyclopentyl)methanol **226**

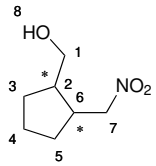

226

To a solution of (*S*)-(-)-5-(2-pyrrolidinyl)-1H-tetrazole (5 mol%, 0.35 mmol, 0.051 g) and DCE (130 mL) previously sonicated for 30 minutes was added the nitro olefin **214** (1.104 g, 7.0 mmol) at -20 °C dropwise in 3 minutes followed by DCE (5 mL) to wash the syringe used and the sides of the reaction flask. The reaction mixture was left stirring at -20 °C for 99 hours. The progress of the reaction was monitored by TLC and ^{1}H NMR. Once the reaction went to completion the reaction was reduced *in situ*. $NaBH_4$ (0.397 g, 10.5 mmol) was added at -20 °C followed by MeOH (10.9 mL). The reaction went to completion in 1 hour. A saturated aqueous solution of NH_4Cl (15 mL) was added, followed by brine (50 mL) and H_2O (20 mL). The organic phase was extracted first with a mixture of chloroform and isopropanol (3:1, 80 mL x 5), then with diethyl ether (3 x 150 mL) and finally with ethyl acetate (3 x 100 mL) because of the high affinity of the product with the aqueous phase. The organic phase was then dried (Na_2SO_4), filtered and concentrated *in vacuo*. The crude product was then purified by flash chromatography on silica gel (25% ethyl acetate in hexane) to afford separately both diastereomers, *cis* and *trans*, as a colourless oil (0.820 g, 9:1 *cis/trans* ratio, 74%). *Cis*-**226**: 92% *ee*; HPLC analysis: Chiralpack OD, 2% isopropanol in hexane, flow rate = 0.8 mL/min, λ = 210 nm.

$[\alpha]^{20}{}_D$ -14 (c = 0.1, CH_2Cl_2). IR (neat, cm^{-1}) 3376, 2958, 2877, 1543, 1383, 1022; ^{1}H NMR (400 MHz, $CDCl_3$) δ 4.55 (2H, ABX, J_{AX} = 6.6 Hz, J_{BX} = 9.1 Hz, J_{AB} = 12.7, ν_{AB} = 138.5, H-7), 3.67 – 3.50 (2H, m, H-1), 2.87 – 2.71 (1H, m, H-6), 2.38 – 2.25 (1H, m, H-2), 1.91 – 1.79 (2H, m, H-5'and H-3'), 1.79 – 1.69 (1H, m, H-4'), 1.71 – 1.56 (1H, m, H-4''), 1.57 – 1.32 (2H, m, H-5'', H3''). ^{13}C NMR (101 MHz, $CDCl_3$) δ C 77.2 (C-7), 63.2 (C-1), 43.1 (C-2), 40.3 (C-6), 29.3 (C-5), 28.0 (C-3), 23.1 (C-4); HRMS required for $C_7H_{43}NO_3$ $[M+H]^+$ is 160.0974, found 160.0980. *Trans*-**226**: 45% *ee*; HPLC analysis: Chiralpack OD, 1% isopropanol in hexane, flow rate = 1 mL/min, λ = 210 nm. $[\alpha]^{20}{}_D$ - 8 (c = 0.1, CH_2Cl_2). ^{1}H NMR (400 MHz, $CDCl_3$) δ 4.44 (2 H, ABX, J_{AX} = 5.7 Hz, J_{BX} = 8.8 Hz,J_{AB} = 11.8 Hz, ν_{AB} = 110.5, H-7), 3.77 - 3.50 (2 H, m, H-1), 2.54 - 2.38 (1 H, m, H-6), 2.01 - 1.88 (1 H, m, H-5'), 1.88 - 1.75 (2 H, m, H-2 and H-3'), 1.71 - 1.53 (2 H, m, H-4), 1.53 - 1.33 (1 H, m, H-5''and H-3'').^{13}C NMR ($CDCl_3$, 101 MHz) δ 79.1 (C-7), 64.9 (C-1), 44.1 (C-2), 40.6 (C-6), 29.8 (C-5), 27.9 (C-3), 23.1 (C-4).

6.9 Synthesis of nitroalcohol derivative 241

((1*S*,2*R*)-2-(nitromethyl)cyclopentyl)methyl (1*S*,4*R*)-4,7,7-trimethyl-3-oxo-2-oxabicyclo[2.2.1]heptane-1-carboxylate **241**

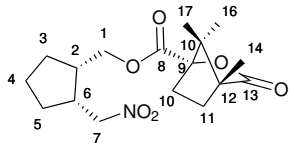

241

To a solution of the nitro alcohol *cis*-**226** (0.040 g, 0.25 mmol) and imidazole (17 μl, 0.30 mmol) in anhydrous THF (2.5 mL), (*S*)-(-)-camphanic chloride was added at 0 °C. The reaction mixture was refluxed for 4 hours and then left stirring at rt for 20 more hours as the reaction was not gone to completion yet. Then, H_2O (5 mL) was added and the organic phase was extracted with diethyl ether (3 x 10 mL), then dried (Na_2SO_4), filtered and concentrated *in vacuo*. The crude product was then recrystallised in a solvent mixture of methanol, ethyl acetate and hexane (2:1:4) to obtain the X-ray crystal of the title compound **241** as a white solid. mp = 71.5 - 73.6 °C; $[\alpha]^{20}{}_D$ - 12.0 (c = 0.1, CH_2Cl_2); IR (neat, cm^{-1}) 2969, 1778, 1743, 1546, 1449, 1398, 1381, 1315, 1266, 1225, 1173, 1154, 1113, 1063, 1034, 1020; ^{1}H

NMR (400 MHz, $CDCl_3$) δ 4.36 (2H, ABX, J_{AX} = 6.7 Hz, J_{BX} = 8.9 Hz, J_{AB} = 12.6 Hz, ν_{AB} = 96,4 Hz, H-7), 4.10 (2H, qd, J = 11.5, 6.7, H-1), 2.85 - 2.70 (1H, m, H-6), 2.51 - 2.42 (1H, m, H-2), 2.42 - 2.29 (1H, m, H-10'), 2.06 - 1.92 (1H, m, H-10''), 1.92 - 1.77 (3H, m, H-5'and H-4', H-11'), 1.72 (2H, m, H-3), 1.68 - 1.51 (1H, m, H-11''), 1.51 - 1.31 (3H, m, H-4''and H-5'') 1.05 (3H, s, H-14), 1.00 (3H, s, H-16), 0.90 (3H, s, H-17). ^{13}C NMR (101 MHz, $CDCl_3$) δ 178.0 (C-13), 167.5 (C-8), 91.0 (C-9), 76.5 (C-7), 65.3 (C-1), 54.8 (C-12), 54.3 (C-15), 40.2 (C-6), 39.9 (C-2), 30.7 (C-10), 29.0 (C-11), 28.9 (C-5), 28.1 (C-4), 22.6 (C-3), 16.8 (C-16), 16.8 (C-17), 9.7 (C-14). HRMS required for $C_{17}H_{26}NO_6$ $[M+H]^+$ is 340.1760, found 340.1762.

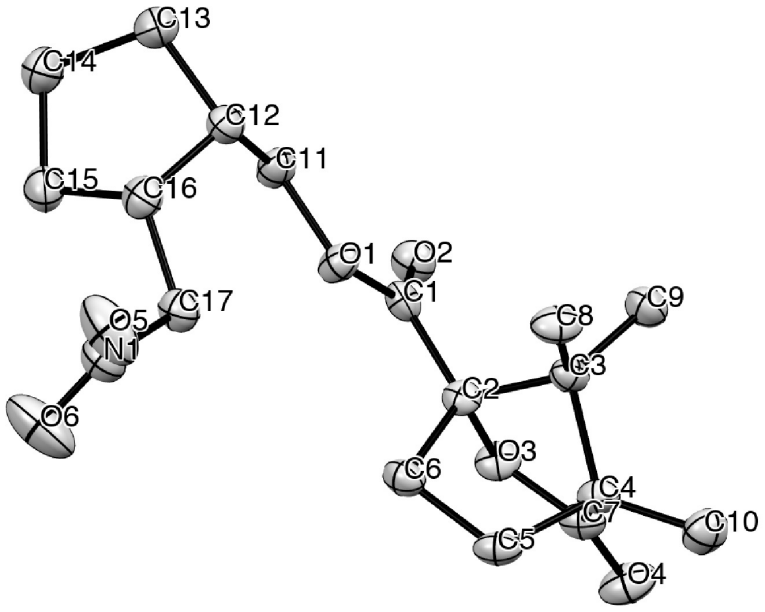

Figure 6.4: X-ray crystal structure of the nitro alcohol derivative **241** (CCDC : 1947228).

Table 6.1: Crystal data and structure refinement for **241**.

Identification code	RF266A
Empirical formula	$C_{17}H_{25}NO_6$
Formula weight	339.38
Temperature/K	153(5)
Crystal system	monoclinic
Space group	$P2_1$
a/Å	6.4204(2)
b/Å	11.9299(4)
c/Å	11.1764(4)
α/°	90
β/°	95.772(3)
γ/°	90
Volume/Å^3	851.71(5)
Z	2
ρ_{calc}g/cm^3	1.323
μ/mm^{-1}	0.832
F(000)	364.0
Crystal size/mm^3	0.09 × 0.07 × 0.05
Radiation	CuKα (λ = 1.54184)
2Θ range for data collection/°	7.95 to 119.994
Index ranges	-7 ≤ h ≤ 6, -13 ≤ k ≤ 13, -12 ≤ l ≤ 12
Reflections collected	6574
Independent reflections	2431 [R_{int} = 0.0266, R_{sigma} = 0.0283]
Data/restraints/parameters	2431/1/220
Goodness-of-fit on F^2	1.097
Final R indexes [I>=2σ (I)]	R_1 = 0.0292, wR_2 = 0.0719
Final R indexes [all data]	R_1 = 0.0310, wR_2 = 0.0737
Largest diff. peak/hole / e Å^{-3}	0.15/-0.17
Flack parameter	-0.10(9)

6.10 Synthetic procedure for the synthesis of α-substituted nitroolefins

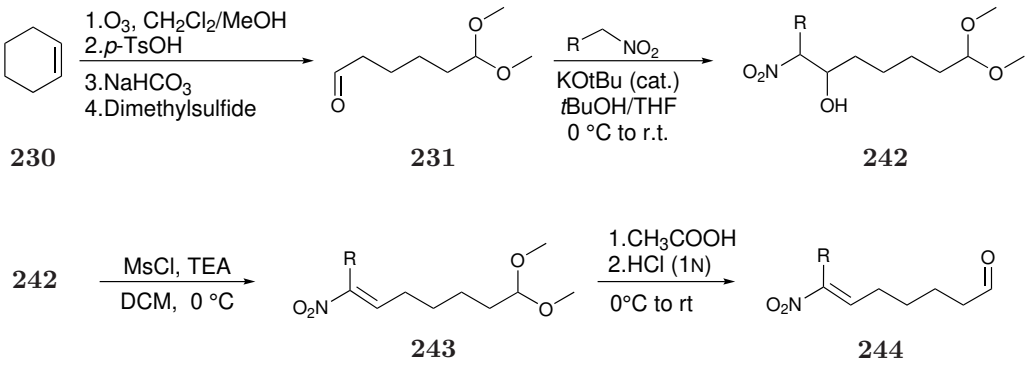

Scheme 6.7: Synthesis of α-substituted nitro olefin substrates.

General procedure H for the synthesis of nitro alcohols 242.

Potassium *tert*-butoxide (0.2 eq.) was added to a solution of **231** (1 eq.) (obtained as described in Method F), nitroalkane (3 eq.) in a mixture of *t*-BuOH and THF (*v/v* = 1:1) and it was left stirring for 3 h. The reaction mixture was then diluted with ethyl acetate and the organic phase was washed with H_2O and brine. The aqueous phase was back extracted with ethyl acetate and the combined organic layers were then dried (Na_2SO_4), filtered and concentrated *in vacuo*. The crude product was then purified *via* combiflash on silica gel (gradient ethyl acetate in hexane).

8,8-dimethoxy-2-nitrooctan-3-ol **242a**

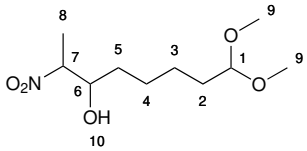

242 a

Following the general procedure H, potassium *tert*-butoxide (0.140 g, 1.3 mmol) was added to a solution of **231** (1.0 g, 6.2 mmol), 1-nitroethane (1.3 mL, 18.7 mmol) in a mixture of *t*-BuOH and THF (12.4 mL, *v/v* = 1:1) to afford two diastereomers of the nitro alcohol **242a** as a colourless oil (0.73 g, 50% yield). Mixture of diastereomers (1:1 *syn/anti*): IR (neat, cm^{-1}) 2945, 1546, 1454, 1390, 1126, 1022, 984; ^1H NMR ($CDCl_3$, 400 MHz) δ 4.53 – 4.37 (2H, m, H-7), 4.29 (2H, td, J = 5.7, 0.7 Hz, H-1), 4.12 (1H, ddd, J = 8.6, 4.0, 2.9 Hz, H-6), 3.84 (1H, ddd, J = 9.7, 4.7, 2.2 Hz,

H-6), 3.42 and 3.25 (12H, d, J = 0.9 Hz, H-9), 1.60 – 1.51 (4H, m, H-2 and H-3), 1.49 (3H, J = 1.5 Hz, H-8), 1.48 (3H, d, J = 1.5 Hz, H-8), 1.43 – 1.25 (12H, m, H-2, H-3, H-4 and H-5). ^{13}C NMR ($CDCl_3$, 101 MHz) δ 104.4 (C-1), 87.7 (C-7), 86.4 (C-7), 72.7 (C-6), 71.9 (C-6), 52.7 (C-9), 50.9 (C-9), 32.9 (C-5), 32.9 (C-2), 32.3 (C-2), 25.6 (C-5), 25.0 (C-3), 24.7 (C-3), 24.3 (C-4), 24.3 (C-4), 16.3 (C-8), 12.4 (C-8). HRMS required for $C_{12}H_{24}N_2O_5$ $[M+CH_3CN+Na]^+$ 299.1583, found 299.1582.

9,9-dimethoxy-3-nitrononan-4-ol **242b**

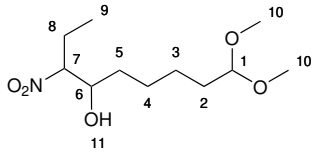

242 b

Following the general procedure H, potassium *tert*-butoxide (0.140 g, 1.3 mmol) was added to a solution of **231** (1.0 g, 6.2 mmol), 1-nitropropane (1.7 mL, 18.7 mmol) in a mixture of *t*-BuOH and THF (12.4 mL, v/v = 1:1) to afford two diastereomers of the nitro alcohol **242b** as a colourless oil (0.83 g, 54% yield). Mixture of diastereomers (1:1 *syn/anti*): IR (neat, cm^{-1}) 3429, 2944, 1545, 1460, 1375, 1126, 1049, 954, 808; ^{1}H NMR ($CDCl_3$, 400 MHz) δ 4.36 – 4.21 (4H, m, H-7 and H-1), 3.95 (1H, dt, J = 8.3, 4.1 Hz, H-6), 3.89 – 3.77 (1H, m, H-6), 3.41 and 3.25 (12H, s, H-10), 2.58 – 2.19 (2H, m, H-11), 2.14 - 1.89 (2H, m, H-8), 1.88 – 1.69 (2H, m, H-8), 1.61 – 1.20 (16H, m, H-2, H-3, H-4 and H-5), 0.92 (6H, td, J = 7.4, 3.5 Hz, H-9). ^{13}C NMR ($CDCl_3$, 101 MHz) δ 104.3 (C-1), 94.4 (C-7), 93.9 (C-7), 72.1 (C-6), 71.6 (C-6), 52.8 (C-10), 52.7 (C-10), 33.7 (C-5), 33.4 (C-5), 33.1 (C-2), 32.3 (C-2), 25.5 (C-4), 25.1 (C-4), 24.3 (C-3), 24.3 (C-3), 23.9 (C-8), 21.5 (C-8). , 21.5, 10.6 (C-9), 10.2 (C-9). HRMS required for $C_{11}H_{23}NO_5$ $[M+Na]^+$ 272.1474, found 272.1470.

1,1-dimethoxy-7-nitroundecan-6-ol **242c**

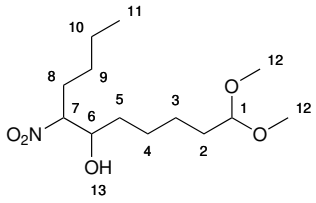

242 c

Following the general procedure H, potassium *tert*-butoxide (0.13 g, 1.1 mmol) was added to a solution of **231** (0.91 g, 5.7 mmol), 1-nitropentane (2.1 mL, 17.1 mmol) in a mixture of *t*-BuOH and THF (11.4 mL, *v/v* = 1:1) to afford two diastereomers of the nitro alcohol **242c** as a colourless oil (1.0 g, 64% yield). Mixture of diastereomers (1:1 *syn/anti*): IR (neat, cm^{-1}) 3429, 2938, 1547, 1460, 1382, 1127, 1049; ^{1}H NMR ($CDCl_3$, 400 MHz) δ 4.37 (1H, ddt, J = 12.6, 6.2, 3.9 Hz, H-7), 4.29 (1H, td, J = 5.7, 1.3 Hz, H-1), 3.94 (0.4H dq, J = 8.4, 4.1 Hz, H-6), 3.82 (0.6H, dd, J = 9.4, 6.3 Hz, H-6), 3.25 (6H, s, H-12), 2.33 (0.4H, d, J = 4.7 Hz, H-13), 2.19 (0.6H, d, J = 7.9 Hz, H-13), 2.12 – 1.89 (1H, m, H-8), 1.72 (1H, dddd, J = 15.6, 14.2, 5.9, 3.7 Hz, H-8), 1.64 – 1.15 (12H, m, H-2, H-3, H-4, H-5, H-9 and H-10), 0.90 – 0.75 (3H, m, H-11). ^{13}C NMR ($CDCl_3$, 101 MHz) δ 104.4 (C-1), 92.9 (C-7), 92.3 (C-7), 72.2 (C-6), 71.9 (C-6), 52.8 (C-12), 52.7 (C-12), 33.5 (C-5), 33.1 (C-5), 32.3 (C-2), 32.3 (C-2), 30.2 (C-8), 28.1 (C-8), 27.8 (C-9), 27.7 (C-9), 25.5 (C-10), 25.1 (C-10), 24.3 (C-3), 24.3 (C-3), 22.2 (C-4), 22.1 (C-4), 13.7 (C-11), 13.7 (C-11). HRMS required for $C_{13}H_{27}NO_5$ $[M+Na]^+$ 300.1787, found 300.1795.

(2-Nitroethyl)benzene 312[186]

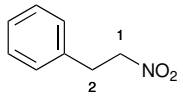

312

To a solution of sodium nitrite (3.59 g, 52 mmol) in anhydrous DMF (230 mL) at -78 °C was added 2-bromo ethyl benzene (5.5 mL, 40 mmol) and it was left stirring overnight leaving the cooling bath to warm up to rt. The reaction was monitored by TLC, and after 20 hours the reaction mixture was concentrated *in vacuo* to reduce the amount of DMF. The reaction mixture was then diluted with ethyl acetate (50 mL) and the organic phase was washed with H_2O (3 x 50 mL). The combined organic

layers were dried (Na_2SO_4), filtered and concentrated *in vacuo*. The crude product was purified via flash chromatography on silica gel (10% ethyl acetate in hexane) to afford the title product as a yellow liquid (2.32 g, 38% yield). ^{1}H NMR ($CDCl_3$, 400 MHz) δ 7.41 – 7.33 (2 H, m, Ar-H), 7.33 – 7.26 (1 H, m, Ar-H), 7.28 – 7.17 (2 H, m, Ar-H), 4.64 (2 H, t, J = 7.4 Hz, H-1), 3.35 (2 H, t, J = 7.4 Hz, H-2); ^{13}C NMR ($CDCl_3$, 101 MHz) δ 135.6 (Ar-C), 129.0 (Ar-C), 128.6 (Ar-C), 127.5 (Ar-C), 76.3 (C-1), 33.5 (C-2).

8,8-dimethoxy-2-nitro-1-phenyloctan-3-ol **242d**

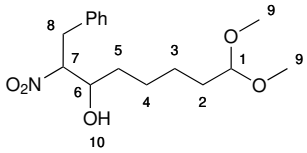

242 d

Following the general procedure H, potassium *tert*-butoxide (0.140 g, 1.3 mmol) was added to a solution of **231** (1.0 g, 6.2 mmol), (2-nitroethyl)benzene **312** (2.83 g, 18.7 mmol) in a mixture of *t*-BuOH and THF (12.4 mL, *v/v* = 1:1) to afford two diastereomers of the nitro alcohol **242d** as a yellow oil (1.51 g, 78% yield). Mixture of diastereomers (1:1 *syn/anti*): IR (neat, cm^{-1}) 3431, 2942, 1723, 1547, 1497, 1456, 1371, 1128, 1051, 858, 749, 699; ^{1}H NMR ($CDCl_3$, 400 MHz) δ 7.32 – 7.17 (3H, m, Ar-H), 7.16 – 7.03 (2H, m, Ar-H), 4.68 – 4.56 (1H, m, H-7), 4.28 (1H, t, J = 5.6 Hz, H-1), 4.13 – 3.98 (0.3H, m, H-6), 3.78 (0.7H, tt, J = 8.7, 4.5 Hz, H-6), 3.39 - 3.00 (8H, m, H-8 and H-9), 2.40 – 2.35 (0.3H, m, H-5), 2.30 – 2.23 (1H, m, H-5), 1.60 – 1.25 (6H, m, H-2, H-3, H-4). ^{13}C NMR ($CDCl_3$, 101 MHz) δ 135.7 (Ar-C), 135.1 (Ar-C), 128.9 (Ar-C), 128.9 (Ar-C), 128.9 (Ar-C), 128.8 (Ar-C), 127.6 (Ar-C), 127.4 (Ar-C), 104.4 (C-1), 104.3 (C-1), 93.5 (C-7), 93.4 (C-7), 72.2 (C-6), 71.2 (C-6), 52.8 (C-9), 52.8 (C-9), 36.6 (C-8), 34.4 (C-8), 33.8 (C-5), 33.2 (C-5), 32.3 (C-2), 25.4 (C-3), 25.3 (C-3), 24.3 (C-4), 24.2 (C-4). HRMS required for $C_{16}H_{25}NO_5$ $[M+Na]^+$ 334.1630, found 334.1629.

6.10.1 Synthesis of the aldehyde 315 for the final synthesis of 244e.

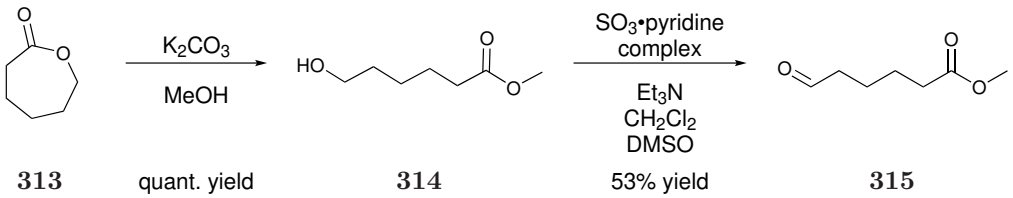

Scheme 6.8: Synthesis of the aldehyde **315** for the final synthesis of **244e**.

Methyl 6-hydroxyhexanoate **314**[187]

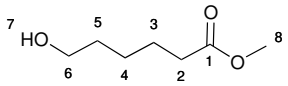

314

To a solution of ϵ-caprolactone **313** (9.7 mL, 87.6 mmol) in anhydrous methanol (175 mL), potassium carbonate (1.21 g, 8.8 mmol) was added and the reaction mixture was stirred vigorously for 20 minutes. H_2O (200 mL) was then added and the organic phase was extracted with CH_2Cl_2 (5 x 200 mL). The combined organic layers were dried (Na_2SO_4), filtered and concentrated at 25 °C *in vacuo*. The alcohol **314** was achieved as a colourless oil (12.8 g, quantitative yield) and it did not need any further purification. ^{1}H NMR ($CDCl_3$, 400 MHz) δ 3.62 – 3.53 (5 H, m, H-8 and H-6), 2.26 (2 H, t, J = 7.5 Hz, H-2), 1.65 – 1.55 (2 H, m, H-3), 1.55 – 1.47 (2 H, m, H-5), 1.45 (1 H, s, H-7), 1.39 – 1.28 (2 H, m, H-4). ^{13}C NMR ($CDCl_3$, 101 MHz) δ 174.2 (C-1), 62.6 (C-6), 51.5 (C-8), 34.0 (C-2), 32.3 (C-5), 25.3 (C-3), 24.6 (C-4).

Methyl 6-oxohexanoate **315**[188]

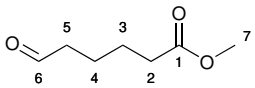

315

To a solution of the alcohol **314** (6.60 g, 45.1 mmol) in a mixture of CH_2Cl_2 and DMSO (v/v, 1:1, 90.2 mL), anhydrous triethylamine (37.7 mL, 270.8 mmol) was added at -5 °C, followed by the addition of the SO_3·pyridine complex (8.97 g, 56.4 mmol) in a single portion. CH_2Cl_2 (5 mL) was added dropwise to clean the neck of the round bottom flask. The reaction mixture was stirred at -5 °C for 2 hours and

then another portion of SO_3·pyridine complex (8.97 g, 56.4 mmol) was added. After 2 extra hours, a saturated aqueous solution of NH_4Cl (100 mL). Diethyl ether (100 mL) was added to dilute the solution and then the organic phase was washed with NH_4Cl (3 x 50 mL), followed by a saturated solution of $CuSO_4$ (2 x 50 mL), then with brine (50 mL) and finally with $NaHCO_3$ (50 mL). The organic layer was then dried (Na_2SO_4), filtered and concentrated *in vacuo*. The product **315** was achieved as a colourless oil (3.48 g, 53% yield) and did not need any further purification. ^{1}H NMR ($CDCl_3$, 400 MHz) δ 9.70 (1 H, t, J = 1.6 Hz, H-7), 3.61 (3 H, s, H-7), 2.40 (2 H, ddq, J = 5.8 Hz, 4.4 Hz, 1.4 Hz, H-5), 2.33 – 2.20 (2 H, m, H-2), 1.68 – 1.46 (4 H, m, H-3 and H-4). ^{13}C NMR ($CDCl_3$, 101 MHz) δ 202.0 (C-6), 173.7 (C-1), 51.6 (C-7), 43.5 (C-5), 33.7 (C-2), 24.4 (C-3), 21.5 (C-4).

Methyl 6-hydroxy-7-nitro-7-phenylheptanoate **242e**

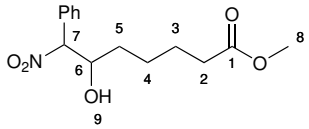

242 e

To a solution of **315** (0.80 g, 5.6 mmol) and nitrotoluene (2.28 g, 16.7 mmol) in a mixture of *t*-BuOH and THF (11.2 mL, *v/v* = 1:1) was added potassium *tert*-butoxide (0.125 g, 1.1 mmol) at 0 °C. The reaction mixture was left stirring at rt for 4 hours and then it was diluted with ethyl acetate (30 mL). The organic phase was washed with H_2O (30 mL) and with brine (30 mL). The organic phase was back extracted from the aqueous phase with ethyl acetate (3 x 50 mL). The combined organic layers were dried (Na_2SO_4), filtered and concentrated *in vacuo*. The crude product was purified *via* flash chromatography on silica gel (25% ethyl acetate in hexane) to afford the nitro alcohol **242e** as a yellow solid (0.81 g, 52% yield). Mixture of two diastereomers *syn/anti*: mp = 58.6 - 60.0 °C; IR (neat, cm^{-1}) 3424, 3381, 2952, 2924, 1724, 1562, 1456, 1436, 1366, 1250, 1228, 1195, 1177, 1115, 962, 725, 695, 622; ^{1}H NMR ($CDCl_3$, 400 MHz) δ 7.47 – 7.35 (5H, m, Ar-H), 5.32 (1H, d, J = 9.7 Hz, H-7), 4.66 – 4.48 (1H, m, H-6), 3.64 (3H, s, H-8), 2.85 - 2.69 (1H, m, H-9), 2.39 - 2.20 (2H, m, H-2), 1.74 – 1.10 (6H, m, H-3 and H-4 and H-5). ^{13}C NMR ($CDCl_3$, 101 MHz) δ 174.1 (C-1), 132.0 (Ar-C), 131.3 (Ar-C), 130.3 (Ar-C), 130.2 (Ar-C), 129.3 (Ar-C), 129.1 (Ar-C), 129.1 (Ar-C), 128.0 (Ar-C), 96.7

(C-7), 94.0 (C-7), 72.2 (C-6), 71.7 (C-6), 51.6 (C-8), 33.8 (C-2), 33.7 (C-2), 32.9 (C-5), 31.8 (C-5), 24.9 (C-3), 24.5 (C-3), 24.4 (C-4), 24.3 (C-4). HRMS required for $C_{16}H_{22}N_2O_5$ $[M+Na]^+$ 345.1426, found 345.1430.

General procedure I for the synthesis of nitro olefins 243.

To a solution of the nitro alcohol **242** in anhydrous CH_2Cl_2, trifluoroacetic anhydride (1.05 eq) followed by triethylamine (2.1 eq.) were added dropwise at 0 °C. The reaction mixture was left stirring at 0 °C for 3.5 hours and then an aqueous saturated solution of NH_4Cl was added, followed by H_2O. The organic phase was extracted with CH_2Cl_2 and then dried over Na_2SO_4 and filtered through a short plug of celite and concentrated *in vacuo*. Purification of the crude product was performed by combiflash on silica gel (gradient diethyl ether in hexane).

(*E*)-8,8-dimethoxy-2-nitrooct-2-ene **243a**

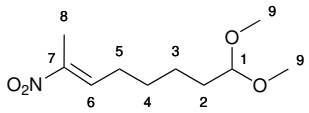

243 a

Following the general procedure I, the nitro alcohol **242a** (0.70 g, 3.0 mmol) was reacted with trifluoroacetic anhydride (0.43 mL, 3.1 mmol) and anhydrous triethylamine (0.9 mL, 6.3 mmol) to afford the nitro olefin **243a** as colourless oil (0.49 g, 75% yield). IR (neat, cm^{-1}) 2944, 1517, 1437, 1390, 1331, 1123, 1072, 1049, 963, 912, 722; ^{1}H NMR ($CDCl_3$, 400 MHz) δ 7.06 (1H, tq, J = 7.9, 1.1 Hz, H-6), 4.29 (1H, t, J = 5.6 Hz, H-1), 3.25 (6H, s, H-9), 2.24 – 2.12 (2H, m, H-5), 2.09 (3H, d, J = 1.0 Hz, H-8), 1.62 – 1.52 (2H, m, H-2), 1.52 – 1.41 (2H, m, H-4), 1.41 – 1.24 (2H, m, H-3). ^{13}C NMR ($CDCl_3$, 101 MHz) δ 147.7 (C-7), 136.0 (C-6), 104.3 (C-1), 52.9 (C-9), 32.3 (C-2), 28.2 (C-4), 28.1 (C-5), 24.3 (C-3), 12.5 (C-8). HRMS required for $C_{10}H_{18}NO_4$ $[M-H]^-$ 216.1230, found 216.1228.

(*E*)-9,9-dimethoxy-3-nitronon-3-ene **243b**

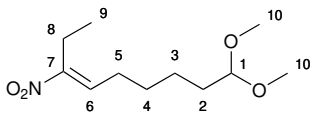

243 b

Following the general procedure I, the nitro alcohol **242b** (0.80 g, 3.2 mmol) was reacted with trifluoroacetic anhydride (0.47 mL, 3.4 mmol) and anhydrous triethylamine (0.94 mL, 6.7 mmol) to afford the nitro olefin **243b** as a colourless oil (0.34 g, 46% yield). IR (neat, cm^{-1}) 2940, 1517, 1460, 1337, 1124, 1072, 1051; ^1H NMR ($CDCl_3$, 400 MHz) δ 6.99 (1H, t, J = 7.9 Hz, H-6), 4.29 (1H, t, J = 5.7 Hz, H-1), 3.25 (6H, s, H-10), 2.53 (2H, q, J = 7.4 Hz, H-8), 2.17 (2H, q, J = 7.6 Hz, H-5), 1.62 – 1.50 (3H, m, H-2 and), 1.50 – 1.42 (2H, m, H-4), 1.41 – 1.27 (2H, m, H-3), 1.04 (3H, t, J = 7.4 Hz, H-9). ^{13}C NMR ($CDCl_3$, 101 MHz) δ 153.3 (C-7), 135.6 (C-6), 104.3 (C-1), 52.9 (C-10), 32.3 (C-2), 28.4 (C-4), 27.8 (C-5), 24.4 (C-3), 19.9 (C-8), 12.7 (C-9). HRMS required for $C_{11}H_{22}NO_4$ $[M+H]^+$ 232.1543, found 232.1548.

(*E*)-11,11-dimethoxy-5-nitroundec-5-ene **243c**

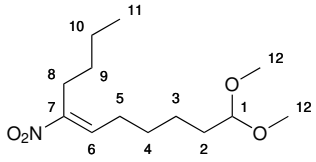

243 c

Following the general procedure I, the nitro alcohol **242c** (0.96 g, 3.4 mmol) was reacted with trifluoroacetic anhydride (0.50 mL, 3.6 mmol) and anhydrous triethylamine (1.0 mL, 7.1 mmol) to afford the nitro olefin **243a** as colourless oil (0.49 g, 55% yield). IR (neat, cm^{-1}) 2933, 1517, 1456, 1336, 1125, 1072, 1051, 957; ^1H NMR ($CDCl_3$, 400 MHz) δ 7.00 (1H, t, J = 7.9 Hz, H-6), 4.29 (1H, t, J = 5.6 Hz, H-1), 3.26 (6H, s, H-12), 2.60 – 2.44 (2H, m, H-8), 2.17 (2H, q, J = 7.6 Hz, H-5), 1.61 – 1.51 (3H, m, H-2 and), 1.51 – 1.21 (8H, m, H-3, H-4, H-9 and H-10), 0.86 (3H, t, J = 7.2 Hz, H-11). ^{13}C NMR ($CDCl_3$, 101 MHz) δ 152.0 (C-7), 136.0 (C-6), 104.3 (C-1), 52.9 (C-12), 32.3 (C-2), 30.0 (C-9), 28.4 (C-4), 28.0 (C-5), 26.1 (C-8), 24.4 (C-3), 22.4 (C-10), 13.8 (C-11). HRMS required for $C_{15}H_{28}N_2O_4$ $[M+CH_3CN+Na]^+$

323.1947, found 323.1947.

(*E*)-(8,8-dimethoxy-2-nitrooct-2-en-1-yl)benzene **243d**

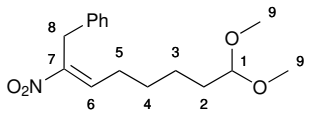

243 d

Following the general procedure I, the nitro alcohol **242d** (1.75 g, 5.6 mmol) was reacted with trifluoroacetic anhydride (0.82 mL, 5.9 mmol) and anhydrous triethylamine (1.6 mL, 11.8 mmol) to afford the nitro olefin **243d** as a colourless oil (0.51 g, 31% yield). ^{1}H NMR ($CDCl_3$, 400 MHz) δ 7.26 – 7.08 (7H, m, Ar-H and H-6), 4.28 (1H, t, J = 5.6 Hz, H-1), 3.90 (2H, s, H-8), 3.25 (6H, s, H-9), 2.29 (2H, q, J = 7.6 Hz, H-5), 1.62 – 1.42 (4H, m, H-2 and H-4), 1.42 – 1.29 (2H, m, H-3). ^{13}C NMR ($CDCl_3$, 101 MHz) δ 150.4 (C-7), 137.6 (Ar-C), 136.5 (Ar-C), 128.7 (Ar-C), 128.0 (C-6), 126.9 (Ar-C), 104.3 (C-1), 52.9 (C-9), 32.3 (C-2), 32.0 (C-8), 28.3 (C-4), 28.3 (C-5), 24.4 (C-3). HRMS required for $C_{16}H_{23}N_2O_4$ $[M+Na]^+$ 316.1525, found 316.1521.

Methyl (*E*)-7-nitro-7-phenylhept-6-enoate **243e**

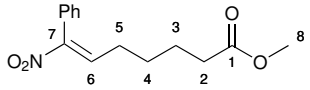

243 e

Following the general procedure I, the nitro alcohol **242e** (0.81 g, 2.9 mmol) was reacted with trifluoroacetic anhydride (0.42 mL, 3.0 mmol) and anhydrous triethylamine (0.84 mL, 6.0 mmol) to afford the nitro olefin **243e** as a yellow oil (0.51 g, 67% yield). IR (neat, cm^{-1}) 2952, 2862, 1733, 1635, 1521, 1495, 1437, 1332, 1277, 1196, 1173, 772, 701; ^{1}H NMR ($CDCl_3$, 400 MHz) δ 7.54 – 7.42 (3H, m, Ar-H), 7.39 (1H, t, J = 8.0 Hz, H-6), 7.34 – 7.21 (2H, m, Ar-H), 3.68 (3H, s, H-8), 2.29 (2H, t, J = 7.2 Hz, H-2), 2.17 (2H, dt, J = 8.0, 7.2 Hz, H-5), 1.70 – 1.58 (2H, m, H-3), 1.58 – 1.47 (2H, m, H-4). ^{13}C NMR ($CDCl_3$, 101 MHz) δ 173.6 (C-1), 151.6 (C-7), 137.9 (C-6), 130.3 (Ar-C), 129.7 (Ar-C), 129.5 (Ar-C), 128.6 (Ar-C), 51.6 (C-8), 33.6 (C-2), 28.2 (C-5), 27.9 (C-4), 24.4 (C-3). HRMS required for $C_{14}H_{18}N_2O_4$ $[M+H]^+$ 264.1230, found 264.1222.

General procedure L for the synthesis of aldehydes 244.

To neat nitro olefin **243** glacial acetic acid (1 mL/mmol) was added at 0 °C. Once frozen, 1N aqueous HCl solution (0.33 mL/mmol) was added and the reaction mixture was left stirring at rt for 17 hours. CH_2Cl_2 was added to the reaction mixture, and the organic phase was washed with H_2O and then with $NaHCO_3$. The aqueous phase was back extracted with CH_2Cl_2 and then the combined organic layers were dried (Na_2SO_4), filtered and concetrated *in vacuo*. The crude product was then purified *via* combiflash on silica gel (gradient 0-30% diethyl ether in hexane) to afford the title compound as a colourless liquid.

(*E*)-7-nitrooct-6-enal **244a**

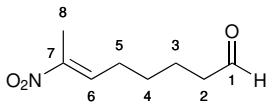

244 a

Following the general procedure L, glacial acetic acid (2.2 mL, 1 mL/mmol) and 1N aqueous HCl solution (0.73 mL) were added to the neat nitro olefin **243a** (0.476 g, 2.2 mmol) to afford the aldehyde **244a** as a pale yellow oil (0.20 g, 54% yield). IR (neat, cm^{-1}) 2936, 2862, 1721, 1671, 1460, 1437, 1390, 1329, 1090, 1058, 1036, 966, 907, 855, 722, 669, 659; ^{1}H NMR ($CDCl_3$, 400 MHz) δ 9.72 (1H, t, J = 1.4 Hz, H-1), 7.04 (1H, t, J = 7.9 Hz, H-6), 2.43 (2H, td, J = 7.1, 1.5 Hz, H-2), 2.28 – 2.14 (2H, m, H-5), 2.10 (3H, s, H-8), 1.71 – 1.57 (2H, m, H-3), 1.57 – 1.41 (2H, m, H-4). ^{13}C NMR ($CDCl_3$, 101 MHz) δ 201.8 (C-1), 147.9 (C-7), 135.4 (C-6), 43.5 (C-2), 27.9 (C-5), 27.8 (C-4), 21.6 (C-3), 12.6 (C-8). HRMS required for $C_8H_{14}N_2O_3$ $[M+H]^+$ 172.0968, found 172.0967.

(*E*)-7-nitronon-6-enal **244b**

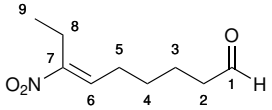

244 b

Following the general procedure L, glacial acetic acid (8.9 mL, 1 mL/mmol) and 1N aqueous HCl solution (2.9 mL) were added to the neat nitro olefin **243b** (2.1 g, 8.9 mmol) to afford the aldehyde **244b** as a pale yellow oil (0.46 g, 28% yield). ^{1}H

NMR ($CDCl_3$, 400 MHz) δ 9.80 (1H, t, J = 1.5 Hz, H-1), 7.06 (1H, t, J = 7.9 Hz, H-6), 2.63 (2H, q, J = 7.4 Hz, H-8), 2.52 (2H, td, J = 7.1, 1.5 Hz, H-2), 2.28 (2H, q, J = 7.6 Hz, H-5), 1.79 – 1.65 (2H, m, H-3), 1.65 – 1.49 (2H, m, H-4), 1.14 (3H, t, J = 7.4 Hz, H-9). ^{13}C NMR ($CDCl_3$, 101 MHz) δ 201.7 (C-1), 153.5 (C-7), 134.9 (C-6), 43.5 (C-2), 28.0 (C-4), 27.6 (C-5), 21.7 (C-3), 19.9 (C-8), 12.7 (C-9).

(*E*)-7-nitroundec-6-enal **244c**

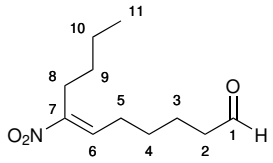

244 c

Following the general procedure L, glacial acetic acid (1.8 mL, 1 mL/mmol) and 1N aqueous HCl solution (0.6 mL) were added to the neat nitroolefin **243c** (0.48 g, 1.8 mmol) to afford the aldehyde **244c** as a pale yellow oil (0.22 g, 57% yield). IR (neat, cm^{-1}) 2957, 2933, 2864, 2327, 2321, 1723, 1700, 1685, 1670, 1636, 1517, 1437, 1335, 1126, 731, 668, 639; ^{1}H NMR ($CDCl_3$, 400 MHz) δ 9.72 (1H, t, J = 1.5 Hz, H-1), 6.99 (1H, t, J = 7.8 Hz, H-6), 2.56 – 2.47 (2H, m, H-8), 2.43 (2H, td, J = 7.1, 1.5 Hz, H-2), 2.19 (2H, q, J = 7.5 Hz, H-5), 1.70 – 1.57 (2H, m, H-3), 1.54 – 1.43 (3H, m, H-4), 1.43 – 1.34 (2H, m, H-9), 1.35 – 1.22 (2H, m, H-10), 0.86 (3H, t, J = 7.2 Hz, H-11). ^{13}C NMR ($CDCl_3$, 101 MHz) δ 201.8 (C-1), 152.3 (C-7), 135.3 (C-6), 43.5 (C-2), 30.0 (C-9), 28.0 (C-4), 27.8 (C-5), 26.2 (C-8), 22.4 (C-10), 21.7 (C-3), 13.8 (C-11). HRMS required for $C_{11}H_{20}NO_3$ $[M+H]^+$ 214.1438, found 214.1442.

(*E*)-7-nitro-8-phenyloct-6-enal **244d**

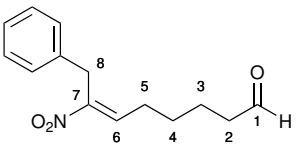

244 d

Following the general procedure L, glacial acetic acid (1.5 mL, 1 mL/mmol) and 1N aqueous HCl solution (0.5 mL) were added to the neat nitro olefin **243a** (0.43 g, 1.5 mmol) to afford the aldehyde **244d** as a pale yellow oil (0.21 g, 58% yield). IR (neat, cm^{-1}) 1721, 1515, 1330, 697; ^{1}H NMR ($CDCl_3$, 400 MHz) δ 9.69 (1H, t, J = 1.4 Hz, H-1), 7.27 – 7.13 (5H, m, Ar-H and H-6), 7.13 - 7.05 (2H,m, Ar-H),

3.90 (2H, d, J = 7.8 Hz, H-8), 2.40 (2H, td, J = 7.1, 1.4 Hz, H-2), 2.31 (2H, dd, J = 15.0, 7.6 Hz, H-5), 1.68 – 1.56 (2H, m, H-3), 1.56 – 1.44 (2H, m, H-4). ^{13}C NMR ($CDCl_3$, 101 MHz) δ 201.7 (C-1), 150.6 (C-7), 137.0 (C-6), 136.4 (Ar-C), 128.8 (Ar-C), 128.0 (Ar-C), 127.0 (Ar-C), 43.4 (C-2), 32.1 (C-8), 28.1 (C-5), 27.9 (C-4), 21.7 (C-3). HRMS required for $C_{14}H_{18}NO_3$ $[M+H]^+$ 248.1281, found 248.1276.

(*E*)-7-nitro-7-phenylhept-6-enal **244e**

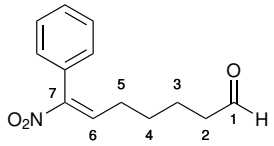

244 e

To a solution of the nitro olefin **243e** (0.49 g, 1.9 mmol) in CH_2Cl_2 (10 mL), DIBAL-H (2.0 mL, 1M in cyclohexane) was added dropwise at -78 °C. The reaction was stopped after 7 hours adding an aqueous solution of 1N HCl (5.7 mL) and the reaction mixture was then left stirring at rt overnight. H_2O (5 mL) was then added and the organic phase was extracted with CH_2Cl_2 (10 mL x 3). The combined organic layers were dried (Na_2SO_4), filtered and concentrated *in vacuo*. Purification of the crude product was performed by combiflash on silica gel (gradient diethyl ether in hexane) to afford the title aldehyde as pale yellow oil (0.17 g, 38% yield). IR (neat, cm^{-1}) 2939, 2863, 1720, 1495, 1331, 1235, 1074, 1050, 1028, 1001, 803, 772, 700, 668; ^{1}H NMR ($CDCl_3$, 400 MHz) δ 9.66 (1H, t, J = 1.5 Hz, H-1), 7.43 – 7.35 (3H, m, Ar-H), 7.29 (1H, t, J = 8.0 Hz, H-6), 7.23 – 7.14 (2H, m, Ar-H), 2.33 (2H, td, J = 7.0, 1.5 Hz, H-2), 2.09 (2H, dt, J = 8.1, 7.3 Hz, H-5), 1.62 – 1.50 (2H, m, H-3), 1.50 – 1.40 (2H, m, H-4). ^{13}C NMR ($CDCl_3$, 101 MHz) δ 201.7 (C-1), 151.7 (C-7), 137.6 (C-6), 130.3 (Ar-C), 129.7 (Ar-C), 129.5 (Ar-C), 128.6 (Ar-C), 43.4 (C-2), 28.3 (C-5), 27.9 (C-4), 21.5 (C-3). HRMS required for $C_{13}H_{16}NO_3$ $[M+H]^+$ 234.1125, found 234.1126.

6.10.2 Synthetic procedure for the synthesis of ketones 249a, 249b and 249c

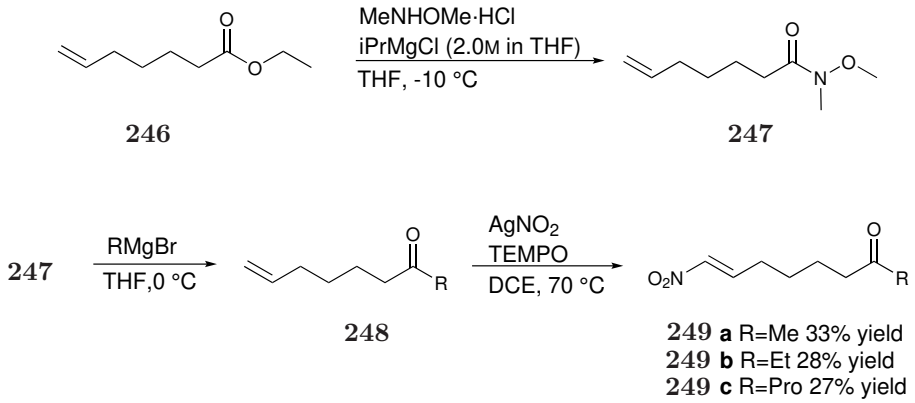

Scheme 6.9: Synthesis of ketones **249a**, **249b** and **249c**.

N-methoxy-*N*-methylhept-6-enamide **247**

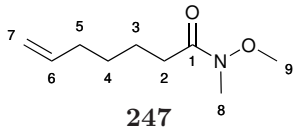

To a solution of *N*,*O*-dimethylhydroxylamine hydrochloride (4.84 g, 49.6 mmol) in anhydrous THF (50 mL) was added a solution of ethyl-6-heptenoate in anhydrous THF (14 mL). The reaction mixture was then cooled to -15 °C and *iPr*MgCl (2.0M in THF, 48 mL) was added steadily dropwise in 30 min. The reaction mixture was stirred at -10° for 2 hours and then a saturated aqueous solution of NH_4Cl (50 mL). The organic phase was extracted with diethyl ether (3 x 50 mL) and then washed with brine (50 mL). The combined organic layers were then dried ($MgSO_4$), filtered and concentrated *in vacuo*. The crude product was purified *via* flash chromatography on silica gel (30% ethyl acetate in hexane) to afford the title product in quantitative yield as a colourless oil. IR (neat, cm^{-1}) 2938, 1664, 1652, 1414, 1384, 1177, 993, 909; ^{1}H NMR ($CDCl_3$, 400 MHz) δ 5.74 (1H, ddt, J = 16.9, 10.2, 6.7 Hz, H-6), 5.02 – 4.75 (2H, m, H-7), 3.61 (3H, s, H-9), 3.11 (3H, s, H-8), 2.36 (2H, t, J = 7.6 Hz, H-2), 2.13 – 1.93 (2H, m, H-5), 1.68 – 1.51 (2H, m, H-3), 1.46 – 1.27 (2H, m, H-4). ^{13}C NMR ($CDCl_3$, 101 MHz) δ 138.7 (C-6), 114.6 (C-7), 61.2 (C-9), 33.6 (C-5), 32.2 (C-8), 31.7 (C-2) 28.7 (C-4), 24.2 (C-3). HRMS required for $C_9H_{17}NO_2$ $[M+H]^+$ 172.1332, found 172.1333.

6.10.3 General procedure M for the synthesis of the olefins 248

To a solution of **247** (1 eq.) in anhydrous THF at 0 °C, the Grignard reagent (4 eq.) was added dropwise in 15 min. The reaction was left stirring at 0 °C for 30 minutes and then a saturated aqueous solution of NH_4Cl was slowly added. The orgnic phase was extracted with diethyl ether and then washed with brine. The combined organic layers were dried ($MgSO_4$), filtered and concentrated at a maximum pressure of 100 mbar keeping the water bath at 25 °C to avoid any evaporation of the volatile product. The product obtained does not need any further purification.

Oct-7-en-2-one **248a**

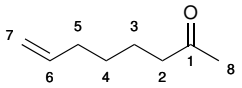

248 a

Following the general procedure M, methylmagnesium bromide (3.0M in THF, 10.7 mL) was added dropwise in 15 minutes to a solution of **247** (1.37 g, 8.0 mmol) in anhydrous THF (80 mL) at 0 °C. The reaction was left stirring at 0 °C for 30 minutes and then a saturated aqueous solution of NH_4Cl (50 mL) was slowly added to finally achieve the desired product **248a** as a colourless oil (0.90 g, 89% yield). IR (neat, cm^{-1}) 2933, 1715, 1642, 1413, 1359, 1164, 995, 910; ^1H NMR ($CDCl_3$, 400 MHz) δ 5.72 (1H, ddt, J = 16.9, 10.2, 6.7 Hz, H-6), 5.06 – 4.82 (2H, m, H-7), 2.38 (1H, d, J = 7.4 Hz, H-2), 2.07 (3H, s, H-8), 2.04 – 1.92 (2H, m, H-5), 1.64 – 1.49 (1H, m, H-3), 1.45 – 1.25 (2H, m, H-4). ^{13}C NMR ($CDCl_3$, 101 MHz) δ 209.2 (C-1), 138.5 (C-6), 114.7 (C-7), 43.6 (C-2), 33.5 (C-5), 29.9 (C-8), 28.4 (C-4), 23.3 (C-3). HRMS required for $C_8H_{15}O$ $[M+H]^+$ 127.1120, found 127.1117.

Non-8-en-3-one **248b**

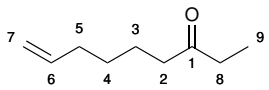

248 b

Following the general procedure M, ethylmagnesium bromide (3.0M in THF, 32 mL) was added dropwise in 10 minutes to a solution of **247** (1.37 g, 8.0 mmol) in anhydrous THF (80 mL) at 0 °C. The reaction was left stirring at 0 °C for 50 minutes and then a saturated aqueous solution of NH_4Cl (50 mL) was slowly added

to finally achieve the desired product **248b** as a colourless oil (1.1 g, 99% yield). IR (neat, cm^{-1}) 2937, 1713, 1641, 1460, 1414, 1376, 1111, 992, 910; ^1H NMR ($CDCl_3$, 400 MHz) δ 5.78 (1H, ddt, J = 16.9, 10.2, 6.7 Hz, H-6), 5.07 – 4.87 (m,2H, H-7), 2.40 (4H, m, H-2 and H-8), 2.11 – 2.00 (2H, m, H-5), 1.68 – 1.52 (2H, m, H-3), 1.47 – 1.32 (2H, m, H-4), 1.04 (3H, t, J = 7.3 Hz, H-9). ^{13}C NMR ($CDCl_3$, 101 MHz) δ 211.8 (C-1), 138.5 (C-6) 114.6 (C-7), 42.2 (C-2), 35.9 (C-8), 33.5 (C-5), 28.5 (C-4), 23.4 (C-3), 7.9 (C-9). HRMS required for $C_9H_{17}O$ $[M+H]^+$ 141.1274, found 141.1275.

Dec-9-en-4-one **248c**

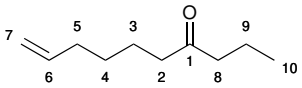

248 c

Following the general procedure M, *n*-propylmagnesium bromide (1.0M in THF, 25 mL) was added dropwise in 10 minutes to a solution of **247** (1.07 g, 6.3 mmol) in anhydrous THF (60 mL) at 0 °C. The reaction was left stirring at 0 °C for 1 hour and then a saturated aqueous solution of NH_4Cl (40 mL) was slowly added to finally achieve the desired product **248c** as a colourless oil (1.04 g, quantitative yield). IR (neat, cm^{-1}) 2934, 1711, 1456, 1412, 1371, 1128, 992, 910; ^1H NMR ($CDCl_3$, 400 MHz) δ 5.72 (1H, ddt, J = 16.9, 10.2, 6.7 Hz, H-6), 5.03 – 4.79 (2H, m, H-7), 2.44 – 2.25 (4H, m, H-2 and H-8), 2.09 – 1.88 (2H, m, H-5), 1.70 – 1.43 (4H, m, H-3 and H-9), 1.43 – 1.24 (2H, m, H-4), 0.84 (3H, t, J = 7.4 Hz, H-10). ^{13}C NMR ($CDCl_3$, 101 MHz) δ 211.4 (C-1), 138.5 (C-6), 114.6 (C-7), 44.7 (C-2), 42.6 (C-8), 33.5 (C-5), 28.5 (C-4), 23.3 (C-3), 17.3 (C-9), 13.8 (C-10). HRMS required for $C_{10}H_{19}O$ $[M+H]^+$ 155.1436, found 155.1429.

General procedure N for the synthesis of **249**

To a solution of $AgNO_2$ (4 eq.), TEMPO (0.4 eq.), 4Å molecular sieves in anhydrous DCE, **248** was added and the reaction mixture was left stirring in a close reaction tube at 70 °C for 16 hours. The reaction mixture was then left to cool down to rt and then filtered over a short pad of celite and washed with ethyl acetate. The crude product was then purified *via* combiflash on silica gel (gradient 0-20% ethyl acetate in hexane).

(*E*)-8-nitrooct-7-en-2-one **249a**

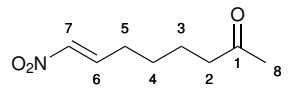

249 a

Following the general procedure N, the olefin **248a** (1.05 g, 8 mmol) was added to a solution of $AgNO_2$ (4.49 g, 26.4 mmol), TEMPO (0.625 g, 4.0 mmol), 4Å molecular sieves (2 g) in anhydrous DCE (32 mL) to afford the title product as a colourless oil (0.45 g, 33% yield). ^{1}H NMR ($CDCl_3$, 400 MHz) δ 7.29 – 7.12 (1H, m, H-6), 6.93 (1H. dt, J = 13.5, 1.6 Hz, H-7), 2.41 (2H, t, J = 7.0 Hz, H-2), 2.23 (2H, qd, J = 7.3, 1.6 Hz, H-5), 2.08 (3H, s, H-8), 1.65 – 1.52 (2H, m, H-3), 1.52 – 1.40 (2H, m, H-4). ^{13}C NMR ($CDCl_3$, 101 MHz) δ 208.2 (C-1), 142.1 (C-6), 139.8 (C-7), 43.0 (C-2), 30.0 (C-8), 28.4 (C-5), 27.2 (C-4), 23.0 (C-3). HRMS required for $C_8H_{13}NO_3$ $[M+H]^+$ 172.0974, found 172.0980.

(*E*)-9-nitronon-8-en-3-one **249b**

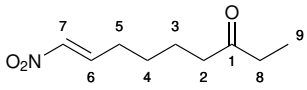

249 b

Following the general procedure N, the olefin **248b** (1.050 g, 7.5 mmol) was added to a solution of $AgNO_2$ (5.09 g, 30 mmol), TEMPO (0.47 g, 3.0 mmol), 4Å molecular sieves (2 g) in anhydrous DCE (30 mL) to afford the title product as a colourless oil (0.39 g, 28% yield). IR (neat, cm^{-1}) 2937, 1711, 1700, 1648, 1521, 1460, 1351, 1115, 959, 732; ^{1}H NMR ($CDCl_3$, 400 MHz) δ 7.35 – 7.16 (1H, m, H-6), 7.01 (1H, dt, J = 13.4, 1.6 Hz, H-7), 2.54 – 2.38 (4H, m, H-2 and H-8), 2.30 (2H, qd, J = 7.3, 1.6 Hz, H-5), 1.73 – 1.61 (2H, m, H-3), 1.61 – 1.45 (2H, m, H-4), 1.07 (3H, t, J = 7.4 Hz, H-9). ^{13}C NMR ($CDCl_3$, 101 MHz) δ 210.9 (C-1), 142.1 (C-6), 139.8 (C-7), 41.9 (C-2), 41.7 (C-8), 36.0 (C-5), 28.4, 27.3 (C-4), 23.1 (C-3), 7.8 (C-9). HRMS required for $C_9H_{16}NO_3$ $[M+H]^+$ 186.1125, found 186.1127.

(*E*)-10-nitrodec-9-en-4-one **249c**

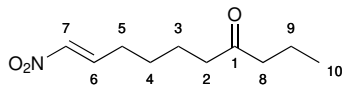

249 c

Following the general procedure N, the olefin **248c** (1.020 g, 6.6 mmol) was added to a solution of $AgNO_2$ (4.49 g, 26.5 mmol), TEMPO (0.41 g, 2.6 mmol), 4Å molecular sieves (2 g) in anhydrous DCE (26 mL) to afford the title product as a colourless oil (0.36 g, 27% yield). IR (neat, cm^{-1}) 2936, 1709, 1700, 1648, 1521, 1458, 1412, 1350, 1127, 961, 732; ^{1}H NMR ($CDCl_3$, 400 MHz) δ 7.35 – 7.21 (1H, m, H-6), 7.01 (1H, dt, J = 13.4, 1.6 Hz, H-7), 2.45 (2H, t, J = 7.0 Hz, H-8), 2.39 (2H, t, J = 7.3 Hz, H-2), 2.30 (2H, qd, J = 7.3, 1.6 Hz, H-5), 1.71 – 1.56 (4H, m, H-3 and H-9), 1.60 – 1.47 (2H, m, H-4), 0.93 (3H, t, J = 7.4 Hz, H-10). ^{13}C NMR ($CDCl_3$, 101 MHz) δ 210.5 (C-1), 142.1 (C-6), 139.8 (C-7), 44.8 (C-2), 42.1 (C-8), 28.4 (C-5), 27.3 (C-4), 23.1 (C-3), 17.3 (C-9), 13.8 (C-10). HRMS required for $C_{10}H_{16}NO_3$ $[M\text{-}H]^-$ 198.1125, found 198.1127.

6.11 Synthesis of nitro olefin 255

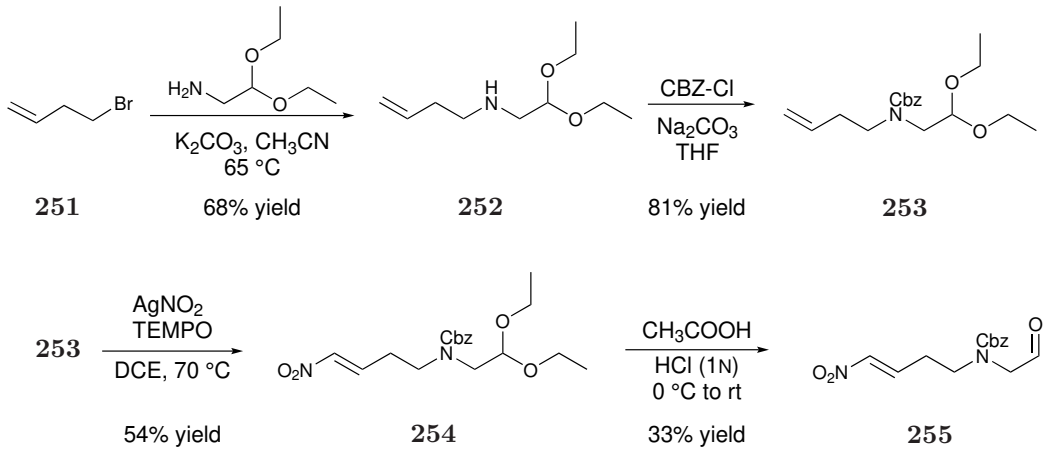

251 68% yield **252** 81% yield **253**

253 54% yield **254** 33% yield **255**

Scheme 6.10: Synthesis of substrate **255**

N-(2,2-diethoxyethyl)but-3-en-1-amine 252

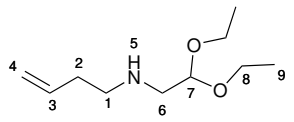

252

To a solution of aminoacetaldehyde diethyl acetal (11.6 mL, 80 mmol) in acetonitrile (200 mL), K_2CO_3 (8.29 g, 60 mmol) and a solution of 4-bromobutene (4 mL, 40 mmol) in acetonitrile (80 mL) were added and left stirring at 65°C for 18 hours. The reaction mixture was then concentrated *in vacuo* and the residue was diluted with ethyl acetate (100 mL) and washed with first with H_2O (100 mL) and then with brine (100 mL). The organic phase was dried over Na_2SO_4, filtered and concentrated *in vacuo*. The crude product was purified *via* combiflash on silica gel (gradient hexane/ethyl acetate) to afford the title compound as a oil (5.05 g, 68% yield). IR (neat, cm^{-1}) 2976, 2901, 1457, 1373, 1123, 1059, 994, 913; ^{1}H NMR ($CDCl_3$, 400 MHz) δ 5.80 (1H, ddt, J = 17.1, 10.2, 6.9 Hz, H-3), 5.17 – 4.97 (2H, m, H-4), 4.62 (1H, t, J = 5.6 Hz, H-7), 3.64 (4H, ddq, J = 64.2, 9.4, 7.0 Hz, H-8), 2.75 (2H, d, J = 5.7 Hz, H-6), 2.71 (2H, t, J = 6.9 Hz, H-1) 2.27 (2H, qt, J = 6.9, 1.3 Hz, H-2), 1.23 (6H, t, J = 7.1 Hz, H-9).^{13}C NMR ($CDCl_3$, 101 MHz) δ 136.3 (C-3), 116.3 (C-4), 102.2 (C-7), 62.4 (C-8), 52.1 (C-6), 48.9 (C-1), 34.3 (C-2), 15.4 (C-9). HRMS required for $C_{10}H_{22}NO_2$ $[M+H]^+$ 188.1651, found 188.1654.

Benzyl but-3-en-1-yl(2,2-diethoxyethyl)carbamate 253

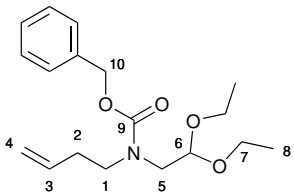

253

To a solution of **252** (5.0 g, 26.7 mmol) in THF (108 mL) was added Na_2CO_3 (8.2 g, 77.4 mmol) and benzyl chloroformate (4.6 mL, 32 mmol) and the reaction mixture was left vigorously stirring at rt for 19 hours. H_2O (50 mL) was added and the organic phase was extracted with ethyl acetate (3 x 70 mL). The organic layers were then washed with brine (50 mL), dried over Na_2SO_4, filtered and concentrated

in vacuo. The crude product was then purified *via* combiflash on silica gel (gradient to 15% ethyl acetate in hexane) to afford the **253** as a yellow oil (6.985 g, 21.8 mmol, 81% yield). IR (neat, cm^{-1}) 2976, 1697, 1474, 1416, 1374, 1284, 1238, 1159, 1121, 1058, 1029, 913, 770, 752, 734, 697; ^{1}H NMR ($CDCl_3$, 400 MHz) δ 7.46 – 7.30 (5H, m, Ar-H), 5.76 (1H, dddt, J = 24.1, 17.1, 10.1, 7.0 Hz, H-3), 5.16 (2H, s, H-10), 5.08 – 4.94 (2H, m, H-4), 4.66 and 4.51 (split because of N-CBZ rotamers, 1H, t, J = 5.4 Hz, H-6), 3.65 and 3.53 (2H, ddq, J = 78.7, 9.5, 7.1 Hz, H-7), 3.49 – 3.40 (2H, m, H-5), 3.34 (2H, dd, J = 10.6, 5.4 Hz, H-1), 2.32 (2H, dq, J = 14.8, 7.2 Hz, H-2), 1.19 (6H, dt, J = 20.5, 7.0 Hz, H-8). ^{13}C NMR ($CDCl_3$, 101 MHz, rotamers) δ 156.4 and 156.0 (C-9), 136.8 and 135.4 (C-3), 135.3 (Ar-C) 128.5 and 128.0 (Ar-C), 127.9 and 127.7 (Ar-C), 116.7 and 116.6 (C-4), 102.2 and 101.7 (C-6), 67.1 and 67.0 (C-10), 63.5 and 63.4 (C-7), 50.9 and 50.3 (C-5), 48.4 and 48.1 (C-1), 33.1 and 32.4 (C-2), 15.4 and 15.3 (C-8). HRMS required for $C_{18}H_{27}NO_4$ $[M+Na]^+$ 344.1838, found 344.1845.

Benzyl (*E*)-(2,2-diethoxyethyl)(4-nitrobut-3-en-1-yl)carbamate 254

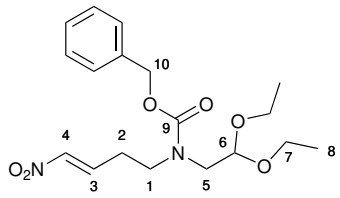

254

To an oven-dried two-neck round bottom flask charged with magnetic stir-bar was added activated 4Å molecular sieves (0.6 g), $AgNO_2$ (17.61 g, 103.7 mmol) and TEMPO (2.03 g, 13.0 mmol), **253** (6.95 g, 21.6 mmol) and anhydrous DCE (67 mL) were added. The tube was then placed in a preheated oil bath at 70 °C and the reaction mixture was left stirring vigorously for 41 hours. The progress of the reaction was monitored by TLC and then the reaction mixture was left to cool down to rt. The reaction mixture was then filtered through a short pad of celite washed with ethyl acetate (500 mL) and concentrated *in vacuo*. The crude product was then purified *via* combiflash using silica gel columns (gradient up to 50% diethyl ether in hexane) to afford the title compound **254** as a colourless oil (4.29 g, 11.7 mmol, 54%). IR (neat, cm^{-1}) 2976, 2885, 1700, 1523, 1454, 1416, 1350, 1238, 1191,

935, 770, 733, 697; ^{1}H NMR ($CDCl_3$, 400 MHz) δ 7.45 – 7.32 (5H, m, Ar-H), 7.32 – 7.13 (1H, m, H-3), 7.01 and 6.96 (1H, d, J = 13.5 Hz, H-4), 5.16 (2H, s, H-10), 4.66 and 4.49 (1H, t, J = 5.2 Hz, H-6), 3.82 -3.39 (6H, m, H-7 and H-1), 3.35 and 3.32 (2H, d, J = 5.1 Hz, H-5), 2.64 – 2.47 (2H, m, H-2), 1.22 and 1.17 (t, J = 7.0 Hz, 6H). ^{13}C NMR ($CDCl_3$, 101 MHz) δ 156.1 and 156.0 (C-9), 140.5 (C-4) 139.3 and 139.1 (C-3), 136.3 and 136.2 (Ar-C), 128.6 and 128.6 (Ar-C), 128.3 and 128.1 (Ar-C), 102.0 and 101.5 (C-6), 67.6 and 67.5 (C-10), 63.7 and 63.5 (C-7), 51.3 and 50.9 (C-1), 47.5 and 47.0 (C-5), 27.9 and 27.4 (C-2), 15.4 and 15.3 (C-8). HRMS required for $C_{18}H_{26}N_2O_6$ $[M+Na]^+$ 389.1689, found 389.1694.

Benzyl (*E*)-(4-nitrobut-3-en-1-yl)(2-oxoethyl)carbamate 255

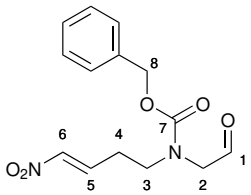

255

To the protected nitro olefin **254** (1.47 g, 4.0 mmol) at ice-cold condition was added acetic acid (4 mL). After the solution started to freeze HCl (1N, 1.3 mL) was added and the mixture was left stirring at rt for 28 hours. CH_2Cl_2 (15 mL) was added and the organic phase was washed with H_2O (2 x 15 mL) and saturated aqueous $NaHCO_3$ (35 mL). The aqueous phase was back extracted with CH_2Cl_2 (3 x 30 mL) and then the combined organic layers were dried over $MgSO_4$, filtered and concentrated under reduced pressure. The crude product was purified *via* combiflash on silica gel (gradient up to 55% ethyl acetate in hexane) to afford compound **255** as a colourless oil (33% yield, 0.389 g). IR (neat, cm^{-1}) 1697, 1521, 1454, 1351, 1235, 1134, 1028, 771, 734, 699; ^{1}H NMR ($CDCl_3$, 400 MHz) δ 9.64 and 9.59 (1H, s, H-1), 7.48 – 7.25 (5H, m, Ar-H), 7.25 – 7.13 (1H, m, H-5), 7.04 and 6.97 (1H, d, J = 13.4 Hz, H-6), 5.18 and 5.13 (1H, s, H-8), 4.15 and 4.09 (1H, s, H-2), 3.53 (2H, dt, J = 10.4, 6.9 Hz, H-3), 2.54 (2H, dq, J = 25.7, 7.3 Hz, H-4). ^{13}C NMR ($CDCl_3$, 101 MHz) δ 197.0 and 196.9 (C-1), 156.0 and 155.6 (C-7), 140.9 (C-6), 138.4 and 138.3 (c-5), 135.8 (Ar-C), 128.7 and 128.6 (Ar-C), 128.5 and 128.4 (Ar-C), 128.2 and 128.0 (Ar-C), 68.2 and 68.0 (C-8), 58.2 and 58.0 (C-2), 47.8 and 47.1 (C-3), 28.1 and 27.6

(C-4). HRMS required for $C_{14}H_{17}N_2O_5$ $[M+H]^+$ 293.1137, found 293.1140.

6.12 Synthesis of nitro olefin 265

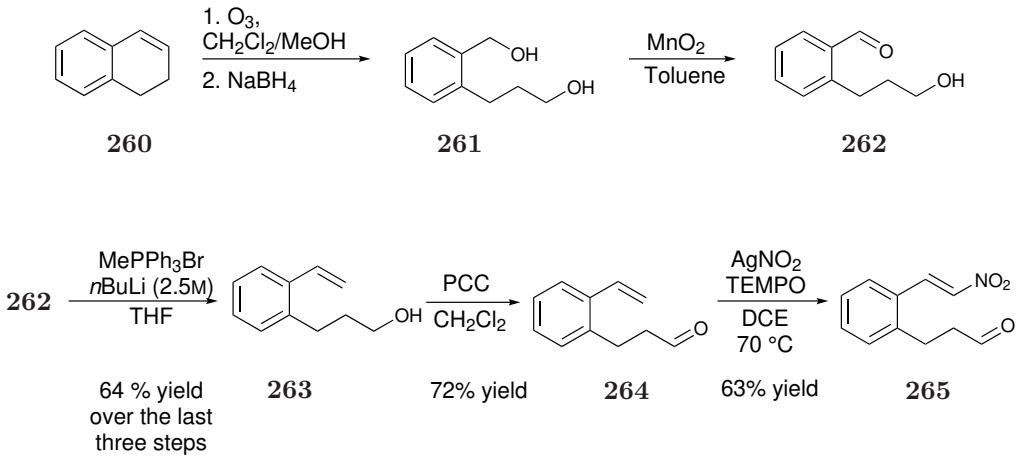

Scheme 6.11: Synthesis of the indane derivative precursor

3-(2-vinylphenyl)propan-1-ol 263[189]

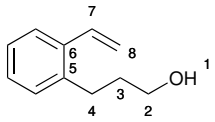

263

1,2-dihydronaphtalene (3.0 g, 23 mmol) was dissolved in a mixture of CH_2Cl_2 and MeOH (*V/V* 1:1, 120 mL) and the mixture was cooled to -78°C. O_3 was then bubbled through until a blue colour developed. Excess of O_3 was removed bubbling through N_2 until the blue colour was discharged. $NaBH_4$ (1.74 g, 46.0 mmol) was added slowly and then the reaction mixture was stirred at rt for 1 h. The reaction was quenched with saturated aq. NH_4Cl solution (100 mL) and then the organic phase was extracted with CH_2Cl_2 (3 x 100 mL). The combined organic layers were dried over Na_2SO_4, filtered and concentrated *in vacuo* to afford compound **261** as a dense colourless liquid. To a solution of **261** (3.30 g, 19.9 mmol) in toluene (81 mL) was added activated MnO_2 powder (8.63 g, 99.3 mmol) every hour for the first three hours for a total of 15 eq. added. The reaction mixture was left stirring at rt for further 18 h. MnO_2 was filtered through a short pad of celite, washed with ethyl acetate (250 mL) and concentrated *in vacuo*. Compound **262** was used for Wittig

olefination without further purification. To a suspension of $MePPh_3Br$ (10.7 g, 30.0 mmol) in THF (36 mL) was added *n*-BuLi (2.5M in hexane, 12 mL) dropwise at 0°C. The reaction mixture was stirred at 0°C for 30 minutes and then a solution of **262** (2.46 g, 15.0 mmol) in THF (9.5 mL) was added dropwise. The reaction mixture was left stirring at rt for 20 hours and then it was quenched with a saturated aq. solution of NH_4Cl (85 mL) at 0°C. The organic phase was extracted with diethyl ether (3 x 90 mL) and then combined organic layers were then dried over Na_2SO_4, filtered and concentrated *in vacuo*. The residue was purified *via* combiflash on silica gel (gradient from 20 to 30% ethyl acetate in hexane) to afford the title product **263** as a colourless oil (2.03 g, 64% yield for three steps). ^{1}H NMR ($CDCl_3$, 400 MHz) δ 7.60 – 7.44 (1H, m, Ar-H), 7.26 – 7.14 (3H, m, Ar-H), 7.04 (1H, dd, J = 17.3, 10.9 Hz, H-7), 5.68 (1H, dd, J = 17.3, 1.4 Hz, H-8), 5.33 (1H, dd, J = 11.0, 1.4 Hz, H-8), 3.70 (2H, t, J = 6.3 Hz, H-2), 2.91 – 2.74 (2H, m, H-4), 1.97 – 1.79 (2H, m, H-3), 1.45 (1H, s, H-1). ^{13}C NMR ($CDCl_3$, 101 MHz) δ 139.2 (C-6), 136.5 (C-5), 134.6 (C-7), 129.5 (Ar-C), 127.9 (Ar-C), 126.4 (Ar-C), 125.9 (Ar-C), 115.6 (C-8), 62.3 (C-2), 33.8 (C-3), 29.4 (C-4).

3-(2-vinylphenyl)propanal 264[189]

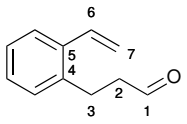

316

To a solution of **263** (0.487 g, 3.0 mmol) in CH_2Cl_2 (17 mL) was added a solution of PCC (1.29 g, 6.0 mmol) in CH_2Cl_2 (3 mL) and the reaction mixture was left stirring at rt for 3 h. Silica gel was added and the crude product was purified *via* combiflash on silica gel (gradient up to 10% ethyl acetate in hexane) to afford compound **264** as a colourless oil (0.346 g, 72% yield). ^{1}H NMR ($CDCl_3$, 400 MHz) δ 9.84 (1H, t, J = 1.4 Hz, H-1), 7.64 – 7.47 (1H, m, Ar-H), 7.40 – 7.12 (3H, m, Ar-H), 6.97 (1H, dd, J = 17.3, 11.0 Hz, H-6), 5.68 (1H, dd, J = 17.3, 1.4 Hz, H-7), 5.36 (1H, dd, J = 11.0, 1.4 Hz, H-7), 3.04 (2H, dd, J = 8.4, 7.1 Hz, H-3), 2.76 (2H, ddd, J = 8.7, 7.1, 1.4 Hz, H-2). ^{13}C NMR ($CDCl_3$, 101 MHz) δ 201.4 (C-1), 137.6 (C-5), 136.6 (C-4), 134.2 (C-6), 129.3 (Ar-C), 128.0 (Ar-C), 126.8 (Ar-C), 126.2 (Ar-C), 116.3 (C-7), 44.8 (C-2), 25.6 (C-3). HRMS required for $C_{11}H_{13}O$ $[M+H]^+$ 161.0966,

found 161.0970.

(*E*)-3-(2-(2-nitrovinyl)phenyl)propanal 265

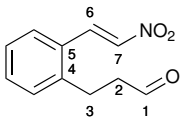

265

To an oven-dried quick-fit cap test tube charged with magnetic stir-bar was added activated 4Å molecular sieves (0.15 g), $AgNO_2$ (1.00 g, 5.9 mmol) and TEMPO (0.125 g, 0.8 mmol). Compound **264** (0.314 g, 2.0 mmol) and anhydrous DCE (8 mL) were added. The tube was then placed in a preheated oil bath at 70 °C and the reaction mixture was left stirring vigorously for 17 hours. The progress of the reaction was monitored by TLC and then the reaction mixture was left to cool down to rt. The reaction mixture was then filtered through a short pad of celite washed with ethyl acetate (250 mL) and concentrated *in vacuum*. The crude product was then purified *via* combiflash using silica gel columns (gradient up to 20% ethyl acetate in hexane) to afford the title compound **265** as a yellow solid (0.257 g, 63% yield). mp = 63.0 - 64.8 °C IR (neat, cm^{-1})2841, 1713, 1700, 1627, 1597, 1500, 1331, 1299, 1270, 1211, 966, 957, 774, 750, 606; ^{1}H NMR ($CDCl_3$, 400 MHz) δ 9.85 (1H, t, J = 1.1 Hz, H-1), 8.35 (1H, d, J = 13.5 Hz, H-7), 7.62 – 7.51 (2H, m, H-6 and Ar-H), 7.50 – 7.39 (1H, m, Ar-H), 7.33 (1H, d, J = 7,6 Hz, Ar-H), 7.32 - 7.29 (1H, m, Ar-H) 3.15 (2H, t, J = 7.4 Hz, H-3), 2.82 (2H, td, J = 7.5, 1.1 Hz, H-2). ^{13}C NMR ($CDCl_3$, 101 MHz) δ 200.0 (C-1), 141.5 (C-5), 138.3 (C-6), 136.0 (C-7), 132.1 (Ar-C), 130.4 (Ar-C), 128.6 (C-4), 127.6 (Ar-C), 127.4 (Ar-C), 44.9 (C-2), 25.3 (C-3). HRMS required for $C_{11}H_{10}NO_3$ $[M\text{-}H]^-$ 204.0661, found 204.0665.

6.13 Organocatalytic products 249, 317 and 266

6.13.1 General procedure O for the organocatalytic reactions

To a solution of (*S*)-(-)-5-(2-pyrrolidinyl)-1H-tetrazole (5 mol%) and DCE (0.05M) previously sonicated for 30 minutes was added the nitro olefin (1 eq.) at -20 °C dropwise in 3 minutes followed by DCE to wash the syringe used and the sides of the reaction flask. The reaction mixture was left stirring at -20 °C until completion of the reaction. $NaBH_4$ (1.5 eq.) was added at -20 °C followed by MeOH. The reaction

went to completion in 1 hour. A saturated aqueous solution of NH_4Cl was added, followed by brine and H_2O. The organic phase was extracted first with a mixture of chloroform and isopropanol (*V/V*, 3:1), then with diethyl ether and finally with ethyl acetate because of the high affinity of the product with the aqueous phase. The organic phase was then dried (Na_2SO_4), filtered and concentrated *in vacuo*. The crude product was then purified by flash chromatography on silica gel to afford the target product.

6.13.2 General procedure P for the organocatalytic racemic reactions

To a solution of the nitro olefin in DCE (0.2M), L-Proline (10 mol%) and D-Proline (10 mol%) were added at -20 °C. The reaction was monitored by TLC and once gone to completion, $NaBH_4$ (1.5 eq.) and MeOH were added. The reaction mixture was left stirring at -20 °C until the reduction was completed. Then, a saturated aqueous solution of NH_4Cl was added, followed by brine and H_2O. The organic phase was extracted with CH_2Cl_2. The combined organic layers were dried (Na_2SO_4), filtered and concentrated *in vacuo*. The crude product was then purified by flash chromatography on silica gel (gradient 10-20% ethyl acetate in hexane).

1-(2-(nitromethyl)-1l3,2l3-cyclopentyl)ethan-1-one **250a**

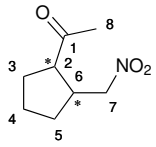

250 a

Following general procedure O, the nitro olefin **248a** (0.100 g, 0.58 mmol) was added to a mixture of catalyst **29** (0.017 g, 0.12 mmol) in DCE (10.6 mL) at 0 °C. After 5 hours, the reaction did not show any formation of the product, therefore the reaction mixture was left stirring at rt. After 48 hours, the reaction was monitored by ^1H NMR, showing only partial formation of the product. Acetic acid (20 mol%, 7μL) was added as co-catalyst. After 8 days from start of the reaction, the reaction mixture was concentrated *in vacuo*. The crude product was purified *via* flash chromatography on silica gel (20% ethyl acetate in hexane) to afford separately *cis*- and *trans*-**250a** as colourless oils (0.56 g, 56% yield of both

diastereomers combined). *cis*-**250a**: 84% *ee*; HPLC analysis: Chiralpack OD, 2% isopropanol in hexane, flow rate = 0.8 mL/min, λ = 210 nm. $[\alpha]^{20}{}_D$ + 24.0 (c = 0.1, CH_2Cl_2); IR (neat, cm^{-1}) 2960, 1699, 1545, 1422, 1382, 1355, 1178; ^{1}H NMR ($CDCl_3$, 400 MHz) δ 4.59 (2H, ABX, J_{AX} = 8.5 Hz, J_{BX} = 6.9 Hz, J_{AB} = 12.9 Hz, ν_{AB} = 92.1 Hz, H-7), 3.23 (1H, ddd, J = 8.4, 7.1, 4.8 Hz, H-2), 2.77 (1H, tq, J = 8.9, 7.3 Hz, H-6), 2.22 (3H, s, H-8), 2.11 – 1.96 (1H, m, H-3), 1.96 – 1.76 (3H, m, H-5, H-3 and H-4), 1.76 – 1.62 (2H, m, H-5 and H-4). ^{13}C NMR ($CDCl_3$, 101 MHz) δ 210.6 (C-1), 75.9 (C-7), 52.1 (C-2), 40.9 (C-6), 30.7 (C-8), 29.4 (C-3), 29.2 (C-5), 23.2 (C-4). HRMS required for $C_8H_{14}NO_3$ $[M+H]^+$ 172.0968, found 172.0972. *trans*-**250a**: 38% *ee*; HPLC analysis: Chiralpack AD-H, 0.5% isopropanol in hexane, flow rate = 0.5 mL/min, λ = 210 nm. $[\alpha]^{20}{}_D$ + 2.0 (c = 0.1, CH_2Cl_2); IR (neat, cm^{-1}) 2960, 1705, 1545, 1431, 1371, 1356, 1174; ^{1}H NMR ($CDCl_3$, 400 MHz) δ 4.31 (2H, ABX, J_{AX} = 6.8 Hz, J_{BX} = 7.2 Hz, J_{AB} = 12.1 Hz, ν_{AB} = 30.2 Hz, H-7), 2.94 (1H, m, H-2), 2.79 – 2.61 (1H, m, H-6), 2.13 (3H, s, H-8), 2.10 – 1.97 (1H, m, H-5), 1.97 – 1.85 (1H, m, H-3), 1.79 – 1.61 (3H, m, H-4 and H-5), 1.49 – 1.26 (2H, m, H-3). ^{13}C NMR ($CDCl_3$, 101 MHz) δ 208.8 (C-1), 78.9 (c-7), 55.2 (C-6), 39.2 (C-2), 30.0 (C-8), 30.0 (C-5), 29.1 (C-3), 24.4 (C-4). HRMS required for $C_8H_{14}NO_3$ $[M+H]^+$ 172.0968, found 172.0972.

1-(2-(nitromethyl)cyclopentyl)propan-1-one **250b**

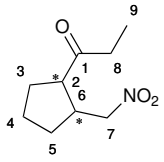

250 b

Following general procedure O, the nitro olefin **248b** (0.150 g, 0.81 mmol) was added to a mixture of catalyst **29** (0.023 g, 0.16 mmol), acetic acid (9.5 μL, 0.16 mmol) in DCE (16.2 mL) at rt. After 8 days, H_2O (20 mL) was added to the reaction mixture and the organic phase was extracted with CH_2Cl_2 (3 x 20 mL). The organic phase was washed with an aqueous solution of 1N HCl (20 mL) and then it was back-extracted with CH_2Cl_2 (20 mL). The combined organic layers were dried (Na_2SO_4), filtered and concentrated in vacuo. The crude product was purified by flash chromatography on silica gel (gradient 10-20% ethyl acetate in hexane) to

afford separately *cis*- and *trans*-**250b** as colourless oils (0.23 g, 15% yield of both diastereomers combined). *cis*-**250b**: IR (neat, cm^{-1}) 2964, 1705, 1700, 1545, 1452, 1379, 1107; ^1H NMR ($CDCl_3$, 400 MHz) δ 4.47 (2H, ABX, J_{AX} = 8.6 Hz, J_{BX} = 6.7 Hz, J_{AB} = 12.9 Hz, ν_{AB} = 84.1 Hz, H-7), 3.13 (1H, ddd, J = 8.0, 7.2, 5.3 Hz, H-2), 2.80 – 2.60 (1H, m, H-6), 2.54 – 2.33 (2H, m, H-8), 2.01 – 1.87 (1H, m, H-3), 1.86 – 1.66 (3H, m, H-3, H-5 and H-4), 1.66 – 1.50 (2H, m, H-5 and H-4), 0.96 (3H, t, J = 7.2 Hz, H-9). ^{13}C NMR ($CDCl_3$, 101 MHz) δ 213.4 (C-1), 76.0 (C-7), 51.1 (C-2), 41.0 (C-6), 36.7 (C-8), 29.8 (C-3), 29.5 (C-5), 23.4 (C-4), 7.6 (C-9). HRMS required for $C_9H_{16}NO_3$ $[M+H]^+$ 186.1125, found 186.1126.

trans-**250b**: -57% *ee*; HPLC analysis: Chiralpack AD-H, 3% isopropanol in hexane, flow rate = 0.3 mL/min, λ = 210 nm. $[\alpha]^{20}{}_D$ - 3.0 (c = 0.1, CH_2Cl_2); IR (neat, cm^{-1}) 2958, 1707, 1547, 1526, 1377, 1346, 1119; ^1H NMR ($CDCl_3$, 400 MHz) δ 4.30 (2H, ABX, J_{AX} = 7.0 Hz, J_{BX} = 7.0 Hz, J_{AB} = 12.1, ν_{AB} = 24.7 Hz, H-7), 3.05 - 2.86 (1H, m, H-6), 2.68 (1H, dt, J = 9.1, 7.7 Hz, H-2), 2.59 – 2.29 (2H, m, H-8), 2.07 – 1.86 (2H, m, H-5 and H-3), 1.74 – 1.56 (3H, m, H-3 and H-4), 1.47 – 1.25 (1H, m, H-5), 1.00 (3H, t, J = 7.3 Hz, H-9). ^{13}C NMR ($CDCl_3$, 101 MHz) δ 211.6 (C-1), 79.0 (C-7), 54.2 (C-2), 39.5 (C-6), 35.3 (C-8), 30.3 (C-3), 30.0 (C-5), 24.4 (C-4), 7.7 (C-9). HRMS required for $C_9H_{16}NO_3$ $[M+H]^+$ 186.1125, found 186.1126.

1-(2-(nitromethyl)cyclopentyl)butan-1-one 250c

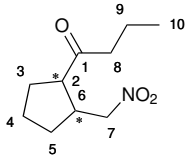

250 c

Following general procedure O, the nitro olefin **248c** (0.150 g, 0.75 mmol) was added to a mixture of catalyst **29** (0.021 g, 0.15 mmol), acetic acid (9 μL, 0.15 mmol) in DCE (15 mL) at rt. After 8 days, H_2O (20 mL) was added to the reaction mixture and the organic phase was extracted with CH_2Cl_2 (3 x 20 mL). The organic phase was washed with an aqueous solution of 1N HCl (40 mL) and then it was back-extracted with CH_2Cl_2 (2 x 30 mL). The combined organic layers were dried (Na_2SO_4), filtered and concentrated in vacuo. The crude product was purified by flash chromatography on silica gel (gradient 10-20% ethyl acetate in hexane) to

afford separately *cis*- and *trans*-**250c** as colourless oils (0.14 g, *dr* 1:2, 9% yield of both diastereomers combined). *cis*-**250**c: 87% *ee*; HPLC analysis: Chiralpack OD, 0.5% isopropanol in hexane, flow rate = 0.5 mL/min, λ = 210 nm. $[\alpha]^{20}{}_D$ + 6.0 (c = 0.1, CH_2Cl_2); IR (neat, cm^{-1}) 2960, 1704, 1547, 1451, 1381, 1123, 1047; ^{1}H NMR ($CDCl_3$, 400 MHz) δ 4.57 (2H, ABX, J_{AX} = 8.6 Hz, J_{BX} = 6.7 Hz, J_{AB} = 12.9 Hz, ν_{AB} = 87.0 Hz, H-7), 3.20 (1H, ddd, J = 8.2, 7.1, 5.1 Hz, H-2), 2.87 – 2.69 (1H, m, H-6), 2.58 – 2.36 (2H, m, H-8), 2.08 – 1.93 (1H, m, H-3), 1.93 – 1.75 (3H, m, H-3, H-5 and H-4), 1.75 – 1.64 (2H, m, H-5 and H-4), 1.67 – 1.53 (2H, m, H-9), 0.93 (3H, t, J = 7.4 Hz, H-10). ^{13}C NMR ($CDCl_3$, 101 MHz) δ 212.9 (C-1), 76.0 (C-7), 51.3 (C-2), 45.4 (C-8), 41.0 (C-6), 29.6 (C-3), 29.4 (C-5), 23.4 (C-4), 16.8 (c-9), 13.7 (C-10). HRMS required for $C_{10}H_{18}NO_3$ $[M+H]^+$ 200.1281, found 200.1282.

trans-**250**c: -55% *ee*; HPLC analysis: Chiralpack AD-H, 3% isopropanol in hexane, flow rate = 0.3 mL/min, λ = 210 nm. $[\alpha]^{20}{}_D$ + 6.0 (c = 0.1, CH_2Cl_2) IR (neat, cm^{-1}) 2963, 1705, 1547, 1452, 1431, 1379, 1129; ^{1}H NMR ($CDCl_3$, 400 MHz) δ 4.30 (2H, ABX, J_{AX} = 7.0 Hz, J_{BX} = 7.0 Hz, J_{AB} = 12.0, ν_{AB} = 24.3 Hz, H-7), 3.04 – 2.88 (1H, m, H-6), 2.67 (1H, dt, J = 9.3, 7.6 Hz, H-2), 2.52 – 2.26 (2H, m, H-8), 2.08 – 1.83 (2H, m, H-3 and H-5), 1.72 – 1.59 (3H, m, H-3 and H-4), 1.59 – 1.44 (2H, m, H-9), 1.44 – 1.29 (1H, m, H-5), 0.85 (3H, t, J = 7.4 Hz, H-10). ^{13}C NMR ($CDCl_3$, 101 MHz) δ 211.1 (C-1), 79.0 (C-7), 54.4 (C-2), 44.0 (C-8), 39.3 (C-6), 30.2 (C-3), 30.0 (C-5), 24.4 (C-4), 17.1 (C-9), 13.7 (C-10). HRMS required for $C_{10}H_{18}NO_3$ $[M+H]^+$ 200.1281, found 200.1280.

Benzyl 2-(hydroxymethyl)-3-(nitromethyl)pyrrolidine-1-carboxylate 317

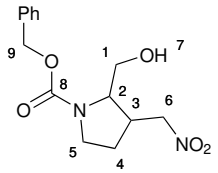

317

Following general procedure O, the nitro olefin **255** (0.187 g, 0.64 mmol) was added to catalyst **29** (0.019 g, 0.13 mmol) in DCE (12.8 mL) at -20 °C. The reaction was left stirring at -20 °C for 7 days and then reduced to the alcohol. The crude product was purified *via* flash chromatography to achieve both diastereomers of the

nitro alcohol **317** (0.092 g, 1:1 *cis/trans* ratio, 48% yield of both diastereomers combined) *cis*-**317**:-77% *ee*; HPLC analysis: Chiralpack AD-H, 10% isopropanol in hexane, flow rate = 1.0 mL/min, λ = 210 nm. $[\alpha]^{20}{}_D$ + 7.0 (c = 0.1, CH_2Cl_2); IR (neat, cm^{-1}) 3427, 2954, 1701, 1549, 1384, 1359, 1292, 1115, 1030, 1003, 769, 698, 668; ^{1}H NMR ($CDCl_3$, 400 MHz) δ 7.36 – 7.21 (5H, m, Ar-H), 5.17 – 4.90 (2H, m, H-9), 4.66 (1H, dd, J = 13,9, 7,7 Hz, H-6), 4.54 – 4.30 (1H, m, H-6), 4.14 – 3.93 (1H, m, H-2), 3.71 (1H, m, H-1), 3.59 (1H, m, H-1), 3.57 – 3.47 (1H, m, H-3), 3.43 – 3.26 (1H, m, H-3), 3.05 – 2.88 (1H, m, H-5), 2.03 – 1.74 (2H, m, H-4). ^{13}C NMR ($CDCl_3$, 101 MHz) δ 155.4 (C-8), 136.4 (Ar-C), 128.6 (Ar-C), 128.2 (Ar-C), 127.9 (Ar-C), 74.9 (C-6), 67.2 (C-9), 61.3 (C-1), 61.0 (C-5), 45.4 (C-3), 38.7 (C-2), 27.0 (C-4). *trans*-**317**: $[\alpha]^{20}{}_D$ + 22.2 (c = 0.1, CH_2Cl_2) IR (neat, cm^{-1}) 3418, 2953, 2887, 1697, 1547, 1416, 1384, 1357, 1213, 1113, 769, 737, 697; ^{1}H NMR ($CDCl_3$, 400 MHz) δ 7.42 - 7.29 (5H, m, Ar-H), 5.25 – 5.06 (2H, m, H-8), 4.60 – 4.42 (1H, m, H-6), 4.36 (1H, dd, J = 12.7, 8.7 Hz, H-6), 3.82 – 3.63 (3H, m, H-5 and H-1 and H-3), 3.45 (2H, dt, J = 11.2, 7.3 Hz, H-3), 2.97 – 2.70 (1H, m, H-2), 2.29 – 2.10 (1H, m, H-4), 1.83 – 1.66 (1H, m, H-4). ^{13}C NMR ($CDCl_3$, 101 MHz) δ 136.2 (Ar-C), 128.6 (Ar-C), 128.3 (Ar-C), 128.1 (Ar-C), 72.0 (C-6), 67.5 (C-8), 65.1 (C-1) 45.1 (C-3), 39.3 (C-2), 28.2 (C-4). HRMS required for $C_{14}H_{19}N_2O_5$ $[M+H]^+$ 295.1288, found 295.1293.

(1-(nitromethyl)-1,3-dihydro-2H-1l3,2l3-inden-2-yl) methanol 266

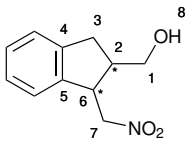

266

Following general procedure O, the nitro olefin **265** (0.131 g, 0.64 mmol) was added to a solution of catalyst **29** (0.019 g, 0.13 mmol) in DCE (12.8 mL). After 24 hours the reaction went to completion and it was reduced to the alcohol. The crude product was purified by flash chromatography on silica gel (25% ethyl acetate in hexane) to obtain a combination of *cis*- and *trans*-**266** as a colourless oil (0.97 g, 1:1 *cis/trans* ratio, 73% yield).

Mixture of diastereomers: $[\alpha]^{20}{}_D$ - 16.0 (c = 0.1, CH_2Cl_2) IR (neat, cm^{-1}) 3569, 3366, 2922, 1543, 1479, 1459, 1430, 1377, 1198, 1020, 752, 668; *cis*-**266**: 90%

ee; HPLC analysis: Chiralpack AD-H, 5% isopropanol in hexane, flow rate = 0.6 mL/min, λ = 210 nm. ^{1}H NMR ($CDCl_3$, 400 MHz) δ 7.34 – 7.09 (4H, m, Ar-H), 4.71 (2H, ABX, J_{AX} = 7.5 Hz, J_{BX} = 7.8 Hz, J_{AB} = 13.2 Hz, ν_{AB} = 128.3 Hz, H-7), 4.14 (1H, q, J = 7.5 Hz, H-6), 3.94 – 3.73 (2H, m, H-1), 3.10 – 2.90 (2H, m, H-2 and H-3), 2.83 (1H, dd, J = 14.8, 7.2 Hz, H-3). ^{13}C NMR ($CDCl_3$, 101 MHz) δ 142.3 (C-5), 141.4 (C-4), 128.0 (Ar-C), 127.0 (Ar-C), 125.0 (Ar-C), 124.0 (Ar-C), 76.0 (C-7), 62.6 (C-1), 44.5 (C-6), 44.3 (C-2), 33.9 (C-3). *trans*-**266**: 52% *ee*; HPLC analysis: Chiralpack AD-H, 5% isopropanol in hexane, flow rate = 0.6 mL/min, λ = 210 nm. ^{1}H NMR ($CDCl_3$, 400 MHz) δ 7.26 – 7.04 (4H, m, Ar-H), 4.65 – 4.42 (2H, m, H-7), 3.80 (1H, td, J = 7.0, 4.7 Hz, H-6), 3.70 – 3.49 (2H, m, H-1), 2.91 (2H, ABX, J_AX = 8.4 Hz, J_BX = 5.0 Hz, J_AB = 16.5 Hz, ν_{AB} = 19.4 Hz, H-3), 2.57 – 2.38 (1H, m, H-2). ^{13}C NMR ($CDCl_3$, 101 MHz) δ 142.3 (C-5), 140.4 (C-4), 128.2 (Ar-C), 127.1 (Ar-C), 125.3 (Ar-C), 124.3 (Ar-C), 79.2 (C-7), 65.3 (C-1), 46.3 (C-6), 45.0 (C-2), 34.0 (C-3). HRMS required for $C_{11}H_{12}NO_3$ $[M\text{-}H]^-$ 206.0812, 206.0816.

6.14 Kinetic studies

Kinetic studies were performed at the University of Manchester under the supervision of Dr. Jordi Burés. Nuclear Magnetic Resonance (NMR) spectra were recorded using a B500 Bruker Avance II+ 500 MHz. A stock solution of the nitro olefin **214**

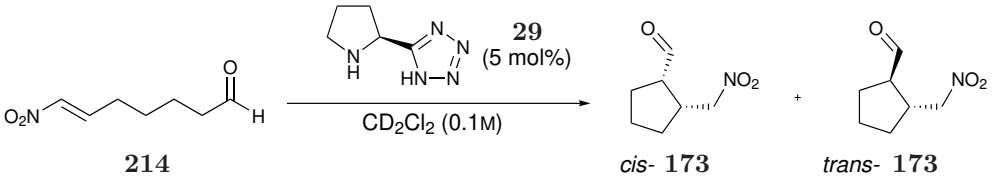

Scheme 6.12: Reaction monitored by ^{1}H NMR to study the kinetic profile.

(400 μL, 0.1M in CD_2Cl_2) was added to a stock solution of the catalyst **29** (100 μL, 1M in CD_2Cl_2) and CD_2Cl_2 (100 μL), directly in a NMR tube. The reaction was monitored by ^{1}H NMR at 25 °C.

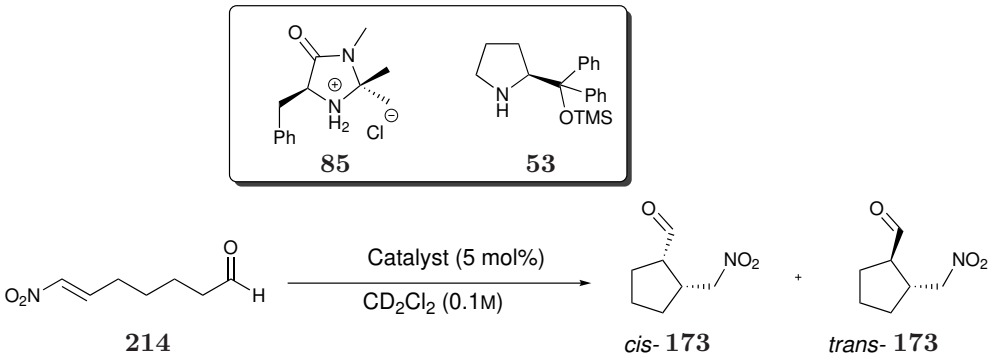

Scheme 6.13: Reactions monitored by ^{1}H NMR to study the kinetic profile.

A stock solution of the nitro olefin **214** (400 μL, 0.1M in CD_2Cl_2) was added to a stock solution of the catalyst **85** or **53** (100 μL, 1M in CD_2Cl_2) and CD_2Cl_2 (100 μL), directly in a NMR tube. The reaction was monitored by ^{1}H NMR at 25 °C.

6.15 Calculated Energies

Table 6.2: Calculated energies and Gibbs free energies. Values were obtained at the ω-B97X-D/6-311G(d,p) level of theory, unless basis specified and are in hartree. G_{therm} is given at 298 K and 1 atm, qRRHO data is calculated at the concentration of 0.04 M

	E_{SP}	G_{therm}	$G_{qRRHO(253)}$	$G_{qRRHO(298)}$	$G_{solv=DCE}$	E(6-311++G(3df,3pd))
V	-469.621079737	-469.495528	-469.488611	-469.494561	-469.621079737	-469.665243816
1	-553.635288342	-553.496528	-553.486999	-553.494122	-553.635288342	-553.687704343
water	-76.423353397	-76.416192	-76.416192	-76.41622	-76.423353397	-76.4383130367
214b (pre-*cis*)	-946.836877190	-946.568887	-946.556856	-946.565660	-946.836877190	-946.922377559
214b (pre-*trans*)	-946.838583781	-946.572888	-946.559697	-946.568646	-946.838583781	-946.924128500
(*1S,2S*)-**214b**‡	-946.814746140	-946.543569	-946.532832	-946.541237	-946.814746140	-946.900771093
(*1R,2R*)-**214b**‡	-946.809430513	-946.537152	-946.526685	-946.535044	-946.809430513	-946.894996939
(*1S,2R*)-**214b**‡	-946.826248358	-946.552554	-946.542915	-946.551166	-946.826248358	-946.910825548
(*1R,2S*)-**214b**‡	-946.815806039	-946.543154	-946.533140	-946.541487	-946.815806039	-946.901350324
(*1S,2S*)-**214c**	-946.827251799	-946.554637	-946.542746	-946.551180	-946.827251799	-946.911608405
(*1R,2R*)-**214c**	-946.826485766	-946.554625	-946.542557	-946.551036	-946.826485766	-946.910800024
(*1S,2R*)-**214d**	-946.858429165	-946.585606	-946.573633	-946.581965	-946.858429165	-946.941568527
(*1R,2S*)-**214d**	-946.856453377	-946.585550	-946.572697	-946.581216	-946.856453377	-946.940468880
(*1S,2S*)-**214e**	-946.844975318	-946.571869	-946.560276	-946.568667	-946.844975318	-946.931214192
(*1R,2R*)-**214e**	-946.843954863	-946.570881	-946.559302	-946.567673	-946.843954863	-946.930217381
(*1S,2R*)-**214e**	-946.855548328	-946.581345	-946.570058	-946.578347	-946.855548328	-946.939941142
(*1R,2S*)-**214e**	-946.852894447	-946.578434	-946.567200	-946.575474	-946.852894447	-946.938840908
(*1S,2S*)-**214e**‡	-1023.26458131	-1022.974427	-1022.961950	-1022.970903	-1023.26458131	-1023.35749357
(*1R,2R*)-**214e**‡	-1023.26086660	-1022.969795	-1022.957859	-1022.966749	-1023.26086660	-1023.35273521
(*1S,2R*)-**214e**‡	-1023.25970289	-1022.967407	-1022.955583	-1022.964426	-1023.25970289	-1023.35113506
(*1R,2S*)-**214e**‡	-1023.26125226	-1022.968186	-1022.956924	-1022.965711	-1023.26125226	-1023.35272650
trans-**173**	-553.667031153	-553.520748	-553.512493	-553.519080	-553.667031153	-553.71648698
cis-**173**	-553.663855226	-553.518404	-553.510002	-553.516670	-553.663855226	-553.713705105

6.16 Synthesis of γ/α-peptides

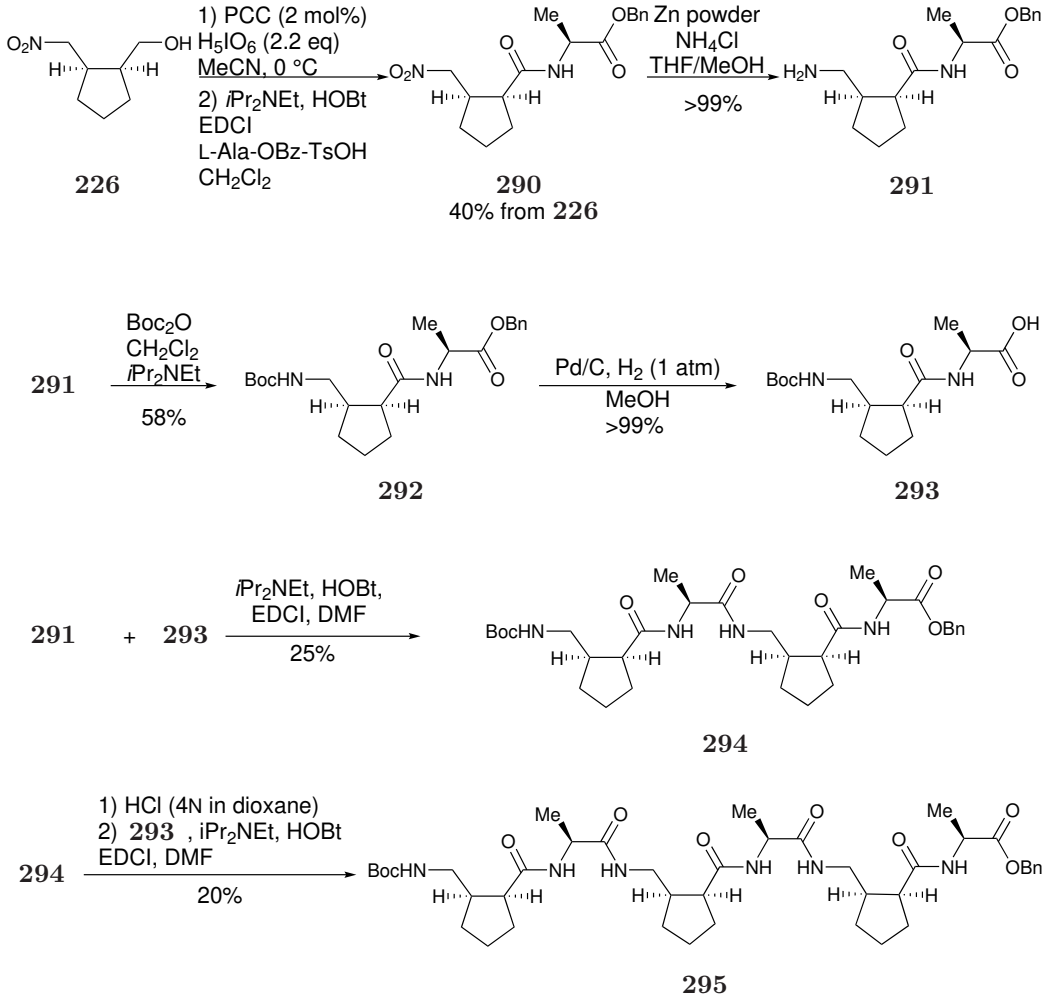

Figure 6.5: Synthetic procedure for the synthesis of γ/α-peptides **292**, **294** and **295**.

(1*S*,2*R*)-2-(nitromethyl)cyclopentane-1-carboxylic acid **288**

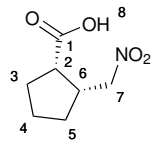

288

To a solution of H_5IO_6 (2.198 g, 9.7 mmol) in anhydrous acetonitrile (19 mL) stirred vigorously for 15 minutes at rt was added ***cis*-226** (0.699 g, 4.4 mmol) at 0 °C in anhydrous acetonitrile (2 mL) followed by PCC (0.019 g, 0.09 mmol) in acetonitrile (4 mL). The reaction mixture was stirred at 0 °C for 45 minutes until the reaction went to completion. The reaction was monitored by TLC. Ethyl acetate

(50 mL) was then added and the organic phase was washed first with brine (50 mL), then with a saturated aqueous solution of $NaHSO_3$ (70 mL) and brine (50 mL) again. The organic layers were then combined and dried on Na_2SO_4, filtered and concentrated *in vacuo*. The product obtained was a colourless oil (0.674 g, 3.9 mmol, 88%) and it did not require further purification. $[\alpha]^{20}{}_D$ +21.0 (c = 0.1, CH_2Cl_2); IR (neat, cm^{-1}) 2963, 1701 , 1547, 1383; ^1H NMR (400 MHz, $CDCl_3$) δ 4.56 (2H, ABX, J_{AX} = 7.2 Hz, J_{BX} = 8.1 Hz, J_{AB} = 13.2 Hz, ν_{AB} = 99.0 Hz, H-7), 3.07 (1 H, td, *J* 7.4, 6.1, H-2), 2.90 (1 H, dt, *J* 9.3, 7.5, H-6), 2.12 – 1.99 (2 H, m, H-3), 2.00 – 1.84 (2 H, m, H-4', H-5'), 1.82 – 1.67 (1 H, m, H-4''), 1.67 – 1.50 (1 H, m, H-5''). ^{13}C NMR (101 MHz, $CDCl_3$) δ 179.6 (C-1), 76.1 (C-7), 45.2 (C-2), 40.4 (C-6), 29.1 (C-3), 28.9 (C-5), 23.0 (C-4); HRMS required for $C_7H_{10}NO_4$ $[M-H]^-$ is 172.0610, found 172.0612.

benzyl ((1*S*,2*R*)-2-(nitromethyl)cyclopentane-1-carbonyl)-D-alaninate **318**

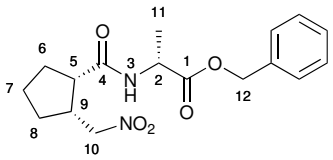

318

To a solution of the carboxylic acid **288** (0.087 g, 0.5 mmol) in CH_2Cl_2 (3.4 mL), DIPEA (0.1 mL, 0.6 mmol), HOBt· H_2O (0.081 g, 0.6 mmol) and EDCI (0.115 g, 0.6 mmol) were added and the reaction mixture was stirred for 15 minutes at rt. D-Ala benzyl ester (0.090 g, 0.5 mmol) was then added and the reaction mixture was left stirring at rt for 16 hours. The reaction was monitored by TLC and after 24 hours ethyl acetate (50 mL) was added. The organic phase was washed first with an aqueous 1N solution of aqueous HCl (75 mL), then with an aqueous saturated solution of $NaHCO_3$ (25 mL) and finally with brine (25 mL). The acidic aqueous phase was then extracted again with CH_2Cl_2 (2 x 25 mL) and the same procedure was carried out for the basic phase ($NaHCO_3$ and brine phases combined) too. The organic phase was then dried over Na_2SO_4, filtered and concentrated *in vacuo*. The crude product was purified *via* combiflash on 80 g silica gel columns (gradient ethyl acetate in hexane). The product was obtained as a white solid (0.056 g, 34%). mp = 48.8 - 50.4 °C; IR (neat, cm^{-1}) 3315, 2932, 1733, 1638, 1538, 1450, 1385, 1334,

1316, 1207, 1144, 958, 757, 731; ^{1}H NMR (400 MHz, $CDCl_3$) δ 7.36 – 7.23 (5 H, m, Ar-H), 6.10 (1 H, d, J = 7.4 Hz, H-3), 5.10 (2 H, ABq, J_{AB} = 12.3 Hz, H-12), 4.58 – 4.31 (3 H, ABX unresolved, m, H-10 and H-2), 2.84 – 2.66 (2 H, m, H-5 and H-9), 1.94 - 1.78 (2 H, m, H-8 and H-7'), 1.81 - 1.70 (1 H, m, H-6'), 1.62 – 1.48 (2 H, m, H-7''and H-6''), 1.32 (3 H, d, J = 7.2 Hz, H-11); ^{13}C NMR (101 MHz, $CDCl_3$) δ 173.2 (C-4), 172.8 (C-1), 135.3 (Ar-C), 128.6 (Ar-C), 128.5 (Ar-C), 128.2 (Ar-C), 76.3 (C-10), 67.2 (C-12), 48.1 (C-2), 46.7 (C-5), 41.1 (C-9), 29.9 (C-8), 29.7 (C-6), 24.0 (C-7), 18.2 (C-11). HRMS required for $C_{17}H_{23}N_2O_5$ $[M+H]^+$ is 335.1607, found 335.1600.

Benzyl ((1*S*,2*R*)-2-(nitromethyl)cyclopentane-1-carbonyl)- L-alaninate **290**

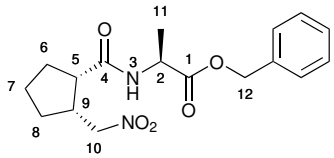

290

To a solution of the carboxylic acid **288** (0.660 g, 3.8 mmol) in CH_2Cl_2 (27 mL), DIPEA (0.80 mL, 4.6 mmol), HOBt· H_2O (0.622 g, 4.6 mmol) and EDCI (0.882 g, 4.6 mmol) were added and the reaction mixture was stirred for 15 minutes at rt. L-Ala benzyl ester *p*-toluene sulfonate salt was then added and the reaction mixture was left stirring at rt for 16 hours. The reaction was monitored by TLC and once gone to completion ethyl acetate (150 mL) was added. The organic phase was washed first with an aqueous 1N solution of $NaHSO_4$ (75 mL), then with an aqueous saturated solution of $NaHCO_3$ (75 mL) and finally with brine (75 mL). The acidic aqueous phase was then extracted again with CH_2Cl_2 (2 x 75 mL) and the same procedure was carried out for the basic phase ($NaHCO_3$ and brine phases combined) too. The organic phase was then dried over Na_2SO_4, filtered and concentrated *in vacuo*. The crude product was purified *via* combiflash on 80 g silica gel columns (gradient ethyl acetate in hexane). The product was obtained as a white solid (0.40 g, 1.2 mmol, 31%). mp = 94.2 - 97.1 °C; $[\alpha]^{20}{}_D$ +15.0 (c = 0.1, CH_2Cl_2); IR (neat, cm^{-1}) 3316, 2959, 1744, 1640, 1550, 1527, 1456, 1389, 1376, 1188, 1168, 1153; ^{1}H NMR (400 MHz, $CDCl_3$) δ 7.46 – 7.32 (3 H, m, Ar-H), 6.14 (1 H, d, J 7.3, H-3), 5.19 (2H, AB, J_{AB} = 12.2 Hz, ν_{AB} = 27.9 Hz, H-12), 4.55 (2H, ABX, J_{AX} = 8.2 Hz,

J_{BX} = 6.6 Hz, J_{AB} = 13.5 Hz, ν_{AB} = 119.4 Hz, H-10), 4.56 (1 H, p, *J* 7.2, H-2), 2.91 (1 H, td, *J* 7.7, 4.8, H-5), 2.87 – 2.71 (1 H, m, H-9), 2.10 – 1.89 (3 H, m, H-6, H-7'), 1.91 – 1.74 (1 H, m, H-8'), 1.74 – 1.58 (2 H, m, H-8'', H-7''), 1.43 (3 H, d, *J* 7.2, H-11). ^{13}C NMR (101 MHz, $CDCl_3$) δ 173.4 (C-4), 172.8 (C-1), 135.4 (Ar-C), 128.8 (Ar-C), 128.6 (Ar-C), 128.4 (Ar-C), 76.5 (C-10), 67.4 (C-12), 48.3 (C-2), 46.9 (C-5), 41.9 (C-9), 29.7 (C-8), 29.5 (C-6), 23.8 (C-7), 18.0 (C-11); HRMS required for $C_{17}H_{23}N_2O_5$ $[M+H]^+$ is 335.1607, found 335.1596.

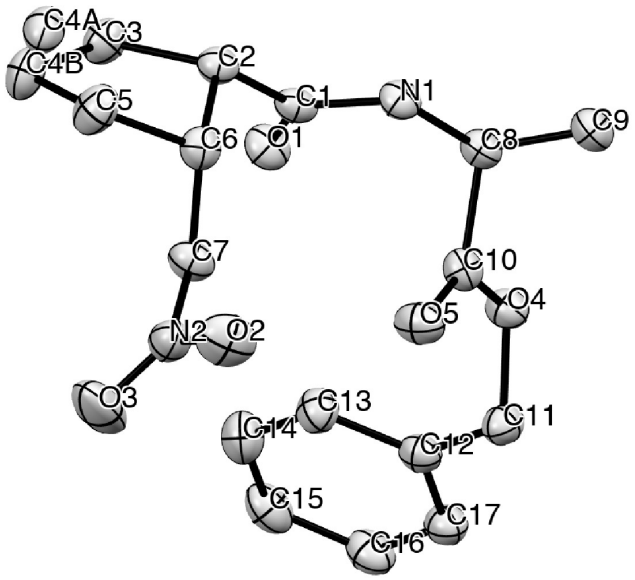

Figure 6.6: Crystal structure of the nitrodimer **290**.

Table 6.3: Crystal data and structure refinement for the nitrodimer **290**

Identification code	RF435-F32-34
Empirical formula	$C_{17}H_{22}N_2O_5$
Formula weight	334.36
Temperature/K	149.95(10)
Crystal system	monoclinic
Space group	$P2_1$
a/Å	9.4637(2)
b/Å	9.36340(10)
c/Å	9.9797(2)
α/°	90
β/°	109.791(2)
γ/°	90
Volume/Å^3	832.09(3)
Z	2
ρ_{calc}g/cm^3	1.335
μ/mm^{-1}	0.819
F(000)	356.0
Crystal size/mm^3	0.26 × 0.05 × 0.02
Radiation	CuKα (λ = 1.54184)
2Θ range for data collection/°	9.418 to 140.84
Index ranges	-11 ≤ h ≤ 11, -11 ≤ k ≤ 11, -12 ≤ l ≤ 12
Reflections collected	15121
Independent reflections	3114 [R_{int} = 0.0432, R_{sigma} = 0.0291]
Data/restraints/parameters	3114/1/232
Goodness-of-fit on F2	1.046
Final R indexes [I>=2σ (I)]	R_1 = 0.0327, wR_2 = 0.0838
Final R indexes [all data]	R_1 = 0.0342, wR_2 = 0.0856
Largest diff. peak/hole / e Å^{-3}	0.17/-0.18
Flack parameter	0.03(10)

Benzyl ((1*S*,2*R*)-2-(((tert-butoxycarbonyl)amino)methyl)cyclopentane-1-carbonyl)-L-alaninate **292**

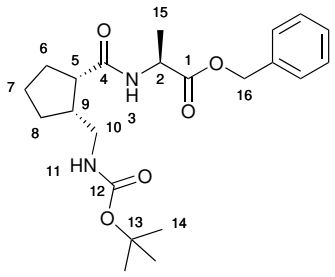

292

To a solution of compound **290** (0.56 g, 1.7 mmol) in anhydrous MeOH (33 mL) and anhydrous THF (33 mL), Zn powder (1.64 g, 24.9 mmol) and NH_4Cl (1.33 g, 24.9 mmol) were added. The reaction mixture was stirred at rt for 1 hour and it was worked up after monitoring it *via* TLC. Ehtyl acetate (500 mL) was added and it was then filtered through a short pad of celite. The white solid obtained was then dissolved in CH_2Cl_2 and filtered through cotton wool to remove any NH_4Cl left in solution. The product **291** obtained was a pale yellow paste (0.57 g, 1.8 mmol, quantitative yield) and it did not require further purifcation. To a solution of the free amine **291** (0.552 g, 1.81 mmol) in anhydrous CH_2Cl_2 (14 mL), isopropyl amine (0.63 mL, 3.6 mmol) and Boc_2O (0.64 mol, 2.7 mmol) were added and the reaction mixture was stirred at rt. The reaction was monitored by TLC and it went to completion in 45 minutes. The reaction mixture was diluted with ethyl acetate (45 mL) and washed with an aqueous solution of 1M $NaHSO_4$ (30 mL) followed by brine (30 mL). The organic layers were then combined, dried over Na_2SO_4, filtered and concentrated *in vacuo*. The crude product was then purified *via* flash chromatography on silica gel (30% ethyl acetate in hexane). The title product was obtained as a white solid (0.270 g, 36%). mp = 131.3 - 133.9 °C; $[\alpha]^{20}{}_D$ +103.8 (c = 0.08, MeOH); IR (neat, cm^{-1}) 3350, 3322, 2958, 1739, 1676, 1640, 1533, 1454, 1370, 1281, 1152, 1058; ^1H NMR (400 MHz, $CDCl_3$) δ 7.36 – 7.21 (5 H, m, Ar-H), 6.16 (1 H, d, *J* 6.7, H-3), 5.39 (1 H, t *J* 6.2, H-11)), 5.19 (1 H, ABq, J_AB = 12.3 Hz, ν_{AB} = 30.5, H-16), 4.60 (1 H, p, *J* 7.3, H-2), 3.19 (1 H, dt, *J* 13.9, 5.9, H-10'), 3.11 - 2.91 (1 H, m, H-10''), 2.73 – 2.60 (1 H, m, H-5), 2.48 - 2.29 (1 H, m, H-9), 2.00 - 1.79 (3 H, m, H-6, H-7'), 1.79 - 1.69 (1 H, m, H-8'), 1.60 – 1.48 (2H, m H-7''and H-8''), 1.44 (9H, s,

H-14), 1.41 (3H, m, H-15); ^{13}C NMR (101 MHz, $CDCl_3$) δ 174.6 (C-4), 173.4 (C-1), 156.4 (C-12), 135.3 (Ar-C), 128.7 (Ar-C), 128.5 (Ar-C), 128.3 (Ar-C), 67.3 (C-16), 48.0 (C-2), 47.4 (C-5), 44.2 (C-9), 41.8 (C-10), 29.7 (C-8), 29.2 (C-6), 28.5 (C-14), 24.1(C-7), 18.0 (C-15); HRMS required for $C_{22}H_{33}N_2O_5$ $[M+H]^+$ is 405.2389, found 405.2399.

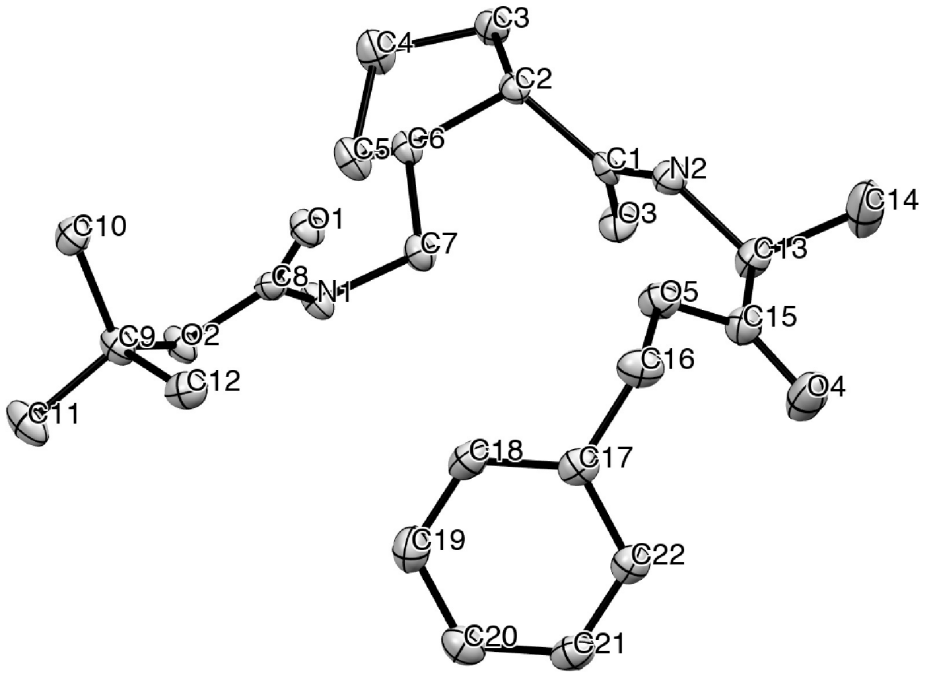

Figure 6.7: X-Ray crystal structure of the dimer **292** (CCDC : 1947227).

Table 6.4: Crystal data and structure refinement for **292**.

Identification code	exp_{13}
Empirical formula	$C_{22}H_{32}N_2O_5$
Formula weight	404.49
Temperature/K	100.00(10)
Crystal system	monoclinic
Space group	$P2_1$
a/Å	5.03210(10)
b/Å	18.5414(4)
c/Å	11.6101(2)
α/°	90
β/°	94.440(2)
γ/°	90
Volume/Å^3	1080.00(4)
Z	2
ρ_{calc}g/cm^3	1.244
μ/mm^{-1}	0.716
F(000)	436.0
Crystal size/mm^3	0.14 × 0.03 × 0.03
Radiation	CuKα (λ = 1.54184)
2Θ range for data collection/°	7.638 to 134.094
Index ranges	-5 ≤ h ≤ 4, -22 ≤ k ≤ 22, -13 ≤ l ≤ 13
Reflections collected	16639
Independent reflections	3822 [R_{int} = 0.0575, R_{sigma} = 0.0462]
Data/restraints/parameters	3822/1/266
Goodness-of-fit on F_2	1.068
Final R indexes [I>= 2σ (I)]	R_1 = 0.0343, wR_2 = 0.0828
Final R indexes [all data]	R_1 = 0.0383, wR_2 = 0.0848
Largest diff. peak/hole / e Å^{-3}	$0.20/-0.17$
Flack parameter	0.02(11)

6.16.1 General procedure Q for deprotection of the acid moiety

To a solution of benzyl ester in MeOH (20 mL/mmol), a spatula tip of Pd/C (10 %w/w) was added followed by 3 H_2 balloons that were emptied in the reaction mixture. The reaction was monitored by ^{1}H NMR and TLC. The reaction mixture was then filtered through a short pad of celite with a short pad of silica on top and it was washed with MeOH (50 mL). The organic phase was then concentrated *in vacuo*. The title product is obtained pure and did not need any further purification.

6.16.2 General procedure R for deprotection of the amine moiety

To a solution of protected amine dissolved in a minimal amount of 1,4-dioxane, a solution of 4N HCl in 1,4-dioxane (5 mL/0.5 mmol) was added. The reaction flask was then sealed with a septum and stirred at rt. The reaction was monitored by ^{1}H NMR and TLC and after 4.5 hours, the reaction mixture was then concentrated *in vacuo* to give pure free amine ready to be used for the following step.

γ/α-peptide BocNH(AMCP-L-Ala)$_2$-OBn **294**

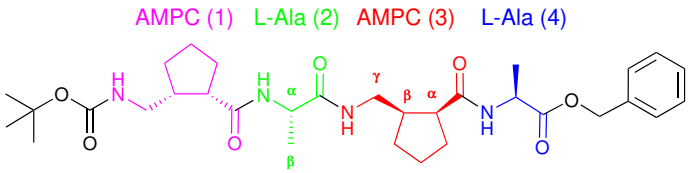

294

To a solution of the dimer acid **293** (0.063 g, 0.2 mmol) in DMF (0.5 mL), DIPEA (0.2 mL, 1.2 mmol), HOBt· H_2O (0.032 g, 0.24 mmol) and EDCI (0.046 g, 0.24 mmol) were added. The solution was stirred at rt for 15 minutes and then a solution of dimer amine **291** (0.061 g, 0.2 mmol) in DMF (0.5 mL) was added. The reaction mixture was stirred at rt for 24 hours. Ethyl acetate (10 mL) was then added and the organic phase was washed with a 1M aqueous solution of $NaHSO_4$ (2 x 5 mL), a saturated aqueous solution of $NaHCO_3$ (2 x 5 mL) and then brine (2 x 5 mL). Acid and basic aqueous layers were then extracted twice with CH_2Cl_2. All organic layers were combined, dried over Na_2SO_4, filtered and concentrate *in vacuo*. The crude product was then purified by flash chromatography on silica gel (gradient hexane/ethyl acetate/methanol) to obtain the title product **294** as a white solid (0.031 g, 0.05 mmol, 26%). $[\alpha]^{20}{}_D$ +69.2 (c = 0.12, MeOH). IR (neat, cm^{-1})

3300, 2931, 1741, 1636, 1534, 1449, 1366, 1278, 1247, 1169, 1114, 1034 . ^{1}H NMR (600 MHz, $CDCl_3$) δ 8.31 (1 H, m), 8.11 (1 H, d, *J* 7.0), 7.44 – 7.27 (5 H, m), 6.11 (1 H, d, *J* 4.9), 6.08 (1 H, d, *J* 6.7), 5.26 (1 H, d, *J* 12.3), 5.20 (1 H, dd, *J* 39.7, 12.3), 4.52 (1 H, t, *J* 7.3), 4.18 (1 H, q, *J* 6.9), 3.62 (1 H, ddd, *J* 13.4, 6.1, 4.7), 3.33 (1 H, dd, *J* 13.1, 6.3), 2.91 – 2.81 (2 H, m), 2.82 – 2.65 (3 H, m), 2.59 – 2.49 (1 H, m), 1.99 – 1.80 (6 H, m), 1.81 – 1.72 (2 H, m), 1.60 (9 H, s), 1.60-1.54 (2H, m) 1.47 - 1.43 (4 H, m), 1.42 (m, 1H), 1.41 (3 H, d, *J* 7.0). ^{13}C NMR (101 MHz, $CDCl_3$) δ 176.5 (CO AMCP(3)), 176.0 (CO L-Ala(4)), 175.7 (CO L-Ala(2)), 173.3 (CO AMCP(1)), 156.5 (CO-Boc), 135.2 (C-Ar), 128.6 (C-Ar), 128.4 (C-Ar), 128.1 (C-Ar), 67.4 (CH_2-Bn), 50.0 (HCα L-Ala(2)), 48.2 (HCα L-Ala(4)), 46.6 (HCα AMCP(1)), 45.3(HCα AMCP(3)), 44.3 (HCβ AMCP(1)), 42.0 (H2Cγ AMCP(1)), 41.9 (HCγ AMCP(1), 30.8 (C1 AMCP(3)), 30.3, 30.1 (C1-AMCP(1)), 30.0 (C3-AMCP(3)), 29.7 (C3-AMCP(1)), 25.6 (C2 AMCP(3)), 24.5 (C2 AMCP(1)), 17.6 (HCβ L-Ala(2)), 16.8 (HCβ L-Ala(4)). HRMS required for $C_{32}H_{49}N_4O_7$ $[M+H]^+$ is 601.3601, found 601.3604.

Table 6.5: ^{1}H NMR assignments for the γ/α-peptide **294**.

Residue	Hα [ppm]	Hβ [ppm]	Hγ1 [ppm]	Hγ2 [ppm]	NH [ppm]	H1 [ppm]	H2 [ppm]	H3 [ppm]
L-Ala(2)	4.19	1.41	-	-	6.08	-	-	-
AMCP (3)	2.71	2.87	3.62	2.79	8.31	1.75 and 1.42	1.88 and 1.58	1.93 and 1.86
L-Ala(4)	4.52	1.45	-	-	8.11	-	-	-
AMCP (1)	2.73	2.54	3.33	2.69	6.10	1.77 and 1.40	1.88 and 1.57	1.93 and 1.86

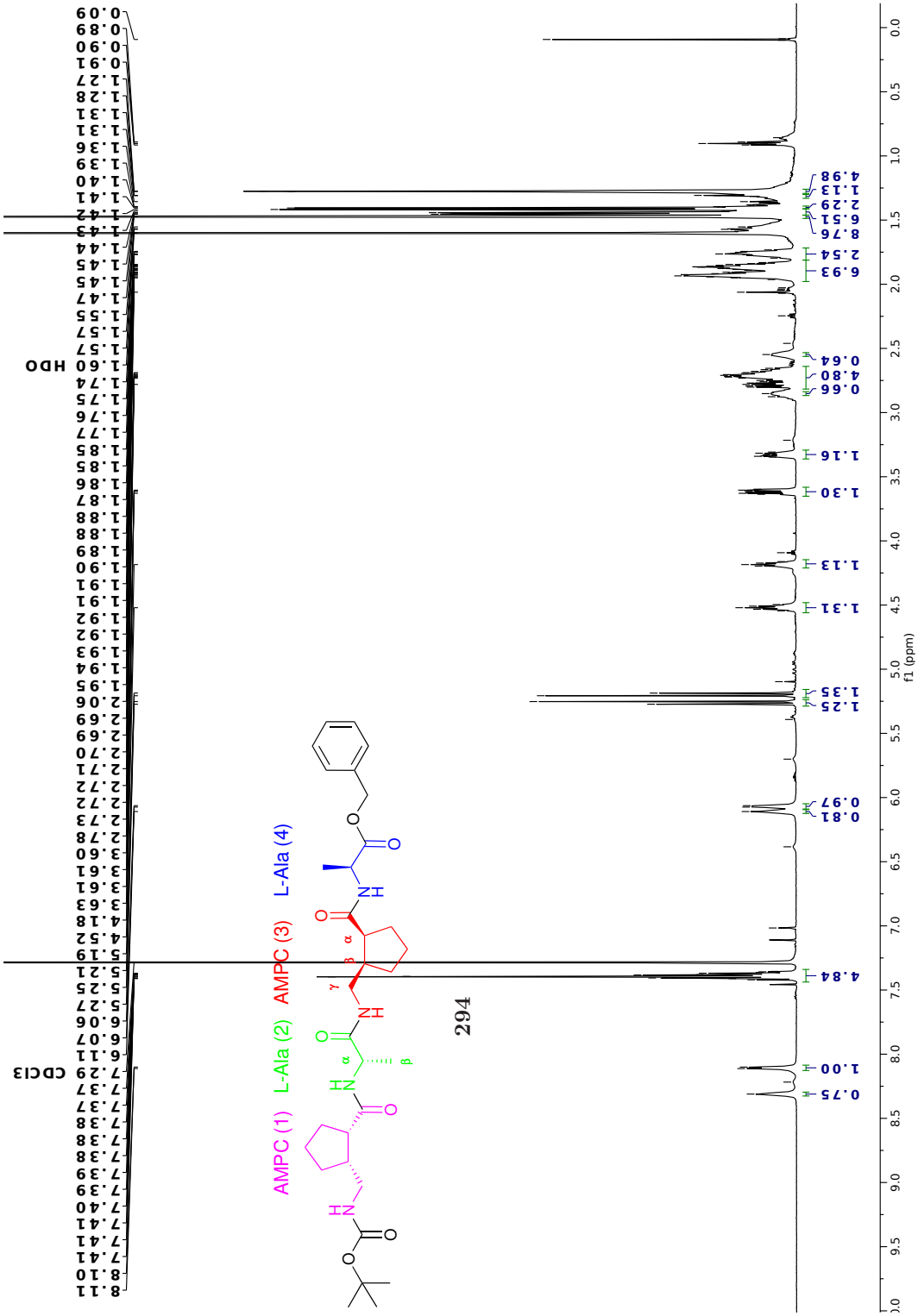
HDO
CDCl3
AMPC (1)
L-Ala (2)
AMPC (3)
L-Ala (4)
294
f1 (ppm)

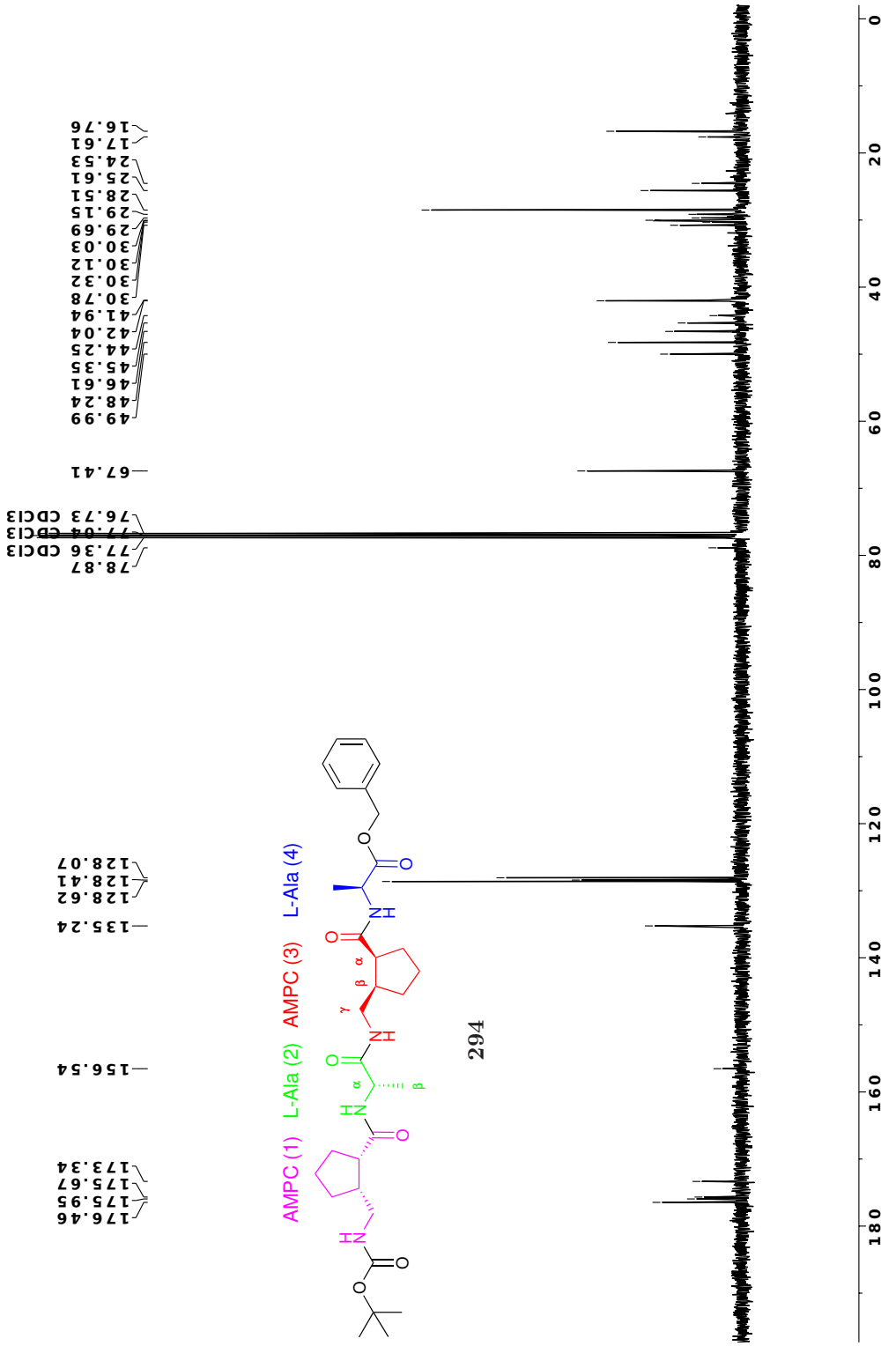
AMPC (1)
L-Ala (2)
AMPC (3)
L-Ala (4)
294
176.46
175.95
175.67
173.34
156.54
135.24
128.62
128.41
128.07
78.87
77.36 CDCl3
77.04 CDCl3
76.73 CDCl3
67.41
49.99
48.24
46.61
45.35
44.25
42.04
41.94
30.78
30.32
30.12
30.03
29.69
29.15
28.51
25.61
24.53
17.61
16.76
0
20
40
60
80
100
120
140
160
180

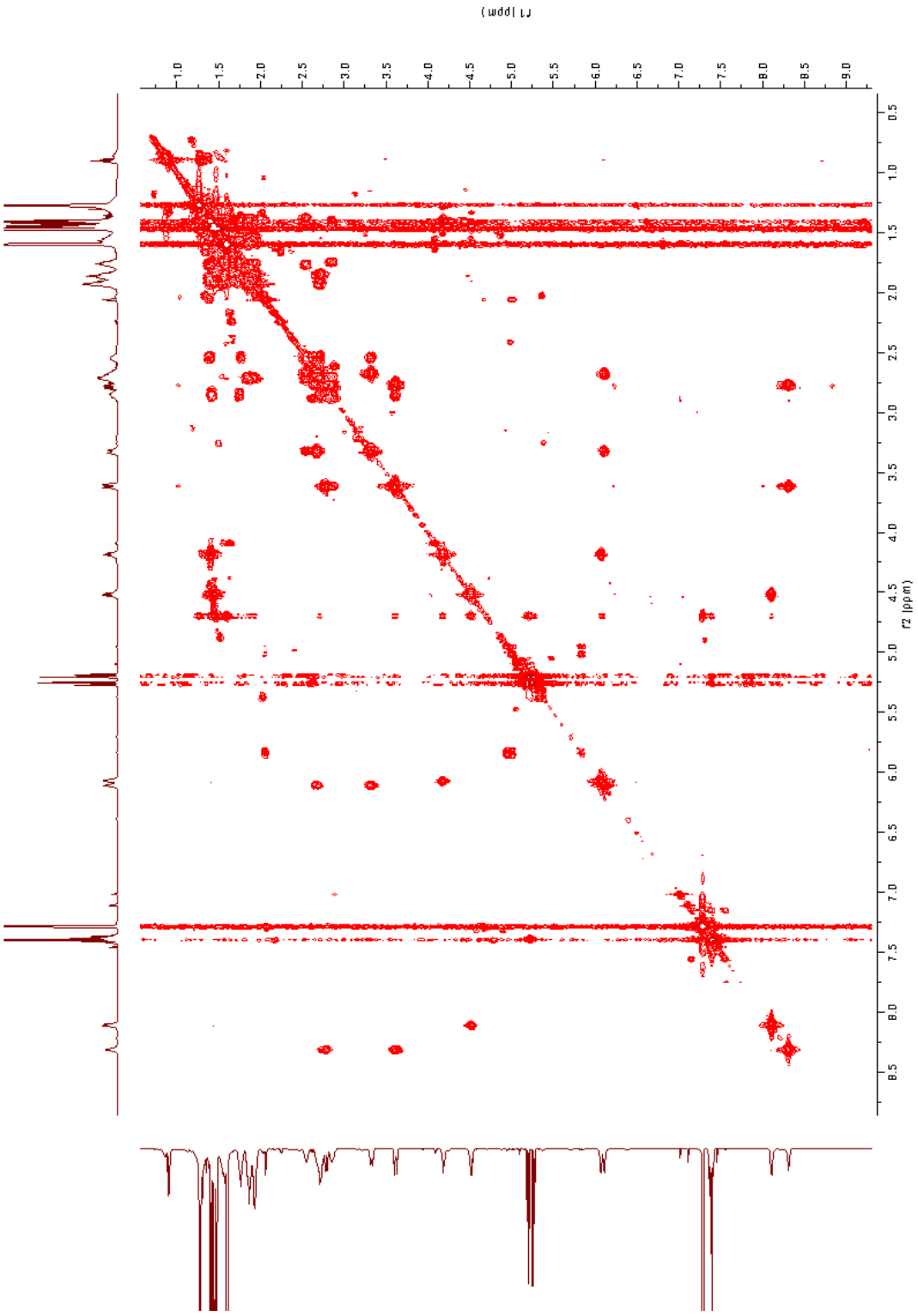

Figure 6.8: COSY NMR spectrum of tetramer **294** at a concentration of 0.2mM in $CDCl_3$ (600 MHz).

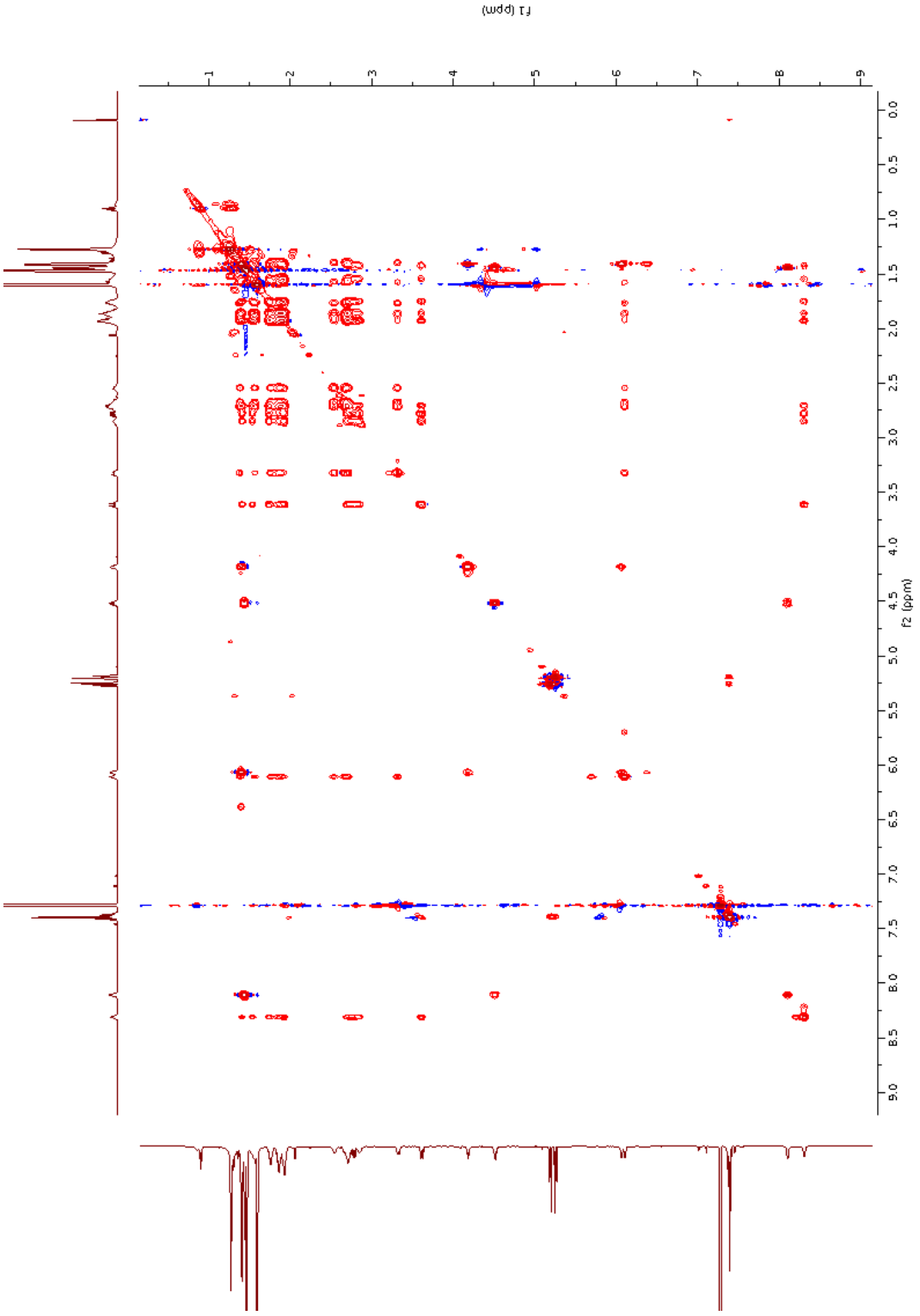

Figure 6.9: TOCSY NMR spectrum of tetramer **294** at a concentration of 0.2mM in $CDCl_3$ (600 MHz).

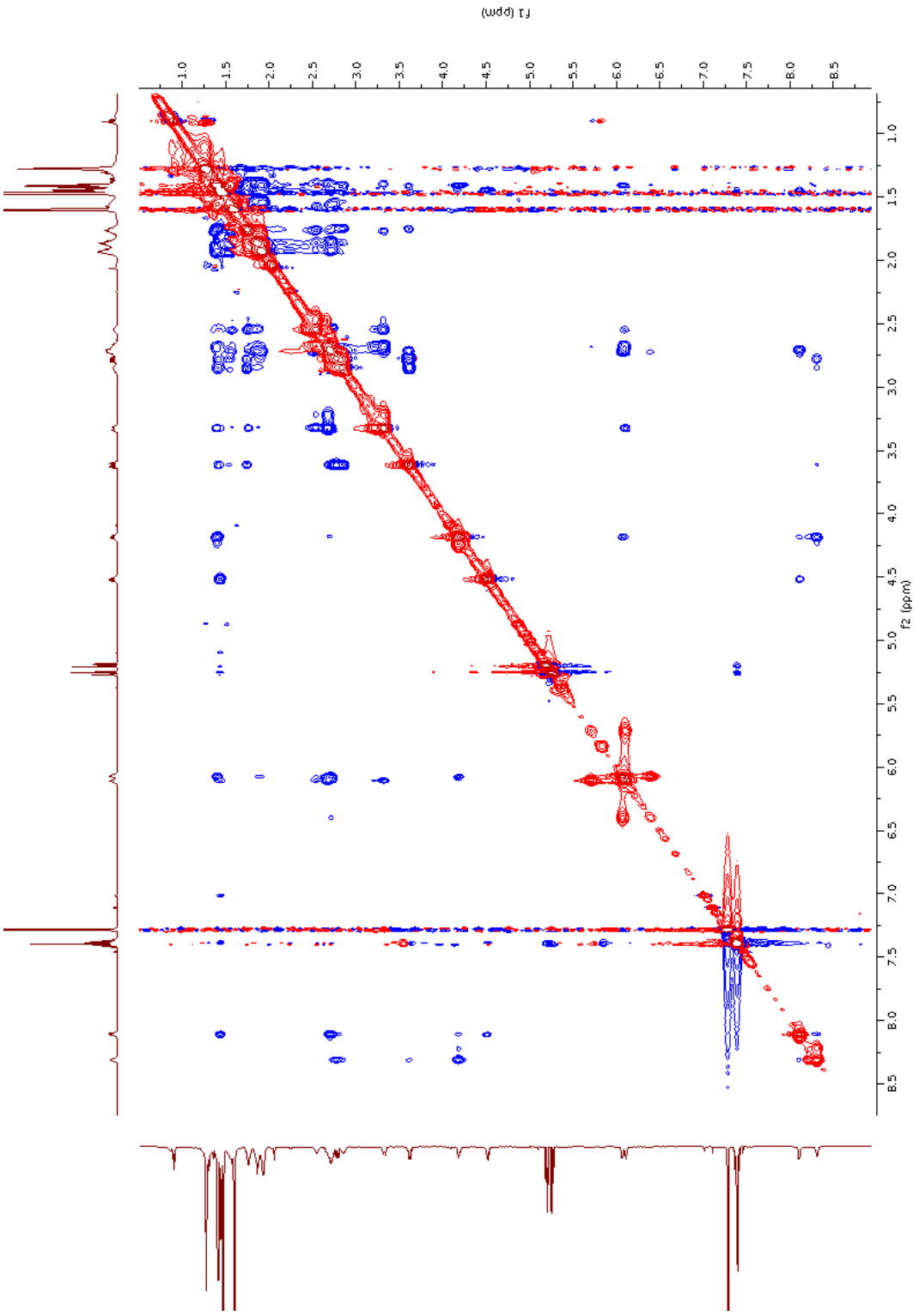

Figure 6.10: ROESY NMR spectrum of tetramer **294** at a concentration of 0.2mM in $CDCl_3$ (600 MHz).

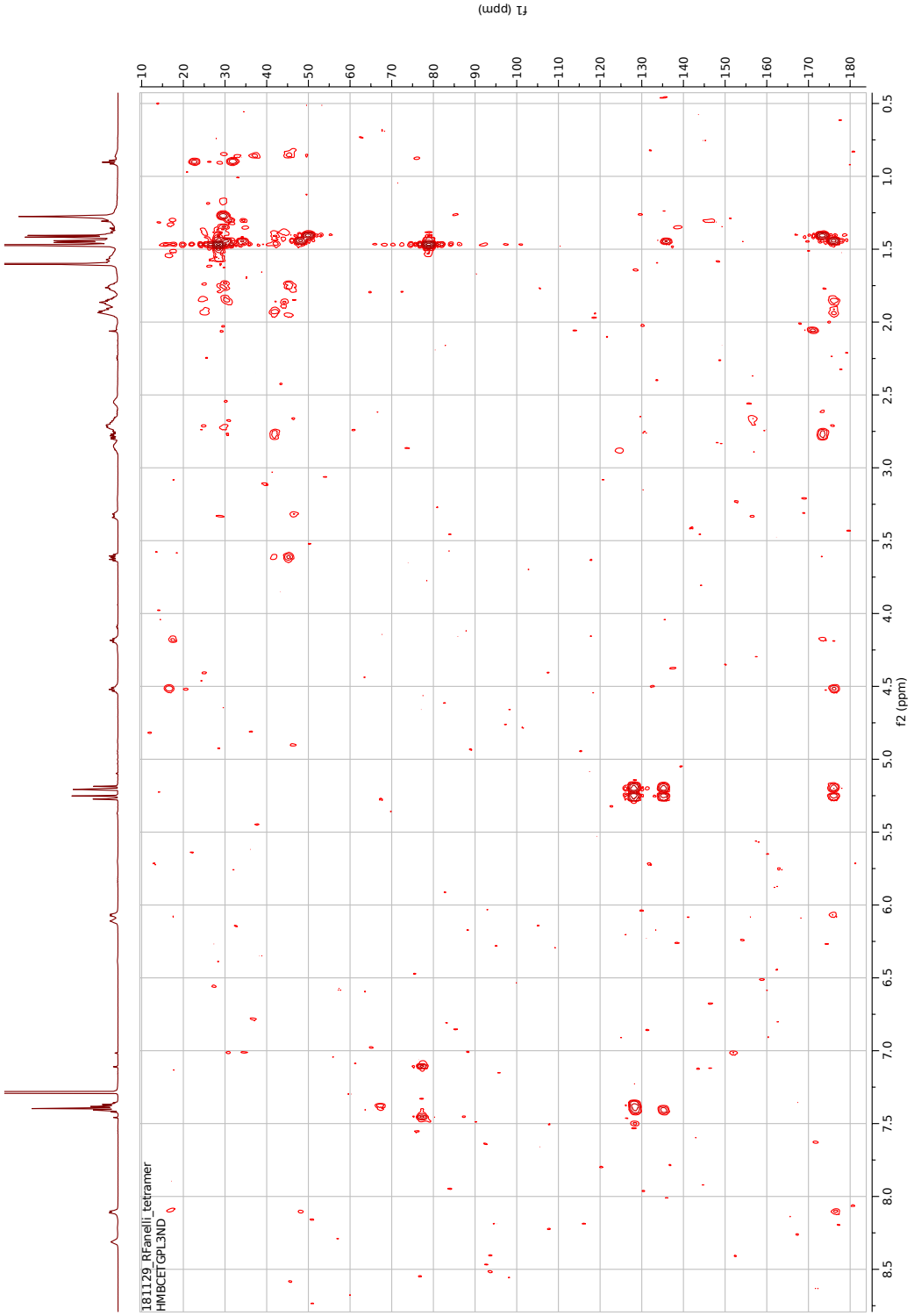

Figure 6.11: HMBC NMR spectrum of tetramer **294** at a concentration of 0.2mM in $CDCl_3$ (600 MHz).

γ/α-peptide Boc(AMCP-L-Ala)$_3$OBn **295**

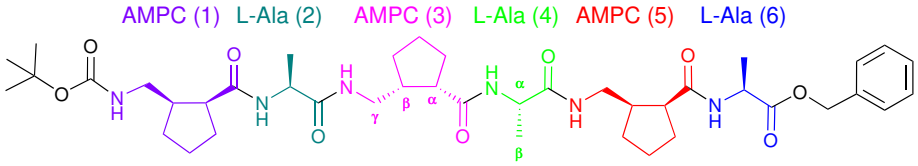

295

To a solution of of **293** (0.036 g, 0.1 mmol) in DMF (1 mL), DIPEA (0.1 mL, 0.6 mmol), HOBt· H_2O (0.018 g, 0.12 mmol), EDCI (0.023 g, 0.12 mmol) were added. The reaction mixture was stirred at rt for 15 minutes and then a solution of the amine deprotected **294** (0.054 g, 0.1 mmol) in DMF (1 mL) was added. The reaction mixture was sealed with a septum and it was left stirring at rt for 24 hours. Ethyl acetate (10 mL) was then added and the organic phase was washed with a 1M aqueous solution of $NaHSO_4$ (2 x 5 mL), a saturated aqueous solution of $NaHCO_3$ (2 x 5 mL) and then brine (2 x 5 mL). Acid and basic aqueous layers were then extracted twice with CH_2Cl_2. All organic layers were combined, dried over Na_2SO_4, filtered and concentrate *in vacuo*. The crude product was then purified by flash chromatography on silica gel (gradient hexane/ethyl acetate/methanol) to obtain the title product **295** as a white solid (0.016 g, 0.02 mmol, 20%).

$[\alpha]^{20}{}_D$ +106.0 (c = 0.05, CH_2Cl_2); IR (neat, cm^{-1}) 3288, 2927, 1739, 1701, 1635, 1529, 1449, 1366, 1247, 1225, 1169; HRMS required for $C_{42}H_{65}N_6O_9$ $[M+H]^+$ is 797.4813, found 797.4832. ^{1}H NMR (600 MHz, $CDCl_3$) δ 8.90 (1 H, s), 8.64 (1 H, d, *J* 6.8), 8.60 – 8.40 (2 H, m), 7.50 – 7.33 (5 H, m), 6.38 (1 H, s), 6.01 (1 H, d, *J* 6.2), 5.27 (1H, d, *J* = 12.3 Hz), 5.19 (1H, d, *J* = 12.3 Hz), 4.48 (1 H, p, *J* 7.3), 4.29 (1 H, q, *J* 6.7), 4.03 (1 H, p, *J* 6.8), 3.66 - 3,54 (2 H, m), 3.45 – 3.31 (1 H, m), 3.04 - 2.89 (2 H, m), 2.88 – 2.77 (2 H, m), 2.77 - 2.68 (2 H, m), 2.68 – 2.55 (2 H, m), 2.54 – 2.42 (1 H, m), 2.02 - 1.92 (2 H, m), 1.94 - 1.83 (4 H, m), 1.83 – 1.70 (3 H, m), 1.48 (10 H, s), 1.46 – 1.43 (5 H, m), 1.41 (3 H, d, *J* 7.5), 1.39 (3 H, d, *J* 7.1).

^{13}C NMR (101 MHz, $CDCl_3$) δ 176.9, 176.7, 176.3, 176.0, 175.4, 173.5, 156.6, 139.3, 135.2, 128.6, 128.4, 128.1, 124.8, 114.1, 78.7, 67.4, 53.4, 50.7, 50.3, 48.3, 46.3, 45.1, 44.8, 44.4, 42.5, 42.3, 41.8, 41.7, 36.5, 34.3, 33.8, 31.9, 31.0, 30.9, 30.3, 30.2, 30.1, 29.7, 29.5, 29.4, 29.2, 29.0, 28.5, 25.7, 25.7, 24.7, 22.7, 17.6, 16.9, 16.6, 14.1.

Table 6.6: ^{1}H NMR assignment for the γ/α-peptide **295**.

Residue	Hα [ppm]	Hβ [ppm]	Hγ1 [ppm]	Hγ2 [ppm]	NH [ppm]	CH2 [ppm]	H-Ar [ppm]
L-Ala(2)	4.287	1.438	-	-	6.005	-	-
AMCP(5)	2.821	2.952	3.611	2.8	8.513	-	
L-Ala(4)	4.033	1.387	-	-	8.537	-	-
AMCP(3)	2.739	2.954	3.6	2.483	8.901	-	-
L-Ala(6)	4.483	1.412	-	-	8.642	-	-
AMCP(1)	2.726	2.6	3.377	2.614	6.377	-	-
Benzyl	-	-	-	-	-	5.236	7.33 - 7.44

Table 6.7: ^{13}C NMR assignment for the γ/α-peptide **295**.

Residue	Cα [ppm]	Cβ [ppm]	Cγ [ppm]	CH2 [ppm]	HAr [ppm]	CO [ppm]
L-Ala(2)	50.33	17.65	-	-	-	173.38
AMCP(5)	45.1	41.77	42.45	-	-	176.72
L-Ala(4)	50.71	16.98	-	-	-	175.51
AMCP(3)	44.71	41.77	42.33	-	-	176.9
L-Ala(6)	48.32	16.64	-	-	-	176.38
AMCP(1)	46.26	44.42	42	-	-	176.03
Benzyl	-	-	-	67.41	135.22, 128.6, 128.4, 128.1	-

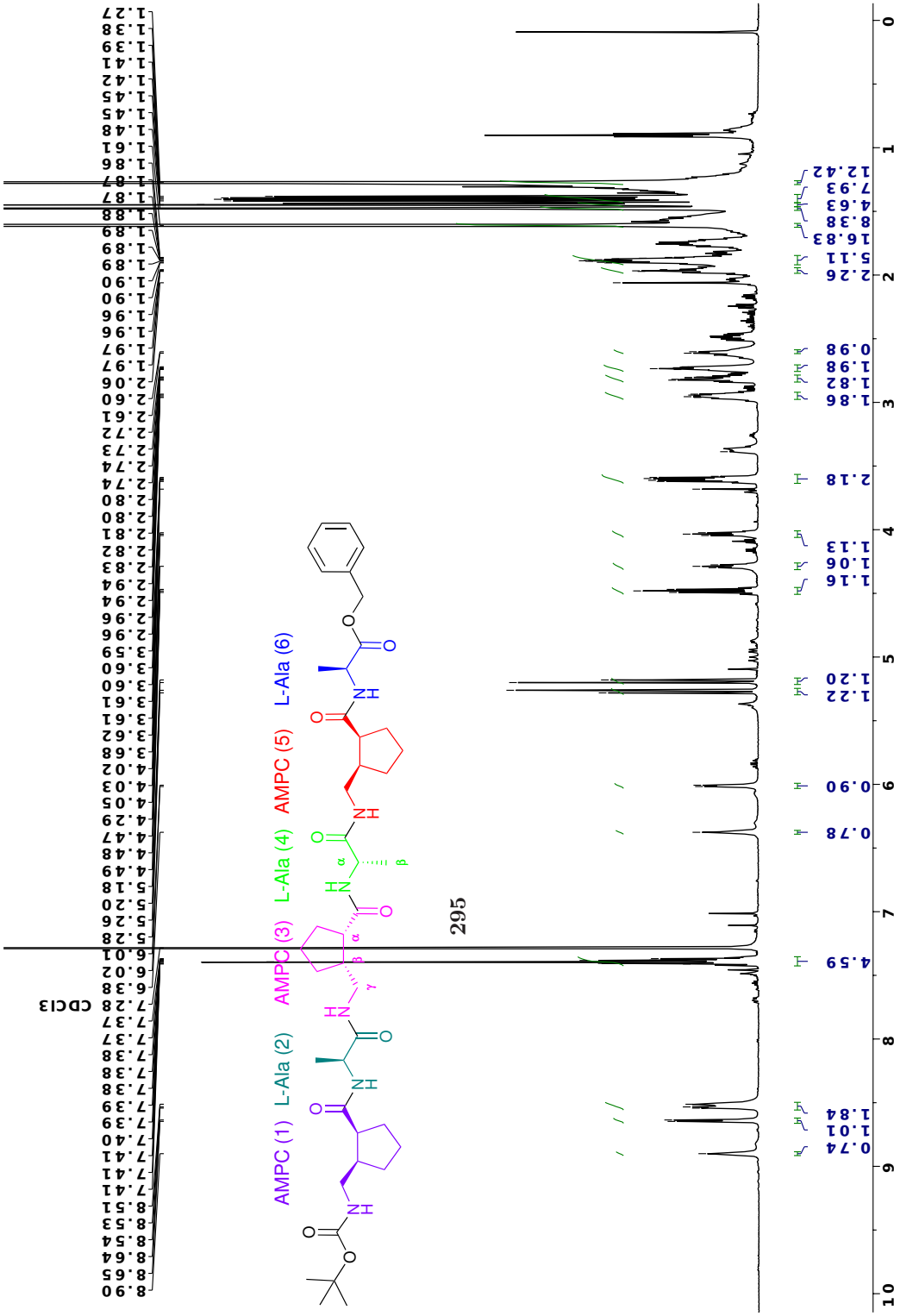
AMPC (1)
L-Ala (2)
AMPC (3)
L-Ala (4)
AMPC (5)
L-Ala (6)
295
CDCl3

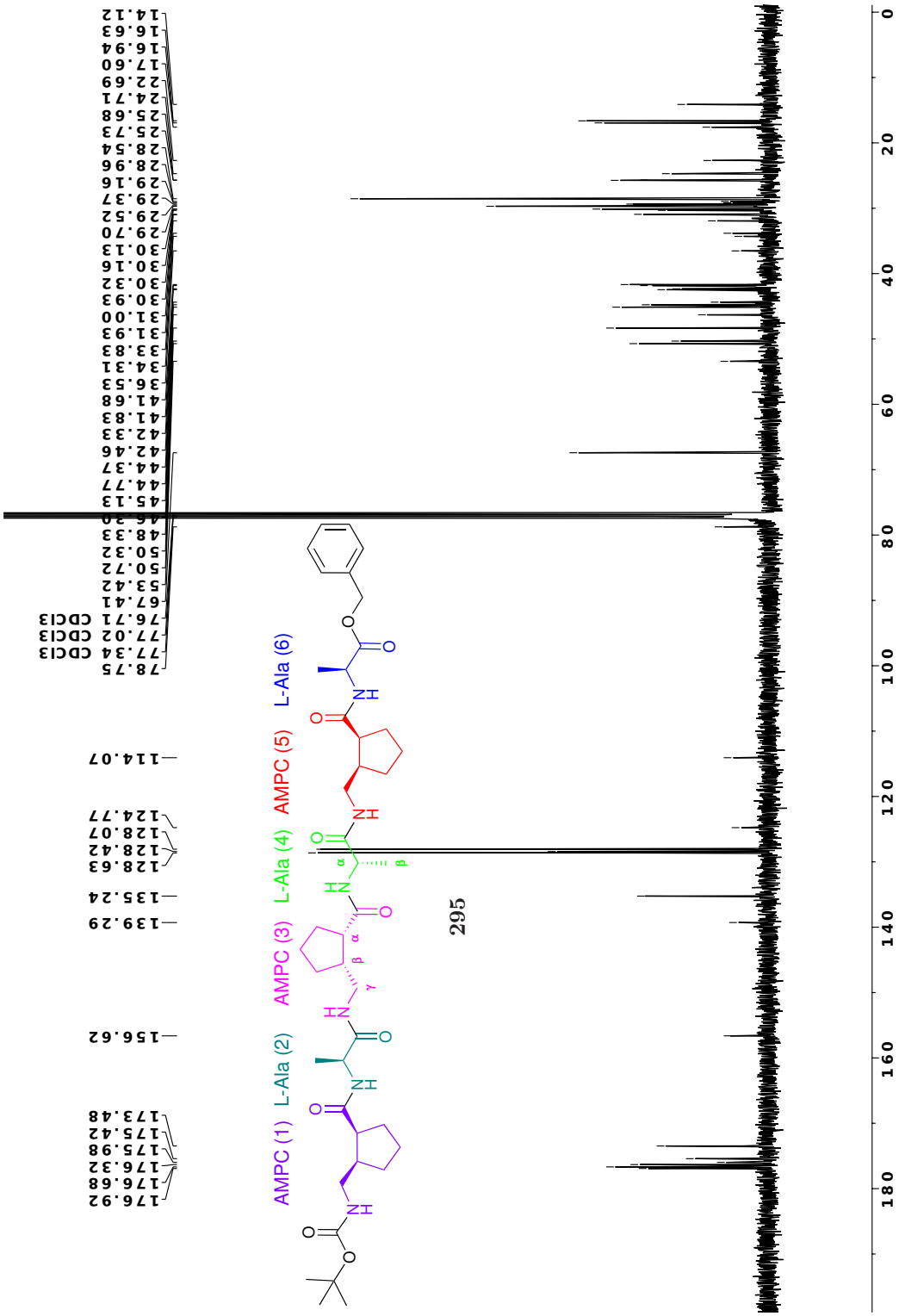
AMPC (1)
L-Ala (2)
AMPC (3)
L-Ala (4)
AMPC (5)
L-Ala (6)
295
CDCl3
CDCl3
CDCl3

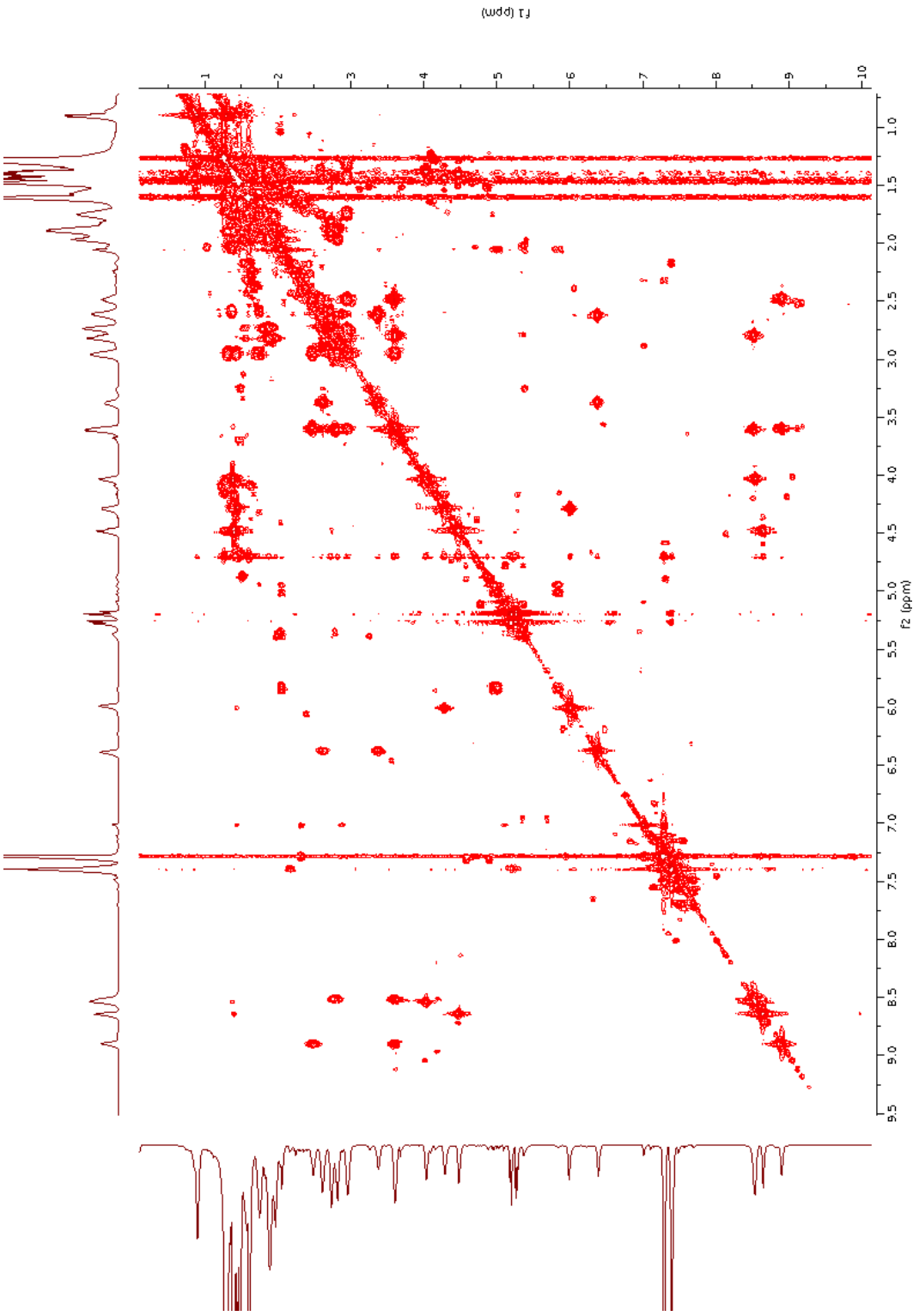

Figure 6.12: COSY NMR spectrum of hexamer **295** at a concentration of 0.2mM in $CDCl_3$ (600 MHz).

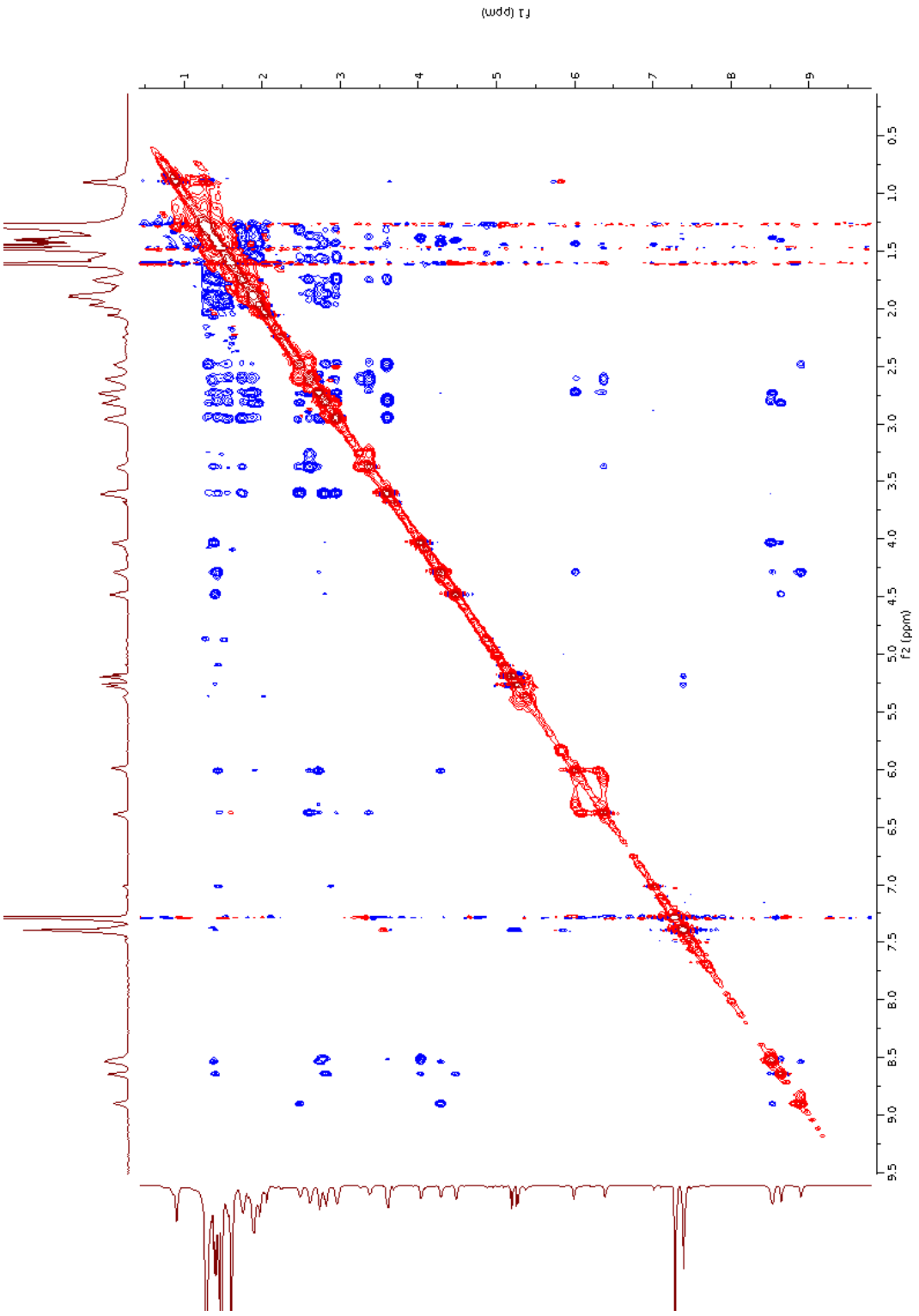

Figure 6.13: ROESY NMR spectrum of hexamer **295** at a concentration of 0.2mM in $CDCl_3$ (600 MHz).

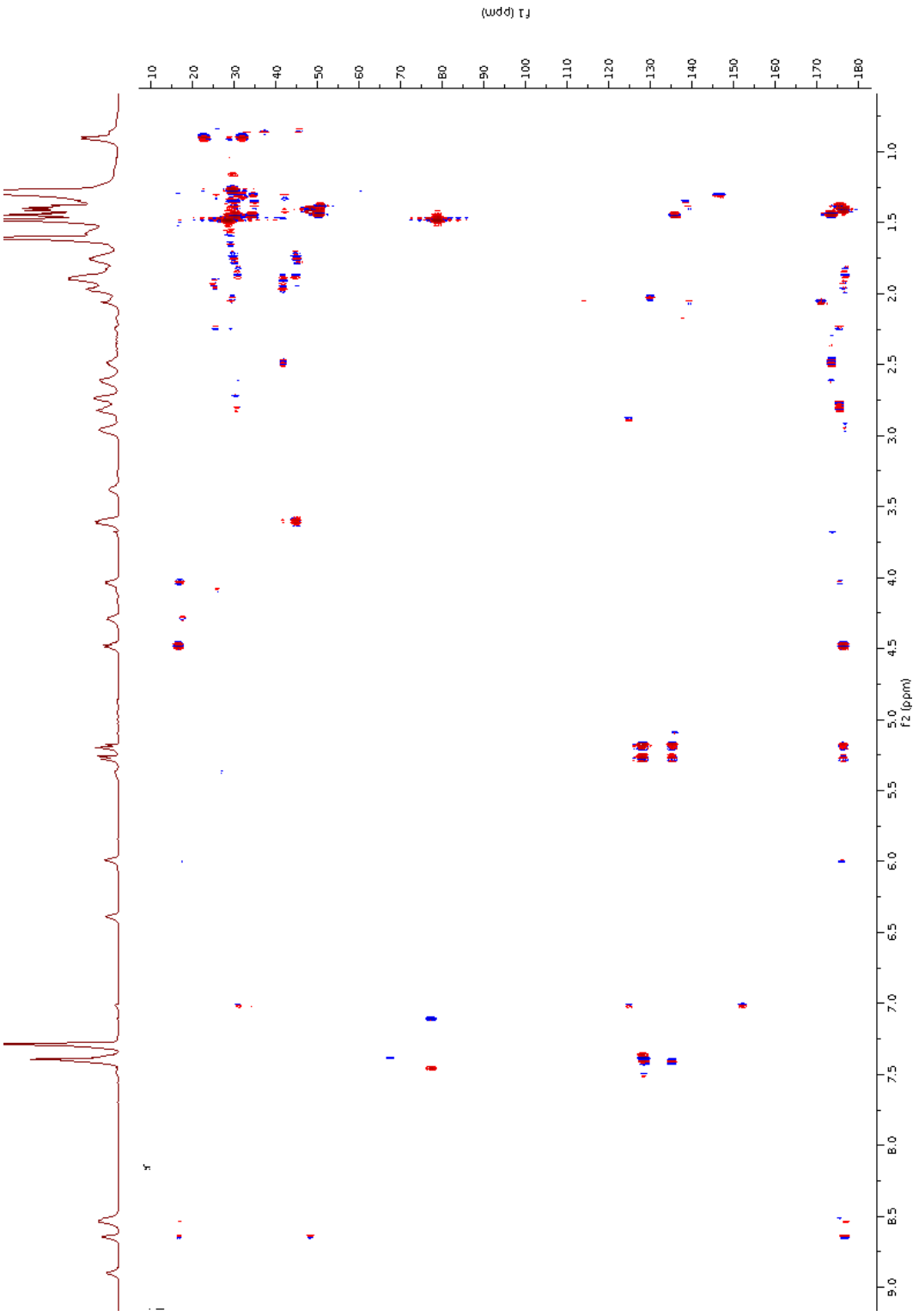

Figure 6.14: HMBC NMR spectrum of hexamer **295** at a concentration of 0.2mM in $CDCl_3$ (600 MHz).

6.17 Computations

6.17.1 Foldamer Conformers

The identified 55 conformers have been processed with DFT as detailed above, apart from the electronic energy calculations with larger basis set. Apart from conformer 23 and 27, all have been optimised to a local minimum according to the vibrational frequencies.

Table 6.8: DFT data for the foldamer conformers, energies shown in hartree, relative free energies (ΔG) are in kcal/mol.

conf	E	G_{therm}	G_{CDCl_3}	ΔG	$Pop\%$
2	-2644.68699609	-2643.728544	-2644.73530155	0.0	40.4
1	-2644.69218238	-2643.731061	-2644.73791821	0.0	38.3
3	-2644.69273043	-2643.726661	-2644.74126282	1.0	7.5
13	-2644.69179647	-2643.727440	-2644.73921455	1.2	5.3
15	-2644.68722408	-2643.725307	-2644.73569671	1.9	1.8
6	-2644.68830318	-2643.723753	-2644.73826996	2.0	1.7
4	-2644.69067077	-2643.726560	-2644.73765846	2.1	1.4
36	-2644.68999239	-2643.728052	-2644.73515110	2.3	1.0
7c	-2644.68664102	-2643.726629	-2644.73320216	2.3	1.0
21	-2644.68281779	-2643.723289	-2644.73226715	2.6	0.6
5	-2644.68624683	-2643.723673	-2644.73469509	3.0	0.3
48c	-2644.68554976	-2643.725689	-2644.73185672	3.0	0.3
19	-2644.68489999	-2643.724086	-2644.73242209	3.3	0.2
9	-2644.68641137	-2643.723480	-2644.73370708	3.8	0.1
29	-2644.68556255	-2643.723266	-2644.73281774	4.0	0.1
17	-2644.68664154	-2643.722931	-2644.73372975	4.3	0.0
12	-2644.68599286	-2643.724920	-2644.73098164	4.4	0.0
42	-2644.68342883	-2643.720420	-2644.73258366	4.6	0.0
8	-2644.68747109	-2643.721151	-2644.73589490	4.6	0.0
18	-2644.68213438	-2643.719856	-2644.73092248	5.1	0.0
44	-2644.68197103	-2643.716164	-2644.73423200	5.3	0.0
30	-2644.68058863	-2643.717996	-2644.73095954	5.3	0.0
16	-2644.68318582	-2643.720860	-2644.73042529	5.5	0.0
11	-2644.68317107	-2643.717081	-2644.73394925	5.6	0.0
23	-2644.68047735	-2643.719414	-2644.72891948	5.6	0.0
49	-2644.67786248	-2643.714263	-2644.73106703	5.9	0.0
33c	-2644.68181786	-2643.720704	-2644.72821781	6.1	0.0
10	-2644.68840009	-2643.721717	-2644.73344859	6.3	0.0
14	-2644.6871915	-2643.721810	-2644.73188780	6.5	0.0
55	-2644.67456623	-2643.714100	-2644.72646804	6.8	0.0
38	-2644.67866302	-2643.716416	-2644.72806146	6.9	0.0
45	-2644.68465842	-2643.720296	-2644.73015004	6.9	0.0
39	-2644.67931606	-2643.718411	-2644.72658773	7.0	0.0
34	-2644.67954929	-2643.716430	-2644.72874308	7.0	0.0
51	-2644.68007288	-2643.716644	-2644.72876918	7.2	0.0
41	-2644.67989286	-2643.715497	-2644.72957564	7.3	0.0
47	-2644.66677457	-2643.708734	-2644.72214856	8.0	0.0
20	-2644.68387582	-2643.715650	-2644.73180148	8.3	0.0
22c	-2644.68603818	-2643.719605	-2644.72995857	8.4	0.0
25	-2644.68093092	-2643.717417	-2644.72703656	8.4	0.0
31	-2644.6822678	-2643.717565	-2644.72820256	8.4	0.0

53	-2644.66985637	-2643.709825	-2644.72308257	8.7	0.0
26	-2644.6848354	-2643.718215	-2644.72934691	8.9	0.0
35c	-2644.67599832	-2643.715935	-2644.72274123	8.9	0.0
54	-2644.67203954	-2643.711219	-2644.72328760	9.0	0.0
40	-2644.6704656	-2643.711772	-2644.72102136	9.1	0.0
27	-2644.67571738	-2643.711273	-2644.72530966	10.0	0.0
37	-2644.67493904	-2643.710936	-2644.72473439	10.1	0.0
24	-2644.67310522	-2643.708253	-2644.72551838	10.2	0.0
43	-2644.67452023	-2643.711053	-2644.72389976	10.3	0.0
28	-2644.67252849	-2643.709870	-2644.72160322	11.2	0.0
46	-2644.66888856	-2643.706041	-2644.72114960	11.6	0.0
32	-2644.67932466	-2643.713084	-2644.72421571	11.8	0.0
50	-2644.67477119	-2643.709797	-2644.72271710	12.0	0.0
52	-2644.66830324	-2643.703964	-2644.71972771	13.5	0.0

In order to show that the computational ensemble conforms the NMR data, the distances originally obtained from the NOESY data are plotted against the original constrains. Note that while in the original Monte-Carlo conformational search, these constrains were in place, but there were not during DFT optimization.

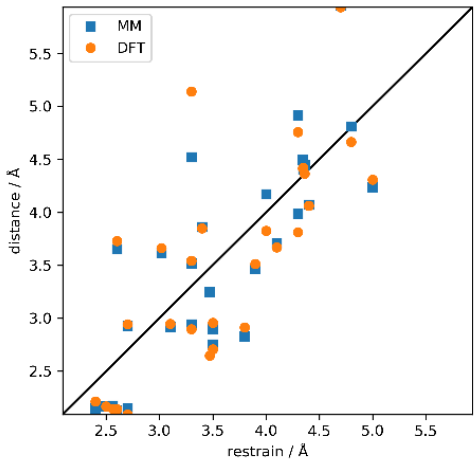

Figure 6.15: Distances for conformer 2.

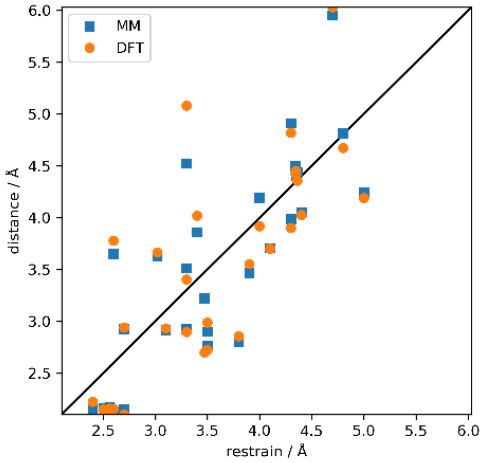

Figure 6.16: Distances for conformer 1.

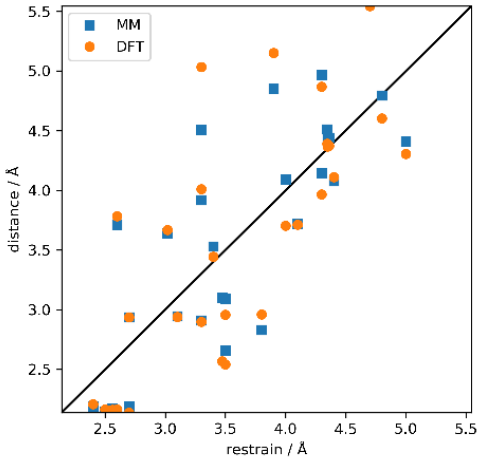

Figure 6.17: Distances for conformer 3.

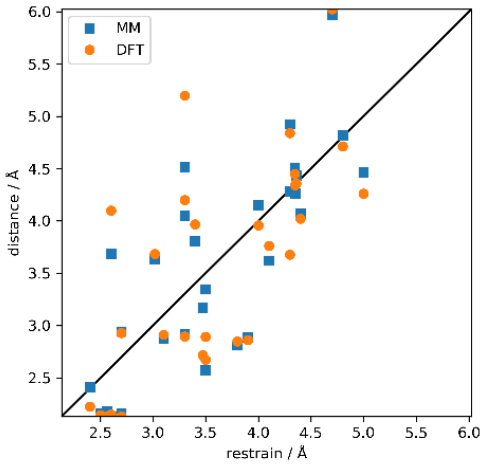

Figure 6.18: Distances for conformer 13.

Table 6.9: Weighted average dihedral angles for the 9 lowest energy foldamer conformers of **295**.

conf:	**conf1**	**conf1 x pop.**	**conf2**	**conf2 x pop.**	**conf3**	**conf3 x pop.**	**conf4**	**conf4 x pop.**
Residue 1								
phi	44	16.97	69	28.04	-139	-10.48	133	1.88
theta	38	14.75	52	21.03	-63	-4.70	54	0.77
zeta	46	17.58	41	16.58	-17	-1.29	36	0.50
psi	-108	-41.57	-100	-40.83	-108	-8.12	-142	-2.00
Residue 2		0.00		0.00		0.00		0.00
phi	-68	-26.03	-76	-30.73	-83	-6.25	-78	-1.09
psi	134	51.72	130	52.73	131	9.87	154	2.17
Residue 3		0.00		0.00		0.00		0.00
phi	61	23.46	64	26.16	57	4.26	55	0.78
theta	44	17.10	45	18.26	45	3.41	36	0.50
zeta	42	16.22	42	17.07	45	3.40	42	0.59
psi	-120	-46.24	-121	-49.24	-112	-8.41	-129	-1.82
Residue 4		0.00		0.00		0.00		0.00
phi	-72	-27.76	-75	-30.31	-81	-6.11	-68	-0.96
psi	142	54.60	145	58.80	144	10.85	144	2.03
Residue 5		0.00		0.00		0.00		0.00
phi	59	22.90	60	24.53	58	4.38	58	0.82
theta	48	18.53	45	18.44	46	3.45	47	0.67
zeta	29	11.09	28	11.54	30	2.24	29	0.42
psi	-118	-45.61	-124	-50.25	-124	-9.30	-118	-1.67
Residue 6		0.00		0.00		0.00		0.00
phi	-65	-24.86	-65	-26.28	-65	-4.88	-64	-0.91
psi*	133	51.33	152	61.93	134	10.07	133	1.87
Population	38.52%		40.64%		7.52%		1.41%	

Table 6.10: Weighted average dihedral angles for the 9 lowest energy foldamer conformers of **295**.

conf:	**conf6**	**conf6 x pop.**	**conf7c**	**conf7c x pop.**	**conf13**	**conf13 x pop.**	**conf15**	**conf15 x pop.**
Residue 1								
phi	-138	-2.32	44	0.43	-98	-5.23	-122	-2.17
theta	-62	-1.05	35	0.34	-88	-4.70	-60	-1.08
zeta	-18	-0.30	46	0.45	51	2.71	-25	-0.45
psi	-108	-1.81	-110	-1.08	-100	-5.34	-95	-1.69
Residue 2		0.00		0.00		0.00		0.00
phi	-82	-1.38	-65	-0.64	-76	-4.04	-77	-1.37
psi	131	2.20	142	1.39	145	7.77	149	2.66
Residue 3		0.00		0.00		0.00		0.00
phi	56	0.94	59	0.57	61	3.28	57	1.02
theta	46	0.77	41	0.40	36	1.93	37	0.67
zeta	46	0.77	42	0.41	43	2.29	42	0.75
psi	-110	-1.84	-122	-1.20	-127	-6.81	-128	-2.27
Residue 4		0.00		0.00		0.00		0.00
phi	-84	-1.42	-71	-0.70	-69	-3.67	-70	-1.25
psi	143	2.41	143	1.41	143	7.65	145	2.58
Residue 5		0.00		0.00		0.00		0.00
phi	60	1.01	59	0.58	58	3.13	58	1.03
theta	45	0.75	47	0.46	48	2.55	47	0.84
zeta	30	0.50	29	0.28	29	1.57	29	0.52
psi	-128	-2.15	-120	-1.17	-118	-6.31	-118	-2.11
Residue 6		0.00		0.00		0.00		0.00
phi	-66	-1.11	-60	-0.59	-64	-3.45	-64	-1.14
psi*	154	2.58	131	1.28	133	7.11	133	2.37
Population	1.68%		0.98%		5.35%		1.78%	

Table 6.11: Weighted average dihedral angles for the 9 lowest energy foldamer conformers of **295**.

conf:	**conf36**	**conf36 x pop.**	**weighted average**
Residue 1			
phi	-115	-1.15	**25.96**
theta	62	0.62	**9.65**
zeta	-53	-0.53	**35.25**
psi	-60	-0.60	**-103.04**
Residue 2		0.00	
phi	-128	-1.28	**-72.81**
psi	-179	-1.79	**128.71**
Residue 3		0.00	
phi	64	0.64	**61.11**
theta	46	0.46	**43.49**
zeta	38	0.38	**41.88**
psi	-119	-1.19	**-119.01**
Residue 4		0.00	
phi	-67	-0.67	**-72.83**
psi	142	1.42	**141.74**
Residue 5		0.00	**0.00**
phi	59	0.59	**58.97**
theta	48	0.48	**46.17**
zeta	29	0.29	**28.44**
psi	-117	-1.17	**-119.73**
Residue 6		0.00	**0.00**
phi	-65	-0.65	**-63.87**
psi*	132	1.32	**139.87**
Population	1.00%		

Bibliography

[1] S. W. Smith, *Toxicol. Sci.*, 2009, **110**, 4–30.

[2] G. Rothenberg, *Catalysis: Concepts and Green Applications*, Wiley-VCH, 2008.

[3] B. M. Trost, *Proc. Natl. Acad. Sci. U. S. A.*, 2004, **101**, 5348–5355.

[4] B. J. A Osborn, F. H. Jardine, J. F. Young, G. Wilkinson, R. D. Gillard, J. A. Osborn and P. B. Stockwell, *J. Chem. Soc. A*, 1966, 1711–1732.

[5] P. I. Dalko and L. Moisan, *Angew. Chem., Int. Ed.*, 2004, **43**, 5138–5175.

[6] P. R. Schreiner, *Chem. Soc. Rev.*, 2003, **32**, 289–296.

[7] Z. G. Parrish and D. R. Hajos, *DE 2102623*, 1971.

[8] Z. G. Hajos and D. R. Parrish, *J. Org. Chem.*, 1974, **39**, 1615–1621.

[9] U. Eder, G. Sauer and R. Weichert, *Angew. Chem., Int. Ed.*, 496–497, title = TOTAL Synthesis OF OPTICALLY ACTIVE STEROIDS .6. NEW TYPE OF ASYMMETRIC CYCLIZATION TO OPTICALLY ACTIVE STEROID CD PARTIAL STRUCTURES, volume = 10, year = 1971.

[10] F. R. Clemente and K. N. Houk, *Angew. Chem., Int. Ed. Engl.*, 2004, **43**, 5765–5768.

[11] B. List, L. Hoang and H. J. Martin, *Proc. Natl. Acad. Sci. U. S. A.*, 2004, **101**, 5839–5842.

[12] S. Mukherjee, J. W. Yang, S. Hoffmann and B. List, *Chem. Rev.* , 2007, **107**, 5471–5569.

[13] J. Seayad and B. List, *Org. Biomol. Chem.*, 2005, **3**, 719–724.

[14] B. List, *Synlett*, 2001, 1675–1686.

[15] B. List, *Acc. Chem. Res.*, 2004, **37**, 548–557.

[16] C. Allemann, R. Gordillo, F. R. Clemente, P. H. Y. Cheong and K. N. Houk, *Acc. Chem. Res.*, 2004, **37**, 558–569.

[17] S. Bahmanyar and K. N. Houk, *J. Am. Chem. Soc.*, 2001, **123**, 12911–12912.

[18] S. Bahmanyar and K. N. Houk, *Org. Lett.*, 2003, **5**, 1249–1251.

[19] P. H. Y. Cheong and K. N. Houk, *J. Am. Chem. Soc.*, 2004, **126**, 13912–13913.

[20] A. Hartikka and P. I. Arvidsson, *Tetrahedron: Asymmetry*, 2004, **15**, 1831–1834.

[21] H. Torii, M. Nakadai, K. Ishihara, S. Saito and H. Yamamoto, *Angew. Chem., Int. Ed.*, 2004, **43**, 1983–1986.

[22] A. J. Cobb, D. M. Shaw and S. V. Ley, *Synlett*, 2004, 558–560.

[23] S. Bahmanyar and K. N. Houk, *J. Am. Chem. Soc.*, 2001, **123**, 11273–11283.

[24] L. Hoang, S. Bahmanyar, K. N. Houk and B. List, *J. Am. Chem. Soc.*, 2003, **125**, 16–17.

[25] A. Hartikka and P. I. Arvidsson, *Eur. J. Org. Chem.*, 2005, 4287–4295.

[26] S. P. Mathew, H. Iwamura and D. G. Blackmond, *Angew. Chem., Int. Ed.*, 2004, **43**, 3317–3321.

[27] H. Iwamura, D. H. Wells, S. P. Mathew, M. Klussmann, A. Armstrong and D. G. Blackmond, *J. Am. Chem. Soc.*, 2004, **126**, 16312–16313.

[28] H. Iwamura, S. P. Mathew and D. G. Blackmond, *J. Am. Chem. Soc.*, 2004, **126**, 11770–11771.

[29] A. J. A. Cobb, D. M. Shaw, D. A. Longbottom, J. B. Gold and S. V. Ley, *Org. Biomol. Chem.*, 2005, **3**, 84–96.

[30] J. Franzen, M. Marigo, D. Fielenbach, T. C. Wabnitz, A. Kjaersgaard and K. A. Jorgensen, *J. Am. Chem. Soc.*, 2005, **127**, 18296–18304.

[31] G. Zuo, Q. H. Zhang and J. X. Xu, *Heteroat. Chem.*, 2003, **14**, 42–45.

[32] Y. Hayashi, H. Gotoh, T. Hayashi and M. Shoji, *Angew. Chem., Int. Ed.*, 2005, **44**, 4212–4215.

[33] D. Seebach and J. Golinski, *Helv. Chim. Acta*, 1981, **64**, 1413–1423.

[34] K. Patora-Komisarska, M. Benohoud, H. Ishikawa, D. Seebach and Y. Hayashi, *Helv. Chim. Acta*, 2011, **94**, 719–745.

[35] J. Burés, A. Armstrong and D. G. Blackmond, *J. Am. Chem. Soc.*, 2012, **134**, 6741–6750.

[36] J. Burés, A. Armstrong and D. G. Blackmond, *J. Am. Chem. Soc.*, 2012, **134**, 14264.

[37] G. Sahoo, H. Rahaman, Á. Madarász, I. Pápai, M. Melarto, A. Valkonen and P. M. Pihko, *Angew. Chem., Int. Ed.*, 2012, **51**, 13144–13148.

[38] J. Duschmalé, J. Wiest, M. Wiesner and H. Wennemers, *Chem. Sci.*, 2013, **4**, 1312–1318.

[39] F. Bächle, J. Duschmalé, C. Ebner, A. Pfaltz and H. Wennemers, *Angew. Chem., Int. Ed.*, 2013, **52**, 12619–12623.

[40] T. Földes, A. Madaraz, A. Revesz, Z. Dobi, S. Varga, A. Hamza, P. Nagy, P. M. Pihko and I. Papai, *J. Am. Chem. Soc*, 2017, **139**, 17052–17063.

[41] K. A. Ahrendt, C. J. Borths, D. W. C MacMillan and D. W. C. MacMillan, *J. Am. Chem. Soc.*, 2000, **122**, 4243–4244.

[42] N. A. Paras and D. W. C. MacMillan, *J. Am. Chem. Soc.*, 2002, **124**, 7894–7895.

[43] J. N. Brönsted, *Recl. Trav. Chim. Pays-Bas*, 1923, **42**, 718–728.

[44] T. M. Lowry, *J. Soc. Chem. Ind.*, 1923, **42**, 43–47.

[45] W. B. Jensen, *J. Adhes. Sci. Technol.*, 1991, **5**, 1–21.

[46] J. M. Friedel, C., Crafts, *C. R. Acad. Sci.*, 1884, 449–532.

[47] A. Wassermann, *J. Chem. Soc.*, 1942, 618–621.

[48] S. J. Connon, *Chem. - Eur. J.*, 2006, **12**, 5418–5427.

[49] Z. G. Zhang and P. R. Schreiner, *Chem. Soc. Rev.*, 2009, **38**, 1187–1198.

[50] M. C. Etter, Z. Urbanczyklipkowska, M. Ziaebrahimi and T. W. Panunto, *J. Am. Chem. Soc.*, 1990, **112**, 8415–8426.

[51] M. C. Etter, *Acc. Chem. Res.*, 1990, **23**, 120–126.

[52] D. P. Curran and L. H. Kuo, *J. Org. Chem.*, 1994, **59**, 3259–3261.

[53] D. P. Curran and L. H. Kuo, *Tetrahedron Lett.*, 1995, **36**, 6647–6650.

[54] M. S. Sigman and E. N. Jacobsen, *J. Am. Chem. Soc.*, 1998, **120**, 4901–4902.

[55] P. Vachal and E. N. Jacobsen, *J. Am. Chem. Soc.*, 2002, **124**, 10012–10014.

[56] T. Akiyama, J. Itoh and K. Fuchibe, *Adv. Synth. Catal.*, 2006, **348**, 999–1010.

[57] T. Okino, S. Nakamura, T. Furukawa and Y. Takemoto, *Org. Lett.*, 2004, **6**, 625–627.

[58] L. S. Aitken, N. R. Arezki, A. Dell'Isola and A. J. A. Cobb, *Synthesis-Stuttgart*, 2013, **45**, 2627–2648.

[59] C. M. Starks, *J. Am. Chem. Soc.*, 1971, **93**, 195–199.

[60] A. W. Herriott and D. Picker, *J. Am. Chem. Soc.*, 1975, **97**, 2345–2349.

[61] E. J. Corey, F. Xu and M. C. Noe, *J. Am. Chem. Soc.*, 1997, **119**, 12414–12415.

[62] A. Nelson, *Angew. Chem., Int. Ed.*, 1999, **38**, 1583–1585.

[63] W. Notz, F. Tanaka and C. F. Barbas, *Acc. Chem. Res.*, 2004, **37**, 580–591.

[64] E. Gomez-Bengoa, A. Linden, R. Lopez, I. Mugica-Mendiola, M. Oiarbide and C. Palomo, *J. Am. Chem. Soc.*, 2008, **130**, 7955–7966.

[65] W. J. Nodes, D. R. Nutt, A. M. Chippindale and A. J. A. Cobb, *J. Am. Chem. Soc.*, 2009, **131**, 16016–16017.

[66] H. Chen, D. Zhang, F. Xue and Y. Qin, *Tetrahedron*, 2013, **69**, 3141–3148.

[67] A. Giannis and T. Kolter, *Angew. Chem., Int. Ed. Engl.*, 1993, **32**, 1244–1267.

[68] L. P. Graham, *An Introduction to Medicinal Chemistry*, Oxford University Press, 2013.

[69] M. Heim, L. Römer and T. Scheibel, *Chem. Soc. Rev.*, 2010, **39**, 156–164.

[70] D. Voet and J. G. Voet, *Biochemistry*, John Wiley & Sons, Ltd, 1990, p. 1223.

[71] A. Trabocchi and A. Guarna, *Peptidomimetics in Organic and Medicinal Chemistry: The Art of Transforming Peptides in Drugs*, Wiley, 2014.

[72] V. Santagada and G. Caliendo, *Peptidi e peptidomimetici*, Piccin, 2003.

[73] S. H. Gellman, *Acc. Chem. Res.*, 1998, **31**, 173–180.

[74] D. J. Hill, M. J. Mio, R. B. Prince, T. S. Hughes and J. S. Moore, *Chem. Rev.* , 2001, **101**, 3893–4011.

[75] S. Hecht, I. Huc, S. H. Huc and Ivan, *Foldamers*, WILEY-VCH, 2007, pp. 229–265.

[76] G. N. Tew, R. W. Scott, M. L. Klein and W. F. Degrado, *Acc. Chem. Res.*, 2010, **43**, 30–39.

[77] A. Tanatani, T. S. Hughes and J. S. Moore, *Angew. Chem., Int. Ed.*, 2002, **41**, 325.

[78] J. L. Hou, X. B. Shao, G. J. Chen, Y. X. Zhou, X. K. Jiang and Z. T. Li, *J. Am. Chem. Soc.*, 2004, **126**, 12386–12394.

[79] M. Inouye, M. Waki and H. Abe, *J. Am. Chem. Soc.*, 2004, **126**, 2022–2027.

[80] A. M. Ramos, S. C. Meskers, E. H. Beckers, R. B. Prince, L. Brunsveld and R. A. Janssen, *J. Am. Chem. Soc.*, 2004, **126**, 9630–9644.

[81] T. A. Zeidan, Q. Wang, T. Fiebig and F. D. Lewis, *J. Am. Chem. Soc.*, 2007, **129**, 9848–9849.

[82] W. Cai, G. T. Wang, Y. X. Xu, X. K. Jiang and Z. T. Li, *J. Am. Chem. Soc.*, 2008, **130**, 6936–6937.

[83] M. Wolffs, N. Delsuc, D. Veldman, N. V. Anh, R. M. Williams, S. C. J. Meskers, R. A. Janssen, I. Huc and A. P. H. J. Schenning, *J. Am. Chem. Soc.*, 2009, **131**, 4819–4829.

[84] B. Gole, B. Kauffmann, V. Maurizot, I. Huc and Y. Ferrand, *Angew. Chem., Int. Ed.*, 2019, **131**, 8147–8151.

[85] M. M. Müller, M. A. Windsor, W. C. Pomerantz, S. H. Gellman and D. Hilvert, *Angew. Chem., Int. Ed.*, 2009, **48**, 922–925.

[86] J. Aguesseau-Kondrotas, M. Simon, B. Legrand, J. Bantigniés, Y. K. Kang, D. Dumitrescu, A. Van der Lee, J. J.-M. Campagne, R. M. de Figueiredo and L. T. Maillard, *Chem. - Eur. J.*, 2019, **25**, 7396–7401.

[87] T. A. Martinek, A. Hetényi, L. Fülöp, I. M. Mándity, G. K. Tóth, I. Dékány and F. Fülöp, *Angew. Chem., Int. Ed.*, 2006, **45**, 2396–2400.

[88] G. Guichard and I. Huc, *Chem. Commun.*, 2011, **47**, 5933–5941.

[89] S. Hanessian, X. Luo and R. Schaum, *Tetrahedron Lett.*, 1999, **40**, 4925–4929.

[90] S. Hanessian, X. Luo, R. Schaum and S. Michnick, *J. Am. Chem. Soc.*, 1998, **120**, 8569–8570.

[91] D. Seebach, M. Brenner, M. Rueping, B. Schweizer and B. Jaun, *Chem. Commun.*, 2000, 207–208.

[92] T. Hintermann, K. Gademann, B. Jaun and D. Seebach, *Helv. Chim. Acta*, 1998, **81**, 983–1002.

[93] C. Baldauf, R. Günther and H.-J. Hofmann, *Helv. Chim. Acta*, 2003, **86**, 2573–2588.

[94] M. Hagihara, N. J. Anthony, T. J. Stout, J. Clardy and S. L. Schreiber, *J. Am. Chem. Soc.*, 1992, **114**, 6568–6570.

[95] P. Coutrot, C. Grison, S. Gen, C. Didierjean and M. Marraud, *Lett. Pept. Sci.*, 1997, **4**, 415–422.

[96] C. Baldauf, R. Gü and H.-J. Hofmann, *J. Org. Chem.*, 2005, **70**, 5351–5361.

[97] L. Mathieu, B. Legrand, C. Deng, L. Vezenkov, E. Wenger, C. Didierjean, M. Amblard, M.-C. Averlant-Petit, N. Masurier, V. Lisowski, J. Martinez and L. T. Maillard, *Angew. Chem.*, 2013, **125**, 6122–6126.

[98] W. S. Horne, *Expert Opin. Drug Discovery*, 2011, **6**, 1247–1262.

[99] K. Ananda, P. G. Vasudev, A. Sengupta, K. Muruga, P. Raja, N. Shamala and P. Balaram, *J. Am. Chem. Soc.*, 2005, **127**, 16668–16674.

[100] C. Baldauf, R. Günther and H.-J. Hofmann, *J. Org. Chem.*, 2006, **71**, 1200–1208.

[101] G. V. M. Sharma, V. B. Jadhav, K. V. S. Ramakrishna, P. Jayaprakash, K. Narsimulu, V. Subash and A. C. Kunwar, *J. Am. Chem. Soc.*, 2006, **128**, 14657–14668.

[102] M. Ganesh Kumar, V. J. Thombare, M. M. Katariya, K. Veeresh, K. Muruga Poopathi Raja and H. N. Gopi, *Angew. Chem., Int. Ed.*, 2016, **55**, 7847–7851.

[103] J. P. Greenstein and J. Wyman, *J. Am. Chem. Soc.*, 1938, **60**, 2341–2347.

[104] T. P. Johnston, G. S. McCaleb, S. D. Clayton, J. L. Frye, C. A. Krauth and J. A. Montgomery, *J. Med. Chem.*, 1977, **20**, 279–290.

[105] R. Allan, G. Johnston and B. Twitchin, *Aust. J. Chem.*, 1981, **34**, 2231–2236.

[106] N. Rodríguez-Vázquez, S. Salzinger, L. F. Silva, M. Amorín and J. R. Granja, *Eur. J. Org. Chem.*, 2013, 3477–3493.

[107] M. Amorín, L. Castedo and J. R. Granja, *J. Am. Chem. Soc.*, 2003, **125**, 2844–2845.

[108] Y. Hu, S.-L. Yu, Y.-J. Yang, J. Zhu and J.-G. Deng, *Chin. J. Chem.*, 2006, **24**, 795–799.

[109] M. Badland, C. A. Bains, R. Howard, D. Laity and S. D. Newman, *Tetrahedron: Asymmetry*, 2010, **21**, 864–866.

[110] S. Karlsson, *Org. Process Res. Dev.*, 2016, **20**, 1336–1340.

[111] R. Sundaram, *PhD thesis*, University of Reading, 2013.

[112] R. Kumar, D. Kumar and A. K. Chakraborti, *Synthesis*, 2007, **2**, 299–303.

[113] P. G. M. Wuts and T. W. T. W. Greene, *Greene's Protective Groups in Organic Synthesis, Fourth Edition*, 2007, p. 1082.

[114] L. H. Wang, B. Prabhudas and D. L. J. Clive, *J. Am. Chem. Soc.*, 2009, **131**, 6003–6012.

[115] N. M. Yoon and Y. S. Gyoung, *J. Org. Chem.*, 1985, **50**, 2443–2450.

[116] J. W. Yang, M. T. Hechavarria Fonseca and B. List, *Angew. Chem., Int. Ed.*, 2004, **43**, 6660–6662.

[117] S. G. Ouellet, J. B. Tuttle and D. W. C MacMillan, *J. Am. Chem. Soc.*, 2005, **127**, 32–33.

[118] C. Zheng and S. L. You, *Chem. Soc. Rev.*, 2012, **41**, 2498–2518.

[119] M. Procházka and L. Lešetický, *Collection of Czechoslovak Chem. Commun.*, 1971, **327**, 307–311.

[120] V. Kral and L. Leseticky, *Collection of Czechoslovak Chem. Commun.*, 1975, **40**, 2816–2825.

[121] L. Lešetický, V. Fidler and M. Procházka, *Collection of Czechoslovak Chem. Commun.*, 1971, **38**, 459–464.

[122] W. Yan, X. Shi and C. Zhong, *Asian J. Org. Chem.*, 2013, **2**, 904–914.

[123] L. Bianchi, F. Ghelfi, G. Giorgi, M. Maccagno, G. Petrillo, D. Spinelli, M. Stenta and C. Tavani, *Eur. J. Org. Chem.*, 2013, **2013**, 6298–6309.

[124] I. R. Baxendale, M. Ernst, W.-R. Krahnert and S. V. Ley, *Synlett*, 2002, **10**, 1641–1644.

[125] D. Enders, C. Wang, J. W. Bats, D. Enders, C. Wang and J. W. Bats, *Angew. Chem., Int. Ed.*, 2008, **47**, 7539–7542.

[126] M. W. Giuliano, S. J. Maynard, A. M. Almeida, A. G. Reidenbach, L. Guo, E. C. Ulrich, I. A. Guzei and S. H. Gellman, *J. Org. Chem.*, 2013, **78**, 12351–12361.

[127] L. Bernardi, M. Fochi, R. Carbone, A. Martinelli, M. E. Fox, C. J. Cobley, B. Kandagatla, S. Oruganti, V. H. Dahanukar and A. Carlone, *Chem. - Eur. J.*, 2015, **21**, 19208–19222.

[128] S. Maity, S. Manna, S. Rana, T. Naveen, A. Mallick and D. Maiti, *J. Am. Chem. Soc.*, 2013, **135**, 3355–3358.

[129] T. He, J.-Y. Qian, H.-L. Song and X.-Y. Wu, *Synlett*, 2009, **19**, 3195–3197.

[130] C.-L. Cao, M.-C. Ye, X.-L. Sun and Y. Tang, *Org. Lett.*, 2006, **8**, 2901–2904.

[131] H. Liang, W. Sun, D. Yang, G. Li and R. Wang, *Chem. Rev.* , 2016, **116**, 4006–4123.

[132] J. Burés, A. Armstrong and D. G. Blackmond, *J. Am. Chem. Soc*, 2011, **133**, 8822–8825.

[133] D. Seebach, X. Sun, M.-O. Ebert, W. B. Schweizer, N. Purkayastha, A. K. Beck, J. Duschmalé, H. Wennemers, T. Mukaiyama, M. Benohoud, Y. Hayashi and M. Reiher, *Helv. Chim. Acta*, 2013, **96**, 799–852.

[134] D. Seebach, X. Sun, C. Sparr, M.-O. Ebert, W. B. Schweizer and A. K. Beck, *Helv. Chim. Acta*, 2012, **95**, 1064–1078.

[135] C. Moberg, *Angew. Chem., Int. Ed.*, 2013, **52**, 2160–2162.

[136] K. L. Jensen, G. Dickmeiss, H. Jiang, Ł. Albrecht, K. Anker Jørgensen, L. Albrecht and K. A. Jorgensen, *Acc. Chem. Res.*, 2012, **45**, 248–264.

[137] K. S. Halskov, B. S. Donslund, B. Matos Paz and K. A. Jørgensen, *Acc. Chem. Res.*, 2016, **49**, 974–986.

[138] A. J. A. Cobb, S. V. Ley, D. A. Longbottom, D. M. Shaw, A. J. André Cobb, R. J. Mutton and S. V. Ley, *Encyclopedia of Reagents for Organic Synthesis*, John Wiley & Sons, Ltd, Chichester, UK, 2016, pp. 1–9.

[139] A. J. A. Cobb, D. A. Longbottom, D. M. Shaw and S. V. Ley, *Chem. Commun.*, 2004, 1808–1809.

[140] P. J. Dyson and P. G. Jessop, *Catal. Sci. Technol.*, 2016, **6**, 3302–3316.

[141] R. Pagni, *J. Chem. Educ.*, 2005, **82**, 382.

[142] R. C. Sovish and W. Boettcher, *J. Polym. Sci., Part A: Gen. Pap.*, 1964, **2**, 5247–5255.

[143] R. H. Wiley and N. R. Smith, *J. Polym. Sci.*, 1947, **2141**, 444–447.

[144] H. B. Jang, H. S. Rho, J. S. Oh, E. H. Nam, S. E. Park, H. Y. Bae and C. E. Song, *Org. Biomol. Chem.*, 2010, **8**, 3918–3922.

[145] R. Salvio, L. Massaro, A. Puglisi, L. Angelini, A. Antenucci, S. Placidi, F. Sciubba, L. Galantini and M. Bella, *Org. Biomol. Chem.*, 2018, **16**, 7041.

[146] A. Lu, K. Hu, Y. Wang, H. Song, Z. Zhou, J. Fang and C. Tang, *J. Org. Chem.*, 2012, **77**, 6208–6214.

[147] A. Preciado and P. G. Williams, *J. Org. Chem.*, 2008, **73**, 9228–9234.

[148] W. R. Roush, T. D. Bannister, M. D. Wendt, M. S. VanNieuwenhze, D. J. Gustin, G. J. Dilley, G. C. Lane, K. A. Scheidt and W. J. Smith, *J. Org. Chem.*, 2002, **67**, 4284–4289.

[149] L. C. Dias, A. M. Aguilar, A. G. Salles, L. J. Steil and W. R. Roush, *J. Org. Chem.*, 2005, **70**, 10461–10465.

[150] G. Chang, W. C. Guida and W. C. Still, *J. Am. Chem. Soc.*, 1989, **111**, 4379–4386.

[151] I. Kolossváry and W. C. Guida, *J. Am. Chem. Soc.*, 1996, **118**, 5011–5019.

[152] I. Kolossváry and W. C. Guida, *J. Comp. Chem.*, 1999, **20**, 1671–1684.

[153] S. Grimme, *Chem. - Eur. J.*, 2012, **18**, 9955–9964.

[154] L. Guo, Y. Chi, A. M. Almeida, I. A. Guzei, B. K. Parker and S. H. Gellman, *J. Am. Chem. Soc.*, 2009, **131**, 16018–16020.

[155] B. F. Fisher and S. H. Gellman, *J. Am. Chem. Soc.*, 2016, **138**, 10766–10769.

[156] M. W. Giuliano, S. J. Maynard, A. M. Almeida, L. Guo, I. A. Guzei, L. C. Spencer, S. H. Gellman and S. M. S, *J. Am. Chem. Soc.*, 2014, **136**, 15046–15053.

[157] L. Guo, W. Zhang, I. A. Guzei, L. C. Spencer, S. H. Gellman, G. Guichard, I. Huc, D. Seebach, A. K. Beck and D. J. Bierbaum, *Chem. Biodiversity*, 2012, **14**, 2582–2585.

[158] R. Knorr, A. Trzeciak, W. Bannwarth and D. Gillessen, *Tetrahedron*, 1989, **30**, 1927–1930.

[159] A. El-Faham and F. Albericio, *Chem. Rev.*, 2011, **111**, 6557–6602.

[160] K. Wuthrich, G. Wider, G. Wagner and W. Braun, *J. Mol. Biol.*, 1982, **155**, 311–319.

[161] J. Decatur, *NOESY on the 400 and 500 Using Topspin*, 2007.

[162] D. Neuhaus and M. P. Williamson, *The nuclear Overhauser effect in structural and conformational analysis*, Wiley, 2000, p. 619.

[163] Ł. Berlicki, L. Pilsl, E. Wéber, I. M. Mándity, C. Cabrele, T. A. Martinek, F. Fülöp and O. Reiser, *Angew. Chem., Int. Ed.*, 2012, **51**, 2208–2212.

[164] I. M. M'andity, E. W'eber, T. A. Martinek, G. Olajos, G. K. Tóth, E. Vass and F. Fülöp, *Angew. Chem., Int. Ed.*, 2009, **48**, 2171–2175.

[165] P. Vasudev, S. Chatterjee, K. Ananda, N. Shamala and P. Balaram, *Angew. Chem., Int. Ed.*, 2008, **47**, 6430–6432.

[166] A.-B. Bornhof, A. Bauzá, A. Aster, M. Pupier, A. Frontera, E. Vauthey, N. Sakai and S. Matile, *J. Am. Chem. Soc*, 2018, **140**, 4884–4892.

[167] S. K. Maity, S. Maity, P. Jana and D. Haldar, *Chem. Commun.*, 2012, **48**, 711–713.

[168] Y. Wang, Y. He, Z. Yu, J. Gao, S. T. Brinck, C. Slebodnick, G. B. Fahs, C. J. Zanelotti, M. Hegde, R. B. Moore, B. Ensing, T. J. Dingemans, R. Qiao and L. A. Madsen, *Nat. Commun.*, 2019, **10**, 801.

[169] J. Lees, B. Smith, F. Wien, A. Miles and B. Wallace, *Anal. Biochem.*, 2004, **332**, 285–289.

[170] *Schrödinger Release 2017-1: MacroModel,*, Schrödinger, LLC, New York, NY, 2019.

[171] W. L. Jorgensen and J. Tirado-Rives, *J. Am. Chem. Soc.*, 1988, **110**, 1657–1666.

[172] W. L. Jorgensen, Maxwell, D. S. and J. Tirado-Rives, 1996.

[173] D. Shivakumar, J. Williams, Y. Wu, W. Damm, J. Shelley and W. Sherman, *J. Chem. Theory Comput.*, 2010, **6**, 1509–1519.

[174] M. J. Frisch, G. W. Trucks, H. B. Schlegel, G. E. Scuseria, M. A. Robb, J. R. Cheeseman, G. Scalmani, V. Barone, B. Mennucci, G. A. Petersson, H. Nakatsuji, M. Caricato, X. Li, H. P. Hratchian, A. F. Izmaylov, J. Bloino, G. Zheng, J. L. Sonnenberg, M. Hada, M. Ehara, K. Toyota, R. Fukuda, J. Hasegawa, M. Ishida, T. Nakajima, Y. Honda, O. Kitao, H. Nakai, T. Vreven, J. A. Montgomery, Jr., J. E. Peralta, F. Ogliaro, M. Bearpark, J. J. Heyd, E. Brothers, K. N. Kudin, V. N. Staroverov, R. Kobayashi, J. Normand, K. Raghavachari, A. Rendell, J. C. Burant, S. S. Iyengar, J. Tomasi, M. Cossi, N. Rega, J. M. Millam, M. Klene, J. E. Knox, J. B. Cross, V. Bakken, C. Adamo, J. Jaramillo, R. Gomperts, R. E. Stratmann, O. Yazyev, A. J. Austin, R. Cammi, C. Pomelli, J. W. Ochterski, R. L. Martin, K. Morokuma, V. G. Zakrzewski, G. A. Voth, P. Salvador, J. J. Dannenberg, S. Dapprich, A. D. Daniels, O. Farkas, J. B. Foresman, J. V. Ortiz, J. Cioslowski and D. J. Fox, *Gaussian09 Revision E.01*, Gaussian Inc. Wallingford CT 2009.

[175] J.-D. Chai and M. Head-Gordon, *Phys. Chem. Chem. Phys.*, 2008, **10**, 6615.

[176] R. Ditchfield, W. J. Hehre and J. A. Pople, *J. Chem. Phys.*, 1971, **54**, 724–728.

[177] W. J. Hehre, R. Ditchfield and J. A. Pople, *J. Chem. Phys.*, 1972, **56**, 2257–2261.

[178] P. C. Hariharan and J. A. Pople, *Theor. Chim. Acta*, 1973, **28**, 213–222.

[179] Paton Lab, J. Rodríguez-Guerra, J. Chen and IFunes, *bobbypaton/GoodVibes: GoodVibes v3.0.0*, 2019, `https://zenodo.org/record/3346166`.

[180] A. V. Marenich, C. J. Cramer and D. G. Truhlar, *J. Phys. Chem. B*, 2009, **113**, 6378–6396.

[181] R. F. Ribeiro, A. V. Marenich, C. J. Cramer and D. G. Truhlar, *J. Phys. Chem. B*, 2011, **115**, 14556–14562.

[182] W. J. Nodes, K. Shankland, S. Rajkumar and A. J. A. Cobb, *Synlett*, 2010, 3011–3014.

[183] L. Lebarillier, F. Outurquin and C. Paulmier, *Tetrahedron*, 2000, **56**, 7483–7493.

[184] R. E. Claus and S. L. Schreiber, *Org. Synth.*, 1986, **64**, 150.

[185] S. E. Denmark and L. Gomez, *The J. Org. Chem.*, 2003, **68**, 8015–8024.

[186] Y.-M. Shao, W.-B. Yang, T.-H. Kuo, K.-C. Tsai, C.-H. Lin, A.-S. Yang, P.-H. Liang and C.-H. Wong, *Bioorg. Med. Chem.*, 2008, **16**, 4652–4660.

[187] X. Chen, Y. Zhang, H. Wan, W. Wang and S. Zhang, *Chem. Commun.*, 2016, **52**, 3532–3535.

[188] H. Tsuji and H. Yamamoto, *J. Am. Chem. Soc*, 2016, **138**, 14218–14221.

[189] E. Marsault, H. R. Hoveyda, M. L. Peterson, C. Saint-Louis, A. Landry, M. Vézina, L. Ouellet, Z. Wang, M. Ramaseshan, S. Beaubien, K. Benakli, S. Beauchemin, R. Déziel, T. Peeters and G. L. Fraser, *J. Med. Chem.*, 2006, **49**, 7190–7197.